Hardy BBT Limited

CONSULTING ENGINEERING & PROFESSIONAL SERVICES

REAL-TIME MARINE RESISTIVITY SYSTEM

Prepared for:

SUPPLY AND SERVICES CANADA

Prepared by:

Hardy BBT Limited

PROJECT NO. CP12100

MARCH, 1987

0,70

TABLE OF CONTENTS

Table of Contents - continued

LIST OF FIGURES

1.0 INTRODUCTION

Recent discoveries of commercial quantities of oil in the Canadian Beaufort Sea make it very probable that major development programs will be carried out in the area in the near future. The detection of sub-bottom permafrost and granular deposits is very important for the design and construction of offshore facilities. Granular deposits will supply valuable borrow material for construction of islands while the presence of permafrost will influence the choice of routes and construction of pipelines.

Marine resistivity measurements offer a valuable complement to seismic and acoustic techniques in mapping permafrost and granular deposits. Electrical resistivity measurements are used routinely on land for detecting permafrost and granular materials. This fact led to the development of a marine resistivity system which has been used at Prudhoe Bay, Alaska, in 1983 and 1984, and in the southern Beaufort Sea, Northwest Territories, in 1985. The system provides apparent resistivity measurements of the sea and sub-bottom which can be interpreted in terms of a layered earth sequence. A major limitation to the system has been the lack of a real-time resistivity interpretation capability. Development of such a capability would provide a reconnaissance level technique that would make a more efficient use of marine survey time and optimize the selection of drillhole locations.

In the present program, the existing marine resistivity system hardware and computer software were redesigned to provide a real-time interpretation of the resistivity data. Funding for this project was provided by the Department of Indian and

Northern Affairs under the direction of Mr. R.J. Gowan. The system was assembled and bench tested prior to carrying out a field trial. Descriptions of the equipment design, bench tests and field trial results are presented in this report.

2.0 BACKGROUND

The use of electrical resistivity measurements has long been accepted on land as a means of mapping the distribution of granular resources and permafrost (Scott et al, 1979). In general, electrical resistivity of soils is a function of grain size, with sands and gravels having a higher resistivities than silts and clays. This relationship holds even when the pore water in the materials is saline. Furthermore, frozen materials have much higher electrical resistivities than the same materials in an unfrozen state.

Figure 1 shows values of electrical resistivity for some typical soils on land as a function of temperature. Figure 2 shows ranges of values of resistivity for typical soils in their unfrozen state. From Figure 1, it is clear that freezing the soil generates a drastic increase in its resistivity. Figure 2 indicates that increasing grain size implies increasing resistivity. The higher the resistivities observed in soils, the more coarse-grained those soils are likely to be, provided that temperature and moisture content conditions are similar.

The use of electrical methods to identify granular materials or permafrost then divides into two parts. The first part is obtaining an estimate of the true electrical resistivity of

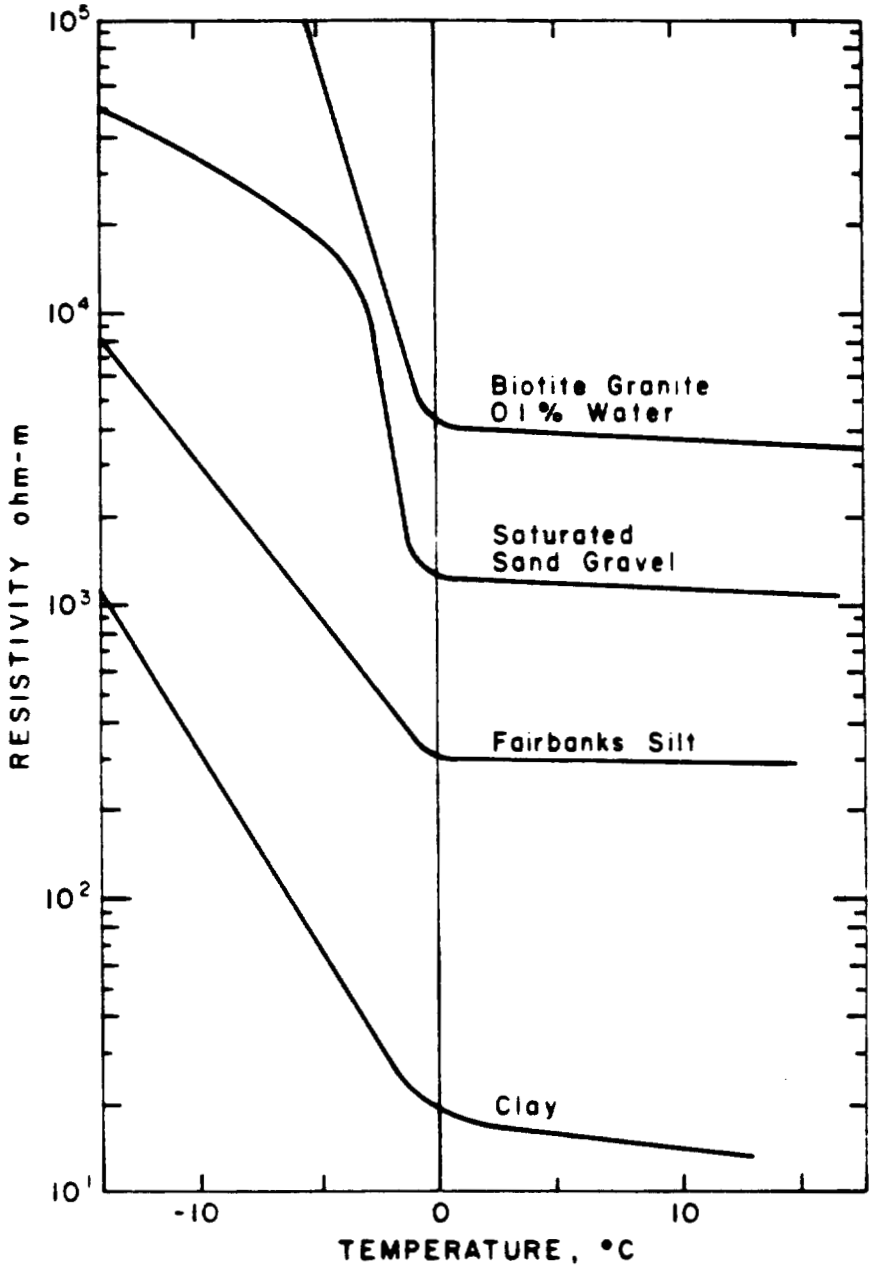

Hardy BBT Limited
CONSULTING ENGINEERING & PROFESSIONAL SERVICES

Supply And Services Canada
Real-Time Marine Resistivity System
Figure 1 - Resistivity vs. Temperature

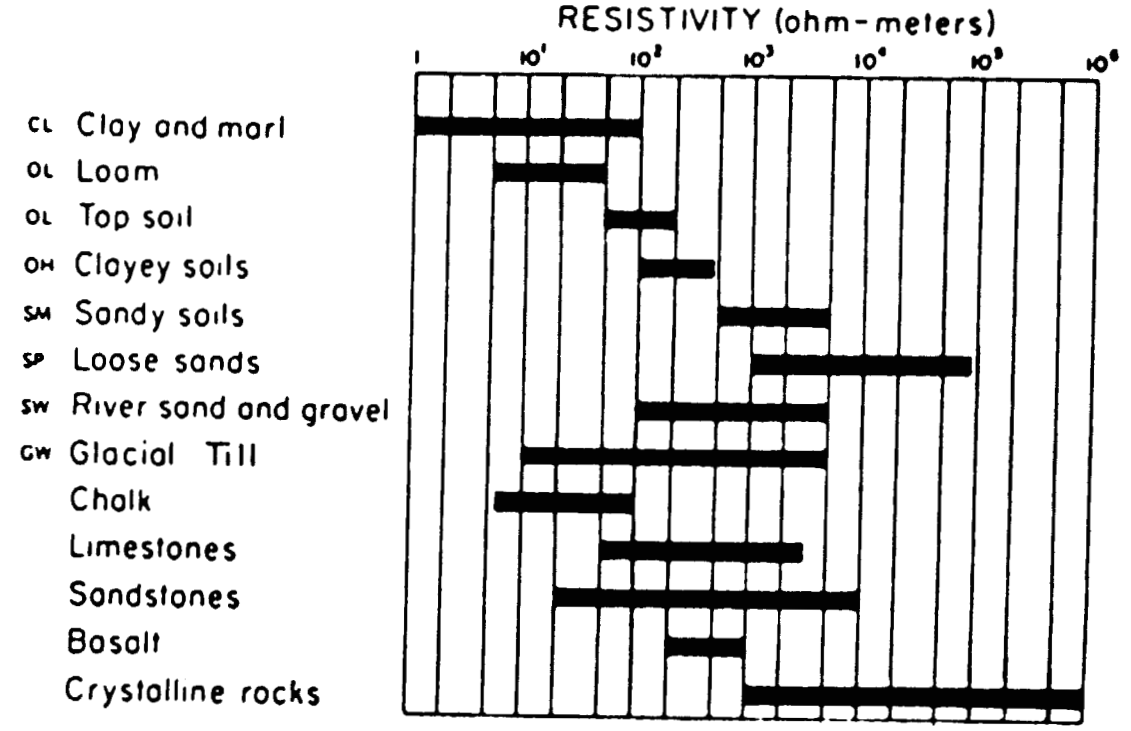

Hardy BBT Limited
CONSULTING ENGINEERING & PROFESSIONAL SERVICES

Supply And Services Canada
Real-Time Marine Resistivity System
Figure 2 - Resistivity vs. Grain Size

the material; and the second part is making the correlation between that resistivity and the type of soil to be expected.

2.1 RESISTIVITY MEASUREMENTS

Measurement of resistivity on land or water involves injection of electrical current through two electrodes and measurement of the resulting potentials between other electrodes. A quantity known as apparent resistivity is calculated from these measurements in the following manner:

$$\rho_a = (V/I)\ f\ (G)$$

WHERE ρ_a is apparent resistivity

I is the injected current

V is the observed voltage

f(G) is a function of the geometry of the electrodes

Figure 3 (Telford et al, 1976) shows some common electrodes arrays and the appropriate formulae for apparent resistivity.

If the ground under the electrode array is homogeneous to a depth much greater than the size of the array, then the measured apparent resistivity would be equal to the true resistivity of the earth. Such a uniform case rarely occurs in nature however, and the apparent resistivity represents some function of the distribution of values in the earth within the range of the measurement.

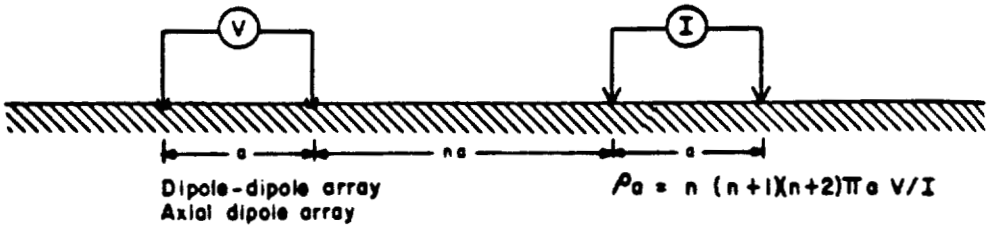

Dipole-dipole array
Axial dipole array

$\rho a = n\,(n+1)(n+2)\pi a\ V/I$

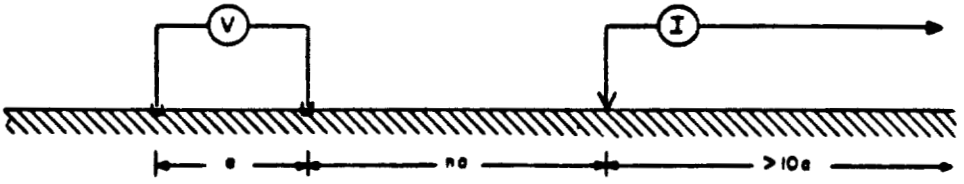

Pole-dipole array
Three array if n = 1

$\rho a = 2n(n+1)\pi a\ V/I$

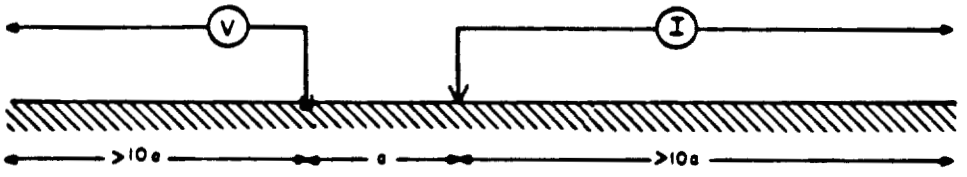

Pole-pole array

$\rho a = 2\pi a\ V/I$

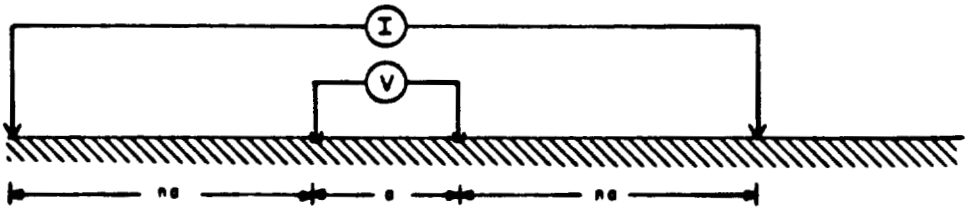

Schlumberger array, n>2

$\rho a = n(n+1)\pi a\ V/I$

Wenner array, n = 1

$\rho a = 2\pi a\ V/I$

Hardy BBT Limited
CONSULTING ENGINEERING & PROFESSIONAL SERVICES

Supply And Services Canada
Real-Time Marine Resistivity System
Figure 3 - Common Electrode Arrays

The general procedure in making electrical resistivity measurements involves varying the size of the array and thus, the volume of ground affected by the measurement, and observing changes in apparent resistivity as a function of this variation. The interpretation process then attempts to explain the observed variation of the apparent resistivity with depth in terms of a model whose geometrical and electrical properties can then be determined. The usual procedure for varying electrode arrays involves increasing the size of the array in some regular manner. The resulting set of observations is called a sounding.

The array most commonly used in marine resistivity is the multi-dipole array. For this array, an increase in depth of penetration is normally accomplished by increasing the spacing between transmitter and receiver dipoles, while keeping the dipole size constant. The expansion of array sizes is carried out in terms of the dipole multiple n (Figure 3). The smallest array is with n=1. In this case, the distance between the nearest transmitter and nearest receiver electrode is one dipole length. Increased penetration is achieved by increasing the number of dipole lengths separating transmitter and receiver dipoles. In practical field situations, the largest separation normally achievable is limited by signal strength to n=6. Thus a multi-dipole sounding consists of six apparent resistivities calculated for n=1 through 6.

2.2 INTERPRETATION OF RESISTIVITY MEASUREMENTS

Resistivity interpretation is carried out in terms of models. In the case of a multi-dipole sounding, only six apparent resistivities are available. Thus, only simple models can be

fitted to the data. For detection of granular resources in the Beaufort Sea however, this is not a significant limitation because adequate models can be developed in terms of a small number of uniform layers. A typical model would involve three layers lying on an infinite half space. The uppermost layer, the water, would have a resistivity and thickness which could be determined by independent means. Thus, the sub-bottom materials could be modelled in terms of two layers lying on a half space. In areas where granular materials are expected to be close to the bottom, variation of resistivity in these upper two layers would be indicative of variation of grain size in the near sub-bottom.

The parameters of the model are obtained from the field observations of the apparent resistivity by an inversion process. The first estimate is made of the model parameters and the apparent resistivities which would be observed for this model are calculated. These resistivities are compared with those observed in the field and adjustments are made in the model parameters in the direction which minimizes the disagreement between observed and calculated apparent resistivities. Normally, several cycles of calculation and adjustment will bring the calculated and observed apparent resistivities into reasonable agreement, provided that a good initial model is used.

It should be understood that it is frequently possible to obtain more than one model which will satisfactorily match the observed apparent resistivities. Thus, it is important that the starting model be reasonably close to the situation which is being investigated. External control such as drill hole information, sub-bottom profile information, and geological

inference can thus be used to help sharpen the precision of the geophysical interpretation. This approach to interpretation is discussed further in Section 4.1.

2.3 HISTORY OF MARINE RESISTIVITY MEASUREMENTS

The published literature on marine resistivity measurements is not extensive. As in so many other aspects of electrical measurements, the earliest paper was by the Schlumberger brothers, this time with Leonardon (in 1934). Boulos (1972) described the use of resistivity soundings to measure depth to bedrock under a branch of the Nile River. Whiteley (1974) described a system for offshore resistivity profiling.

In the early 1970's, studies carried out at the Geological Survey of Canada (Scott, 1975, Appendix C), indicated the feasibility of making marine resistivity measurements and correlating these measurements with material type and permafrost regime. By 1979, the development program at the GSC had resulted in a prototype system for measuring resistivities in a marine environment, (Lobach and Scott, 1979, Appendix C).

During the same time frame, a group at the University of Wisconsin was attempting to use marine resistivity measurements to map granular materials and sub-bottom geology in Lake Michigan, (Nebrija, et al, 1976, Appendix C). So far as is known, the work of this group was discontinued in the late 1970's.

In 1980, Hardy Associates (1978) Ltd. (now Hardy BBT Limited) began the development of the marine resistivity system known as MICRO-WIP, (Micro Processor Controlled Waterborne Induced

Polarization Resistivity). In various stages of development, this system was used for fresh water work in mineral exploration and for salt-water searches for granular materials. Initial results of a survey offshore Alaska were described by Scott et al, 1983 (Appendix C). At that time, design of the system was relatively established and only minor changes were made from then until the commencement of the present program. The system was used in the Canadian southern Beaufort Sea in 1985 in a successful program to map granular materials for island construction (Scott and Maxwell, 1987, Appendix C).

2.4 MEASUREMENT TECHNIQUES - MARINE SYSTEM

Marine resistivity meaurements with the MICRO-WIP system are made by means of a streamer towed behind a survey vessel. This layout is shown schematically in Figure 4. The multi-dipole array is incorporated into the streamer. The two electrodes nearest the survey vessel are used to transmit electrical current into the water and sub-bottom materials. The other seven electrodes on the streamer are used to measure the resulting voltage distribution as a function of distance from the source, and consequently, as a function of penetration into the sub-bottom. These seven electrodes allow the calculation of the six values of apparent resistivities as discussed above. Experience in the Beaufort Sea in 1985 (Appendix C), indicates that current levels of approximately 15 amperes are adequate to give reliable signal levels for measurements of this sort with a dipole length of 25 metres and separations of n=1 to 6.

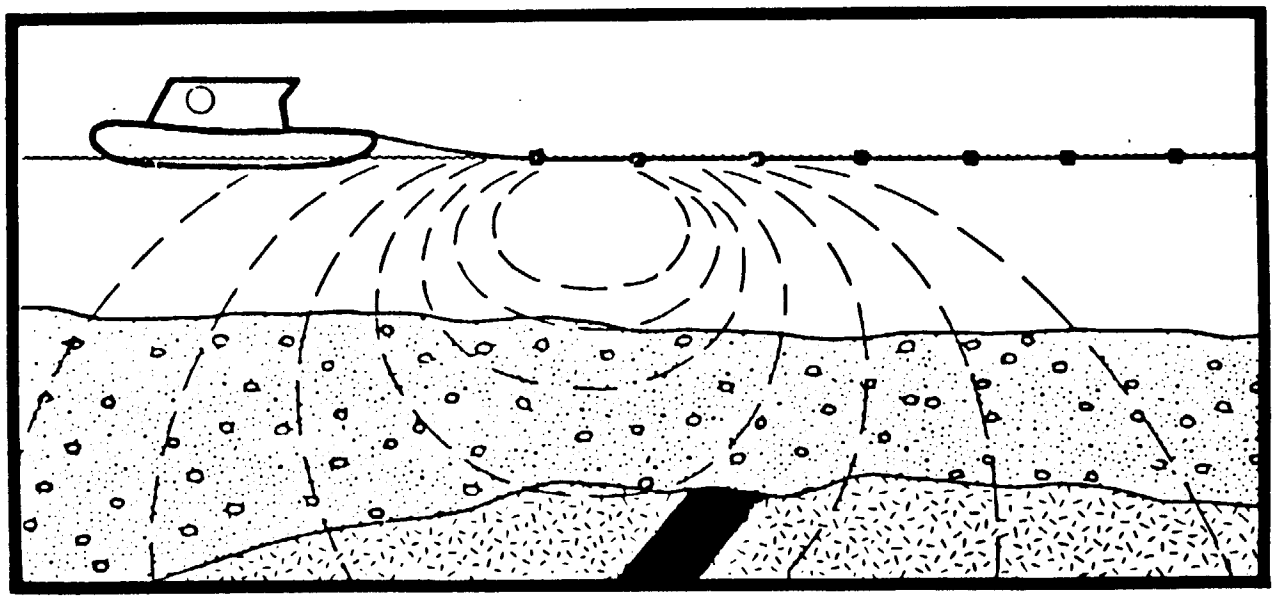

Hardy BBT Limited
CONSULTING ENGINEERING & PROFESSIONAL SERVICES

Supply And Services Canada
Real-Time Marine Resistivity System
Figure 4 - Schematic Diagram of MICRO-WIP Survey

2.5 MICRO-WIP EQUIPMENT IN 1985

In 1985, the MICRO-WIP system was used to carry a search of granular material in the southern Beaufort Sea. The block diagram of the system as used during the period 1981 to 1985, is shown in Figure 5. (After Dyck et al, 1983). The heart of the system at that time was a Sonotek SDS 1200 Data Acquisition System. This system controlled the wave form injected through the current electrodes by a transmitter. The current wave form and the six resulting voltage signals were digitized and the digitized values were stored on magnetic tape. The water depth, the time of day and navigation information were also recorded and keyed to the observed resistivity measurements. Following the survey, the magnetic tapes were read and calculations of the apparent resistivity and in the case of mining surveys, apparent chargeability, were made after the manner shown in Figure 6. The resistivity calculations were made by averaging the digitized values for a large part of the time that current was transmitted, taking the ratio of the current wave form to the observed voltage wave form and applying the appropriate geometric factor. When induced polarization measurements were taken, the transient persisting after interruption of the current was integrated over a fixed time interval and the results normalized with respect to the potential observed during the current flow. This was in general, a fairly unwieldy process and thus, considerable time elapsed between finishing the survey and the preparation of even a preliminary interpretation. This time interval has not been considered a problem with more southerly lake-based mineral exploration surveys, but has been a concern in Arctic marine granular survey programs.

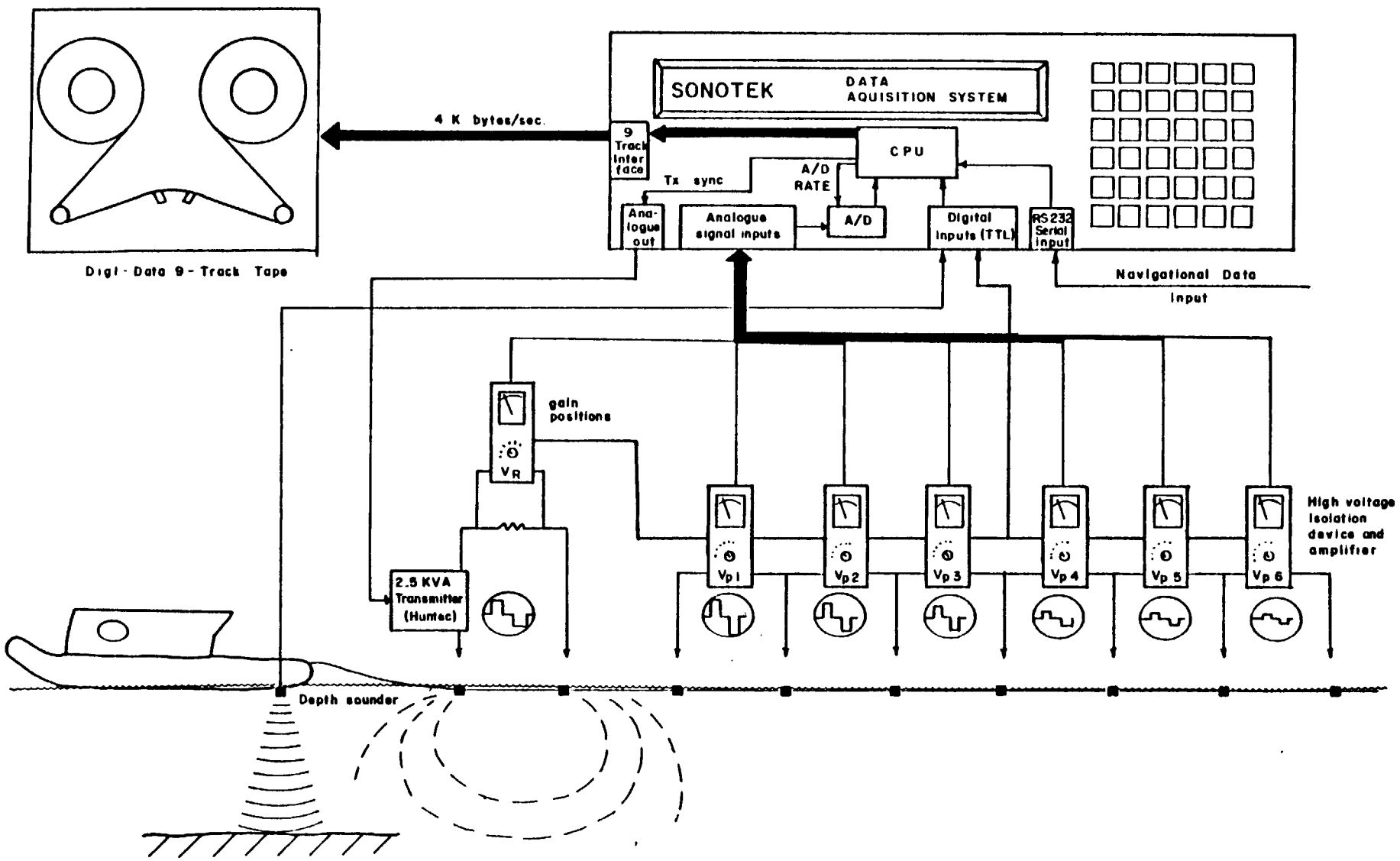

Hardy BBT Limited
CONSULTING ENGINEERING & PROFESSIONAL SERVICES

Supply And Services Canada
Real-Time Marine Resistivity System
Figure 5 - MICRO-WIP Block Diagram,
circa. 1985

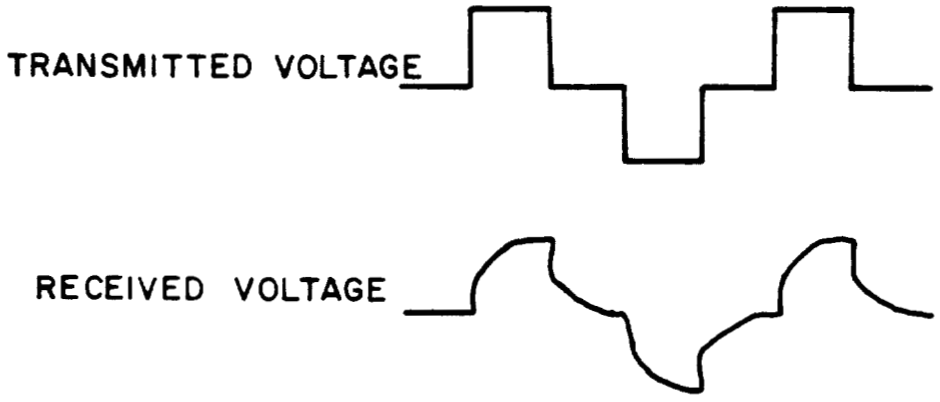

1(a)

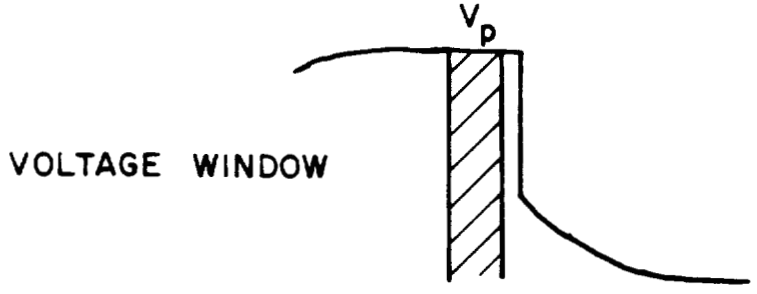

2(b)

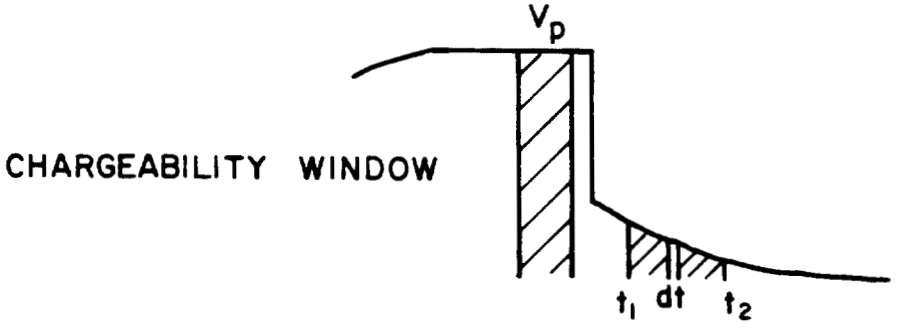

2(c)

Hardy BBT Limited
CONSULTING ENGINEERING & PROFESSIONAL SERVICES

Supply And Services Canada
Real-Time Marine Resistivity System
Figure 6 - Waveform and Calculations

2.6 1985 MICRO-WIP SURVEY, SOUTHERN BEAUFORT SEA

During the summer of 1985, the system was operated in the Beaufort Sea to map resistivities in support of evaluation of granular resources (Scott and Maxwell, 1987, Appendix C). This survey was carried out prior to the dredging of material to build an artificial island. Despite very bad ice conditions which allowed only very limited access to the survey area, some 40 kilometres of survey data were obtained during a two day period. After completion of the survey, however, a ten day period elapsed before the first preliminary interpretation was provided to the client. A further period of a month ensued before presentation of the detailed interpretation.

Fortunately for the future of MICRO-WIP, other geotechnical information had already indicated the presence of granular material, and the borrow pit was successfully established shortly after the preliminary interpretation was supplied. The final interpretation showed that the borrow pit was indeed in the optimum location. After this survey, it was recognized that if the MICRO-WIP were to be used in a reconnaissance mode, it would be impossible to proceed without providing an interpretation without delay.

It was in light of this experience that the present development program was undertaken. The objective of the present program was to develop the capability to carry out interpretation in real-time, in order that reconnaissance surveys could be performed immediately ahead of dredging, and expensive stand-by time for the dredge could be avoided.

2.7 ELECTRICAL CHARACTERISTICS - SOUTHERN BEAUFORT SEA

The interpretation carried out on the data from the 1985 survey showed that the resistivity of the seawater in the southern Beaufort Sea was typically about 2.0 ohm-metres. In electrical terms, the sub-bottom materials in the survey area could be represented by three layers. The uppermost layer appeared to have resistivities ranging from 1.6 to 2.6 ohm-metres. From the limited drilling carried out to a establish the borrow pit, it appears that this range of resistivities spanned materials from clayey silts to coarse sands with occasional pebbles. Within the survey area, none of this material appeared to be frozen. The bottom-most layer interpreted in the 1985 survey had resistivities which ranged from a low of 10 ohm-metres to a high of greater than 500 ohm-metres. The variation of resistivity generally reflected the depth to the top of the layer, with the highest resistivities occurring where the layer was shallowest. A single drill hole intersected permafrost at the interpreted depth to the top of this layer within the borrow area. From the high interpreted resistivities and from the fortuitous intersection in the borehole, it was concluded that the high resistivity parts of this layer represent the ice-bonded material, and that the ice content generally correlated with the interpreted resistivity values.

An unexpected outcome of the interpretation procedure was that between the uppermost layer, (1.6 to 2.6 ohm-metres) and the deepest (permafrost) layer, there appeared to be a layer of significantly lower resistivity (0.5 to 1.5 ohm-metres). This layer has no apparent direct geological correlation. However, work in the Alaska Beaufort Sea, (Sellmann, P.V., 1985

pers.comm.) suggests that there is a pronounced increase in salinity of pore waters immediately above the degrading permafrost. Such an increased salinity would result in lowered resistivities and would provide a reasonable explanation for the observations from the 1985 survey.

From the 1985 survey several things therefore emerged. The first was the need for real-time processing in order to avoid delay in providing interpretation. The second was an understanding of the general range of resistivities to be expected in the sub-bottom materials. These resistivities correlated reasonably well with those initially determined by Scott,(1975), in resistivity soundings carried out through the sea ice in the same general area. The 1985 survey further provided some values of apparent resistivity as a function of dipole spacing which could be used in simulated trials with modified equipment.

3.0 SYSTEM DESIGN AND TESTING

3.1 OVERVIEW

The microprocessor controlled waterborne induced polarization (MICRO-WIP) system was developed to provide exploration services for mineral and engineering application. At the core of the system was the MICRO-WIP amplifier network which allows a simultaneous measurement of seven voltages from receiver dipoles in a marine environment. The design of these amplifiers and supervision of their assembly was provided by Hardy BBT Limited under the direction of Dr. W.J. Scott in 1983.

These amplifiers were also the core around which the system developed under this program was constructed. One of the requirements for a real-time system was the need to sample and perform calculations rapidly on a continuous stream of data acquired during the survey. It was also necessary to design and build calibration and simulation equipment which would allow sufficient bench testing of the system before field trials are undertaken. This was clearly the most efficient and cost-effective approach.

The MICRO-WIP system operated with an interrupted square wave (Figure 6) in which the current was transmitted in one direction for one second, was off for one second, transmitted in the opposite direction for one second, and then was off for a further second. Thus the basic period of the waveform was four seconds and the frequency was 0.25 hz.

The MICRO-WIP amplifiers were designed to measure this signal with a minimum of distortion. The amplifiers are DC-coupled. The front-end has provision for offset adjustments, and was provided with an operator-controlled gain adjustment. After amplification to about one volt or better, the signal was transmitted to the data acquisition system.

The amplifier bandwidth was DC to approximately 12 Hz. The low-pass filter system was designed to provide 60 dB of attenuation at a frequency of 60 Hz.

In order to meet the requirements of designing and building a real-time marine resistivity system a sequence of tasks was assigned with a timetable and budget. This sequence of tasks

and accompanying budget and timetable are shown in Tables 1 and 2, respectively.

To provide real-time interpretations, two functions must be developed within the system. The first of these was the averaging of the digitized waveforms and calculation of apparent resistivity values. The second was to invert the apparent resistivity values by the process described in Section 2.2. Within the time constraints of real-time processing, it did not appear possible to perform both functions in a single computer. It was therefore decided to carry out the first function within the data acquisition system. Unfortunately, the Sonotek SDS 1200 did not have sufficient computing power to carry out this function, and a new controller and data acquisition system was therefore required. The implementation of these two functions was, therefore, the main objective of the study.

The first stage of development consisted of selecting a suitable data acquisition system with the specifications that were required. The interfacing of the three major components (controlling computer, MICRO-WIP amplifiers, and data acquisition system) was then carried out at the same time as the assembly of the simulator and test network. This interfacing required a large amount of computer programming as well as assembling hardware connnections between the instruments. A transmitter controller unit was designed and built to allow the computer to control the timing of the transmitted waveform. It is essential that the system computer keep track, via the pacer clock on the data acquisition unit, of what each component is doing and when.

TABLE 1
REAL-TIME MARINE RESISTIVITY PROJECT TASKS

1. Determine Equipment Availability and Compatibility
2. Determine Specifications for Acquisition System (HP 3852)
3. Get Manuals
4. Redesign Simulator for Free Run
5. Flowchart for HP 3852 Program
6. Inversion Program
7. Test Network for Simulations
8. Get HP 3852 & Other Equipment and Software
9. Display Program
10. Computer Model Suite
11. Interface HP 3852 to IP
12. Interface Computer (HP 9816)
13. Interface Inversion to HP 3852
14. Transmitter Controller Design
15. Simulated Trials
16. Operation Manual
17. Transmitter Controller Assembly
18. Program Manual
19. Field Trials
20. Report
21. Project Management

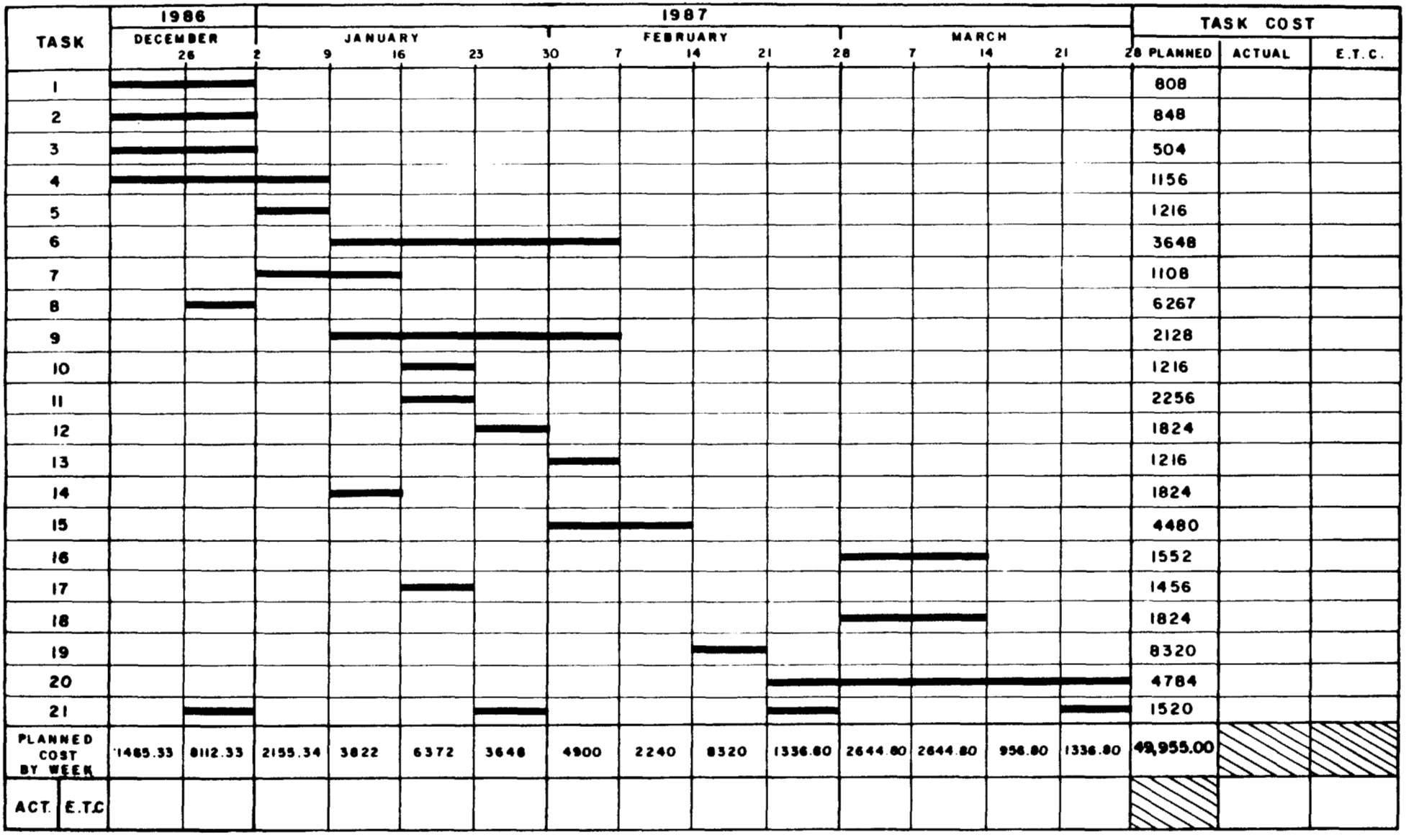

TASK	TASK COST PLANNED	ACTUAL	E.T.C.
1	808		
2	848		
3	504		
4	1156		
5	1216		
6	3648		
7	1108		
8	6267		
9	2128		
10	1216		
11	2256		
12	1824		
13	1216		
14	1824		
15	4480		
16	1552		
17	1456		
18	1824		
19	8320		
20	4784		
21	1520		

PLANNED COST BY WEEK	1485.33	8112.33	2155.34	3822	6372	3648	4900	2240	8320	1336.80	2644.80	2644.80	956.80	1336.80	49,955.00		
ACT. / E.T.C.																	

File No. 38 ST . A7134 - 6 - 0021 Serial No. A7134 - 6 - 0021 / 01 - ST

Hardy BBT Limited
CONSULTING ENGINEERING & PROFESSIONAL SERVICES

SUPPLY AND SERVICES CANADA

PROJECT TIMETABLE AND BUDGET

REAL-TIME MARINE RESISTIVITY MEASUREMENT

Table 2

CP12100

After these devices were built and debugged, then a bench test trial was carried out to simulate a real field test. Finally, the entire system was installed on a suitable vessel for a field trial on Okanagan Lake, British Columbia. There the real-time resistivity interpretation capability of this system was demonstrated during the field trial.

3.2 DATA ACQUISITION SYSTEM

The system selected for this project was the Hewlett Packard HP 3852S data acquisition and control system. A more complete description of the control unit and plug-in accessories is contained in Appendix "A". The system can be configured for a variety of applications. It has built-in intelligence, an internal clock and a programmable pacer which can be used as timing control for remote devices.

3.3 SIMULATOR AND RESISTOR NETWORK

In order to adequately test the system before carrying out field trials, it is necessary to construct devices which can simulate a real environment. During the course of a normal field survey, a towed cable supplies six voltages to the MICRO-WIP amplifiers from a series of electrodes. The output current is obtained by measuring a voltage across a shunt resistor in series with the current electrodes. This can be simulated for a bench test by applying a suitable voltage waveform across a bank of resistors, whose values are chosen from resistivity results obtained during previous offshore surveys. A schematic diagram of the resistor network is illustrated in Figure 7. The simulator box consisted of an existing device which was used on previous surveys to

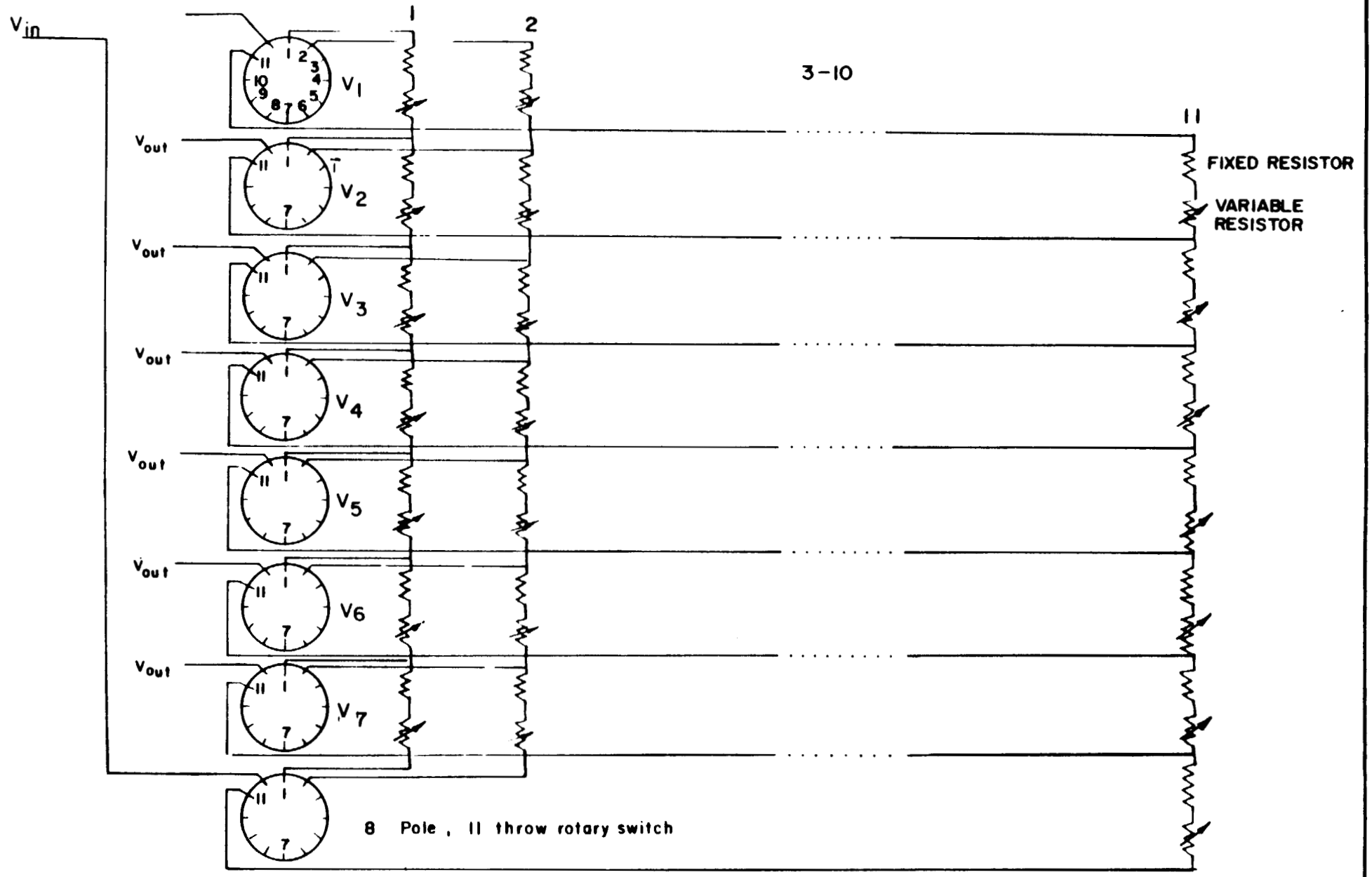

Hardy BBT Limited

Supply And Services Canada
Real-Time Marine Resistivity System

Figure 7 - Simulator Network

HT 139-82/12

calibrate the resistivity/induced polarization system. This was modified to produce a voltage waveform controlled by the system pacer which could be applied to the resistor network.

3.4 TRANSMITTER CONTROLLER

The system must know when the current is transmitted in order to calculate a resistivity value during the correct window. This was accomplished by designing a controller which turns the transmitter on and off in synchronization with the timing supplied by the pacer signal in the HP 3852. A schematic diagram of the transmitter control circuit is shown in Figure 8.

3.5 SYSTEM FUNCTION

As discussed earlier, it is very important that the system electronics be bench tested prior to carrying out a field trial. The system was assembled for bench tests according to Figure 9.

There are two computer programs required to run the system, both of which have been included in Appendix "B". First the program called DOWNLOAD2 is executed in the HP 9816 computer. This "downloads" a set of instructions to the data acquisition system (HP3852) as a callable subroutine. This subroutine sets up the system pacer, scans the amplifier channels, stacks the voltages, and checks the gains. However, this program does not start executing until called from the main program, INV-LD-PL (for inversion-log dipole-plot). This program initializes the plotter, graphics and inversion step size, starts the HP 3852, reads data from the HP 3852 and plots the real-time resistivity section.

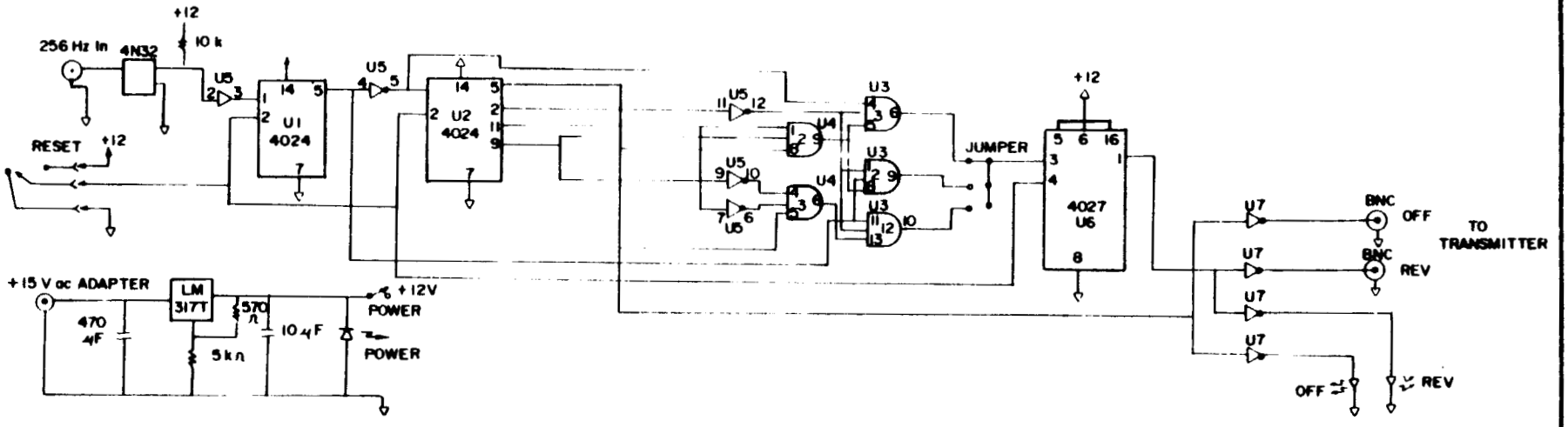

Hardy BBT Limited
CONSULTING ENGINEERING & PROFESSIONAL SERVICES

Supply And Services Canada
Real-Time Marine Resistivity System

Figure 8 - Transmitter Control Network

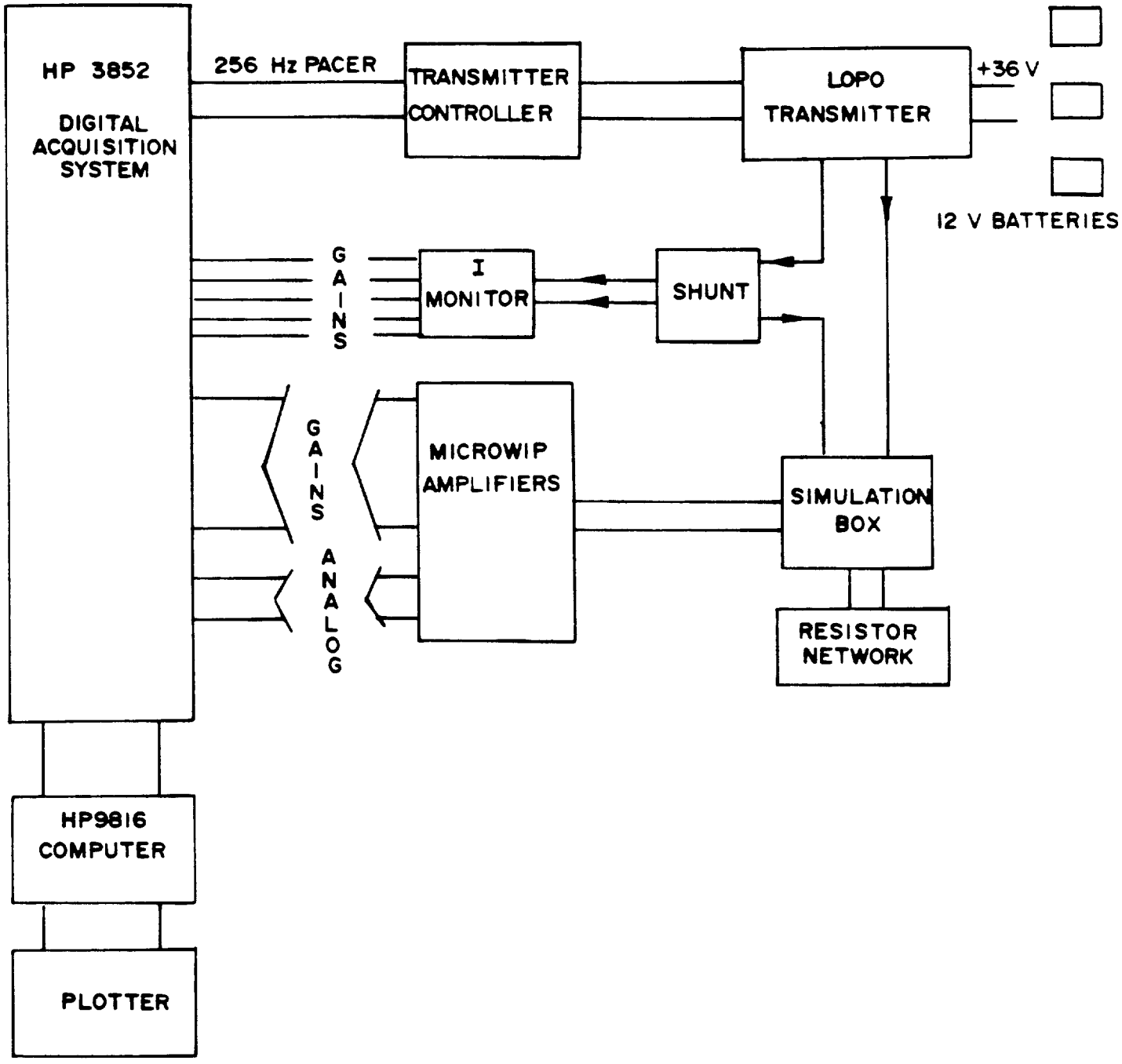

Hardy BBT Limited
CONSULTING ENGINEERING & PROFESSIONAL SERVICES

Supply And Services Canada
Real-Time Marine Resistivity System
Figure 9 - System Diagram, Simulation Trial

HT83-82/03

The sequence of events for the devices shown on Figure 9 is as follows. The HP 9816 starts the HP 3852 as previously discussed. The pacer output from the HP 3852 goes into the transmitter controller which tells the transmitter (a 160 w Huntec Lopo MK3 model in this case), to transmit a current with the appropriate waveform and frequency. The transmitter, already turned on, sits in a waiting state until told to transmit. Power for the transmitter is supplied by three-12 volt car batteries. The output current is measured by a shunt resistor in series with the output. This signal is supplied to the current monitor where is it amplified, and filtered and passed to the HP 3852, along with the gain information. The current output from the transmitter goes into the simulation box which divides it among the six resistor networks which simulate the six receiver dipoles in the water.

The six voltages are then fed into the MICRO-WIP amplifiers which pass both voltage and gain information back to the HP 3852 for processing. After a specified number of cycles is stacked, all of this information is passed to the HP 9816 computer which calculates and fits layered earth models to the measured values of resistivity and then plots the interpreted section.

3.6 STREAMER ELECTRODE ARRAY

The 1985 survey was performed with an array of 25-metre dipoles and n=1 to 6. This array was initially designed for mineral exploration, where arrays with constant dipole size are common. The combination of water depth, water resistivity and sub-bottom conditions in the 1985 Beaufort Sea survey area was such that the 25-metre array gave good definition of the

surface layers and at the same time, adequate penetration to map relic permafrost at depth.

Subsequent computer modelling support by an Industrial Research Assistantship Program (IRAP) Grant suggested that better resolution of deep features and better definition of near-surface resistivities could be obtained with an array in which the receiver dipole size increased logarithmically with distance from the transmitter dipole. As part of the IRAP program, such a streamer was built. The spacings of this streamer are given in Table 3.

TABLE 3

LOGARITHMIC STREAMER

DISTANCE (metres)	IDENTIFICATION	ELECTRODE
0	Start of Cable	-
25	Current Dipole	C1
50		C2
60		P1
70	Potential Channel 1	P2
85.75	Potential Channel 2	P3
107.75	Potential Channel 3	P4
141.25	Potential Channel 4	P5
189.25	Potential Channel 5	P6
260.50	Potential Channel 6	P7

Because the 1985 data were taken with constant dipole lengths, the simulator network was established for this configuration. The data acquisition system and inversion routines were configured to handle either constant-spacing arrays or logarithmic-spacing arrays.

4.0 SIMULATION OF BEAUFORT SEA MEASUREMENTS

Within the time and cost constraints of the present program, it is impossible to provide real data from the Beaufort Sea with the modified system. It is therefore important to look at the variety of likely geological models to be encountered in the Beaufort Sea and to predict the electrical responses of such models. Fortunately, the experience gained in the 1985 survey allows some degree of certainty in predicting the likely range of measurements to be encountered.

A very large number of resistors is required to prepare a single simulated resistivity distribution for measurement with this system in the manner indicated in Figures 7 & 9. It is possible to predict, from forward modelling programs already in existence, the apparent resistivities that would be observed with this system over given geologic conditions. Furthermore, in order to provide a realistic transition from one model to another, it is necessary to prepare a series of intermediate models so that the variation in measurement can proceed incrementally as would be the case in a field survey. Because of this, only three models were chosen to be included in the simulated network as described in Figure 7, and five or six intermediate steps were chosen between the three models. A single simulator network requires fourteen resistors which are adjustable in order to provide precise values. Thus, our three models, with the necessary transition resistor arrays as well, represent an array of one hundred and fifty-four resistors. Physical simulation of larger numbers of models becomes extremely difficult without a large investment in switching and resistor arrays.

Thus, while a significant number of likely geologic configurations was considered for forward modelling only the three most representative of conditions encountered in the 1985 survey were built into the physical simulator.

4.1 GRANULAR BORROW CONFIGURATIONS

Table 4 summarizes the likely set of conditions which would be encountered in looking for granular materials in the southern Beaufort Sea. While this is a reasonably comprehensive set of geologic conditions, the innate perversity of nature is such that it is not possible to predict all configurations which are likely to be encountered. Furthermore, it should be realized that even with the logarithmic array, the maximum number of layers that can be resolved is three layers lying on a half-space. Forward calculations can be carried for all of the models in Table 4 and a set of observed of apparent resistivities can be derived. However, in cases with more than three layers, the inversion will not necessarily lead back to the starting model. This is an intrinsic limitation of resistivity methods and must be recognized if application of marine resistivity is contemplated.

This problem, known as the problem of equivalence, can be resolved to some extent if acoustically determined boundaries coincide with some of the electrically defined boundaries. For example, it is obviously possible to define the bottom of the water (top of seabed) and thus the influence of the water can be removed from any model by calculation. In the case of Group 5, (Table 4), the top of the granular material under the silts and clay will constitute an acoustic reflector. In such a case, fixing the thickness of the fine-grained layer from the

TABLE 4

TYPICAL SUB-BOTTOM GEOLOGICAL CONFIGURATIONS

MODEL NO.	CONFIGURATION* (ρ (Ω-m), t(m))
1A	Granular(2.2,20)/Saline(1,20)/Permafrost (100,∞)
1B	Granular(2.2,10)/Saline(1,10)/Permafrost (500,∞)
1C	Granular(2.2,20)/Saline(1,20)/Unfrozen (10,∞)
2A	Fines (1.6,20)/Saline(1,20)/Permafrost (100,∞)
2B	Fines (1.6,10)/Saline(1,10)/Permafrost (500,∞)
2C	Fines (1.6,20)/Saline(1,20)/Unfrozen (10,∞)
3A	Permafrost(20,2)/Granular(2.2,20)/Saline(1,20)/Permafrost (100,∞)
3B	Permafrost(20,2)/Granular(2.2,10)/Saline(1,10)/Permafrost (500,∞)
3C	Permafrost(20,2)/Granular(2.2,20)/Saline(1,20)/Unfrozen (10,∞)
4A	Permafrost(15,2)/Fines (1.6,20)/Saline(1,20)/Permafrost (100,∞)
4B	Permafrost(15,2)/Fines (1.6,10)/Saline(1,10)/Permafrost (500,∞)
4C	Permafrost(15,2)/Fines (1.6,20)/Saline(1,20)/Unfrozen (10,∞)
5A	Fines (1.6,5)/Granular(2.2,20)/Saline(1,20)/Permafrost (100,∞)
5B	Fines (1.6,20)/Granular(2.2,10)/Saline(1,20)/Permafrost (100,∞)

*TOP LAYER IS ALWAYS WATER (2 Ω-m, 8 m THICK)

acoustic results will allow better resolution of the resistivity of the uppermost layers. Similarily, in any area where acoustic definition of the top of relic permafrost has been obtained, the inversion model can be constrained so that the total thickness of material lying above permafrost is held to that determined by the acoustic results. It is therefore important to recognize that the use of marine resistivity measurements is not a substitute for acoustic surveying in the search for borrow material, but that it is rather a complement which allows additional information to be incorporated in a progressively more precise interpretation.

At the present state of development, it is not possible to incorporate the acoustic information in the real-time inversion because picking of reflectors and determining their depths is not automated. Such refinements can be added on re-interpretation after the survey.

The apparent resistivities expected for the models of Table 4 are calculated for the both constant array, and are presented in detail in Appendix D.

4.2 MODELS SELECTED FOR SIMULATOR TRIALS

Once it is established that the simulator network provides reasonable match to the models used as starting points, then it is reasonable to assume that the theoretical calculations will provide an adequate indication of the detectability of other models. The three models chosen, based on the 1985 survey results, were models 1A,1B, and 2B (Table 4). These models were wired into the simulator resistance network so that model 1B was represented by switch position 1, model 2B

by switch positions 6, and model 1A by switch position 11. The intermediate switch position were used to provide a smooth transition between the models, as this is usually the case in the Beaufort Sea. The complete set of simulated data output is included in the map folder as simulator line T4. The simulator line starts with model 1B (Table 4) and varies through model 2B (Table 4) to model 1A (Table 4). Finally, the switch positions are moved slowly back to model 1B.

In looking at the results of line T4, we will refer to the apparent resistivities by their fiducial number. The fiducial numbers run along the top of the section.

Model 1B is represented by the interpreted resistivities at Fiducials 2 and 108. Model 2B is represented by Fiducials 26 and 78, and Model 1A by Fiducial 52.

It is reassuring to note that there is good agreement between the two interpretations for model 1B,(Fiducials 2 and 106) and for model 2B (Fiducials 26 and 52). Hence the inversion has indeed led back to essentially the original model in each case. The interpreted resistivity of the upper layer repeats within about one and half percent and surprisingly, the resistivity of the deepest layer repeats exactly. The most poorly determined layer is the conductive (saline) middle layer, whose resistivity is interpreted to only within about seven percent.

Note that the resistivities presented on the simulated data set (T4) did not match exactly the model resistivities presented on Table 4. This occurred because the current supplied by the simulation network was incorrect by

approximately ten percent. Since it is a constant difference, it does not affect the conclusions reached for the simulated trial.

In general, resistivity interpretations provide resistivities to a precision of only a few percent. However, the experience in the Beaufort Sea was that with slowly varying apparent resistivities, the repeatability of estimates of resistivity for near surface materials was within two to five percent. The variation in interpreted resistivity values as a function of grain size was in the order of forty percent, and thus well beyond the likely error of interpretation.

5.0 FIELD TRIALS OKANAGAN LAKE

The test area was chosen because it was the nearest body of water of sufficient size which was likely to be navigable during the winter time. The field trials were carried from February 15, to February 19, 1987.

5.1 TEST AREA

Okanagan Lake is a long lake which runs approximately north-south through the central part of B.C. The lake is typically 5 km wide and extends over one hundred kilometres from Penticton in the south to Vernon in the north. The test area was situated at Kelowna, B.C. Figure 10 is a location map that shows the approximate area of the lake in which the trials were carried out and the approximate location of the lines for which the data is included in this report.

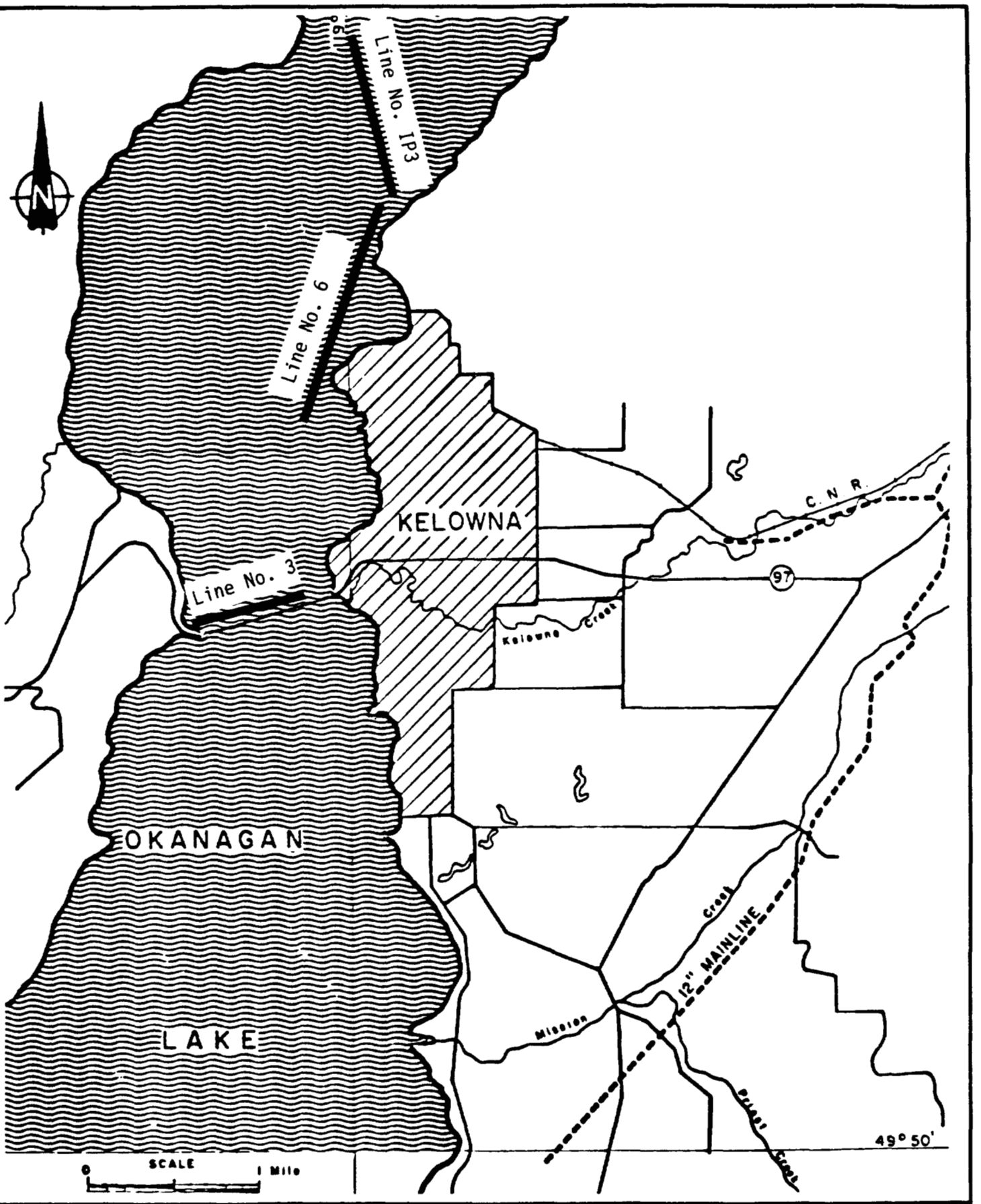

HARDY ASSOCIATES (1978) LTD.
CONSULTING ENGINEERING & PROFESSIONAL SERVICES

Supply And Services Canada
Real-Time Marine Resistivity System
Figure 10 - Location Map, Okanagan Lake

HT09 - 79/05

In the deeper parts of Okanagan Lake, the water depth is up to 300 m. The depth sounder operated with the MICRO-WIP system has a useable water depth of 120 m. This depth was exceeded several times during the trials. In the neighbourhood of Kelowna, there are significant areas where water depths ranged from 4 to 8 m and the bottom was relatively smooth. It was felt that the deeper water would allow an assessment of the noise level of the system in a uniform medium and the shallow areas would represent operating conditions which are similar those expected in the Beaufort Sea. Water resistivities are approximately 30 times greater than those of the Beaufort Sea. By the same token however, sub-bottom resistivities are also 30 times higher; the contrast between water and bottom is therefore reasonably similar to that to be expected in the Beaufort Sea.

Very little is known about the unconsolidated deposits in Okanagan Lake. However, Nasmith (1981), describes the surficial geology of sediments in the neighbourhood of the lake. From Nasmith's description, it appears that the sediments underlying the shallow portions of the test area are deltaic deposits derived from the mixed fine and coarse sediments lying above Kelowna. Figure 11 is a typical surficial geological section taken from Nasmith showing the source materials for the Kelowna delta.

Within the test area, two construction projects have been undertaken in the past. The first is the construction of the famous floating bridge in Okanagan Lake and the second is the laying of a pipe line across the lake. While the results of geotechnical investigations are available, the drilling failed to secure cores to depths greater than one metre, and thus

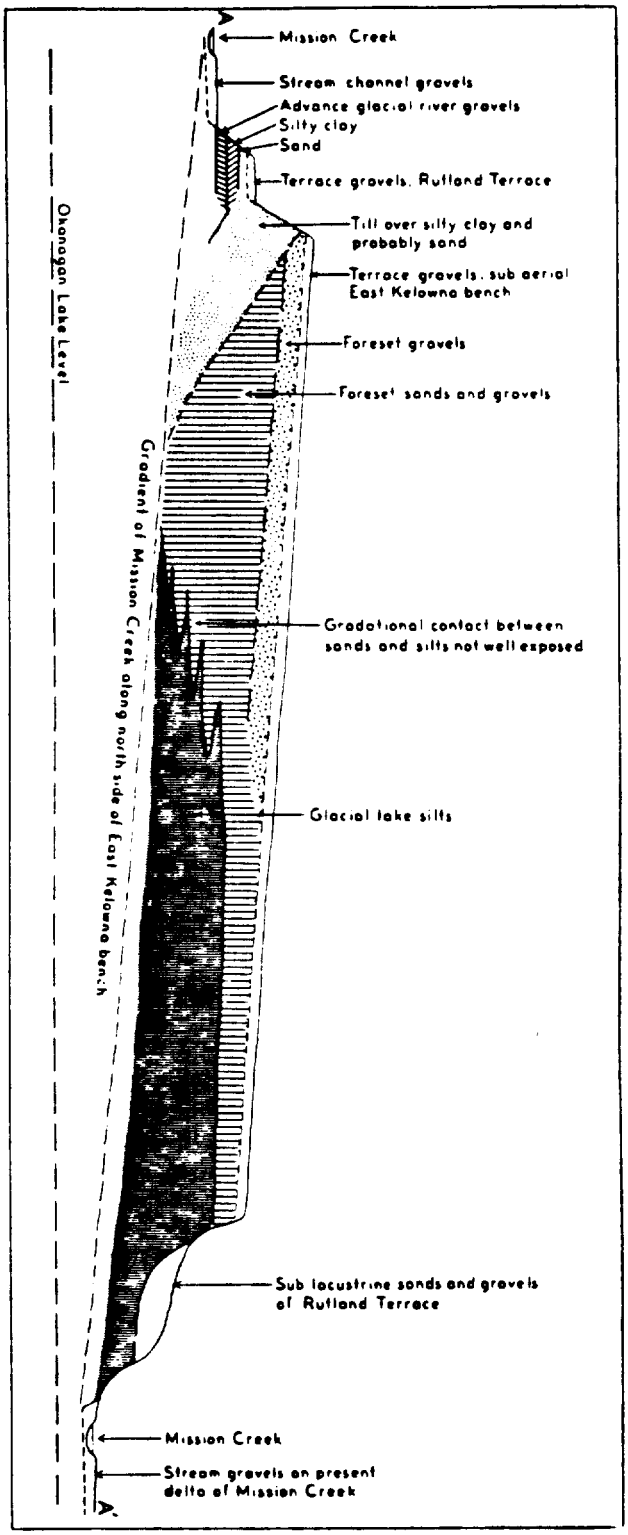

Hardy BBT Limited
CONSULTING ENGINEERING & PROFESSIONAL SERVICES

Supply And Services Canada
Real-Time Marine Resistivity System
Figure 11 - Geological Section

little is known about the sediments at depth. From the on-shore section (Figure 11), it appears that the shallower areas are predominantly by fine grained silts and clays while granular areas are exposed on the slopes on the edges of shallow areas.

The following description of the bedrock geology of Okanagan Lake is based on the summary prepared by Tipper et al, (1981). The lake is underlain by a conjugate set of faults. In the southern part of the lake, a major north-south fault separates plutonic granodiorites of Jurassic age on the west bank from Paleozoic gneisses on the east bank.

In the central part of the lake, this fault is dextrally offset by an east-west fault passing south of Kelowna. The Lake itself, offsets to the east along the course of this fault. North of the east-west fault, the north-south fault continues northward just east of Okanagan Lake.

In the northern part of the lake, the rocks exposed on both shores are intermediate to acidic volcanic flows of upper Cretaceous age which probably overly the older rocks exposed to the south.

Rocks exposed on shore in the neighbourhood of this survey showed intense shearing. The rocks under the lake are probably even more strongly sheared, and water-saturated as well. They would therefore be expected to have resistivities of a few hundred ohm-metres. It is reasonable to assume that the bedrock resistivities would be in the same ratio to the

shallow sub-bottom resistivities as would permafrost resistivities in the southern Beaufort Sea to the overlying sediments.

In general, while the geology of Okanagan Lake is significantly different from that to be expected in the Beaufort Sea, it appears reasonable that the resistivity contrasts from water to sub-bottom sediments to deeper sub-bottom materials should be in the same general proportions as those in the Beaufort Sea. Because resistivity interpretations deal primarily with contrasts between resistivities of layers rather than with absolute values, it is reasonable to use this area as a test site for assessing the performance of a system designed for the Beaufort Sea. The major difference would be that in the Beaufort Sea, to obtain readings at the same level of confidence, much higher transmitter currents would be required. It is probable that currents would have to be approximately 30 times higher to compensate for the approximately 30 times lower general resistivities. In the event, the survey on Okanagan Lake was carried out with 0.5 amperes while measurements in 1985 in the Beaufort Sea used 15 amperes. Thus it appears that the ratio of currents used in the two settings is approximately in proportion to the ratio of the resistivities to be observed.

5.2 SURVEY LOGISTICS

The primary purpose of the field trials was to establish that the modified data processing system could provide inversion of resistivity data in real-time. The field survey was thus broken into two parts. The first was to establish the noise levels in the system and demonstrate that these are low enough

not to interfere with the measurements. The second was to demonstrate that the inversion technique provided answers within the real-time constraints of operating the survey.

Because of budgetary limits, a minimum set of equipment was deployed for the survey. The minimum equipment included the MICRO-WIP and an analogue-recording depth sounder with a digital output.

The budget constraints prevented the deployment of the sub-bottom profiler and magnetometer which normally would be part of this survey system in the field. Furthermore, because no exact geological control was available, it appeared unnecessary to employ the precise navigation system which normally would be part of the survey. This was particularly significant because a large part of the daily costs of operating the system is attributed to the utilization of the microwave ranging system to get positional information. Thus the "bare bones" nature of this survey was considered to demonstrate the system capabilities. Had geological control and a more flexible budget been available, consideration would have been given to a full dress survey.

The survey equipment and streamers were transported from Calgary to Kelowna by road. An eight metre aluminum boat, Figure 13, was chartered in Kelowna for the survey. The survey crew consisted of A. Kay, F. Maxwell, M. Mitchell, and W.J. Scott. R.J. Gowan, Indian and Northern Affairs Canada was present for the final two days of the trial.

As the survey vessel was kept at the Kelowna Yacht Club, the crew stayed at the Siesta Motel in Kelowna. Mobilization in

Calgary occurred on February 15, 1987. On February 16, the system was installed on the survey vessel and the preliminary trials were taken. The final debugging of the trials took place on Tuesday, February 17, 1987. R.J. Gowan joined the crew on the afternoon of the 17th and initial measurements were carried out. On Wednesday, February 18, 1987, a full day of simulated survey was carried out. On Thursday, 19th, W.J. Scott and R.J. Gowan flew back to Calgary while the other crew members returned by road with the equipment.

5.3 SURVEY PERFORMANCE

Figure 12, shows the configuration of the MICRO-WIP as set up in the vessel, and Figure 13 shows the survey vessel. The primary difference between the test configuration and the survey configuration was that the simulator and resistance network were replaced with cables to connect the transmitter and receiver to electrodes in the water. The depth sounder was deployed in order to provide water-depth information as part of the input to the inversion process.

The MICRO-WIP system performed extremely well on trials with only minor modifications necessary to provide smooth functioning. Minor alterations in the grounding and shielding arrangement between the acquisition system and the transmitter system and the controller box were necessary to provide adequate stability in the transmitter control system. The newly delivered streamer (Figure 14), was wired in the reverse of the order originally specified and modifications to the extension cord coupling the streamer to the system were necessary. The Huntec Lopo transmitter used in this survey (Figure 14), produces an extremely noisy wave form. A passive

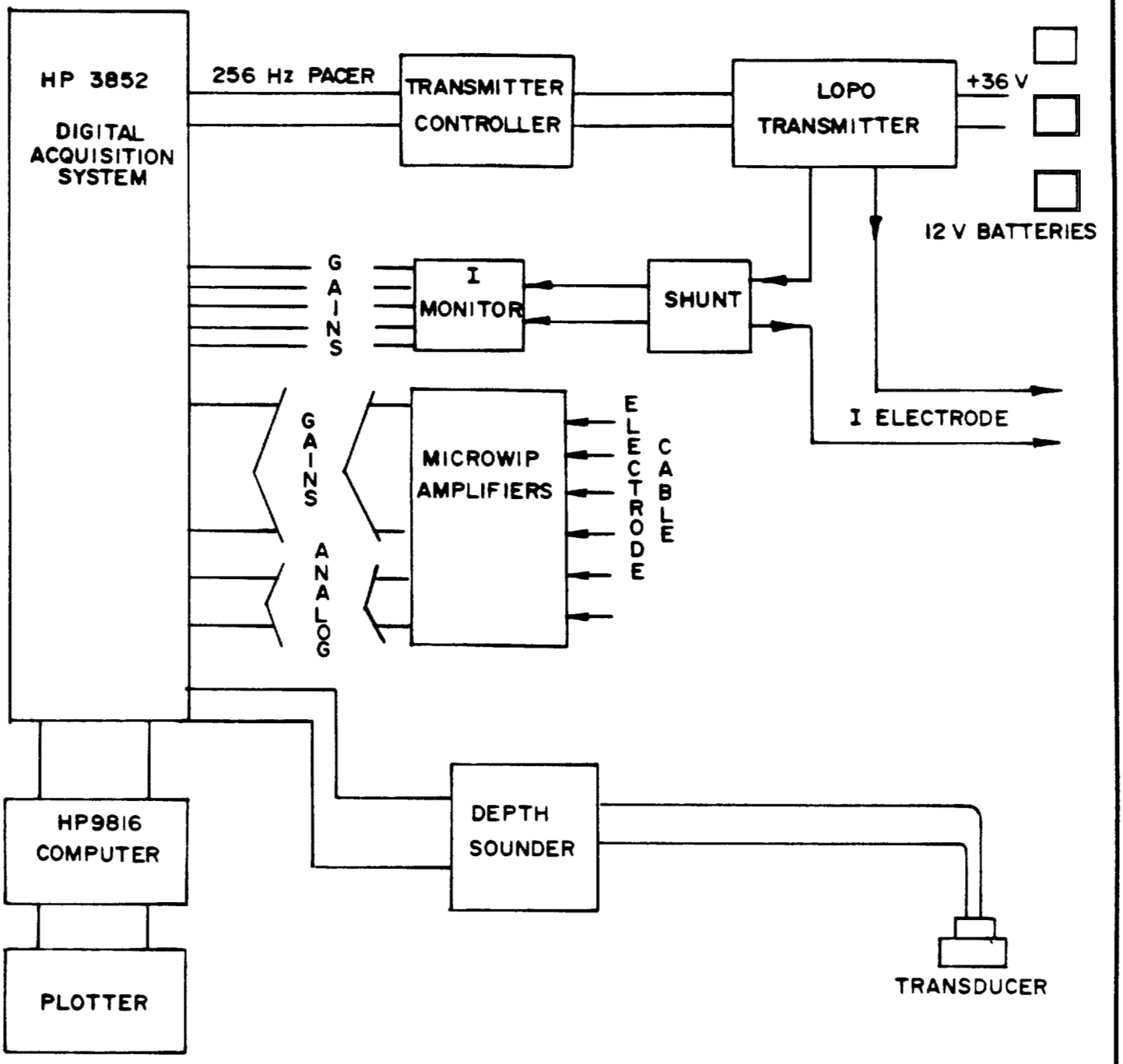

Hardy BBT Limited

Supply And Services Canada
Real-Time Marine Resistivity System
Figure 12 - System Diagram, Field Trial

HTB3-82/03

Supply and Services Canada
Real-Time Marine Resistivity System
Figure 13 - Survey Vessel in Okanagan Lake

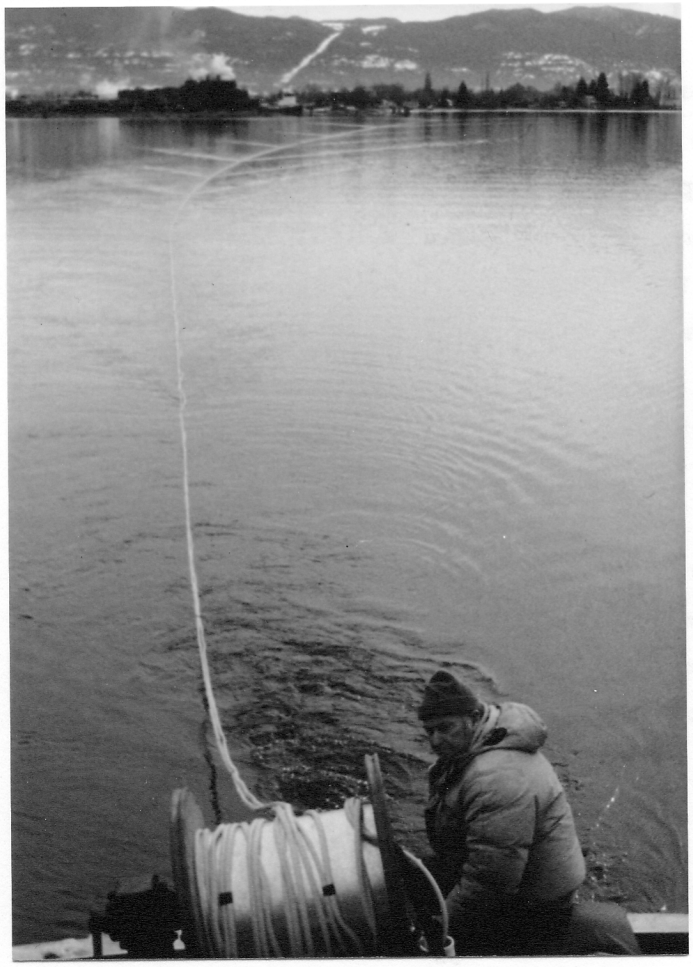

Supply and Services Canada
Real-Time Marine Resistivity System
Figure 14 - Logarithmic Streamer Deployed

filter device was assembled on the boat and applied to the output of the transmitter. The filtered wave form was essentially the same in character and frequency content as that which is normally obtained from the high-powered system used in the Beaufort Sea.

Since the navigation system was not used in the trial, it was not possible to calculate distances or locations, but approximately ten line kilometers were surveyed during roughly eight hours of survey time. An anticipated production rate of from ten to twenty line kilometres is expected during a commercial survey in a twelve (hour) day. The results of the trial surveys are included in the map folder as 3 and 6, and their approximate positions are shown in Figure 10.

The eight metre survey vessel used in the trials provided sufficient cabin and deck space to operate a normal survey. Figure 16 shows the MICRO-WIP amplifiers set-up in the cabin. Figure 17 shows the computer, data acquisition system and recording depth sounder. Note the sounding curve displayed on the computer monitor. Figure 18 shows the plotter which produced real-time interpreted sections. Even with the addition of the high powered transmitter and the navigational and sub-bottom profiler system, the survey vessel would have been adequate with minor modifications to the interior layout. It is recognized that offshore survey in the Beaufort Sea would not be performed in this vessel without a mothership because of the requirements of sea worthiness, although surveys in coastal areas would be feasible. Furthermore, any long-term survey would require crew accommodations on the vessel.

Supply and Services Canada
Real-Time Marine Resistivity System
Figure 15 - Huntec Lopo Transmitter with Battery

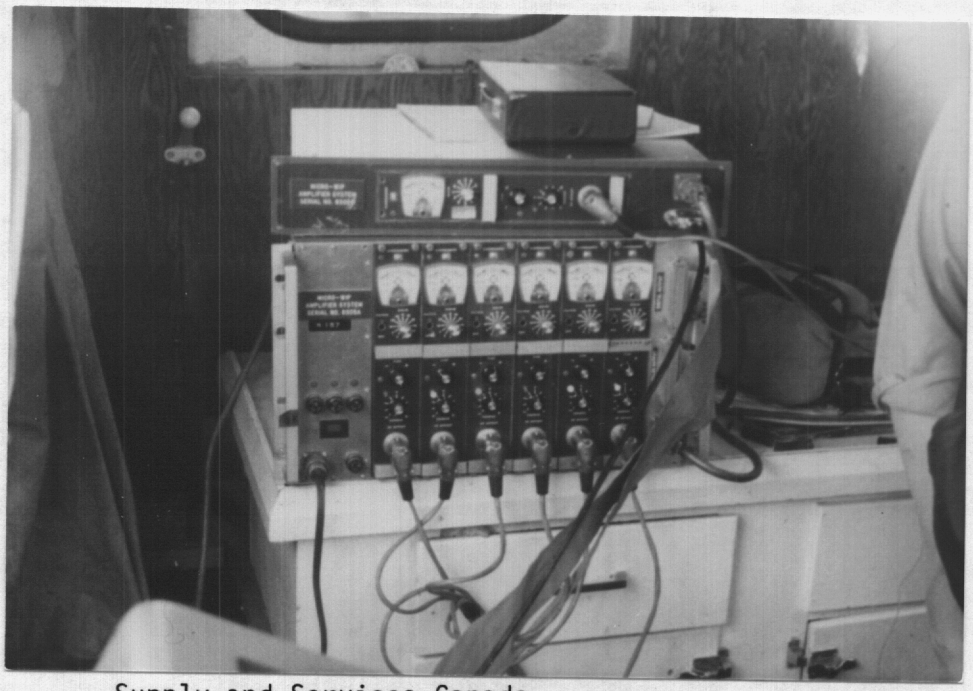

Supply and Services Canada
Real-Time Marine Resistivity System
Figure 16 - MICRO-WIP Amplifiers in Cabin

Supply and Services Canada
Real-Time Marine Resistivity System
Figure 17 - Computer, Data Acquisition System and Recording Depth Sounder in Cabin

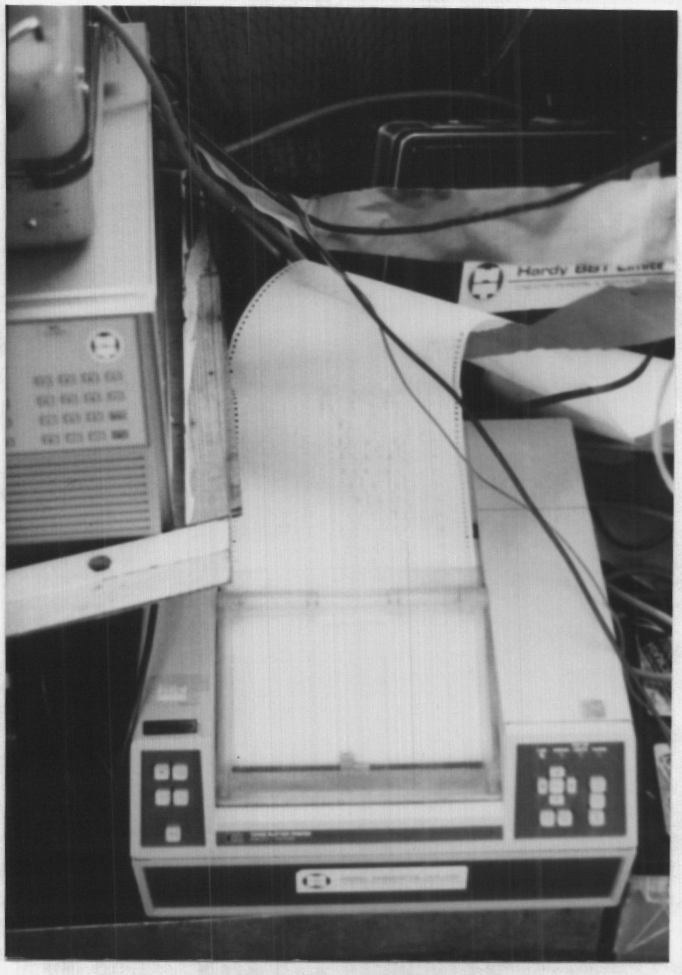

Supply and Services Canada
Real-Time Marine Resistivity System
Figure 18 - Plotter in Cabin

For normal stand-alone surveys, a technical crew of three would be required. One of these would operate the sub-bottom profiler, which in our experience requires the full-time attention of one person. The second would operate the MICRO-WIP system and controlling computer. The third would operate the navigation system and monitor the performance of the magnetometer (if used). The three jobs would be rotated during the survey day, as the navigation job is somewhat less demanding than the other two.

Installation of the MICRO-WIP system could be undertaken within a day of boarding the survey vessel. However, in any vessel, it should be recognized that problems of grounding and noise levels will always be present and will require some time at the beginning of the survey for complete resolution. Furthermore, the time required to complete an installation goes up with the square of the number of systems being installed.

The operation of the system in the Okanagan Lake trials followed the same procedure as would be observed in actual field survey. At the beginning of the day, the streamer was deployed. Because the electrodes must be kept moist, they are normally stored separately from the streamer and are installed on the streamer as it is deployed. As the connection between electrode and streamer is made, silicon grease is used to waterproof the connection.

Once the streamer is deployed and the vessel is approaching the desired survey line, program DOWNLOAD2 is loaded and the data acquisition system turns on the transmitter. The operator then adjusts the current level to the maximum useable value

and regulates the gains of the six channels of the receiver to ensure that the signal provided to the data acquisition system is sufficiently strong to be digitized. Once transmitter current and receiver gains are established, then the main process of data acquisition is begun. In the 1985 version of the MICRO-WIP, the incoming waveforms were digitized and written on tape and therefore constituted the raw data. In the present system, however, the digitization is automatic and the apparent resistivities are calculated as part of the acquisition process. Thus the raw data consists of the six apparent resistivities associated with the six dipoles. This data is normally written on disk. Line IP3 (Pocket) shows a plot of the pseudosections of apparent resistivity derived in the field and plotted in real-time. The northwest part of Line IP3 is in very deep water and represents essentially the noise level of the system in a homogeneous medium. The southeast end of the line is in very shallow water (4-8 m) and represents actual resistivities of water and sub-bottom materials as calculated in real-time. These resistivities, and chargeabilities in mineral surveys, constitute the raw data which is recorded with the system in its present configuration. During resistivity surveys for identification of granular materials, the apparent resistivities are inverted in terms of a layered model. The data from lines 3 and 6 (Pocket) show the results of this inversion in real-time.

One inversion is carried out for every thirty-two seconds worth of data. Thus the lateral resolution of the system is dependent on the survey speed. At a survey speed of one kilometre per hour, each sounding represents a lateral translation of approximately nine metres. At a survey speed of one knot, each reading represents a distance of approximately

sixteen metres and at a survey speed of three knots, each sounding represents a distance of fifty metres. Thus, the choice of survey speed depends upon the the lateral resolution that is required in near surface features. As vessel speed increases, so does the noise level, and a practical upper limit for resistivity surveying appears to be about three knots.

The volume of measurement which is represented by each of the apparent resistivities depends upon the spacing between the transmitter and receiver pair which are used for the calculation. Thus the volume involved in measurement of shallow resistivities is quite small. A movement of fifty metres probably involves significant variation laterally in terms of the shallow measurements. However, for permafrost at depths of fifty to one hundred metres, separation between the transmitter and the farthest spaced dipole is of the order of two hundred metres and thus the lateral translation does not imply a major replacement of the volume of measurement by new material. The desired depth and resolution of the target therefore will have some influence on the selected speed as it appears feasible to make reliable resistivity measurements at the speeds of up to three knots.

There is some evidence (Olhoeft, 1975) that frozen clays give rise to small induced polarization affects. If it appears necessary to distinguish between frozen granular materials and frozen clays, the IP effect may be a useful indicator. The calculation of the IP effect is given in detail in the papers of Appendix C of this report. The IP effect is more noise-sensitive than the resistivity. A survey in which IP affects are measured would probably have to be conducted at a

significantly lower speed than one conducted solely for resistivity measurements. It appears that realistic measurements of IP affects can only be made at survey speeds of one knot or less. The reliability of IP measurements goes up as the survey speed goes down. Thus in a survey for granular materials in the Beaufort Sea, it is likely that IP affects would not be measured unless required to distinguish the subtle effects associated with the frozen fine-grain sediments. In such a case, the original reconnaissance could be carried out at the normal survey speed and then a certain amount of detail work undertaken at slower speeds to provide the required information.

5.4 SURVEY RESULTS

The results of the survey lines are enclosed in the map pocket in the back of the report. It should be emphasized that without control, it is difficult to come to an absolute determination of the accuracy of the interpretations. However, the resistivity values and thicknesses determined for the sediments appear to be consistent with those derived from the on-shore geological model (Figure 11). Resistivities range from sixty to several hundred ohm-metres and the resistivity of near surface materials appears somewhat higher in areas where granular material would be expected. It should be emphasized that geologic interpretation on the basis of these results is very difficult because no control exists.

5.5 RECOMMENDATIONS FOR FUTURE WORK

Before the utility of the modified MICRO-WIP system for granular prospecting is fully demonstrated, it is considered necessary to carry out a demonstration survey in the Beaufort Sea in an area where adequate drill control is available and where bottom sediments contain both fine and coarse grained materials. The test area would ideally have some shallow sub-bottom permafrost as well as some deeper relic permafrost within the range of survey of this system. Since a considerable amount of work has been carried out in the Beaufort Sea by the commercial operators in search of granular material, it appears likely that the necessary control could be assembled from the industry.

A demonstration survey would not necessarily be laid out to provide a detailed map of the distribution of granular material within the area. It would rather be designed to obtain sub-bottom information in the areas where control is adequate to demonstrate the capability of the system.

Two approaches could be taken to carrying out such a demonstration of capability. In the first approach, performance of the survey would depend on finding a survey vessel carrying out other work in the same area and adding a marine resistivity survey system to the complement of equipment on board. Provided some assistance were available for streaming and recovering the streamer, such an operation could be carried out by a single operator with technician backups standing by somewhere in the area in case of electrical and mechanical problems.

The second approach to demonstrating the capabilities of the new MICRO-WIP system would be to undertake a sole-purpose survey in an area with adequate control. Such an approach would obviously be considerably more expensive but would not depend on the fortuitous presence of a survey vessel in the appropriate area at an appropriate time. For a stand alone survey, a total number of three technical people would be required. Depending upon the size of the survey vessel, an additional one or two nautical crew members would be required. Provided that an appropriate test area could be located within reasonable striking distance of shore, a relatively small survey vessel could be used for a survey of this sort. A survey crew would then base themselves at a shore camp in the immediate area of the proving grounds. They would go out by day to obtain the necessary geophysical information to demonstrate the system capability.

No matter which approach is taken, it appears extremely desirable that a demonstration of capability be undertaken for the system in advance of a major call for its employment. From such a demonstration of capability would come an understanding of the strengths of the system, the likely production to be obtained, and the limitation on its application. Planning of a survey at a later date for which ground truthing would be obtained directly after the survey would be much aided if access to such a demonstration of capabilities were available.

6.0 SUMMARY

The objective of this program was to design and produce a real-time marine resistivity interpretation system for

surveying in offshore environments. The results obtained demonstrated the successfulness of this project, both in terms of meeting the objectives and also being within the budget and scheduling estimates. This system is now available for routine surveying in offshore environments to map granular deposits and permafrost with a real-time resistivity interpretation capability. All that remains is a small survey to demonstrate the capability of the system in the environment of interest.

Respectfully Submitted:

Hardy BBT Limited

Per:

A. Kay, M.Sc., P.Geoph.,
Senior Geophysicist

Per:

Frank K. Maxwell

for W.J. Scott, Ph.D., P.Eng., P.Geoph.,
Chief Geophysicist

0,70

REFERENCES

Boulos, F.K., 1972, Electrical Sounding on the Water-Surface at Khor Kundi-El-Bahari in Egypt. Geophysical Prospecting, Vol. 20, p. 304 - 316.

Dyck, A.V., Scott, W.J., and Lobach, J., 1983, Waterborne Resistivity/Induced Polarization Survey of Collins Bay, Wollaston Lake, in Uranium Exploration in Athabasca Basin, Sask. Canada. ed. E.M. Cameron, Geol. Survey Can. Paper 82-11, p 281-289.

Lobach, J. and Scott, W.J., 1979, A System for Resistivity Surveying in Water: in National Research Council of Canada, Tech. Man. 128, p 35-45.

Nasmith, H., 1981, Late Glacial History and Surficial Deposits of the Okanagan Valley, British Columbia. Brit. Col Min. Energy, Mine and Resources, Bull. 46.

Nebrija, E.L., Young, C.T., Meyer, R.P., and Moore, J.R., 1976, Electrical Prospecting for Copper Veins in Shallow Water. Proc. Eighth Offshore Technology conference, Houston, May 1976, p. 319-340.

Olhoeft, G.R., 1975, The Electrical Properties of Permafrost, Unpublished Ph.D. Thesis, University of Toronto, 172 p.

Schlumberger, C., Schlumberger, M., and Leonardon, E.G., 1934, Electrical Exploration of Water Covered Areas. A.I.M.E. Geoph. Prosp.

Scott, W.J., 1975, Preliminary Experiments in Marine Resistivity Near Tuktoyaktuk, District of Mackenzie Geol. Survey Can., Paper 75-1, Part A, p. 141-145.

Scott, W.J., Sellman, P.V., and Hunter, J.A., 1979, Geophysics in the Study of Permafrost: Review Paper, Proc. Third Int. Conf. on Permafrost, Vol. 2, National Research Council of Canada, p. 93-115.

Scott, W.J., Laing, J.S., and Botha, W.J., 1983, Waterborne Resistivity/Induced Polarization Survey in Prudhoe Bay. Proc. Fifteenth Offshore Tech. Conf., Houston, May 1983, p. 227-230.

Scott, W.J., and Maxwell, F.K., 1987, Marine Resistivity Survey for Granular Materials, Beaufort Sea. (Submitted to the Journal of the Canadian Society of Exploration Geophysicists.)

Telford, W.M., Geldart, L.P., Sheriff, R.E, and Keys, D.A, 1976, Applied Geophysics, Cambridge University Press, 860 p.

Tipper, H.W., Woodsworth, G.J., and Gabrielse, H., 1981, Tectonic Assemblage Map of the Canadian Cordillera, Geol. Survey Can. Map 1505 A.

Whiteley, R.G., 1974, Design and preliminary Testing of a Continuous Offshore Resistivity Method. Bull. Aust. Soc. Explor. Geophysics, V.5, No. 1, p. 9-13.

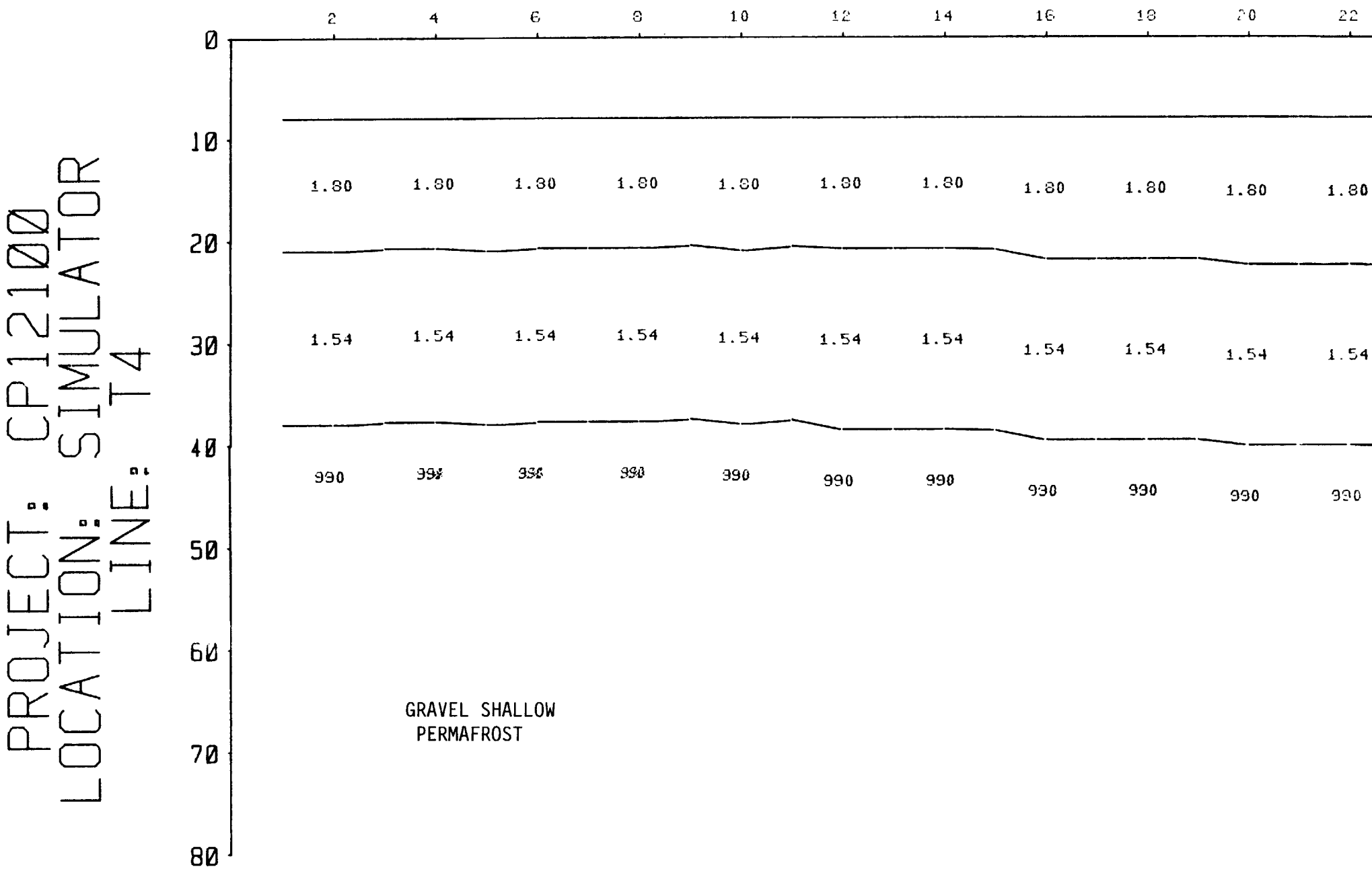
PROJECT: CP12100
LOCATION: SIMULATOR
LINE: T4
2
4
6
8
10
12
14
16
18
20
22
0
10
20
30
40
50
60
70
80
1.80
1.54
990
GRAVEL SHALLOW
PERMAFROST

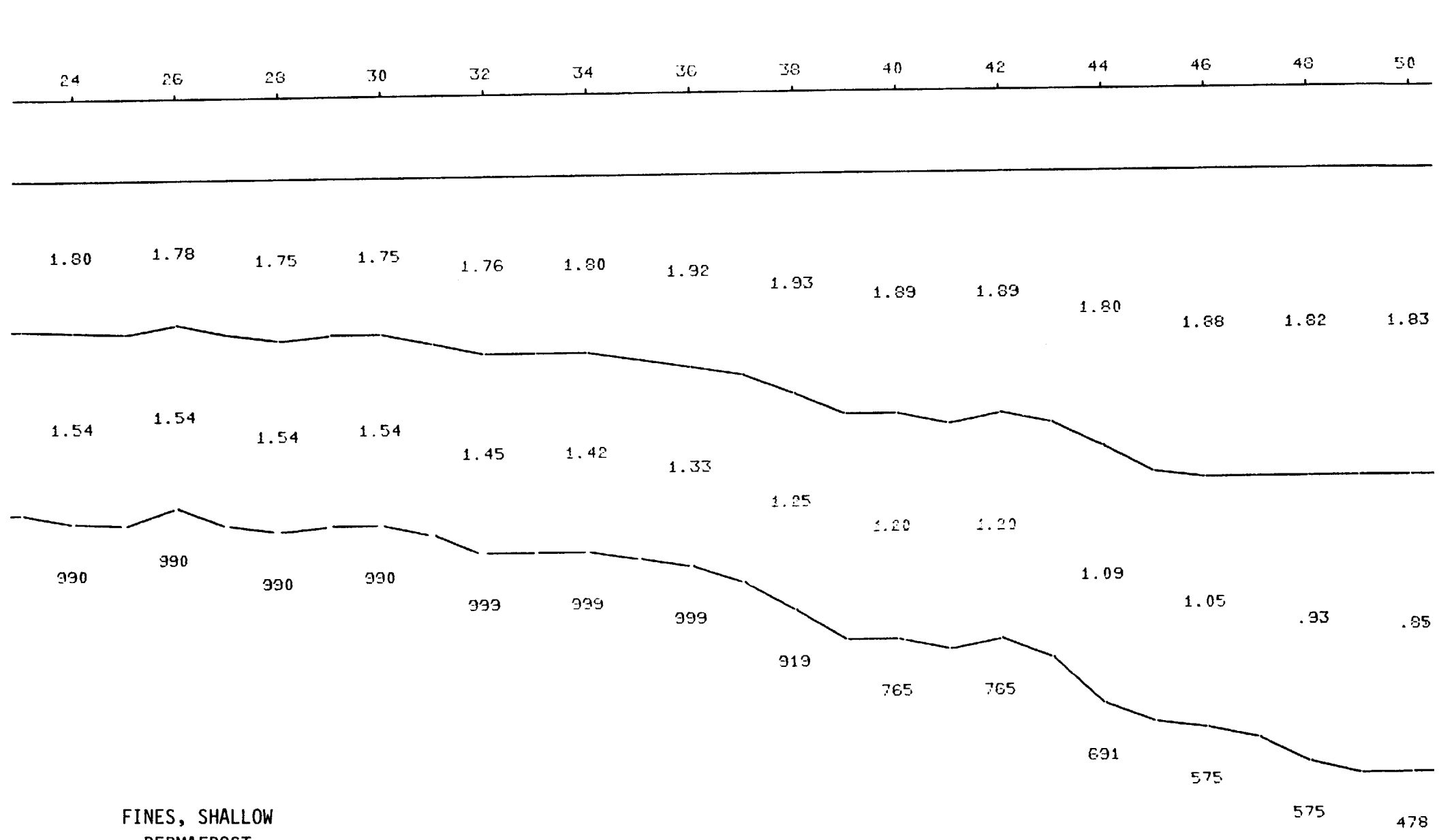

FINES, SHALLOW
PERMAFROST

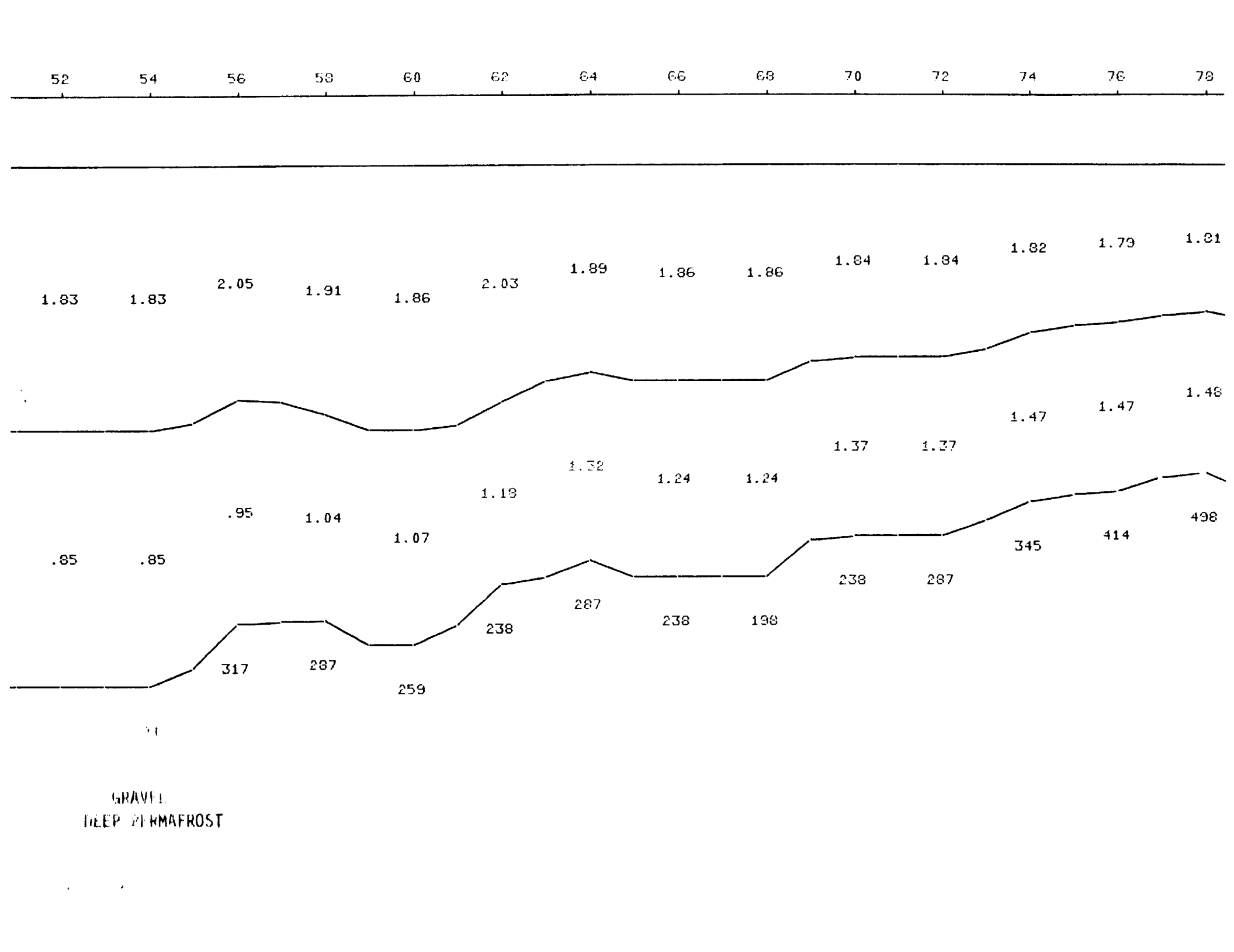
52
54
56
58
60
62
64
66
68
70
72
74
76
78
1.83
1.83
2.05
1.91
1.86
2.03
1.89
1.86
1.86
1.84
1.84
1.82
1.79
1.81
1.48
1.47
1.47
1.37
1.37
1.32
1.24
1.24
1.18
.95
1.04
1.07
.85
.85
498
414
345
238
287
287
238
238
198
317
287
259
GRAVEL
DEEP PERMAFROST

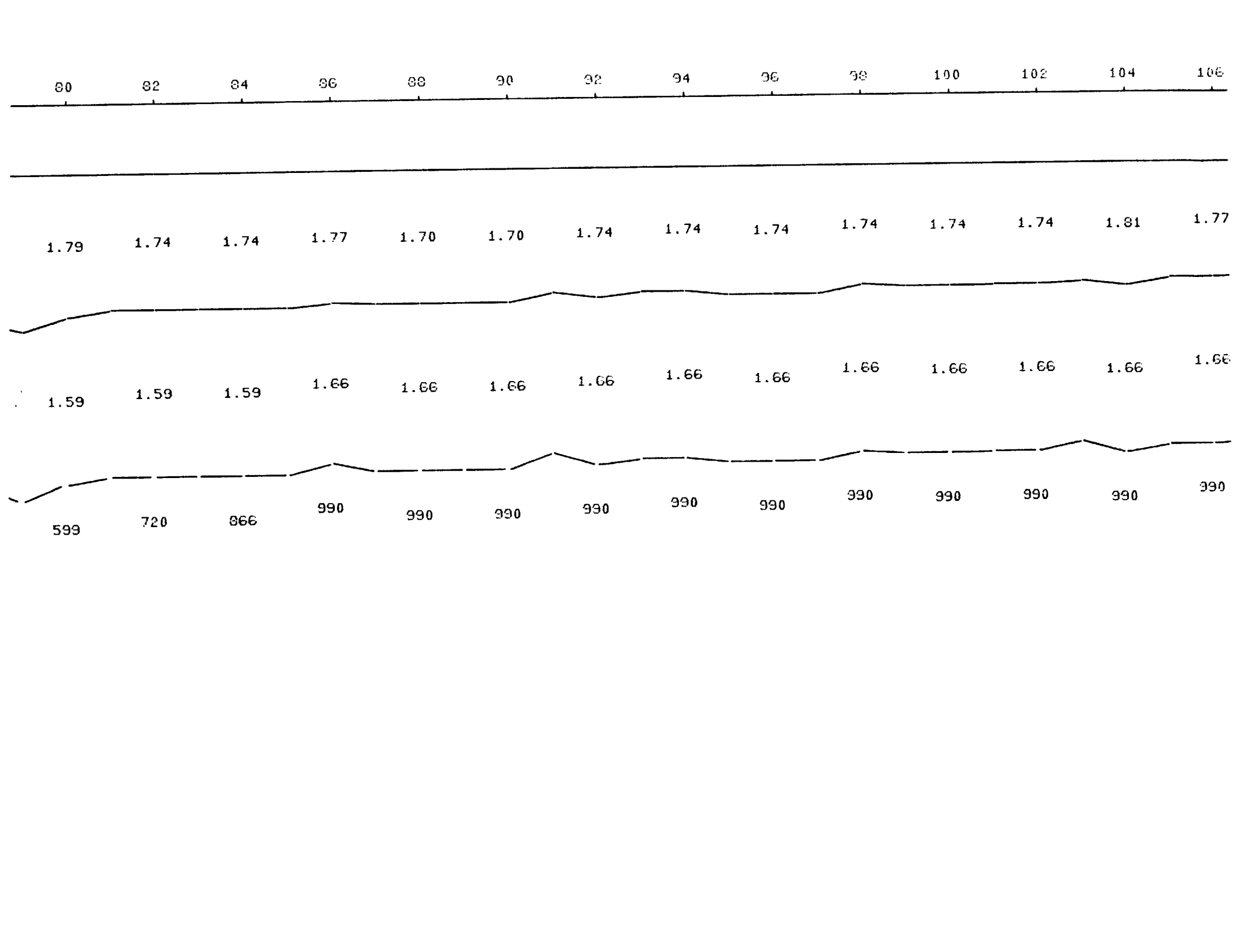
80 82 84 86 88 90 92 94 96 98 100 102 104 106
1.79 1.74 1.74 1.77 1.70 1.70 1.74 1.74 1.74 1.74 1.74 1.74 1.81 1.77
1.59 1.59 1.59 1.66 1.66 1.66 1.66 1.66 1.66 1.66 1.66 1.66 1.66 1.66
599 720 866 990 990 990 990 990 990 990 990 990 990 990

108

1.77

1.66

990

LINE: IP3

RESISTIVITY (ohm-m)

									1		2		3		4		5		6		7	
					63.3		62.7		62.7		62.7		62.7		62.8		62.8		62.8		62.7	
				63.8		63.2		63.3		63.2		63.1		63.2		63		63		63		[illegible]
			62.7		62.1		61.9		61.8		61.7		61.6		61.3		61.1		60.9		60.8	
		64.9		64.3		64.4		63.9		63.5		63.2		62.5		62.1		61.7		61.4		61.[illegible]
	60.3		59.4		61.2		59.2		60		59.1		58.8		58.2		58		57.2		56.6	
62		61.1		61.1		59.5		60		58.3		56.9		47.6		58.6		56.8		56.9		[illegible]

CHARGEABILITY (mV/V)

									1		2		3		4		5		6		7	
					-.01		-.02		-.02		-.01		-.01		-.01		0		0		0	
				0		.03		.03		0		.01		.03		.01		.02		.02		[illegible]
			.03		.04		-.03		0		-.01		-.01		-.01		.01		-.02		-.02	
		-.03		-.06		-.03		.11		0		.07		-.04		-.01		.05		-.15		[illegible]
	.03		-.01		-.08		-.02		.05		-.15		-.17		-.05		0		-.06		.01	
.22		.17		.01		.42		.38		.22		.17		-5.52		.08		-.23		.34		[illegible]

62.8 62.7 62.8 62.8 62.8 62.9 62.9 62.9 62.9 62.9 63 62.9

63 63.1 63.2 63.2 63.3 63.3 63.3 63.3 63 62.8 62.3

60.8 60.9 61.1 61.3 61.3 61.5 61.3 60.9 60.5 59.6 58.6

61.4 61.8 61.6 62.1 62 61.9 61.3 60.5 59.3 57.8

56.7 56.5 56.9 56.5 56.3 56.6 56.1 55.2 54 52.6

55.6 56.6 56.3 56 55.3 55 54.6 52.5 51.1

-.01 -.01 0 -.01 -.01 -.01 -.01 -.01 0 -.01 0 -.01

.03 .01 .03 0 .03 .01 .01 0 .01 .01 .01

.03 0 0 .04 -.05 -.02 .01 -.04 0 -.02 0

.07 .06 -.01 .15 .03 .06 -.11 .03 -.05 -.01

.08 .14 .09 0 -.12 -.01 -.11 -.07 .05 .06

.39 .47 .33 -.03 .22 .05 .12 -.06 .07

APPENDIX "A"

Data Acquisition System

HP 3852S Data Acquisition and Control System

- System Software
- Command Storage
- BASIC Commands
- Reading Storage
- Expandable **RAM**
- Integrating DVM
- FET Multiplexer
- Relay Multiplexer
- High Speed DVM
- Digital **I/O**
- T/C Compensation
- Counter
- Analog Outputs
- Actuators
- General Purpose Switch

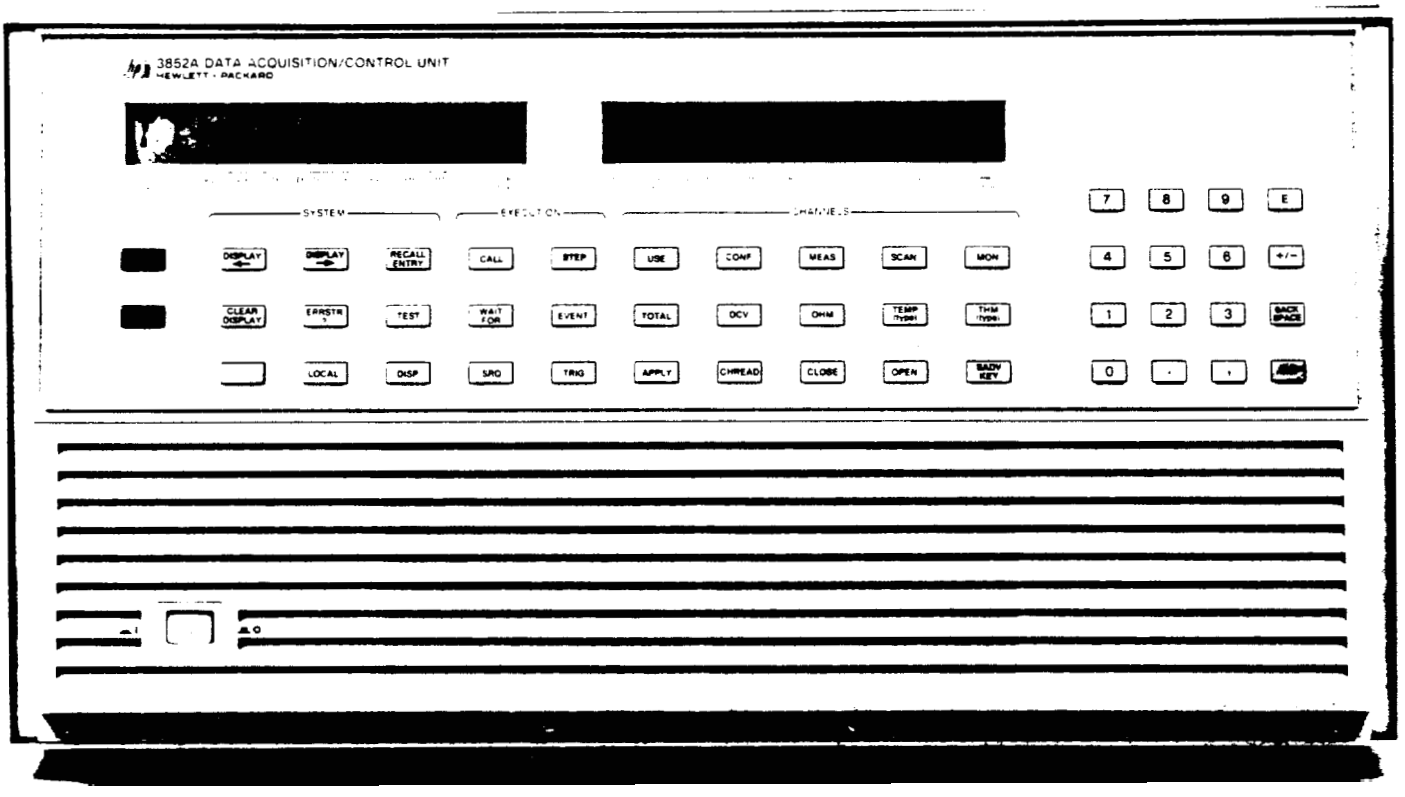

With the HP **3852S** Data Acquisition and Control System you get capable hardware plus system software to create a powerful data acquisition system that you can easily configure to your needs. With this system, you'll find that data acquisition and control **is** fast and easy. A full keyboard with two displays means easy checkout of system wiring. Plug-in voltmeters and input/output accessories with removable terminal modules for field wiring speed up system configuration. You'll have powerful system software for fast and easy start-up using a tool set of capabilities needed in data acquisition such as data analysis, presentation, distribution and archiving.

The **HP 3852S** Data Acquisition and Control System consists of an **HP 3852** mainframe, optional HP **3853** extenders, a selection of plug-in voltmeters, multiplexers and input/output accessories, an optional HP Series **200** or **300** computer and system software. **You** can choose any combination of these capabilities. The HP **3852** Data Acquisition and Control Unit has a full keyboard with displays, a power supply and a controller module built-in. Eight slots are available for plug-in accessories. If more slots are needed, add up to seven extenders with 10 slots per extender.

System Capabilities

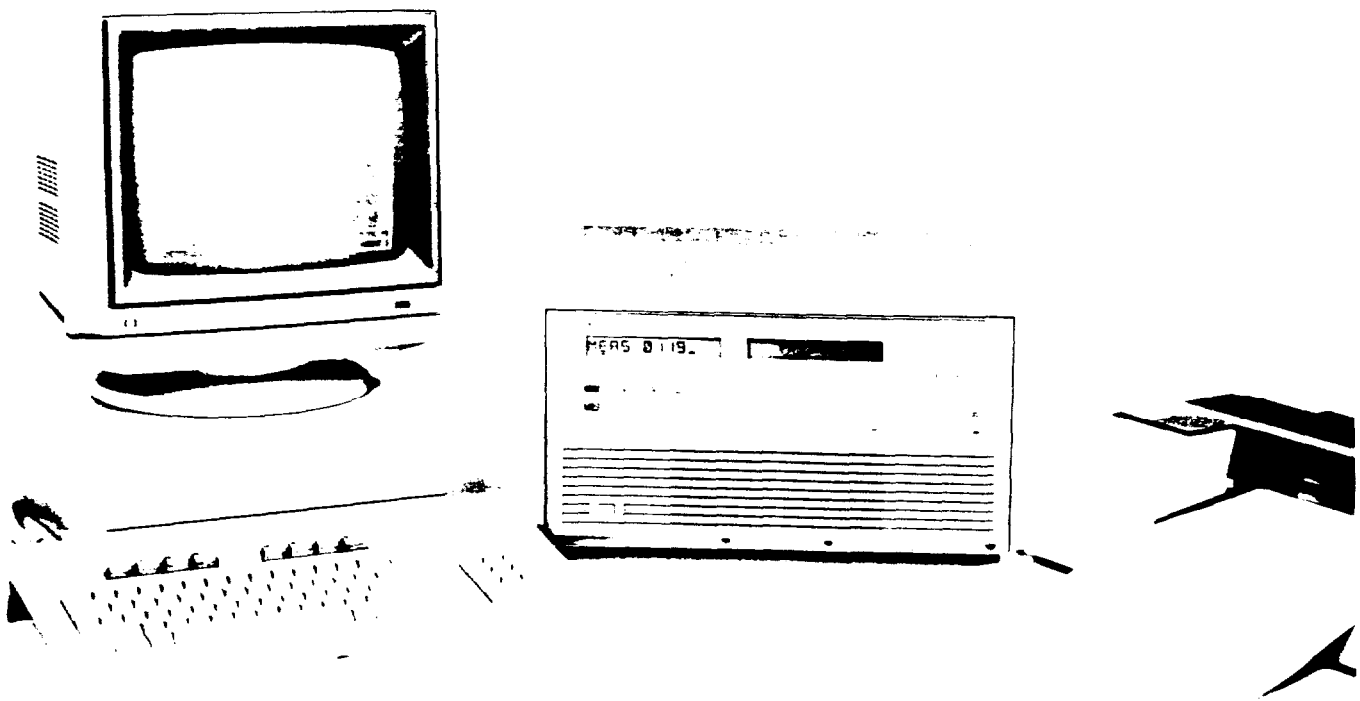

High Performance

You can use the **HP** 3852S to **perform accurate, low-level and noise-rejecting measurements as well as high speed measurements.** You can resolve 1 microvolt signals with the Integrating DVM and make scanned readings at up to 100,000 readings per second with the High Speed DVM. In a single card-cage product you can make a wide range of measurements. Both system voltmeters interface to transducers directly or through a variety of multiplexer accessories. The voltmeters have built-in current sources for measuring resistive transducers. You can even insert shunt resistors in multiplexer accessories and measure current.

Flexible Hardware Configuration

You can use the HP 3852S to **configure exactly the system you need.** The HP **3852S** consists of a HP 3852 Data Acquisition & Control Unit (mainframe). plus an HP 3853 extender if needed. Voltmeter and I/O plug-in accessories can be placed in any slot of the mainframe or extenders. If you need racks. both a 76.2 cm (30 inch) and a **142.24** cm *(56* inch) rack (48.26 cm **(19** inch) wide) are available. An HP Series 200/300 computer and system software for the Series 200/300 computer complete the system with easy-to-use but powerful tools for data acquisition.

Intelligent Computer Front End

Use the HP 3852 Data Acquisition and Control Unit with **any HP-IB (lEEE-488) computer.** While not a "stand-alone" instrument. it has considerable built-in intelligence which frees the computer to handle other tasks. This built-in intelligence increases the speed with which data is collected and decisions made. Download your user routines from the computer. Use the computer to call a routine or let one routine call another. A number of BASIC constructs such as FOR...NEXT, IF..THEN...ELSE and WHILE are built into the HP 3852 **as** are the capabilities for conversion **of** data to user units, transducer linearizations and execution of user stored routines. Limit and alarm capabilities are also included. Channel lists (of channels in random order) can be downloaded and scanned with a single powerful command. Data can be output over HP-IB immediately or stored for later transfer or processing. The HP 3852 can unpack any data stored in the "packed" mode prior to transferring the data over HP-IB to a computer.

System Clock and Pacer

In the HP 3852 Data Acquisition and Control Unit you have an accurate system clock and a programmable pacer. The clock is nonvolatile for four years with 1 millisecond resolution for time stamping data or for timing events. The system pacer gives you 0.25 microsecond resolution and can be used to initiate measurements. scans or events.

Expandable Memory

Store up to 1.000 readings in the standard HP 3852. Expand this memory by 256 kbytes or 1 Megabyte with an Extended Memory card. The Extended Memory card fits inside the controller module and does not use an I/O slot. Memory is used for storage of user routines as well as readings.

Powerful System Software

Use system software for the HP Series 200 or 300 controllers to get the system running quickly and easily. While you can program the HP 3852 mainframe with any HP-IB computer. many of your other tasks are aided by the System Software. These tasks are:

- **Configure the system**
- **Store the data**
- **Acquire high speed data**
- **Analyze the data**

- **Present displays**
- **Present real-time graphics**
- **Control a process**
- **Schedule a task**
- **Distribute Data**

System software runs on the following HP Series 200 and 300 controllers with or without Shared Resource Manager capabilities.

* **Model 216, 217, 236. 220, 310, 320**

Plug-In Accessories

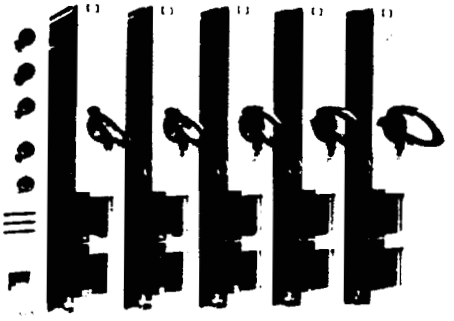

Choose from two digital multimeters to meet your application needs For applications requiring low level. accurate measurements in the presence of noise, the 5½ Digit Integrating DVM provides the solution. If you need speed. the 13 bit (12 bit plus sign). 100.000 readings per second DVM is the answer These DVMs can be used in any mainframe or extender slot. and multiple DVMs are allowed per cardcage.

5½ Digit Integrating Digital Multimeter

In the HP 44701A 5½ Digit Integrating Voltmeter you have **a complete instrument as a plug-in accessory.** It is guarded. single ended and Integrating for making accurate. low-level measurements in the presence of common mode noise. It is software programmable for one or more power line cycles of integration to achieve maximum noise rejection. For speed in situations where noise is not a problem. use the voltmeter in **3½** or 4½ digit modes with less than one power line cycle of integration. In the 3½ digit mode. single channel measurement speed can reach 1600 reading/second.

To measure DC current. use a resistive shunt placed in the appropriate channel of the multiplexer accessory. **AC** (45 - 500 Hz) sinewave voltage measurements are made with a peak detector calibrated in RMS. Two and four wire ohms measurements use a built-in current source. For ohms measurements. the proper multiplexer connections are automatically made by the system.

13 Bit High Speed Multimeter - 100 kHz

Use the HP **44702A/B** High Speed Voltmeter to digitize waveforms or to make fast readings over many channels. It scans and autoranges at up to **100.000** readings per second The inputs are balanced **to** reduce common mode noise without the use of a guard Make voltage or current (with a shunt on the multiplexer) measurements Use its built-in current source for **2** and 4-wire ohms measurements. The High Speed Voltmeter is the only plug-in accessory which uses two slots in the main. frame or extender. All other accessories use one slot.

The HP 44702A High Speed Voltmeter has a memory buffer of 8K readings This is expandable to 64K readings with the HP 44702B version of the voltmeter. Readings can also be stored in the mainframe memory which is expandable to 256 kbytes or 1 Mbyte. The High Speed Voltmeter contains a General Purpose Interface (GPIO) port. This can be used with a Direct Memory Address (DMA) card to transfer readings at a 100,000 reading per second rate to an HP Series *200/300* Computer. The HP **3852S** system software facilitates high speed data transfer to an HP Series 200 or 300 computer and. from there. into a hard disc

Input/Output Accessories

With the HP **3852S** Data Acquisition and Control System you'll have available a complete set of input and output plug-in accessories for interfacing to measurements and for controlling and sequencing your tests.

You'll have **relay and solid state multiplexers** with and without thermocouple compensation. These multiplexers can switch the voltmeter high. low and guard for common mode noise rejection or you can select one configured for single ended measurements (switch high only) to achieve high channel counts at a low cost per channel.

Use **a Five Channel Counter/Totalizer** to make accurate isolated or non-isolated readings of signals with frequencies up to **200** kHz It can measure frequency or totalize. do up down counting and wrap around counting. For low frequency signals. totalizing at low cost is available on all 16 channels of the Digital Input accessory.

For outputs. your choices include **a 16 Channel Digital Output accessory, an *8* Channel Form C Relay Actuator** for switching AC or DC. and **a 4 Channel Analog Output accessory** which provides voltage or current on each channel

For general purpose. low frequency and low level signal switching use **a 16 Channel Form C Switch Accessory.** This accessory has a terminal module which you can wire for genera: purpose switching configurations such as matrix and others.

The I 'O Accessories make system configuration easy in the following ways:

- **I/O accessories all slide easily into slots in the Mainframe and Extender.**
- **Each I/O accessory has a removable Terminal Module for field wiring.**
- **Terminal Modules have easily removable and see-through covers.**
- **Most configuration is done in software.**
- **Most hardware configuration is done with finger movable jumpers (no soldering).**
- **All Accessories work in all slots and require only one slot** (except the High Speed Voltmeter which uses two slots)

You can configure the system **by** connecting the field wiring to the screw-down terminals of the terminal module and plugging the terminal module with its I/O accessory Into the desired slot of the mainframe or extender. You'll do very little hardware configuration. but where required (such as the choice of **5.** 12 **24 or** 48 volts DC on the digital input accessory) it is done with jumpers on the terminal module that are moved by hand In most cases. no tools or soldering are required.

Data Acquisition & Control Unit - HP 3852

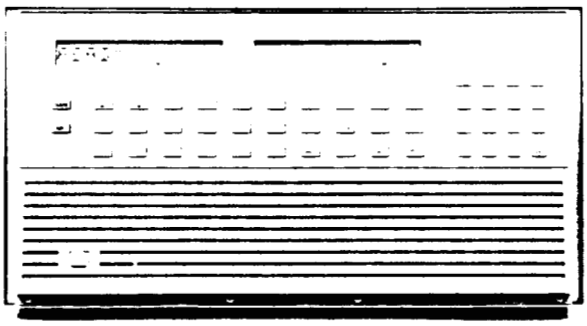

The HP 3852 Data Acquisition & Control Unit is a cardcage mainframe for the system. Use it as a computer front end for measuring voltages and transducer signals. It must normally be linked to a computer via HP-IB but it does have a keyboard and display for local operation. With its built-in intelligence and memory it can often run with minimal communications with the computer.

Features

Full alphanumeric keyboard: Most commands are keyboard executable.
Two displays: Command entry and results
Eight I/O slots
Any accessory in any slot
Interrupts from any slot
Multiple voltmeters allowed

Intelligence

BASIC constructs:
FOR...NEXT
IF THEN...ELSE
WHILE...ENDWHILE
Time Alarms
Limit Checking: Real-time or post-processing
Slot Interrupts
User routines: Callable by computer. by another routine or by Time Alarms. Limits or a Slot Interrupt
Conversion to user units
Temperature linearizations: Thermocouples. Thermistors and RTD
Any type of measurement can be stored
Packed data can be unpacked before transmission over HP-IB
Uses a Motorola 68000 μP

Memory

Usable for program and data storage:
8000 Bytes standard
1/4 **MByte and 1 MByte expansion:** Using HP Model 9000 Series 200/300 memory boards
Memory expansion cards fit into controller module and therefore don't use up a mainframe slot

Memory per reading/# of Readings (using Standard Memory)

Storage Format	High Speed DVM	Integrating DVM'
Integer	2 bytes/4000 rdgs	
Packed	2 bytes/4000 rdgs	4 bytes/2000 rdgs
Real	8 bytes/1000 rdgs	8 bytes/1000 rdgs

For all resolutions

Real Time Clock

Accuracy: 0.004% of elapsed time since setting ± 2 msec
Temperature coefficient: ± $(4.5 \cdot 10^{-6})\%/(°C)^2$
Resolution: 1 msec
Nonvolatile lifetime: 4 years

Time Alarms

Modes: Set alarm
Increment alarm
Read alarm
Resolution: 1 msec

Pacer

Pulses: 1 to 65.535 or continuous
Interval: 1 μsec to 4.19 sec
Step size: 0.25 μsec
Pulse width: 0.5 μsec nominal (low true)
Time jitter: 1st pulse = ±0.005% + 1 μsec - 0 μsec after trigger. Additional pulses = ± 0.005% ± 100 nsec after first pulse

HP 3852 HP-IB Interface Capability Codes

For further explanation of these codes. see a Hewlett-Packard catalog or IEEE Standard 488.

SH1: full source handshake capacity
AH1: full acceptor handshake capacity
T6: a basic talker. serial poll, unaddresses if "my listen address"
L4: a basic listener. unaddresses if "my talk address"
SR1: full capacity service request
RL1: full capacity remote local
PP1: parallel poll with remote configuration
DC1: full capacity device clear
DT1: full capacity for device trigger
C0: no controller capability
Data rate: 140 kbytes/sec from internal buffer to ideal listener with FASTOUTon

Connectors

Six BNC connectors on the rear of the controller module are:
Inputs are TTL compatible and require pulse widths > 0.5 μsec. Outputs can drive CMOS/HCMOS one TTL load or two LSTTL loads.
Event In: use with "WAIT FOR EVENT" command to initiate an action
Channel Advance: advances scan to next channel in channel list
Channel Closed: use to trigger an external voltmeter once channel closes
System Trigger In: provides a backplane trigger to all I/O accessories
Pacer Out: outputs from the system pacer
Pacer Trigger In: hardware trigger for Pacer

Other

Size: 22.225 cm (8 3/4 inches) high, 48.26 cm (19 inches) wide. 50.8 cm (20 inches) deep, System II cabinet
Weight: 16.8 kg (37 pounds) without plug-in accessories: 31.8 kg (70 pounds) loaded
Power: Voltage: 100, 120, 220. 240 VAC ± 10%
Frequency: 47.5 - 66 Hz (auto selected at power up)
Usage: 150 VA max
Temperature: Operation 0 to 55°C, noncondensing
Storage -40 to 75°C
Humidity: to 95% R.H., at 40°C except as noted
Wire Sizes: All accessories with screw terminals can use wire sizes 16-26 AWG except for HP 44722A. 44728A and 44729A accessories. Check their accessory description for details.

APPENDIX "B"

Computer Software Listings

PROGRAM DOWNLOAD?

```
1000  OUTPUT 709;"SCRATCH"                    ! ERASE ALL OLD SUBROUTINES AND VARIABLES
1010  OUTPUT 709;"SUB SYNC"                   ! SYNCHRONIZE TO EVEN SECONDS
1020  OUTPUT 709;"REAL C"
1030  OUTPUT 709;"LET C=999"
1040  OUTPUT 709;"WHILE C>2"
1050  OUTPUT 709;"CHREAD 202 INTO C"
1060  OUTPUT 709;"END WHILE"
1070  OUTPUT 709;"SUBEND"
1080  OUTPUT 709;"SUB DEPTH"                  ! READ DEPTH SOUNDER
1090  OUTPUT 709;"REAL D"
1100  OUTPUT 709;"CHREAD 200 INTO D"
1110  OUTPUT 709;"USE 200;TRIG SGL"
1120  OUTPUT 709;"SUBEND"
1130  OUTPUT 709;"SUB ZERO"
1140  OUTPUT 709;"REAL DP(7),A(6),STK"
1150  OUTPUT 709;"WAITFOR PACER"
1160  OUTPUT 709;"SUBEND"
1170  OUTPUT 709;"SUB SUMA"                   ! STACKING SUBROUTINE
1180  OUTPUT 709;"DISP OFF;PACER,3.906E-3"    ! SET UP PACER AT 256 Hz
1190  OUTPUT 709;"INTEGER I,J,K,L,IW"
1200  OUTPUT 709;"REAL VTS(6),A(6),G1,G2,G3,G4,STK,DP(7)"
1210  OUTPUT 709;"USE 600;SCANMODE ON; SCTRIG HOLD; FUNC DCV, TERM RIBBON"
1220  !                                       SET UP HIGH SPEED VOLTMETER AND FET MUX
1230  OUTPUT 709;"CLWRITE SENSE,500-506;RANGE 10" ! CHANNELS 1-7, FIXED RANGE
1240  OUTPUT 709;"AZERO ONCE"
1250  OUTPUT 709;"USE 202;TRIG HOLD;TERM ISO"! SET UP PACER COUNTER
1260  OUTPUT 709;"EDGE LH"
1270  OUTPUT 709;"FUNC TOTALM;NPER 256;TRIG SGL"
1280  OUTPUT 709;"USE 200;TRIG HOLD"          ! SET UP RATIO COUNTER FOR DEPTH
1290  OUTPUT 709;"TERM ISO,ISO;EDGE LH,LH;FUNC RAT"  ! SOUNDER
1300  OUTPUT 709;"NPER 2;TRIG SGL"
1310  OUTPUT 709;"LET L=0;"
1320  OUTPUT 709;"PTRIG"                      ! START PACER
1330  OUTPUT 709;"WHILE L<16000"              ! OUTER LOOP
1340  OUTPUT 709;"WAITFOR PACER;READ 400 INTO G1"  ! READ GAINS FROM 16ch DIGITAL INPUT IN SLOT 4
1350  OUTPUT 709;"READ 400 INTO G1"
1360  OUTPUT 709;"READ 300 INTO G3"
1370  OUTPUT 709;"LET IW=370;WAITFOR PACER"! SET UP DELAY BETWEEN WINDOWS
1380  OUTPUT 709;"CALL ZERO"                  ! ZERO STACKING ARRAY,DEPTH ARRAY
1390  !                                         AND STACK COUNTER
1400  OUTPUT 709;"FOR K=0 TO 7"               ! STACK 8 COMPLETE WAVEFORMS (4s EACH)
1410  OUTPUT 709;"FOR I=1 TO IW" ! !
1420  OUTPUT 709;"WAITFOR PACER"
1430  OUTPUT 709;"NEXT I"
1440  OUTPUT 709;"LET IW=384"
1450  OUTPUT 709;"READ 400 INTO G2"           ! CHECK GAINS
1460  OUTPUT 709;"READ 300 INTO G4"
1470  OUTPUT 709;"FOR J=1 TO 32"              ! 32 SCANS PER WINDOW
1480  OUTPUT 709;"WAITFOR PACER"              ! SYNCHRONIZE WITH PACER
1490  OUTPUT 709;"USE 600;SCTRIG SGL"         ! SINGLE SCAN OF CHANNELS SPECIFIED IN CLWRITE STATEMENT
1500  OUTPUT 709;"INDEX VTS,0"                ! START STORING AT ELEMENT 0
1510  OUTPUT 709;"XRDGS 600 INTO VTS"         ! TRANSFER READINGS FROM VOLTMETER TO ARRAY VTS
1520  OUTPUT 709;"IF G2=G1 AND G3=G4 THEN" ! STACK IF NO GAIN CHANGE
1530  OUTPUT 709;"STK=STK+1"                  ! INCREMENT STACK COUNTER
1540  OUTPUT 709;"FOR I=0 TO 6"               ! STACK IN ARRAY A
1550  OUTPUT 709;"  LET A(I)=A(I)+VTS(I)"
1560  OUTPUT 709;"NEXT I"
1570  OUTPUT 709;"ELSE"                       ! IF NO STACK
1580  OUTPUT 709;"WAITFOR PACER"              ! WAIT FOR EQUIVALENT AMOUNT OF TIME
1590  OUTPUT 709;"END IF"
```

PROGRAM DOWNLOAD2

```
1000  OUTPUT 709;"SCRATCH"                    ! ERASE ALL OLD SUBROUTINES AND VARIABLES
1010  OUTPUT 709;"SUB SYNC"                   ! SYNCHRONIZE TO EVEN SECONDS
1020  OUTPUT 709;"REAL C"
1030  OUTPUT 709;"LET C=999"
1040  OUTPUT 709;"WHILE C)2"
1050  OUTPUT 709;"CHREAD 202 INTO C"
1060  OUTPUT 709;"END WHILE"
1070  OUTPUT 709;"SUBEND"
1080  OUTPUT 709;"SUB DEPTH"                  ! READ DEPTH SOUNDER
1090  OUTPUT 709,"REAL D"
1100  OUTPUT 709;"CHREAD 200 INTO D"
1110  OUTPUT 709;"USE 200;TRIG SGL"
1120  OUTPUT 709;"SUBEND"
1130  OUTPUT 709;"SUB ZERO"
1140  OUTPUT 709;"REAL DP(7),A(6),STK"
1150  OUTPUT 709;"WAITFOR PACER"
1160  OUTPUT 709;"SUBEND"
1170  OUTPUT 709;"SUB SUMA"                   ! STACKING SUBROUTINE
1180  OUTPUT 709;"DISP OFF;PACER,3.906E-3"    ! SET UP PACER AT 256 Hz
1190  OUTPUT 709;"INTEGER I,J,K,L,IW"
1200  OUTPUT 709,"REAL VTS(6),A(6),G1,G2,G3,G4,STK,DP(7)"
1210  OUTPUT 709;"USE 600;SCANMODE ON; SCTRIG HOLD; FUNC DCV; TERM RIBBON"
1220  !                                       SET UP HIGH SPEED VOLTMETER AND FET MUX
1230  OUTPUT 709;"CLWRITE SENSE,500-506;RANGE 10" ! CHANNELS 1-7; FIXED RANGE
1240  OUTPUT 709;"AZERO ONCE"
1250  OUTPUT 709;"USE 202;TRIG HOLD;TERM ISO"! SET UP PACER COUNTER
1260  OUTPUT 709;"EDGE LH"
1270  OUTPUT 709;"FUNC TOTALM;NPER 256;TRIG SGL"
1280  OUTPUT 709;"USE 200;TRIG HOLD"          ! SET UP RATIO COUNTER FOR DEPTH
1290  OUTPUT 709;"TERM ISO,ISO;EDGE LH,LH;FUNC RAT"  ! SOUNDER
1300  OUTPUT 709;"NPER 2;TRIG SGL"
1310  OUTPUT 709;"LET L=0;"
1320  OUTPUT 709;"PTRIG"                      ! START PACER
1330  OUTPUT 709;"WHILE L<16000"              ! OUTER LOOP
1340  OUTPUT 709;"WAITFOR PACER;READ 400 INTO G1"  ! READ GAINS FROM 16ch DIGITAL INPUT IN SLOT 4
1350  OUTPUT 709;"READ 400 INTO G1"
1360  OUTPUT 709;"READ 300 INTO G3"
1370  OUTPUT 709;"LET IW=370;WAITFOR PACER"! SET UP DELAY BETWEEN WINDOWS
1380  OUTPUT 709,"CALL ZERO"                  ! ZERO STACKING ARRAY,DEPTH ARRAY
1390  !                                         AND STACK COUNTER
1400  OUTPUT 709;"FOR K=0 TO 7"               ! STACK 8 COMPLETE WAVEFORMS (4s EACH)
1410  OUTPUT 709;"FOR I=1 TO IW"
1420  OUTPUT 709;"WAITFOR PACER"
1430  OUTPUT 709;"NEXT I"
1440  OUTPUT 709;"LET IW=384"
1450  OUTPUT 709;"READ 400 INTO G2"           ! CHECK GAINS
1460  OUTPUT 709;"READ 300 INTO G4"
1470  OUTPUT 709;"FOR J=1 TO 32"              ! 32 SCANS PER WINDOW
1480  OUTPUT 709;"WAITFOR PACER"              ! SYNCHRONIZE WITH PACER
1490  OUTPUT 709;"USE 600;SCTRIG SGL"         ! SINGLE SCAN OF CHANNELS SPECIFIED IN CLWRITE STATEMENT
1500  OUTPUT 709;"INDEX VTS,0"                ! START STORING AT ELEMENT 0
1510  OUTPUT 709;"XRDGS 600 INTO VTS"         ! TRANSFER READINGS FROM VOLTMETER TO ARRAY VTS
1520  OUTPUT 709;"IF G2=G1 AND G3=G4 THEN"    ! STACK IF NO GAIN CHANGE
1530  OUTPUT 709;"STK=STK+1"                  ! INCREMENT STACK COUNTER
1540  OUTPUT 709;"FOR I=0 TO 6"               ! STACK IN ARRAY A
1550  OUTPUT 709;"  LET A(I)=A(I)+VTS(I)"
1560  OUTPUT 709;"NEXT I"
1570  OUTPUT 709;"ELSE"                       ! IF NO STACK
1580  OUTPUT 709;"WAITFOR PACER"              ! WAIT FOR EQUIVALENT AMOUNT OF TIME
1590  OUTPUT 709;"END IF"
```

```
1600  OUTPUT 709;"NEXT J"
1610  !                                        DEPTH SOUNDER
1611  OUTPUT 709;"CALL SYNC"
1612  OUTPUT 709;"CALL DEPTH"
1613  OUTPUT 709;"LET DP(K)=D"
1615  OUTPUT 709;"WAITFOR PACER ;WAITFOR PACER,WAITFOR PACER,WAITFOR PACER"
1616  OUTPUT '709;"CALL SYNC"
1620  OUTPUT 709;"FOR J=1 TO 96"              ! DELAY BETWEEN WINDOWS
1630  OUTPUT 709;"WAITFOR PACER"
1641  OUTPUT 709,"NEXT J"
1650  OUTPUT 709;"READ 400 INTO G2"           ! CHECK GAINS
1660  OUTPUT 709,"READ 300 INTO G4"
1670  OUTPUT 709,"FOR J=1 TO 32"              ! NEXT WINDOW - 32 SCANS
1680  OUTPUT 709;"WAITFOR PACER,USE 600;SCTRIG SGL,INDEX VTS,0"
1690  OUTPUT 709,"XRDGS 600 INTO VTS"
1700  OUTPUT 709,"IF G1=G2 AND G3=G4 THEN"    ! STACK IF NO GAIN CHANGE
1710  OUTPUT 709;"STK=STK+1"                  ! INCREMENT STACK COUNTER
1720  OUTPUT 709;"FOR I=0TO6"                 ! STACK THIS WINDOW NEGATIVE
1730  OUTPUT 709;" LET A(I)=A(I)-VTS(I)"
1740  OUTPUT 709;"NEXT I"
1750  OUTPUT 709;"ELSE"                       ! IFNO STACK
1760  OUTPUT 709,"WAITFOR PACER"              ! USEUP EQUIVALENT AMOUNT OF TIME
1770  OUTPUT 709;"END IF"
1780  OUTPUT 709,"NEXT J"
1790  OUTPUT 709;"NEXT K"
1800  OUTPUT 709,"WAITFOR PACER;VREAD A,RASC"! OUTPUT COMPLETE STACK TO 316
1810  OUTPUT 709,"WAITFOR PACER;L=L+1"
1820  OUTPUT 709,"VREAD G1,RASC"              ! OUTPUT GAINS TO 216
1830  OUTPUT 709;"VREAD G3,RASC"
1840  OUTPUT 709;"WAITFOR PACER;VREAD STK,RASC" ! OUTPUT STACK COUNT TO 216
1841  OUTPUT 709;"VREAD DP,RASC"
1850  OUTPUT 709,"END WHILE"                  ! END OF STACKING LOOP
1860  OUTPUT 709;"DISP ON"                    ! TURN ON DISPLAY ON COMPLETION
1870  OUTPUT 709;"PACER,1,0"
1880  OUTPUT 709;"SUBEND"                     ! END OF SUBROUTINE
1890  END
```

```
1000  OPTION BASE 1
1010  DIM Vt(7),Xx(28),Yy(28),Yyp(28),S(28),X0(134),Rt(6),Gf(6),Gn(14),V11(7)
1020  DIM Depth(8),Lpp(4),Pp(4)
1030  COM P(7),R(134),Fltr(29),INTEGER E,M,N
1040  INTEGER G(7),Np,Screen(7500),Ss(6)
1050  ON KEY 4 LABEL " ABANDON SHIP" GOTO Ex      ! GRACEFUL EXIT
1051  !
1053  Water_cal=.06                               ! SPEED OF SOUND IN WATER
1054  !                                             CALIBRATION
1060  ASSIGN @O TO "DAT"                          ! TEMPORARY OUTPUT FILE
1070  OUTPUT 705;"IN;"                            ! INITIALIZE 7245B PLOTTER
1080  OUTPUT 705;"IW-200000,-150000,200000,5000;"
1090  OUTPUT 705,"SCMM,3;"
1100  INPUT "LINE ID",Lid$
1101  INPUT "VC",Lsd
1110  OUTPUT 705;"LOS;"
1120  OUTPUT 705;"PAPU10,90;"
1130  OUTPUT 705,"SI.56,1.;"
1140  OUTPUT 705;"DI0,1;"
1150  OUTPUT 705;"LBLINE: "&Lid$;CHR$(3)          ! PLOT LINE TITLE
1160  OUTPUT 705;"SI.2,.35;"
1170  OUTPUT 705;"DI1,0,"
1180  OUTPUT 705;"LOB;"
1190  OUTPUT 705;"PAPU30,175;"
1200  OUTPUT 705;"PAPD29,175;"
1210  OUTPUT 705,"PAPU28,175;"
1220  OUTPUT 705;"LBO";CHR$(3);                   ! DRAW VERTICAL AXIS
1230  OUTPUT 705;"PAPU30,175;"
1240  FOR I=10 TO 70 STEP 10
1250    Xxs=175-2*I
1260    OUTPUT 705;"PAPD30,";Xxs;";"
1270    OUTPUT 705;"PAPD29,";Xxs;";"
1280    OUTPUT 705;"PAPU28,";Xxs;";"
1290    OUTPUT 705;"LB";VAL$(I);CHR$(3);
1300    OUTPUT 705;"PAPD30,";Xxs;";"
1310  NEXT I
1320  OUTPUT 705;"LOS;"                           ! SETUP FOR PLOTTING SECTIONS
1330  !
1340  GINIT                                       ! INITIALIZE SCREEN GRAPHICS
1350  GRAPHICS ON
1360  Xmin=3-2.2*RATIO
1370  SHOW Xmin,3,-.275,2
1380  MOVE: 1,0                                   ! GRID FOR LOG-LOG PLOT
1390  DRAW 3,0
1400  MOVE 1,1
1410  DRAW 3,1
1420  MOVE 1,2
1430  DRAW 3,2
1440  MOVE: 1,0
1450  DRAW 1,2
1460  MOVE: 2,0
1470  DRAW 2,2
1480  MOVE 3,0
1490  DRAW 3,2
1500  CSIZE 5
1510  LORG 6
1520  MOVE 2.0,0
1530  LABEL "LOG(r)"                              ! LABEL AXES
1540  LDIR 2*ATN(1)
1550  LORG 4
```

```
1560  MOVE 1,1
1570  LABEL "LOG(Rho)"
1580  LORG 2
1590  LDIR 0
1600  MOVE .45,1 876
1610  LABEL "V1"                                  ! DISPLAY LOCATION LABELS
1620  MOVE .45,1.693                              ! FOR RAW VOLTAGE DISPLAY
1630  LABEL "V2"
1640  MOVE  45,1.511
1650  LABEL "V3"
1660  MOVE .45,1.328
1670  LABEL "V4"
1680  MOVE .45,1 145
1690  LABEL "V5"
1700  MOUE  45,.963
1710  LABEL "V6"
1720  MOVE .45,.78
1730  LABEL "CM"                                  ! INCLUDING CURRENT MONITOR
1731  MOVE  45,.597
1732  LABEL "D(m)"
1740  CSIZE 3
1750  LORG 5
1760  GSTORE Screen(*)                            ! STORE BACKGROUND FOR DISPLAY
1770  !
1780  Lpp(1)=0                                    ! TEMPORARY STORAGE FOR
1790  Lpp(2)=0                                    ! PLOTTING SECTIONS
1800  Lpp(3)=0
1810  Lpp(4)=0
1820  !
1830  DATA 1,2.5,5,10,25,50,0,0,100,250,500,1000,2500,5000
1840  HEAD Gn(*)                                  ! GAIN VALUES FOR DECODING
1841  !  LOG DIPOLE GEOMETRIC FACTORS
1842  DATA 143.7393,386 262,1000.56,2185.71,4986.38,10606 8
1850  !  DIPOLE-DIPOLE GEOMETRIC FACTORS
1860  !DATA 471 239,1884.96,4712 39,9424 78,16493  4,26389.4
1870  READ Gf(*)
1880  DATA .00046256,- 0010907,.0017122,- 0020687 ! FILTER COEFFICIENTS
1890  DATA .0043048,-.0021236,.015995,.017065,.098105, 21918,.64722,1 1415
1900  DATA .47819,-3.515,2 7743,-1.201, 4544,- 19427, 097364,-.054099, 031729
1910  DATA -.019109, 011656,- .0071544,.0044042,-.00271.5,.0016749,- 0010335
1920  DATA  00040124
1.930 READ Fltr(*)
1940  !                                           ! ABSCISSAE FOR FILTER POINTS
1950  DATA 20 62,22 70,24.98,27.5,30.27,33 32,36 67,40 364,44 34,48 9,53 83
1960  DATA 59.247,65.21,71.79,79.01,86 96,95 72,105.36,115 97,127.64,140.50
1970  DATA 154 64,170.22,187.36,206.22,226.99,249 84,275
1980  READ S(*)
2010  DATA 8,20,30,65.0,65.,65 5,190              ! INITIAL GUESS
2020  READ P(*)
2030  DATA 4,7,20,28,2
2040  READ E,N,M,Np,Spac                          ! 4 LAYERS
2041                                              ! 7 PARAMETERS
2050  FOR I=1 TO Np
2060    Xx(I)=LOG(S(I))                           ! LOG OF ABSCISSAE   DISTANCES
2070  NEXT I
2080  Spac=LOG(Spac)                              ! SPACED FORM 2 TO 2154
2090  Delx=LOG(10)/6                              ! LOGARITHMIC SPACING
2100  Fine=1/SQR(2)                               ! CHANGE IN STEP SIZE
2110  Adj= 4                                      ! INITIAL STEP SIZE
2120  !
```

```
2150  PRINT CHR$(12)                                  ! CLEAR ALPHA SCREEN
2190  !
2150  OUTPUT 709;"CALL SUMA"                          ! CALL SUBROUTINE IN 3852A
2160  T1=TIMEDATE                                     ! FOR TIMING
2170  T3=T1
2180  FOR I=1 TO 16000
2190  T9=TIMEDATE
2200  !                                                 DATA ENTRY FROM 3852A
2210  ENTER 709;Vt(*)                                 ! READ STACKED VOLTAGES
2220  ENTER 709;Ggg1                                  ! READ GAINS - BINARY FORMAT
2230  ENTER 709;Ggg2
2240  ENTER 709;Stack_count                           ! NUMBER OF STACKS STORED :NUt
2250  ENTER 709;Depth(*)
2260  !
2261  Sd=4*Lsd
2262  Sds=4*Lsd*Lsd
2264  FOR J=1 TO 8
2265    Depth(J)=Depth(J)*Water_cal
2267    Sd=Sd+Depth(J)
2268    Sds=Sds+Depth(J)*Depth(J)
2269  NEXT J
2270  Sdev=SQR(Sds/12-Sd*Sd/144)
2271  Nnn=12
3272  FOR J=1 TO 8
2273    IF ABS(Depth(J)-Sd/12))2*Sdev THEN
2274      Nnn=Nnn-1
2275      Sd=Sd-Depth(J)
2276    END IF
2277  NEXT J
2278  Sd=Sd/Nnn
2279  Lsd=Sd
2281  FOR J=1 TO 4                                    ! DECODE GAINS
2282    K=7-J
2290    L1=(J-1)*4
2300    G(K)=0
2310    FOR L=0 TO 3
2.320     G(K)=G(K)+BIT(Ggg1,L1+L)*2^L
2330    NEXT L
2340  NEXT J
2350  FOR J=1 TO 2                                    ! SECOND BINARY GAIN NUMBER
2360    L1=(J-1)*4
2371    K=3-J
2372    G(K)=0
2380    FOR L=0 TO 3
2390      G(K)=G(K)+BIT(Ggg2,L1+L)*2^L
2400    NEXT L
2410  NEXT J
2420  G(7)=0
2421  L1=8
2422  FOR L=0 TO 3
2423    G(7)=G(7)+BIT(Ggg2,L1+L)*2^L
2424  NEXT L
2425  IF Stack_count=0 THEN 3520
2430  FOR J=1 TO 7                                    ! DIVIDE TO REMOVE STACKING
2440    Vt(J)=Vt(J)/Stack_count
2450  NEXT J
2460  PRINT USING "@,7(/,DDDDD DDD,/),/,DDDDDDD D";Vt(*),Sd
2470 !PRINT TIMEDATE-T9
2480  Vt(7)=Vt(7)/ 1667/Gn(G(7)+1)                    ! SHUNT RESISTANCE
2490  FOR J=1 TO 6
```

```
2500    Cnn Gn(G(J)+1)                          ! REMOVE GAINS
2510    Rt(J)=ABS(Vt(J)/Gnn/Vt(7)*Gf(J))        ! AND CALCULATE RESISTIVITY
2520  NEXT J
2521  P(1)=Sd
2530  GOSUB Logdip                              ! THEORETICAL RESPONSE OF INITIAL MODEL
2540  Er1=Er                                    ! AND ERROR
2550  IF Adj< .06 THEN Adj= .06
2560  FOR Lll=1 TO 3                            ! REPEAT INVERSION LOOP 3 TIMES
2570    Adj=Adj*Fine                            ! STEP SIZE FROM 4.2% TO 2.1%
2580    Fac=1+Adj                               ! STEP SIZE
2590    FOR Kkk=2 TO 7                          ! ALL PARAMETERS VARIED EXCEPT
2600      IF Kkk=4 THEN 2820                    ! WATER DEPTH AND RESISTIVITY
2610      P(Kkk)=P(Kkk)*Fac                     ! INCREASE PARAMETER
2620      IF P(2)>40 THEN                       ! MAXIMUM DEPTH LIMIT
2630        Er=2*Er1
2640        GOTO 2710
2650      END IF
2660      IF P(3)>40 THEN                       ! MAXIMUM DEPTH LIMIT
2670        Er=2*Er1
2680        GOTO 2710
2690      END IF
2700      GOSUB Logdip                          ! CALCULATE THEORETICAL RESPONSE
2710      IF Er1<Er THEN                        ! NO DECREASE IN ERROR
2720        P(Kkk)=P(Kkk)/Fac/Fac               ! DECREASE PARAMETER
2730        GOSUB Logdip                        ! CALCULATE THEORETICAL RESPONSE
2740        IF Er1<Er THEN                      ! NO DECREASE IN ERROR
2750          P(Kkk)=P(Kkk)*Fac                 ! RESTORE ORIGINAL PARAMETER
2760        ELSE
2770          Er1=Er                            ! KEEP LOWER PARAMETER
2780        END IF
2790      ELSE
2800        Er1=Er                              ! KEEP HIGHER PARAMETER
2810      END IF
2820    NEXT Kkk
2830  NEXT Lll
2840    GOSUB logdip                            ! RECALCULATE BEST-FIT MODEL
2850    GLOAD Screen(*)                         ! RESTORE SCREEN BACKGROUND
2860    MOVE LGT(S(1)),LGT(Yy(1)-Yyp(1)/2)-1    ! DISPLAY THEORETICAL CURVE
2870    FOR Li=2 TO 28                          ! ON SCREEN
2880      DRAW LGT(S(Li)),LGT(Yy(Li)-Yyp(Li)/2)-1
2890    NEXT Li
2900    FOR Li=1 TO 6                           ! DISPLAY DATA
2910      Lj=Li*4
2920      MOVE LGT(S(Lj)),LGT(Rt(Li))-1
2930      LABEL "+"
2940    NEXT Li
2950    OUTPUT @0;X_nav,Y_nav,P(*),Vt(*)        ! OUTPUT DATA TO DISC
2960    MOVE .25,1.94
2970    CSIZE 5
2980    LABEL "E:"&VAL$(DROUND(Er1,3))&"%"      ! DISPLAY MODEL ERROR ON SCREEN
2990    CSIZE 3
3000    Pp(1)=0
3050    Pp(2)=P(1)+Pp(1)
3020    Pp(3)=P(2)+Pp(2)
3030    Pp(4)=P(3)+Pp(3)
3040    Xxs=10^ I+30
3050    OUTPUT 705;"PAPU";Xxs-10;",175;"        ! PLOT LAYERED MODEL ON 7245B
3060    OUTPUT 705;"PAPD";Xxs;",175;"
3070    FOR J=2 TO 4
3080      IF I=1 THEN 3140
```

```
3090      Yys=175-Lpp(J)*2
3100      Xx2=Xxs-10
3110      OUTPUT 705;"PAPU";Xx2;",";Yys;";"
3120      Yys=175-Pp(J)*2
3130      OUTPUT 705;"PAPD",Xxs;",",Yys;";"
3140      Lpp(J)=Pp(J)
3150    NEXT J
3160    I2=INT(I/2)*2                          ! EVERY SECOND TIME
3170    IF I2=I THEN                           ! PLOT VALUES OF RESISTIVITY
3180      Yys=Yys-10
3190      OUTPUT 705;"PAPU";Xxs;",";Yys;";"
3200      SELECT P(7)                          ! FORMATING OF NUMBERS
3210        CASE >999                          ! THREE SIGNIFICANT FIGURES
3220          OUTPUT 705 USING "#,D DDESZ";P(7)
3230        CASE >99.9
3240          OUTPUT S$ USING "#,DDD";P(7)
3250        CASE >9.99
3260          OUTPUT SI USING "#,DD D";P(7)
3270        CASE ELSE
3280          OUTPUT 705 USING "#,D DD";P(7)
3290      END SELECT
3300      OUTPUT 705;"LB"&S$&CHR$(3);
3310      OUTPUT 705;"PAPU";Xxs;",175;"
3320      OUTPUT 705;"PAPD";Xxs;",176;"
13330     OUTPUT 705;"PAPU";Xxs;",179;"
3340      OUTPUT 705;"LB"&VAL$(I)&CHR$(3);
3350      FOR J=5 TO 6
3360        SELECT P(J)
3370          CASE >99.9
3380            OUTPUT S$ USING "#,DDD";P(J)
3390          CASE >9.99
3400            OUTPUT SI USING "#,DD D";P(J)
3410          CASE <-9.99
3420            OUTPUT S$ USING "#,D.DD";P(J)
3430          CASE ELSE
3440            OUTPUT SI USING "#,D DDESZ",P(J)
3450        END SELECT
3460        Pp2=(Pp(J-3)+Pp(J-2))/2              ! PLOT FID NUMBER
3470        Yys=175-2*Pp2
3480        OUTPUT 705;"PAPU";Xxs;",";Yys;";"
3490        OUTPUT 705,"LB"&S$&CHR$(3);
3500      NEXT J
3510    END IF
3520  NEXT I
3530 Ex.  !
3540  ASSIGN @O TU *
3550  STOP
3560 Logdip:  !  RESITIVITY RESPONSE OF LAYER-CAKE MODELS USING GHOSH FILTER
3570          Y=Spac-19*Delx- 013069
3580          FOR Li=1 TO 47
3590            CALL Trans(Y,Li)
3600            Y=Y+Delx
3610          NEXT Li
3620          CALL Filter
3630          Y=Spac
3640          FOR Li=1 TO M
3650            X0(Li)=Y
3660            A=EXP(Y)
3670            Y=Y+Delx
3680          NEXT Li
```

```
3690          CALL Spline(X0(*),R(*),Xx(*),Yy(*),Yyp(*),M,Np)
3700          Er=0
3710          FOR Li=1 TO 6
3720            Lj=4*Li
3730            Dd=Yy(Lj)-Yyp(Lj)/2
3740            Er=Er+LGT(Rt(Li)/Dd)^2
3750          NEXT Li
3760          Er=SQR(Er/6)*100
3770  RETURN
3780  END
3790  SUB Trans(Y,I)
3800  OPTION BASE 1
3810  COM P(7),R(134),Fltr(29),INTEGER E,M,N
3820  DIM T(50)
38.30 U=1/EXP(Y)
3840  T(1)=P(N)
3850  FOH J=2 TO E
3860    Arg=-2*U*P(E+1-J)
3870    A=0
3880    IF Arg)-700 THEN A=EXP(Arg)
3890    B=(1-A)/(1+A)
3900    Rs=P(N+1-J)
3910    Tpr=Rs*B
3920    T(J)=(Tpr+T(J-1))/(1+Tpr*T(J-1)/Rs/Rs)
3930  NEXT J
3940  R(I)=T(E)
3950  SUBEND
3960  SUB Filter
3970  OPTION BASE 1
3980  COM P(7),R(134),Fltr(29),INTEGER E,M,N
3990  DIM Res(31)
4000  FOR I=i TO M
40i0    Rr=0
4020    FOR J=i TO 29
4030      B=Fltr(J)*R(I+29-J)
4040      Rr=Rr+B
4050    NEXT J
4060    Res(I)=Rr
4070  NEXT I
4080  FOR I=i TO M
4090    R(I)=Res(I)
4100  NEXT I
4110  SUBEND
41211 SUB Spline(X0(*),F(*),U(*),V(*),W(*),INTEGER N,M)
4130  OPTION BASE 1
4140  !     INPUT:
4i50  !           X0  - ABSCISSAE OF INPUT LINE (in ascending order)
4160  !           F   - ORDINATES OF INPUT LINE
4170  !           N   - NUMBER OF INPUTPOINTS
4180  !           U   - ABSCISSAE OF DESIRED OUTPUT LINE
4190  !           M   - NUMBER OF OUTPUT POINTS
4200  !    OUTPUT:
4210  !           V   - ORDINATES OF OUTPUT LINE CORRESPONDING TO U
4220  !           W   - DERIVATIVE OF FUNCTION AT POINTS SPECIFIED
4230  !                 BY ABSCISSAE U
4240  !
4250  DIM Ys(5,100)
4260  INTEGER I,J,K,M1,M2
4270  M1=N-1
4280  FOR I=2 TO M1
```

```
4290    Ys(2,I)=2
4300    J=I-1
4310    K=I+1
4320    S=X0(K)-X0(J)
4330    S1=X0(K)-X0(I)
4340    S2=X0(I)-X0(J)
4350    Ys(1,I)=S1/S
4360    Ys(3,I)=S2/S
4370    Ys(4,I)=3*(Ys(1,I)*(F(I)-F(J))/S2+Ys(3,I)*(F(K)-F(I))/S1)
4380  NEXT I
4390  !     BOUNDARY CONDITIONS '
4400  Ys(2,1)=2
4410  Ys(3,1)=2/Ys(1,2)
4420  Ys(4,1)=(2*Ys(3,2))*(F(2)-F(1))/(X0(2)-X0(1))
4430  C=(Ys(3,2)*Ys(3,2)/Ys(1,2))*(F(3)-F(2))/(X0(3)-X0(2))
4440  Ys(4,1)=2*(Ys(4,1)+C)
4450  Ys(2,N)=2
4460  Ys(1,N)=2/Ys(3,N-1)
4470  M2=N-2
4480  C=(Ys(1,M1)*Ys(1,M1))/Ys(3,M1)*(F(M1)-F(M2))/(X0(M1)-X0(M2))
44Y0  Ys(4,N)=(2*Ys(1,M1))*(F(N)-F(M1))/(X0(N)-X0(M1))
4500  Ys(4,N)=2*(C+Ys(4,N))
45i0  ! LU decomposition
4520  ! LU matrices stored in first 3 columns of Ys
4530  FOR I=2 TO N
4540    J=I-1
4550    Ys(1,I)=Ys(1,I)/Ys(2,J)
4560    Ys(2,I)=Ys(2,I)-Ys(1,I)*Ys(3,J)
4570  NEXT I
4580  ! Solution of the first triangular system
455'0  ! Solution vector stored in column 4 of Ys
4000  FOR I=2 TO N
4610    J=I-1
4620    Ys(4,I)=Ys(4,I)-Ys(1,I)*Ys(4,J)
46.40  NEXT I
4640  ! Solution of the second triangular system
4650  ! Solution vector stored in column 5 of Ys
4660  Ys(5,N)=Ys(4,N)/Ys(2,N)
4670  FOR I=N-1 TO 1 STEP -1
4680    J=I+1
4690    Ys(5,I)=(Ys(4,I)-Ys(3,I)*Ys(5,J))/Ys(2,I)
4700  NEXT 1                          ' '
4710  ' Interpolation Loop
4720  FOR K=1 TO M
4730    X=U(K)
4'740    IF X(X0(1) THEN PRINT "ERROR S"
4750    IF X)X0(N) THEN PRINT "ERROR 2"
4760    LET J=2
4770    IF X(=X0(J) THEN 4800
4'780    J=J+1
4790    GOTO 4770
4800    I=J-1
4810    H=X0(J)-X0(I)
4820    H2=H*H
4830    X1=X-X0(I)
4840    X2=X0(J) X
4850    Y=F(I)*X2*X2*(2*X1+H)+F(J)*X1*X1*(2*X2+H)
4860    Y=Y/H+(Ys(5,I)*X2 Ys(5,J)*X1)*X1*X2
4870    U(K)=Y/W2
4880    X3=x2-2 X1
```

```
4891      X4 2*X2-X1
4900      Y=6*X1*X2*(F(J)-F(I))/H+Ys(S,I)*X2*X3-Ys(S,J)*X1*X4
4910      W(K)=Y/H2
4920    NEXT K
4930    SUBEND
```

APPENDIX "C"

Published Papers on Marine Resistivity

MARINE RESISTIVITY SURVEY FOR GRANULAR MATERIALS, BEAUFORT SEA

W.J. Scott* and F.K. Maxwell*

(Submitted to the Journal of the Canadian Society of Exploration Geophysicists)

INTRODUCTION

The purpose of this paper is to describe the Hardy MICRO-WIP Marine Resistivity System and its application to a search for granular material in the Beaufort Sea. The paper will describe the system, the method of making measurements, the method of interpretation and finally some results from the survey.

The electrical resistivity of unconsolidated materials depends on the grain size distribution and the resistivity of the pore water. For materials above $0^{o}C$, coarse-grained materials have higher electrical resistivities than fine-grained materials. As the temperature decreases through zero and ice starts to form in the pores, the resistivities of all materials rise. Figure 1 (after King and others 1982) shows the dependence of resistivity on temperature for some typical materials both from onshore and offshore. For temperatures above zero there is a spread in resistivity values among sands and silts and clays. Resistivities of all materials at temperatures below zero are much higher than those of the same materials above zero. Because of these variations, measurements of resistivity of sub-bottom materials can be used to find coarse-grained materials and also to identify the presence of permafrost.

*Hardy BBT Limited, Calgary, Alberta

During the period from 1973 to 1979 studies were carried out at the Geological Survey of Canada directed towards development of a marine resistivity system. To assess the utility of the technique, measurements of sub-bottom resistivity were made during winter time by drilling holes through the sea ice and suspending electrodes in the water.

Figure 2, after Scott (1975), shows the results of a resistivity sounding carried out in the mouth of Kugmallit Bay in the winter of 1973-74. The interpretation of this sounding and others like it showed that the resistivities of sub-bottom materials could be identified with reasonable reliability by electrical measurements made on the surface of the water.

Following the success of these early experiments, development of an initial marine resistivity system was carried out at the GSC. Results of this work appeared in Scott and Hunter (1975) and in Lobach and Scott (1979).

In 1980, development of an improved marine system was undertaken at Hardy Associates (1978) Ltd. This system was designed for two applications. The first was the mapping of the distribution of sands and gravels in the Beaufort Sea and the identification of permafrost in the sub-bottom. The second was the application of resistivity and induced polarization (IP) measurements in fresh water to the search for metallic mineralization. This paper will describe the successful application of the MICRO-WIP (Microprocessor Controlled Waterborne IP) system to the search for granular materials and permafrost in the Beaufort.

SYSTEM

Figure 3 shows a block diagram of the MICRO-WIP system. The controller provides timing signals to the transmitter, to regulate current injected into the water through the first two electrodes on the streamer.
The current waveform is an interrupted square wave (Figure 4A) which is on in one direction for one second, off for one second, on in the other direction for one second and off for a fourth second. The waveform repeats with a period of four seconds.

Also on the streamer is an array of seven electrodes which is connected to the receiver amplifier system (Figure 3). The voltage differences between successive adjacent pairs of electrodes are amplified in six receiver channels. A typical voltage waveform observed at the receiver is shown on Figure 4B. The observed voltage waveform has the same shape and timing as the current except for a small rounding of the leading edge of the voltage waveform and a corresponding small transient voltage after the interruption of current. Signals from the six receiver channels and from a current waveform monitor are digitized in the controller at a rate of 256 Hz and the digital values are stored on magnetic tape.

A total field magnetometer is part of the MICRO-WIP system. To provide noise-free readings the magnetometer is operated during the time the current flow is off. The magnetic readings are stored on tape along with the electrical values.

Navigation for MICRO-WIP surveys is normally performed by an on-board computer which utilizes ranges from systems such as

the Racal MICRO-FIX, Del Norte Trisponder or Motorola Miniranger. The navigation computer prepares a display to guide the pilot of the boat and also digitizes the boat path to store on magnetic tape. Every fifty metres, the navigation computer generates a fiducial mark which is applied to the sub-bottom profilers normally run in unison with the MICRO-WIP system.

Figure 5 shows a photograph of the MICRO-WIP system installed on a survey vessel for work in the Beaufort Sea in the summer of 1985. The transmitter is a Huntec M4 (7.5 KVa) which provides a current of 15 amps. The system will fit in a space approximately 2.0 m x 1 m x 1 m. In addition, deck space is required for the 7.5 KVa motor generator which supplies power for the transmitter.

The streamer is made of two buoyant cables approximately 1 cm in diameter. The receiver cable has seven take outs for the electrodes used to measure the voltage distribution (potential electrodes). The transmitter cable carries the two current electrodes and the two cables are taped together at regular intervals in order to maintain appropriate spacing between current and receiver electrodes. The streamer is light enough that it can be reeled in and out by hand. The potential electrodes, which are kept moist when not in use, are mounted on the streamer when it is reeled out and removed again when it is reeled in.

Because the electrical measurements are considered complementary to normal sub-bottom profiling, work in the Beaufort Sea is carried out with both electrical measurements

and sub-bottom acoustic profiling. In the survey of 1985, a Raytheon RTT-1000 and an EG&G Uniboom were run with the MICRO-WIP system.

In freshwater applications for metallic mineral prospecting the system is frequently operated from a small boat (Figure 7) and in these circumstances the Raytheon RTT-1000 is carried but space limitations preclude the use of the EG&G Uniboom.

PROCESSING AND INTERPRETATION

During surveying all data is recorded on magnetic tape. The tape is filled in about an hour of survey. When removed from the data acquisition system, a tape is available for processing. A tape normally contains the time of day, the water depths, the magnetic readings, navigation information and the digitized waveforms of current and voltage for the MICRO-WIP. The first stage in processing is to extract from the tape the magnetic and water-depth information and to calculate the apparent resistivities associated with the MICRO-WIP measurements. Apparent resistivities are calculated from the digitized current and voltage values. To avoid the problem of turn-on transients, the calculations are based on an average of 50 points digitized on the curve towards the second half of the second during which current is transmitted (Figure 4). These 50 digital values are used to establish an average value of current and an average value of observed voltage. Apparent resistivity is then calculated according to the following formula.

$$\rho_{an} = n(n + 1)(n + 2)x \ V_n/I$$

where ρ_{an} = the apparent resistivity calculated for channel n.

n = the number of the channel (n = 1,....6)

x = the spacing between adjacent electrodes (metres)

V_n = the voltage observed on channel n averaged over the 50-sample window (volts)

I = the current averaged over the 50-sample window (amperes)

Thus for every four seconds of data collection we have a set of apparent resistivities for channels 1 through 6. As well as representing increasing distances between transmitter and receiver, these apparent resistivities represent increasing depths of penetration sampled in the voltage measurement. To be displayed as a pseudosection (Figure 8), the apparent resistivities are plotted at the midpoint of the relevant transmitter and receiver electrode pairs at a depth which is determined by the intersection of lines drawn downwards at 45° from the centre-points of the transmitter and receiver electrode pairs. As the array of electrodes is towed along, successive values of apparent resistivity can be plotted at successive positions. The result is a pseudosection. Figure 9 shows a typical pseudosection of data obtained in the Beaufort Sea in the summer of 1985. In Figure 9 the diagonal slash outlines the six values of apparent resistivity obtained simultaneously from the same transmitted current.

The six values of apparent resistivity obtained for a given transmitter current constitute a vertical electric sounding,

albeit limited in vertical extent. The interpretation of the MICRO-WIP resistivity data is based on treating each successive set of resistivity values as such a sounding. A Monte-Carlo inversion scheme is used to invert the data in terms of a layered model. Figure 10 shows one such set of apparent resistivities plotted in a sounding mode against spacing between current and receiver electrodes. To assess quality of fit, an error expression is calculated as follows:

$$E(\%) = 100 \sqrt{\sum_{n=1}^{6} (\text{Log} \quad \rho_{an} \text{ Obs} / \rho_{an} \text{ model})^2 / 6}$$

An acceptable fit is considered to have been achieved if the error is 1 percent or less.

Figure 10 shows a typical model fitted to the sounding data. The model is based on a generalization of drill control obtained in the area. In this model, the first layer represents the seawater, the second layer represents sand, and the bottom layer, with a much higher resistivity, is interpreted as permafrost. Between the surficial sand layer and the permafrost is a layer of lower resistivity which we tentatively correlate with increasing salinity in the materials above the permafrost. Although we know of no sub-bottom salinity logs in this area, increasing salinity with depth has been observed off the north slope of Alaska (Sellmann et al 1982). In this area increasing salinity with depth is consistent with the model of deltaic development proposed by Blasco (1986) in which the first part of delta

development is sub-aquaeous and thus subject to saline intrusion while later stages are sub-aerial and tend to be fresher in porewater content. The numbers in parentheses beside the model parameters in Figure 10 represent the relative sensitivity of the parameter to small changes in value.

Small variations in water resistivity are reflected in variation of the asymptotic level which the lefthand part of the sounding curve approaches but in the zone of measurement very little impact is felt. Small variations in water depth appear to have very little influence on the sounding curve.

The spacing of the electrodes on the streamer was chosen to maximize the sensitivity of the interpretation to values of resistivity and thickness of the first bottom layer. Even a small variation in resistivity alters the sounding curve enough to be distinguishable. Variations in thickness of 10% are also significant.

For low resistivities (10 ohm-metres), the resistivity of the deepest layer is reasonably well-determined but as resistivities rise above 100 ohm-metres the reliability of determination decreases. Sensitivity to permafrost resistivities at depths of 50 m could be achieved by increasing the spacing between electrodes or by increasing the number of channels sampled. However, for the present survey this was not considered necessary.

Although permafrost on the bottom of the sea was not encountered in this survey, the question of sensitivity to such permafrost is relevant in other parts of the Beaufort

Sea. Figure 17 shows variations in the shape of the sounding curve for a thin layer of high resistivity on the sea bottom. The thickness of the sub-bottom layer is chosen as 2 m. Resistivities of 12 and 24 ohm-metres have dramatic impact on the curve shape. Thus it is clear that the presence of even thin permafrost on the seabottom would be easily detected by the resistivity method. Even when thin permafrost on the sea bottom is detected, the layers beneath remain reasonably well determined. This is in contrast to the acoustic sub-bottom profiling technique which normally finds a thin layer of permafrost on or near the seabottom opaque, so that layering beneath that is difficult to distinguish. Thus in carrying out a combined acoustic and electrical survey, structure can be followed with the electrical resistivity in areas where near-bottom permafrost prevents depth penetration with the acoustic technique.

In the future, it is planned to increase the number of channels and to vary the spacing between electrodes in order to provide a reasonable precision in the nearbottom and at the same time to enhance the sensitivity of the measurements to permafrost at depth.

SURVEY RESULTS

During the summer of 1985, a MICRO-WIP survey with associated sub-bottom acoustic profiling was carried out in the Southern Beaufort Sea east of Pullen Island. Figure 12 shows the approximate location of the survey area, and the location of the three transponders used for navigation during the survey. The purpose of the survey was to outline granular material for use in construction of an artificial island. Figure 13 shows a

very compressed section through approximately 6 km in the southern part of the survey area. The pseudosection of Figure 9 represents several hundred metres of this section. Because of the great compression of the horizontal scale it is not possible to show all of the apparent resistivity values but a representative selection of these is plotted in the bottom part of Figure 13. Contours intervals of 0.5 and 1 ohm-metre have been chosen to illustrate the variation in apparent resistivities.

The model inversion interpretation was carried out for this profile. In the upper part of Figure 13 is a plot of the interpreted thicknesses of the identified layers together with interpreted ranges of resistivities. Only generalized resistivities are shown but it is clear that detailed variations can be represented with reasonable reliability. The borrow pit for construction of the island was established in the central part of this profile where interpreted resistivities in the upper layer were between 2.3 and 2.6 ohm-metres. The material excavated from the pit was clean sand with occasional pebbles.

Very little control was available on this line as heavy ice in the area prevented a significant drilling programme. However, acoustic sub-bottom profiling on this line identified a reflector (Figure 14) over the central part of the profile which is interpreted as hummocky permafrost at a depth of approximately 30 m. Its position is plotted in Figure 13. Thus there is reasonable confidence in the interpretation of high resistivities in the sub-bottom as permafrost.

Because permafrost in this area is all relic, it is likely that the shallowest permafrost was the most ice rich and consequently slowest to degrade. The shallowest permafrost is associated with the highest interpreted resistivities. At greater depths it appears that in places this relic permafrost may be either absent or out of reach of the electrode array at depths beyond about 55 m.

Once the model interpretations have been carried out for all the profile lines it is possible to prepare maps showing the varation of any interpreted parameter of interest. Figure 15 shows the variation of resistivity interpreted in the first sub-bottom layer. We assume that areas of 2 ohm-metres or less correlate with the areas in which the near-bottom materials are silty sands. Increasing resistivities above 2 ohm-metres represent increasing coarseness of the sand; resistivities above 2.3 ohm-metres are interpreted to indicate relatively clean sand.

In the central part of the survey area, high resistivities in this layer are observed near A and B. The borrow pit for the island was developed near B. It is interesting to observe high resistivities off to the east and to to the west. Without control we can only speculate on the likely reason for such high resistivities. It is possible that these resistivities represent coarse sands or possibly fine gravels. It is unlikely that they represent near bottom permafrost because the interpreted resistivities are still less than 3 ohm-metres.

Figure 16 shows the distribution of resistivity values interpreted for the third layer. High resistivites are

tentatively correlated with relic permafrost. Resistivities in this layer range from less than 30 ohm-metres to higher than 700 ohm-metres. In areas where the interpreted resisitivities are higher than a few hundred ohm-metres, the interpreted depths to the top are also shallowest (Figure 13). This is consistent with the concept of increased ice content in these layers. In some areas, interpreted resistivities are less than 30 ohm-metres and the depths are greater than 55 ohm-metres. In these areas, it appears that permafrost is either deeper than the range of sensitivity of the electrode array or entirely absent.

SUMMARY AND CONCLUSIONS

In this paper we have described the present configuration of the Hardy MICRO-WIP system for measuring sub-bottom electrical resistivity in a marine environment. This system was used successfully in the Beaufort Sea in the summer of 1985 to map sub-bottom resistivity variations associated with grain size variation in the near bottom and presumably with the presence of permafrost at greater depths.

This system can be set up in a survey boat of moderate size and can be used successfully in sheltered areas in collapsible boats for mineral exploration surveys as well.

It is clear that the sub-bottom resistivity information cannot be considered as a substitute for acoustic sub-bottom profiling. It is however a valuable complement to the sub-bottom profiling technique. In general, sub-bottom profiling techniques are sensitive to interfaces between materials, while the resistivity measurements represent bulk

values of the layers between interfaces. The ultimate interpretation can be obtained by correlating the thicknesses of electrical layers with the depths obtained in the acoustical profiling. In such a case, the modelling will determine interpreted resistivities for the layering identified in the acoustic sub-bottom profiling. These resistivities can be used to identify the type of material, the presence or absence or permafrost and possibly the presence of ice within permafrost. Future development is intended to be directed towards the refinement of resistivity estimates within layers identified by the profiling. Furthermore, it is expected that studies will show a correlation between resistivities and ice content in sub-bottom materials similar to that observed on land by Hoekstra and McNeil (1973).

ACKNOWLEDGEMENTS

We would like to thank C.S. Nelson of Esso Resources for extensive assistance in the carrying out of this survey and the preparation of the interpretation.

FIGURE CAPTIONS

Figure 1: Complex resistivity of permafrost samples as a function of temperature (after King and others, 1982).

Figure 2: DC resistivity sounding data on Beaufort Sea, April 1974. The dashed line linking the data points corresponds to the layered model shown below the curve.

Figure 3: MICRO-WIP system block diagram

Figure 4: Wave forms of transmitted current (I) and received voltage (V).

Figure 5: System installed in survey vessel. Controller and tape drive are nearest the camera, receiver with current monitor and magnetometer amplifier in centre, and transmitter farthest from camera.

Figure 6: Streamer on hand-powered winch.

Figure 7: Collapsible vessel for sheltered inshore and freshwater surveys.

Figure 8: Method of preparation of pseudosection of apparent resistivity.

Figure 9: Data presentation. The upper half displays bottom profile and sub-bottom reflectors identified with the acoustic systems. The lower half displays apparent resistivity values in pseudosection. The two diagonal lines in the pseudosection enclose a set of simultaneous readings.

Figure 10: Sounding curves and interpretation. The + symbols represent apparent resistivity values plotted against dipole number. The solid curve is derived from the model shown in the lowest part of the figure. The numbers in parentheses represent on an arbitrary scale the reliability to which each parameter is determined.

Figure 11: Theoretical demonstration of the sensitivity of the sytem to the presence of near-bottom permafrost. The data points are those shown in Figure 10. The two theoretical curve represent the soundings which would be observed if a 1-metre layer of permafrost of resistivities 12 and 24 ohm-metres is inserted in the previous model at sea bottom.

Figure 12: Location map, showing the survey area. The site of the island is shown as a black square within the survey area. Locations of the transponders used for navigation are also shown.

Figure 13: Interpretation of part of a line through the survey area near the future island site. The lower part of the figure shows a pseudosection of apparent resistivity, while the upper part shows the interpretation derived from the apparent resistivity measurements.

Figure 14: Acoustic record showing interpreted relic permafrost. The position of this reflector is shown in the section of Figure 13.

Figure 15: Contours of interpreted resistivity in the upper layer. Interpreted resistivity values greater than 2.1 ohm meters are correlated with coarse sands.

Figure 16: Contours of interpreted resistivity in the third layer. Interpreted resistivity values above 100 ohm-meters are correlated with the presence of permafrost.

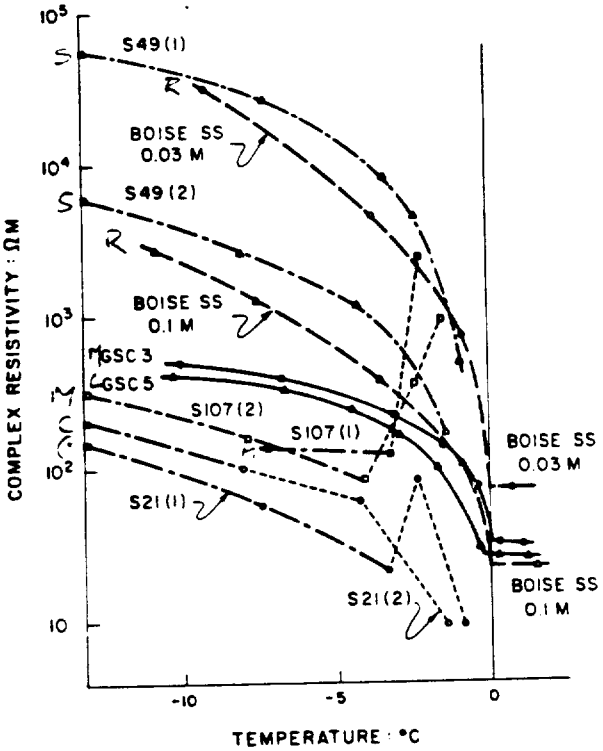

FIGURE 1 Complex resistivity of permafrost samples as a function of temperature.

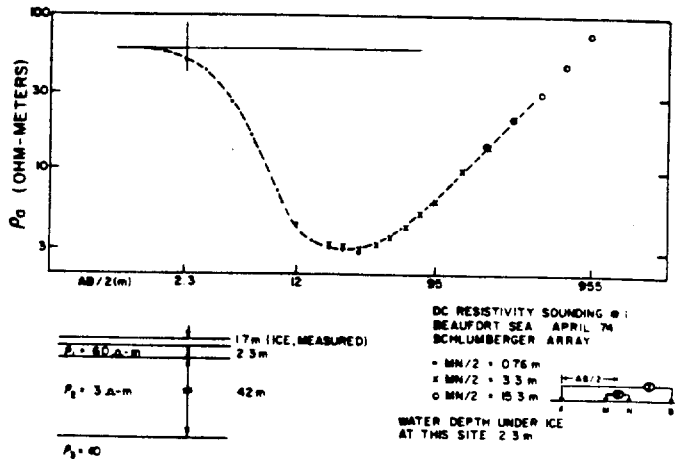

Figure 2 DC resistivity sounding data on Beaufort Sea, April 1974. The dashed line linking the data points corresponds to the layered model shown below the curve.

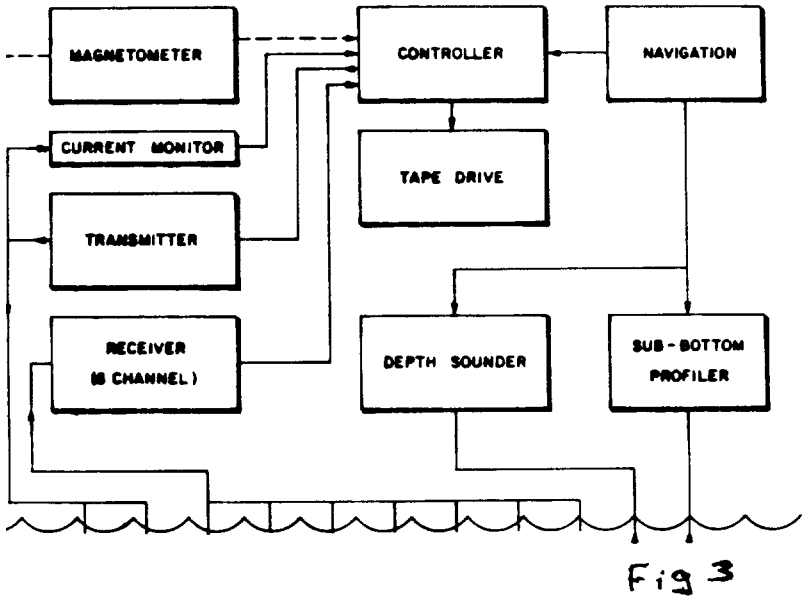

Fig 3

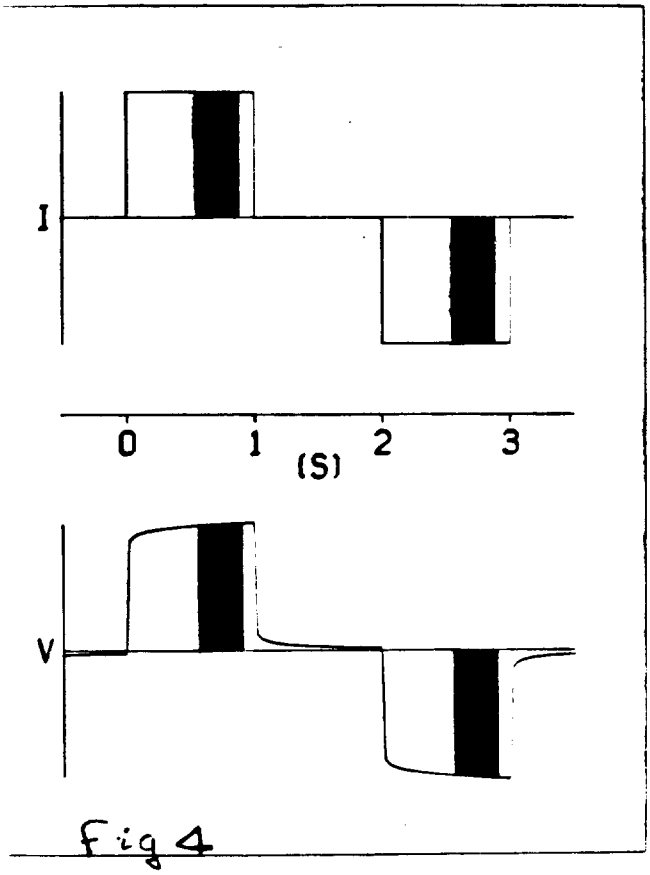

Fig 4

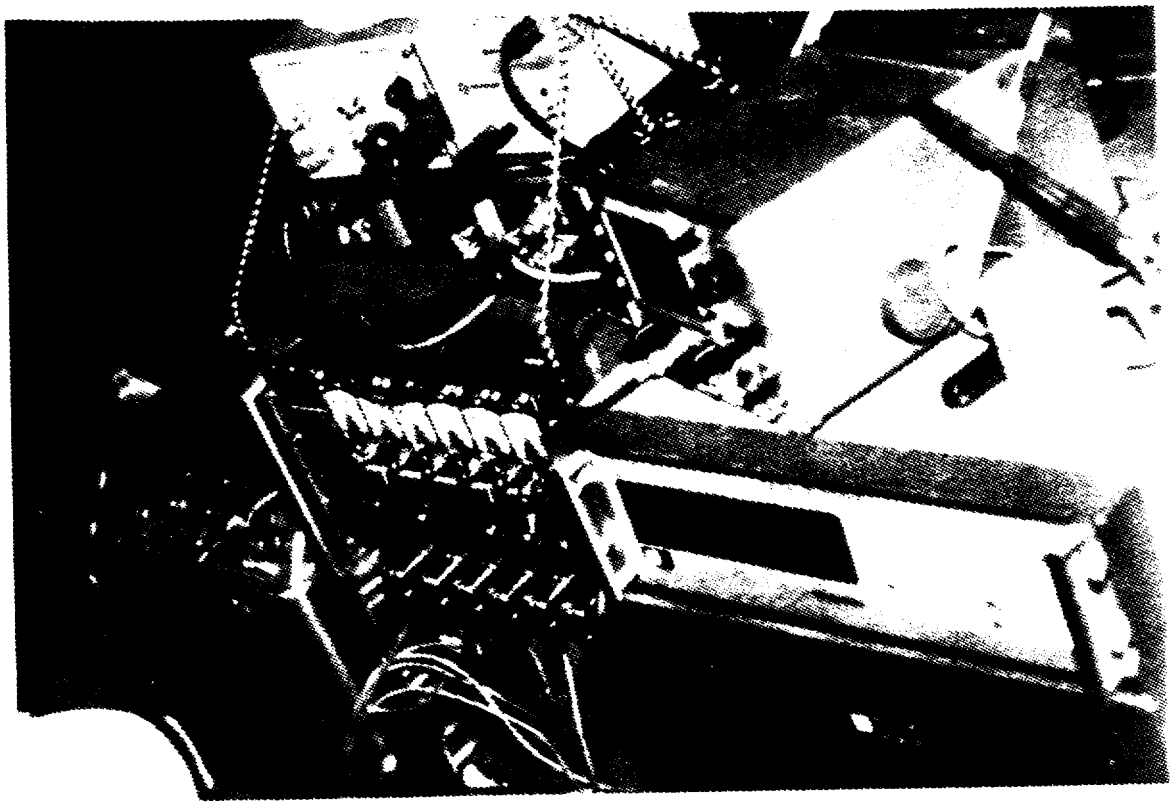

FIG 5

FIG 6

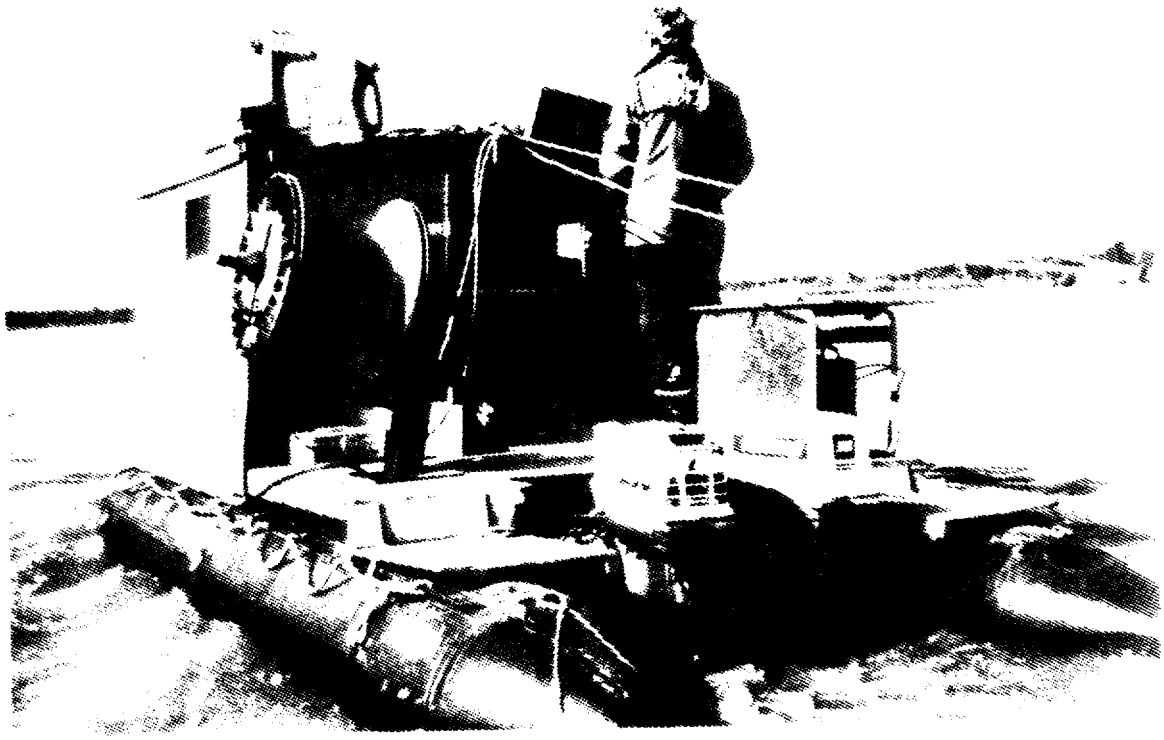

FIG. 7.

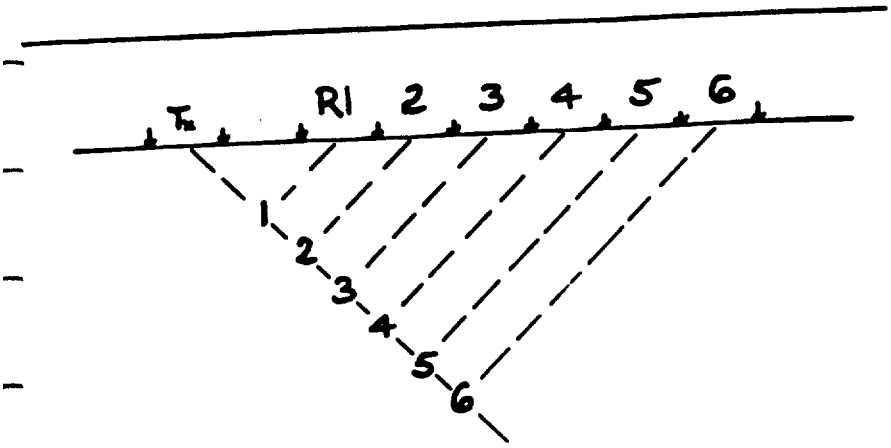

Fig 8 PSEUDO-SECTION

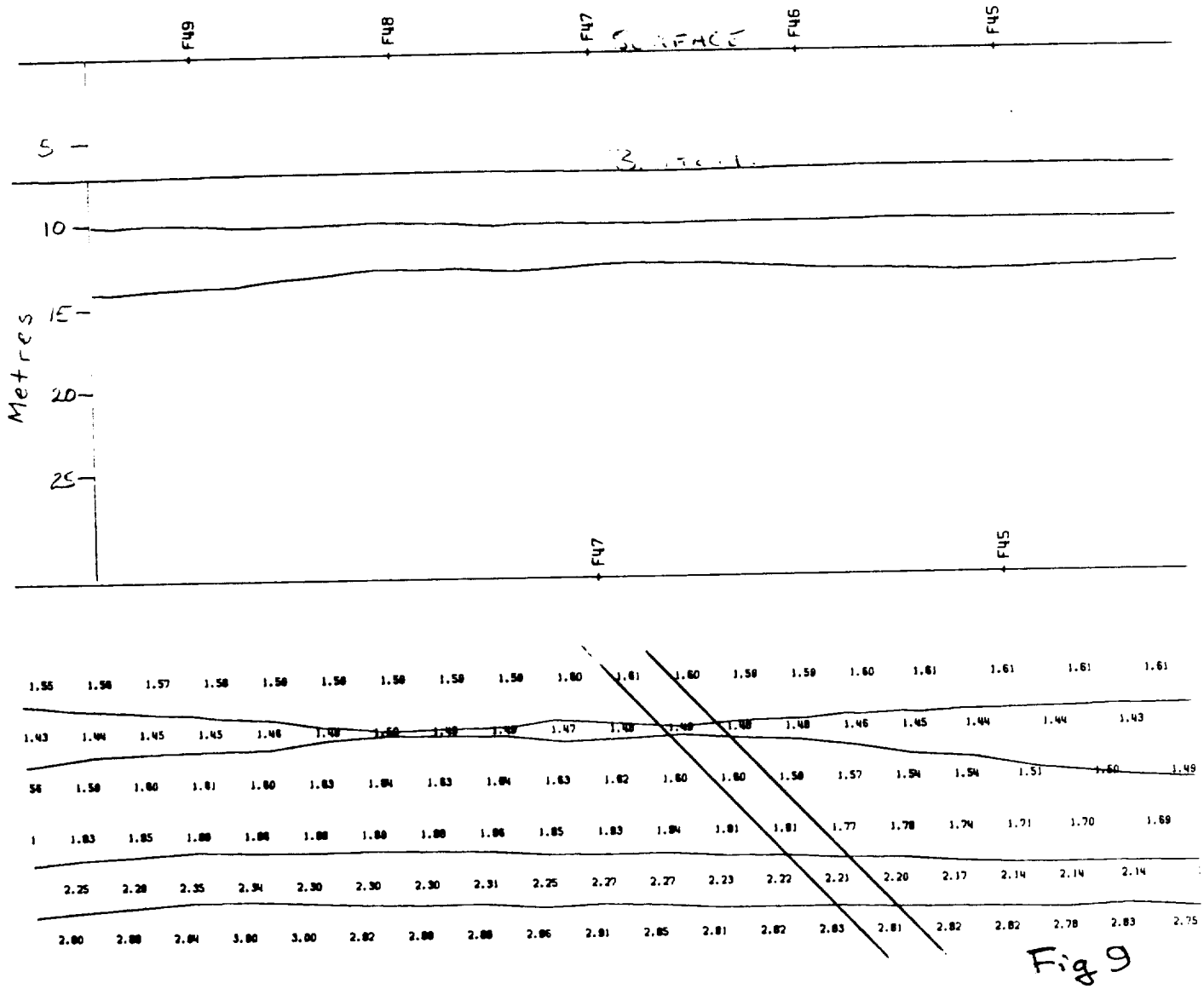

Fig 9

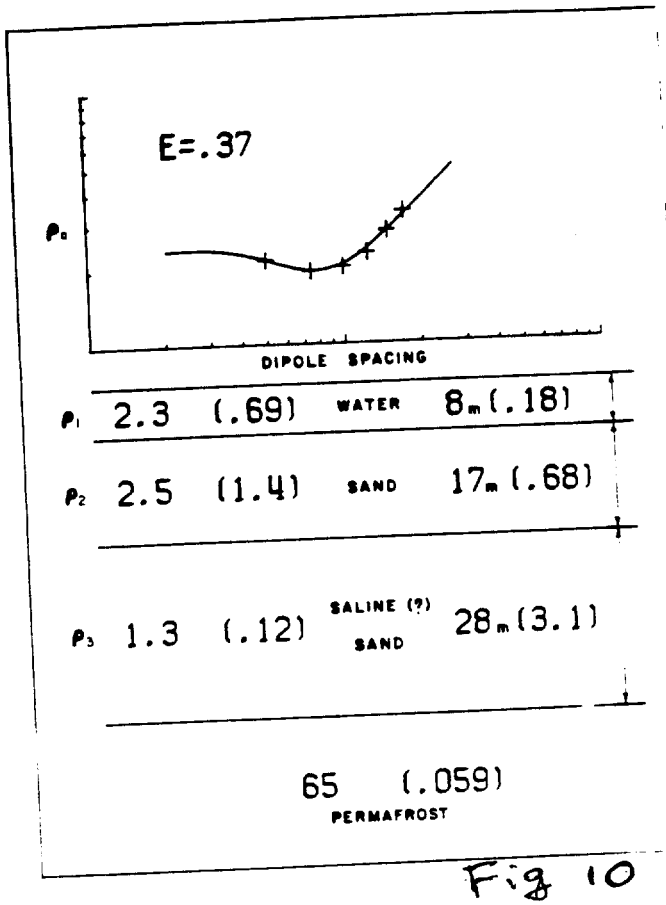
E=.37
ρ_a
DIPOLE SPACING
ρ_1 2.3 (.69) WATER 8m (.18)
ρ_2 2.5 (1.4) SAND 17m (.68)
ρ_3 1.3 (.12) SALINE (?) SAND 28m (3.1)
65 (.059)
PERMAFROST

Fig 10

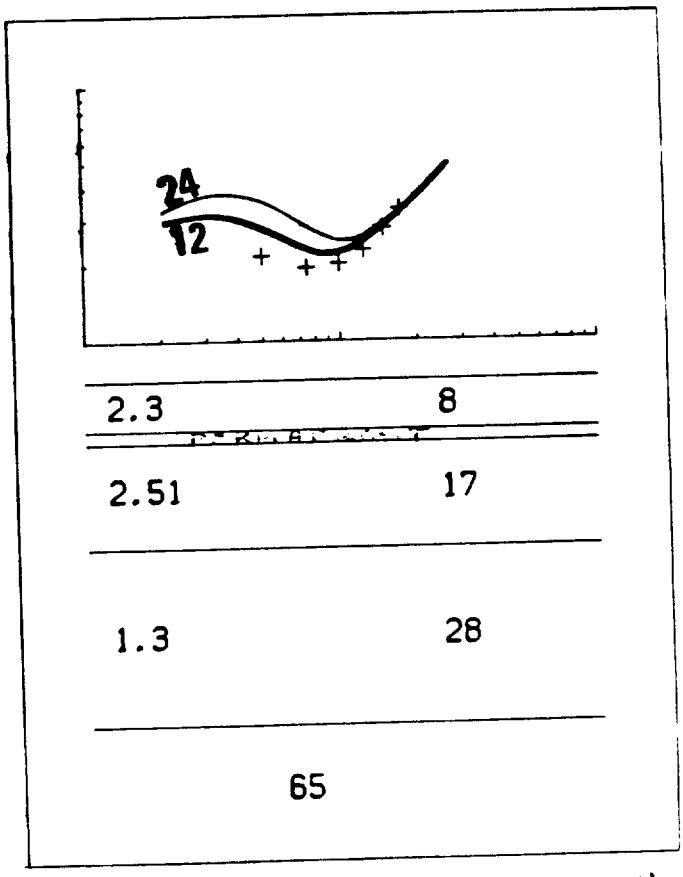
24
12
2.3
8
2.51
17
1.3
28
65

Fig 11

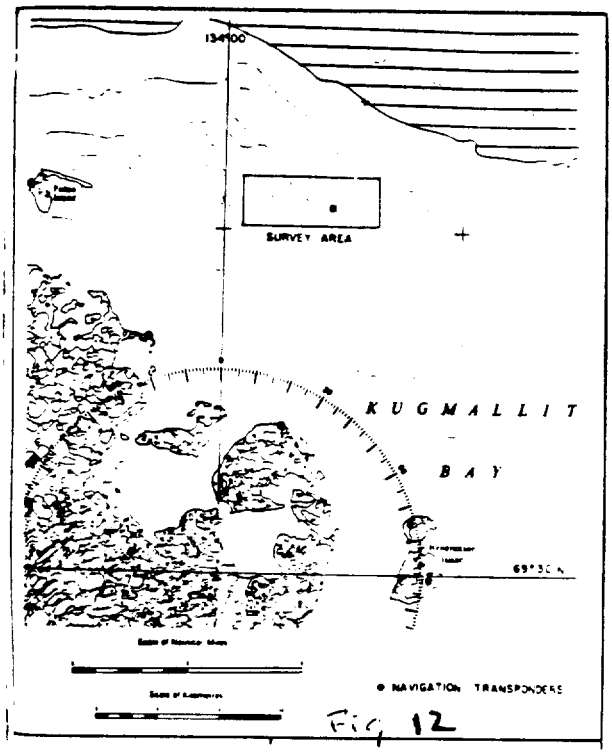

Fig 12

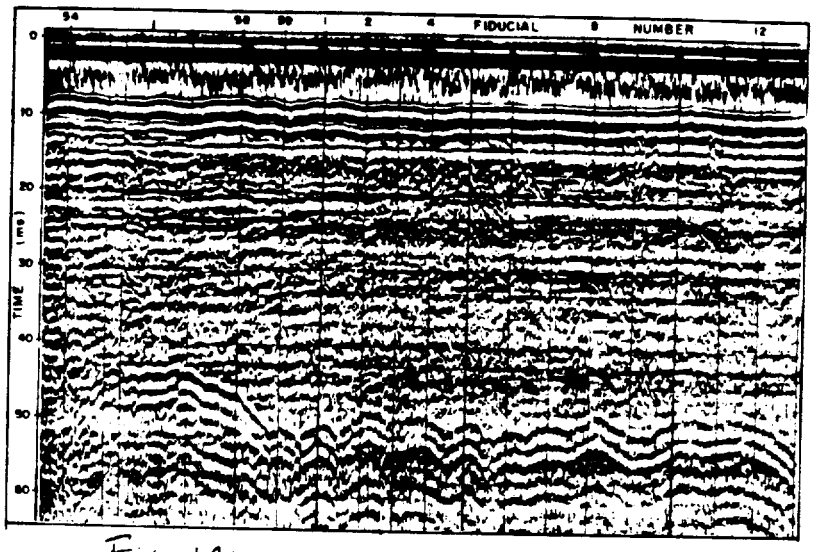

Fig 14

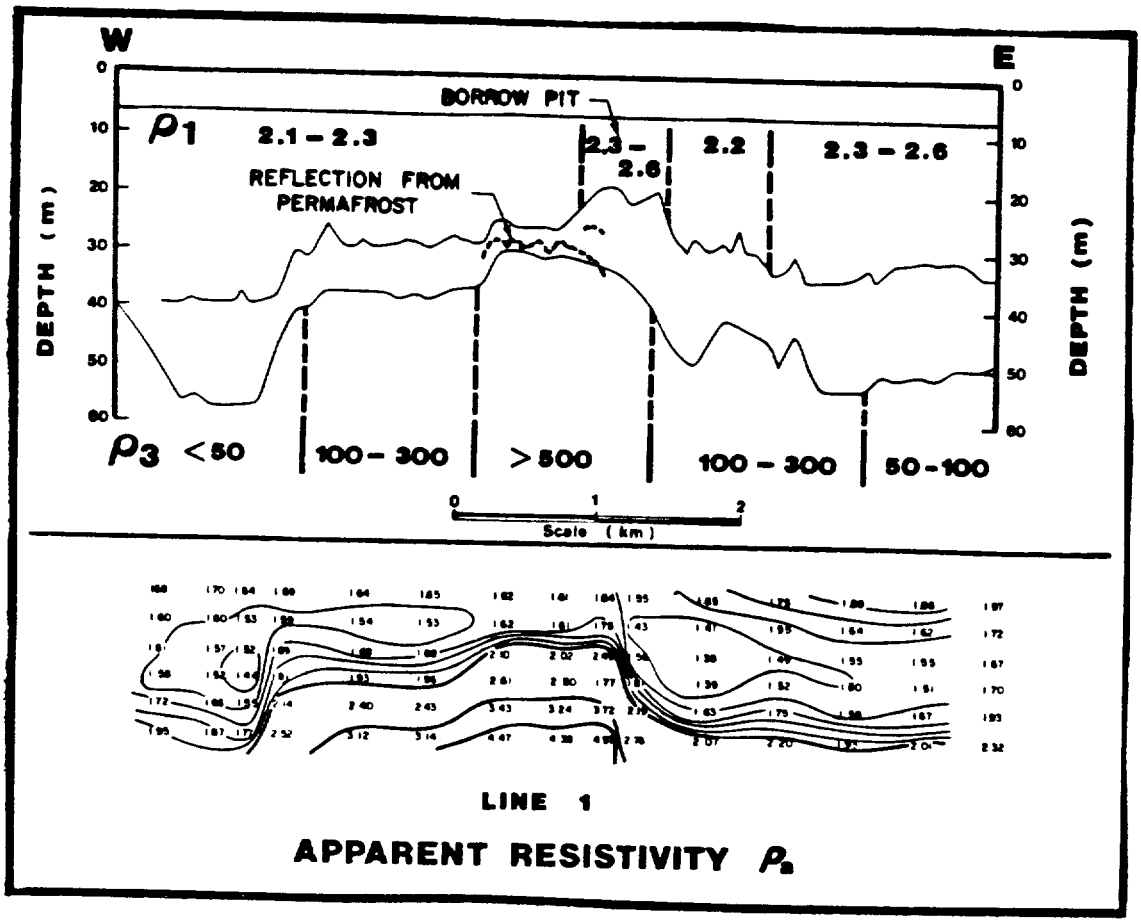

FIGURE 13: Interpreted Resistivity section

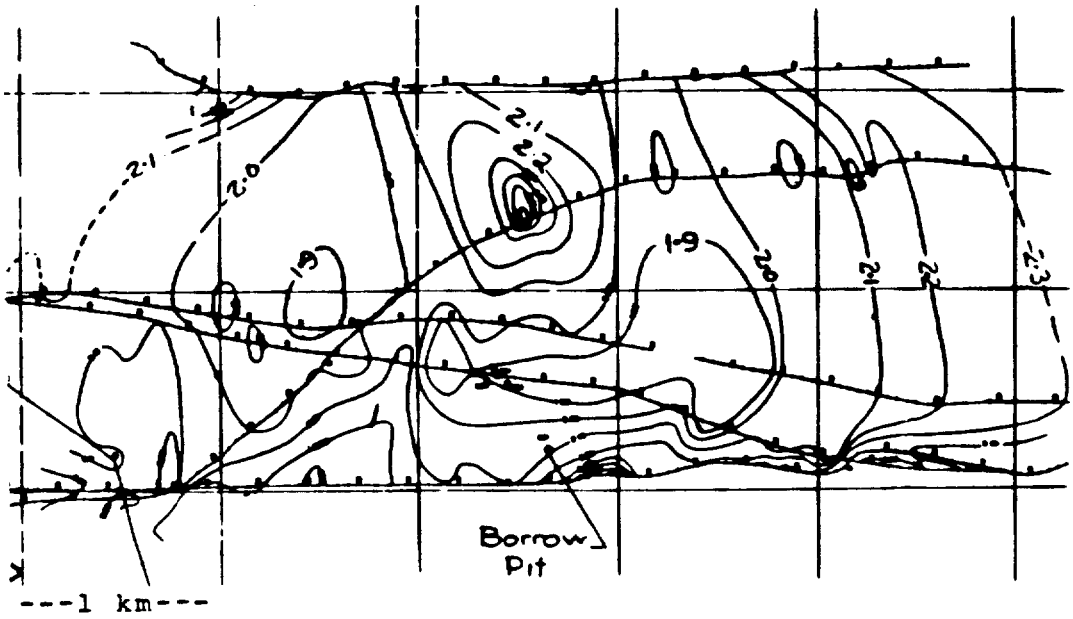

FIGURE 15: Interpreted resistivity of upper layer in ohm-metres

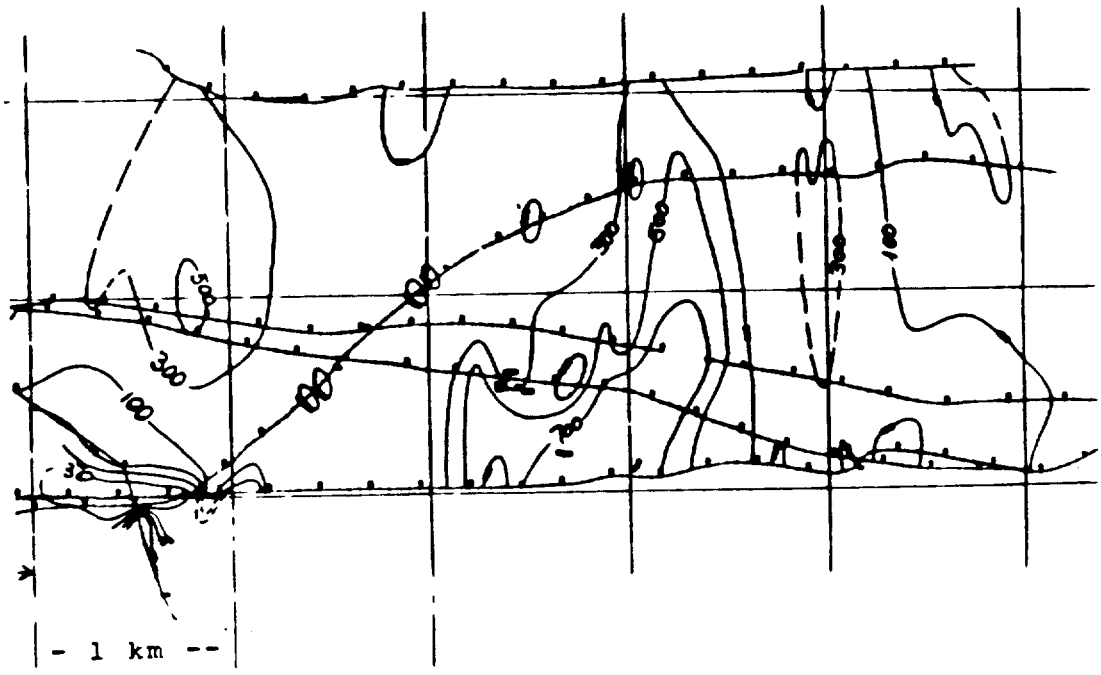

FIGURE 16: Interpreted resistivity of third (permafrost) layer in ohm-metres

37. PRELIMINARY EXPERIMENTS IN MARINE RESISTIVITY NEAR TUKTOYAKTUK, DISTRICT OF MACKENZIE

Project 670041

W.J. Scott
Resource Geophysics and Geochemistry Division

Introduction

During the spring and summer of 1974 marine resistivity soundings and profiles were carried out in three lakes on the Tuktoyaktuk peninsula and on Kugmallit Bay near Tuktoyaktuk.

The spring trials consisted of six resistivity soundings done through the ice, of which three were on Kugmallit Bay (1, 2 and 6, Fig. 1), two on Grass Lake (4 and 5, Fig. 1) and a sixth (3) on Kidney Pond near Grass Lake, not shown on Figure 1. The summer work involved two soundings, one on Grass Lake (7, Fig. 1) and the other on Kugmallit Bay (8, Fig. 1). In addition, the summer work included a number of resistivity profiles, made by towing an array behind a slowly moving boat.

The spring soundings were made in the same manner as soundings carried out on land, except that the electrodes, instead of being planted on the surface, were lowered through holes drilled in the ice and suspended at the base of the ice.

The summer soundings were taken by boat. A Schlumberger array was used. One boat was anchored at the centre of the array to carry the transmitter and receiver, while two other boats pulled out the current leads and tended the current electrodes. Both current and potential electrodes were supported at the water surface by buoys. The summer profiles were taken by towing a Wenner array behind a slowly-moving boat and taking readings at timed intervals.

Inflatable rubber boats 19½ feet in length were used as both electrode tenders and instrument carriers.

For the spring work and most of the summer as well, the electrodes were pieces of ¼" brass stock, bent in the shape of a thin U with legs about 30 cm long. Tin cans were tried during the summer, but were found to offer no advantage. Since the receiver potential values were quite stable, no attempt was made to use porous pots as electrodes, although these will be tried in future experiments.

The receiver for both winter and summer work was a standard McPhar R-103 resistivity receiver. The transmitter was a Huntec Lopo, modified in timing to produce a square wave output with a fundamental frequency of 0.3125 Hz. Current levels up to 500 ma were used, although most of the readings were made with currents of 100 ma.

Results

Table 1 presents in summary form a first interpretation of the sounding data, together with the available control for comparison.

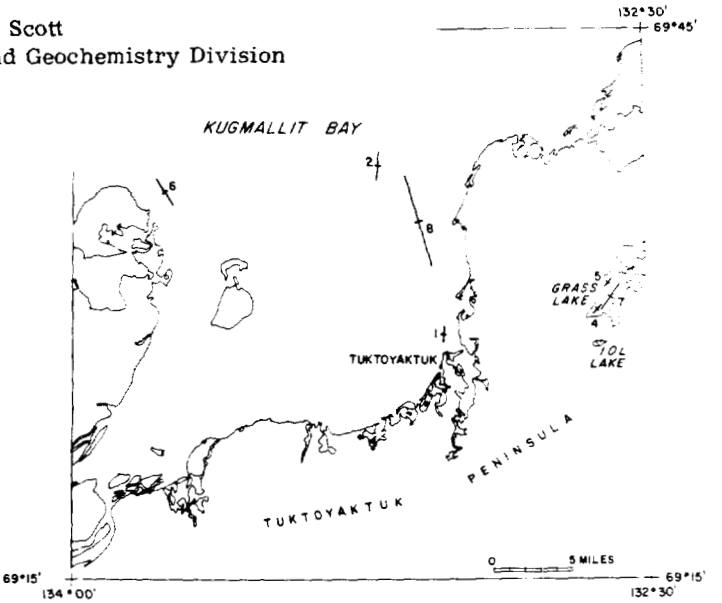

Figure 1. Map showing locations of soundings and profiles near Tuktoyaktuk, N.W.T.

1. Kugmallit Bay

Three spring soundings and one summer sounding were done on Kugmallit Bay. Figure 2a shows one of the spring soundings, and Figure 2b the summer one. The spring sites were those at which holes had been drilled by Hunter and Judge (pers. comm.) to look for the top of permafrost. The summer site was chosen for uniform water depth and ease of navigation (i.e. visibility of the DEW Line radome at Tuktoyaktuk).

The interpretations of the three spring-time soundings (Table I) agree reasonably well with the sparse control available, except for the depth to permafrost in sounding 6. The curve for the data of this sounding is not well-fitted, and a large discrepancy in depth is not surprising. More refined interpretation based on computer techniques will be made during this winter.

The water resistivities obtained from interpretation of the spring soundings may not be very reliable, as small variations in the depth of the potential electrodes made large differences in observed potentials for small values of AB/2. This variation was not observed for larger values of AB/2.

The spring-time soundings show a variable thickness of low-resistivity sediment overlying a layer of very high resistivity identified as permafrost. Since the unfrozen sediment has resistivities of the order of 3 ohm-m, the most that can be said of the high-resistivity layer is that the resistivity contrast is effectively infinite and that the high-resistivity value is probably greater than 300 ohm-m. The thickness of this layer

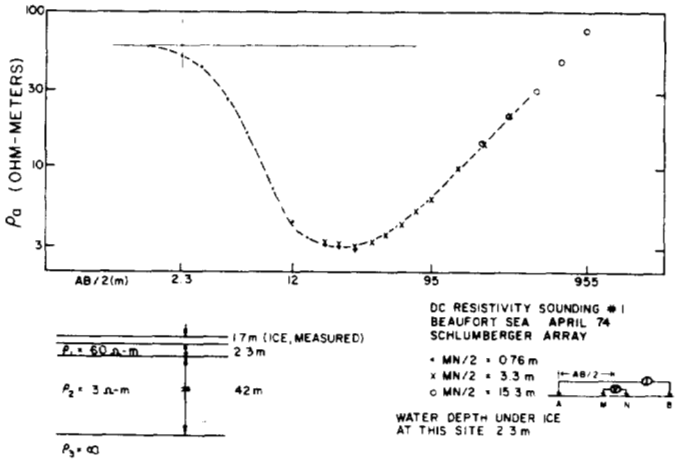

Figure 2a. DC resistivity sounding data on Beaufort Sea, April 1974. The dashed line linking the data points corresponds to the layered model shown below the curve.

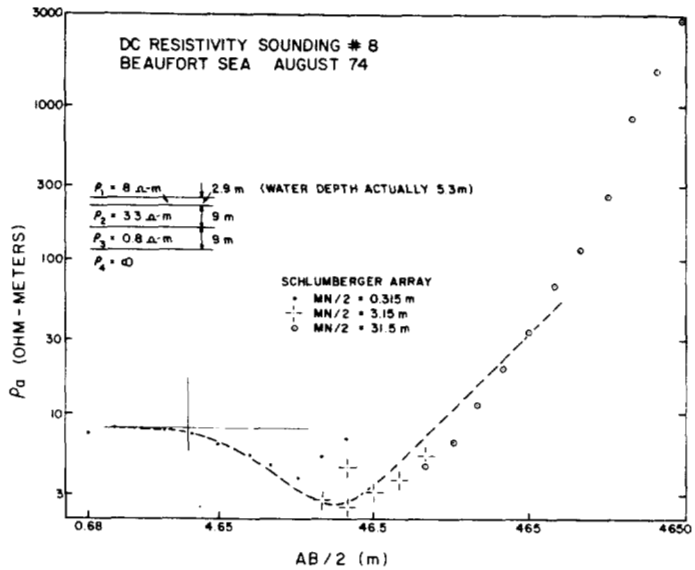

Figure 2b. DC resistivity sounding data on Beaufort Sea, August 1974.

is difficult to determine. A reasonable limit might be of the order of 300 to 400 m, but no evidence of this is seen even at AB/2 values of 1,500 m. A theoretical study is planned for this winter to determine the AB/2 value required to penetrate such thicknesses.

The summer-time sounding was undertaken primarily to try for greater AB/2 values, up to a maximum of 4,650 m. Unfortunately the summer sounding proved unreliable, for reasons which will be discussed below.

2. Grass Lake

At the time of the spring work, Grass Lake had frozen to the bottom, and in places up to 3 decimetres into the bottom sediments. The spring soundings were carried out by inserting the electrodes into the unfrozen sediment exposed at the bottom of holes drilled through the ice and frozen sediment. The two spring soundings were on resistivity lows indicated by an airborne E-Phase survey (Barringer, 1973) which were expected to correlate through taliks underlying at least part of the lake. Figure 3a shows one of the spring soundings, and Figure 3b the summer one.

Although no control is available on Grass Lake, the interpreted resistivities and depths from the winter work are consistent with drilling results on land between Grass and IOL Lakes (Rampton and Walcott, 1974a, b; Scott, unpubl. data). The material identifications in Table 1 are based on the land drilling data. In both spring soundings on Grass Lake, the ρ_a obtained for the largest AB/2 values was probably influenced by the proximity of the shore. In Figure 1, the length of the line indicates approximately the maximum span of the soundings. Thus the sudden rise in ρ_a at AB/2 values of 304 and 457 m is ascribed to the proximity of shore and near-surface permafrost rather than to the presence of permafrost under the lake.

Interpretation of the early (i.e. low AB/2 value) part of the summer sounding (Fig. 3b) agrees well with those of the two spring soundings. However, at greater AB/2 values, there is considerable scatter in ρ_a values, and the results are probably as unreliable as those of the summer sounding on Kugmallit Bay.

Figure 4 shows the results of two profiles made along the line of the summer sounding, with Wenner arrays of 5 and 15 m. At the ends of the line, nearshore, apparent resistivity values are quite high, and the presence of permafrost is thus indicated. Along the major part of the profile, however, ρ_a values are quite low, agreeing well with the values from the soundings. A further profile at a = 15 m was run across Grass Lake, crossing soundings 4 and 7, and penetrating into the southeast bay. The results on this profile resembled those on the first profile line. It appears that along these profile lines there is no permafrost within a few metres of the bottom, except very near the shore.

3. Kidney Pond

One spring-time sounding was carried out on Kidney Pond, a small body of water about 1 km south of Grass Lake. Kidney Pond is so small (200 m x 50 m) that the results were indecisive, as nearly all large AB/2 values reflect the influence of the shores of the pond.

4. IOL Lake

In an effort to outline the distribution of near-bottom permafrost, six Wenner profiles were surveyed during the summer on IOL Lake (Fig. 1) with an a-spacing of 5 m. The results are shown schematically on Figure 5. Apparent resistivities ranged from 30 ohm-m to 500 ohm-m with most values concentrated at the low and high ends of the range, and very few values observed between 50 and 200 ohm-m. A level of 150 ohm-m was

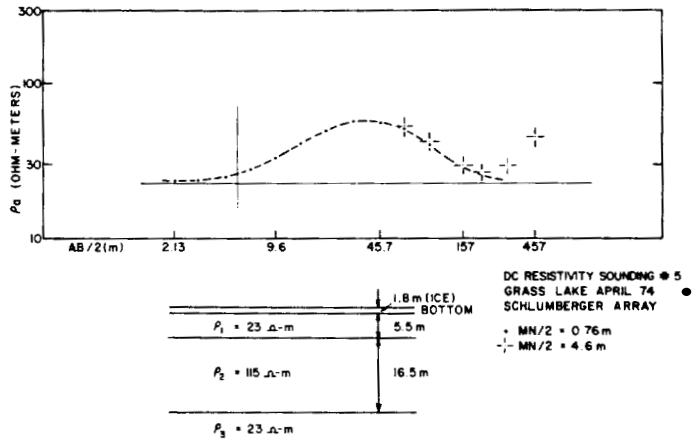

Figure 3a. DC resistivity sounding data on Grass Lake, April 1974. The dashed line linking the data points corresponds to the layered model shown below the curve.

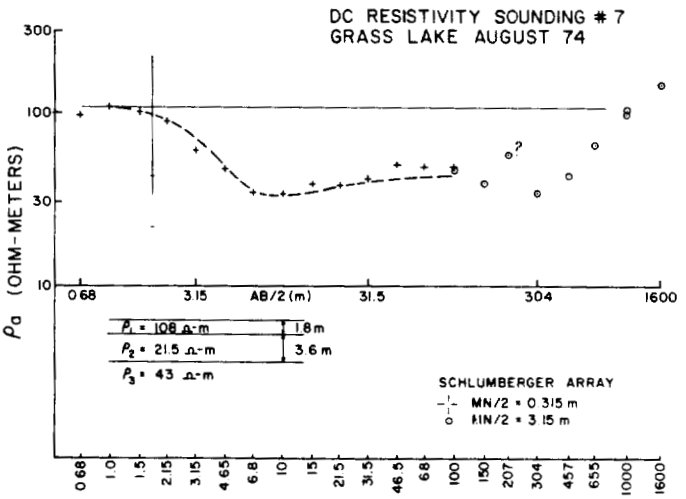

Figure 3b. DC resistivity sounding data on Grass Lake, August 1974.

TABLE I

Preliminary Interpretation of Soundings

SDG	PLACE & SEASON	CONTROL				INTERPRETATION												
		Thicknesses		Depth to Permafrost	ρ water from sample	ρ_1	t_1	ID	ρ_2	t_2	ID	ρ_3	t_3	ID	ρ_4	t_4	ID
		Ice m	Water m	m	Ω-m	Ω-m	m		Ω-m	m		Ω-m	m		Ω-m	m	
1	Kugmallit Bay Spring	1.7	2.3	54	24	60	2.3	water	3	42	Unfrozen sediment (saline?)	∞	?	Permafrost depth=46 m			
2	Kugmallit Bay Spring	2.1	3.6	> 52	-	64	3.7	water	1.6	93	Unfrozen sediment (saline?)	∞	?	Permafrost depth=99 m			
6	Kugmallit Bay Spring	1.1	1.4	67	26	35	1.3	water	2.7	110	Unfrozen sediment (saline?)	∞	?	Permafrost depth=113			
8	Kugmallit Bay Summer	-	5.3	-	-	8	2.9	water	3.3	9	Unfrozen sediment	0.8	9	Unfrozen sediment	∞	?	permafrost
4	Grass Lake Spring	1.3	0	-	-	25	3.6	unfrozen clay	62	54	Unfrozen sands & gravels	25	?	Unfrozen sands			
5	Grass Lake Spring	1.3	0	-	-	23	5.5	unfrozen clay	115	17	Unfrozen sands & gravels	23	?	Unfrozen sands			
7	Grass Lake Summer	-	1.7	-	-	108	18	water	21.5	3.6	Unfrozen clay ?	43	?	Unfrozen sands & gravels			
3	Kidney Pond (near Grass Lake) Spring	2.0	1.2	-	-	124	2.1	water	12.4	2.1	Unfrozen organics?	∞	?	Edge of Pond			

chosen arbitrarily to represent the division between permafrost (ρ_a > 150 Ω-m) and non-permafrost (ρ_a < 150 Ω-m) zones. The transition from permafrost to non-permafrost on each profile appeared to coincide with increases in water depth. The distribution of permafrost shown in Figure 5 agrees approximately with that deduced by Hunter (pers. comm.) from refraction seismic measurements.

Discussion

Both summertime soundings suffered from the problem of current leakage. Some of the wire used in the current leads was somewhat aged, and patched in many places. Prior to the work the wire was inspected closely, and all cuts and splices were taped first with self-vulcanizing rubber tape and then with

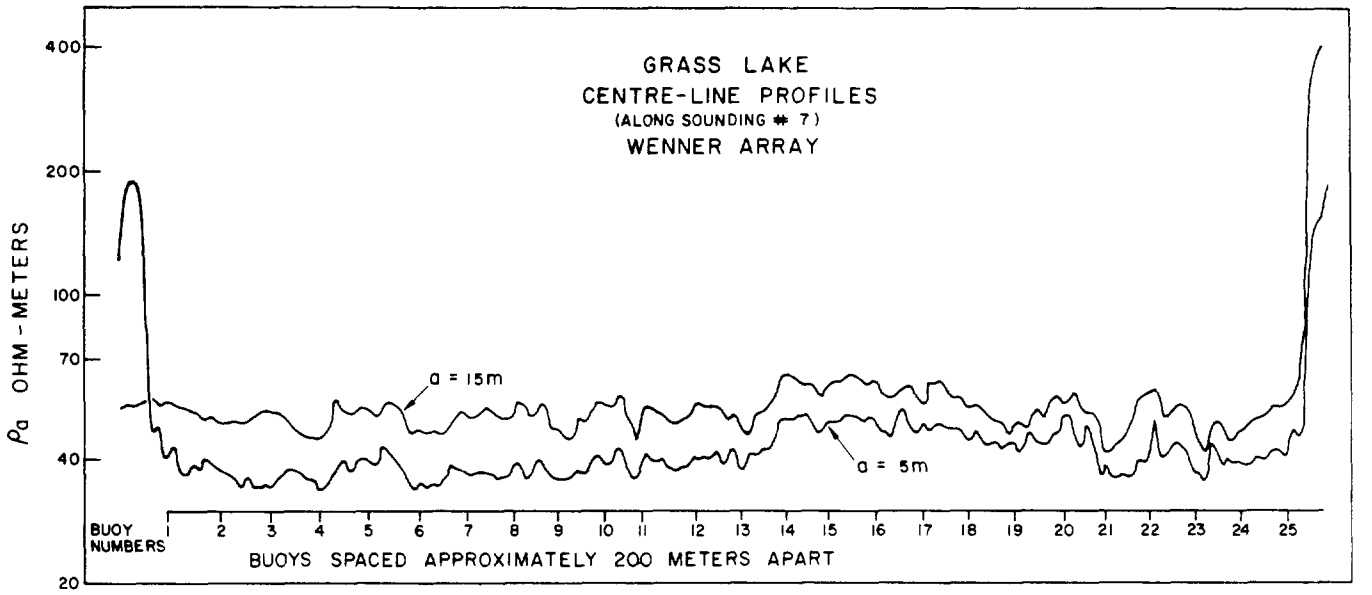

Figure 4. DC resistivity profiles on Grass Lake, along the line of the sounding shown in Figure 3b.

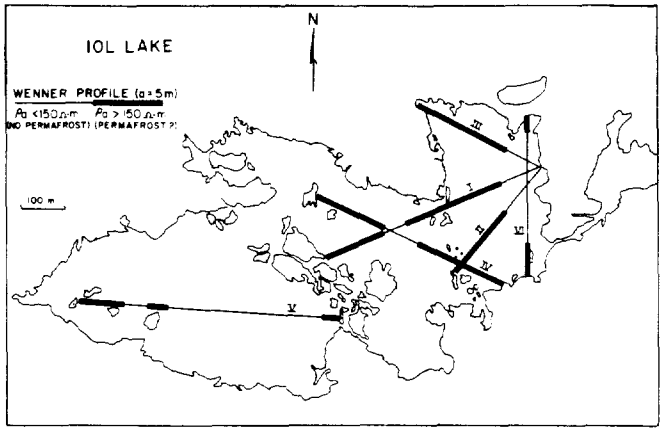

Figure 5. Map of DC resistivity profiles on IOL Lake, August 1974, showing interpreted distribution of permafrost.

standard plastic electrical tape. Erratic readings at large AB/2 values in sounding 7 were attributed to current leakages from specific splices, which were re-taped as well as possible. However, the repair jobs were badly strained during the recovery of wire from the bottom after sounding 7, and it was observed during sounding 8 that for large AB/2 values the resistance between the two current leads with the electrodes out of the water was only two or three times that with the electrodes immersed in the water. Consequently it is felt that particularly for large values of AB/2, the results of soundings 7 and 8 are at best unreliable and at worst useless. Attempts will be made this winter to correct the results for leakage on the assumption of a line-source of current, but the outcome is not viewed with optimism, since it is unlikely that the leaks are uniformly distributed along the wire.

The spring-time soundings, on the other hand, are of reasonably high quality. Since the work was done in early spring, while daytime temperatures were still around -20°F to -40°F, the ice surface was dry, and current leakage was not a problem. Over the length of a sounding, water depth typically varied less than ten per cent and values of ρ_a obtained for different MN/2 but the same AB/2 varied only slightly. Unfortunately the contrast between permafrost and non-permafrost resistivities was so great that very large values of AB/2 may be required to probe beneath the permafrost. Further experiments are planned for this spring on sea ice, both in Kugmallit Bay, and hopefully farther out to sea.

From a logistical point of view, it appears that deep marine soundings may well be more efficiently carried out with a dipole-dipole rather than with a Schlumberger array. The consensus among the crew handling the wire this summer was that six miles of wire was beyond the limit for efficient operation. The disadvantage of a dipole-dipole array is the requirement for higher transmitted power levels, which calls for a motor-generator unit, and a general increase in scale, which in turn precludes the use of small inflatable rubber boats such as were employed this summer. Experiments are planned for next summer, in which both Schlumberger and dipole-dipole arrays will be employed.

The resistivity profiling technique appears most promising. The experiments this year were limited by the fact that the present receiver is single-ended, and thus cannot tolerate small signal levels when both receiver electrodes are far from the receiver location. By next summer it is expected that this problem will have been overcome. Larger arrays will be employed (i.e. larger values of a), and attempts will be made to use multiple a-spacings simultaneously. In these experiments comparisons will be made among various arrays.

Conclusions

The most interesting outcome of these preliminary experiments is that marine resistivity is not only feasible but also potentially very rewarding. Both profiling and sounding techniques appear to offer considerable subsurface information, some of which may not be available through other geophysical techniques.

The results of the work described here are sufficiently encouraging to warrant further experiments in the coming season. Further evaluation of the technique must await the results of this work.

Acknowledgments

The spring-time work was carried out by the author with the able assistance of D.C. Butterfield (GSC) and Ranley Felix (PCSP, Tuktoyaktuk). The name Grass Lake arises from a joke perpetrated by Mr. Felix and not recognized by the author until too late.

The summertime work was carried out by D. Eberle (Geological Survey of Germany), Colin Mathieson, Barry Malmsten, Alan Cox and Euan Mathieson (students employed by the GSC for the summer) and the author.

Special thanks are due Mr. Cox for his selfless dive into the Beaufort Sea to free one of the boats at a critical point in the carrying out of sounding no. 8.

Initial encouragement to experiment with marine resistivity came from J.R. MacKay (UBC) and J.A. Hunter (GSC).

The names of lakes in this paper are strictly abritrary, and have no official standing.

References

Barringer Research Ltd.
1974: Airborne resistivity E-phase surveys over four areas in the Northwest Territories; GSC Open file 222.

Rampton, V.N. and Walcott, R.I.
1974a: The detection of ground ice by gravity profiling; Presented at Symposium on Permafrost Hydrology and Geophysics, Calgary, Feb. 1974.

1974b: Gravity profiles across ice-cored topography: Can. J. Earth Sci., v. 11, no. 1, p. 110-122.

OTC 4468

Water-Borne Resistivity/Induced Polarization Survey in Prudhoe Bay

by W.J. Scott, *Hardy Assocs. (1978) Ltd.*; J.S. Laing,* *Consultant*; and W.J. Botha, *Hardy Assocs. (1978) Ltd.*
*Formerly with Hardy Assocs. (1978) Ltd.

This paper was presented at the 15th Annual OTC in Houston, Texas, May 2-5, 1983. The material is subject to correction by the author. Permission to copy is restricted to an abstract of not more than 300 words.

ABSTRACT

During August 1982, a marine resistivity/induced polarization (IP) Survey was undertaken in Prudhoe Bay, Alaska. Multi-electrode arrays with inter-electrode spacings of 10 metres and 25 metres were used to survey a total of 34 line kilometers. Apparent resistivity values were considerably higher over known granular materials. No strong IP responses were observed. The use of marine resistivity measurements in conjunction with high-resolution sub-bottom profiling can improve the chances of finding granular materials in shallow offshore waters.

INTRODUCTION

During late August 1982, a marine resistivity/induced polarization (IP) survey was undertaken in Prudhoe Bay, Alaska. The purpose of the survey was to determine whether the system could be used to detect and map gravel deposits in the Bay.

TECHNICAL APPROACH

From measurements of resistivity made on land it is clear that the resistivity of sub-surface materials increases with increasing grain size. Thus coarse-grained materials such as sand and gravel have higher resistivities than fine-grained silts and clays. This resistivity-grain size dependence remains true even when the materials are saturated with saline water.

Sub-bottom materials tend to have higher resistivities when frozen (i.e. ice-bonded) than when not frozen. The presence of permafrost in the sub-bottom will be observed as higher resistivities. A frozen clay could in this manner give rise to apparent resistivities comparable to those associated with unfrozen coarse-grained materials. However there is evidence (Olhoeft 1975) that frozen clays exhibit an induced polarization response which is not present in unfrozen coarse-grained materials.

The IP effect can be observed as a small transient voltage which exists in a polarizable medium after interruption of electric current flow. This transient is generally two orders of magnitude lower than the voltage drop in the medium during current flow. It has time constants in the 0.1 to 10 second range. (IP effects also arise in the presence of metallic sulphides; IP measurements are frequently used in prospecting for metals).

The measurement of apparent resistivity and IP effects can be expected to provide sufficient information to detect and map gravel distribution in the sub-bottom. High resistivities with no IP response would imply the presence of gravels, while high resistivities and an IP response would suggest the presence of frozen fine-grained sediments. This situation is analogous to that observed on land, where measurement of electrical response is a widely-accepted means of mapping granular deposits and permafrost distribution.

RESISTIVITY AND INDUCED POLARIZATION MEASUREMENT

The resistivity/IP measurement system used in this survey has been developed by Hardy Associates (1978) Ltd. over the past three years. Figure 1 is a schematic illustration of the system.

The system measures the electrical resistivity of sub-bottom materials by injecting electric current into the water from a pair of electrodes and measuring the resulting voltages between successive pairs of electrodes equally spaced at increasing distances from the current electrodes. The electric current is supplied by a Huntec (70) Ltd. M4 IP transmitter, capable of producing 20 amperes at power levels up to 7.5 KVA. The current waveform is an interrupted square wave with a period of 4 seconds. Current flows in one direction for one second, is interrupted for one second to permit IP measurements, flows in the other direction for one second, and is again interrupted for one second.

The receiver electrodes are non-polarizing Cu-Cu SO_4 systems modified from a design by Corwin and Corti (1973).

References and illustrations at end of paper.

The voltages across 6 successive pairs of receiver electrodes are amplified by the receiver system, and digitized by a Sonotek SDS 1200 data acquisition system, at a rate of 256 Hz. The digitized signals are written on 9-track tape, together with water-depth values and navigation information.

Apparent resistivities are calculated from the digitized voltages during the current "on" time as follows:

$$\rho_a = \pi . X . n(n+1)(n+2) . Vp/I \quad \ldots\ldots\ldots (1)$$

ρ_a = apparent resistivity in ohm-metres

X = spacing between adjacent electrodes

n = number of X values separating the nearer potential electrode from the nearer current electrode

V_p = primary voltage, measured during current flow

I = transmitted current

The IP effect, which is measured in terms of apparent chargeability, is calculated from the intergated transient voltage during the "off" time as follows:

$$M_a = \frac{1}{V_p} \int_{t1}^{t2} Vs\ (t)dt \quad \ldots\ldots (2)$$

Ma = apparent chargeability in millivolt seconds/volt or milliseconds

Vs = transient voltage after current turnoff

t1 = 20 milliseconds after current turnoff

t2 = 920 milliseconds after current turnoff

NAVIGATION

The navigation system employed in the survey was based on a del Norte Trisponder system, which provided ranges to two or more known remote positions, updated every second. Normally the Trisponder ranges are used by an on-board Hewlett-Packard 9835A microcomputer to provide the helmsman with a constantly-updated visual display of ship position relative to shore and to the desired survey line. In this survey, however, because of problems with the HP 9835A, the survey lines were run on dead reckoning, and boat track was subsequently recovered from recorded Trisponder data.

BOAT

The navigation and electrical survey equipment were mounted in a 6-metre Zodiac inflatable rubber boat. The Zodiac has the advantages of portability and adequate seaworthiness for inshore work, combined with shallow draft. For offshore work the system could be mounted in a larger vessel.

SURVEY RESULTS

Figure 2 shows the location of the survey lines. These lines were surveyed with two electrode arrays. The first array had an inter-electrode spacing of 10 metres, while the second had a spacing of 25 metres. Figures 3 and 4 show portions of the results obtained with the two arrays, over the northern part of line C, near Gull Island.

The apparent resistivity and apparent chargeability values are plotted in pseudosection. In this display, the value is plotted midway between the centres of the transmitter and receiver electrode pairs, at a depth determined by the separation between the pairs. Although the pseudosection is a convenient means of display, it does not represent a true depth-section.

In both Figure 3 and Figure 4 higher apparent resistivities are observed in the vicinity of Gull Island, in an area of known granular material. There is unfortunately considerable scatter in the chargeability data. No systematic apparent chargeability increase is observed to correlate with the apparent resistivity increase. Thus it appears that the system is responding to the change in resistivity of the sub-bottom, which results from the presence of the granular material.

In addition to the area of high resistivity close to Gull Island, three areas of higher resistivity were interpreted to represent near-bottom granular material. Figure 2 shows the approximate locations of these areas.

DISCUSSION

This survey has demonstrated the feasibility of making resistivity measurements in a marine environment. The IP results were rather disappointing, however. Subsequent work on the measurement system has reduced the noise level by about 40 db, and subsequent fresh-water surveys have shown that with reduced noise, the IP measurement can be made with reliability. The utility of IP measurement for identifying ice-bonded permafrost remains to be proven.

This system has also been used in prospecting for metallic minerals. For this purpose we have fitted a marine magnetometer with one-gamma total field resolution.

The electrical measurements described in this paper have been designed as an adjunct to seismic sub-bottom profiling, and not as a substitute. In subsequent fresh-water work, a Raytheon RTT-1000 sub-bottom profiler was added to the system. The combined interpretation of electrical and seismic results increased the confidence level of the work considerably. For the future, the integrated seismic and electric survey system offers increased reliability of determining the presence of coarse-grained materials, and possibly enhanced capability for the detection fo sub-bottom permafrost.

REFERENCES

1. Olhoeft, G.R.: The Electrical Properties of Permafrost. Ph.D., Thesis, University of Toronto (1975)

2. Corwin, R.F. and Corti, U.: A rugged silver-silver chloride electrode for field use. Rev. Sci. Inst. (1973) 44, 708-711

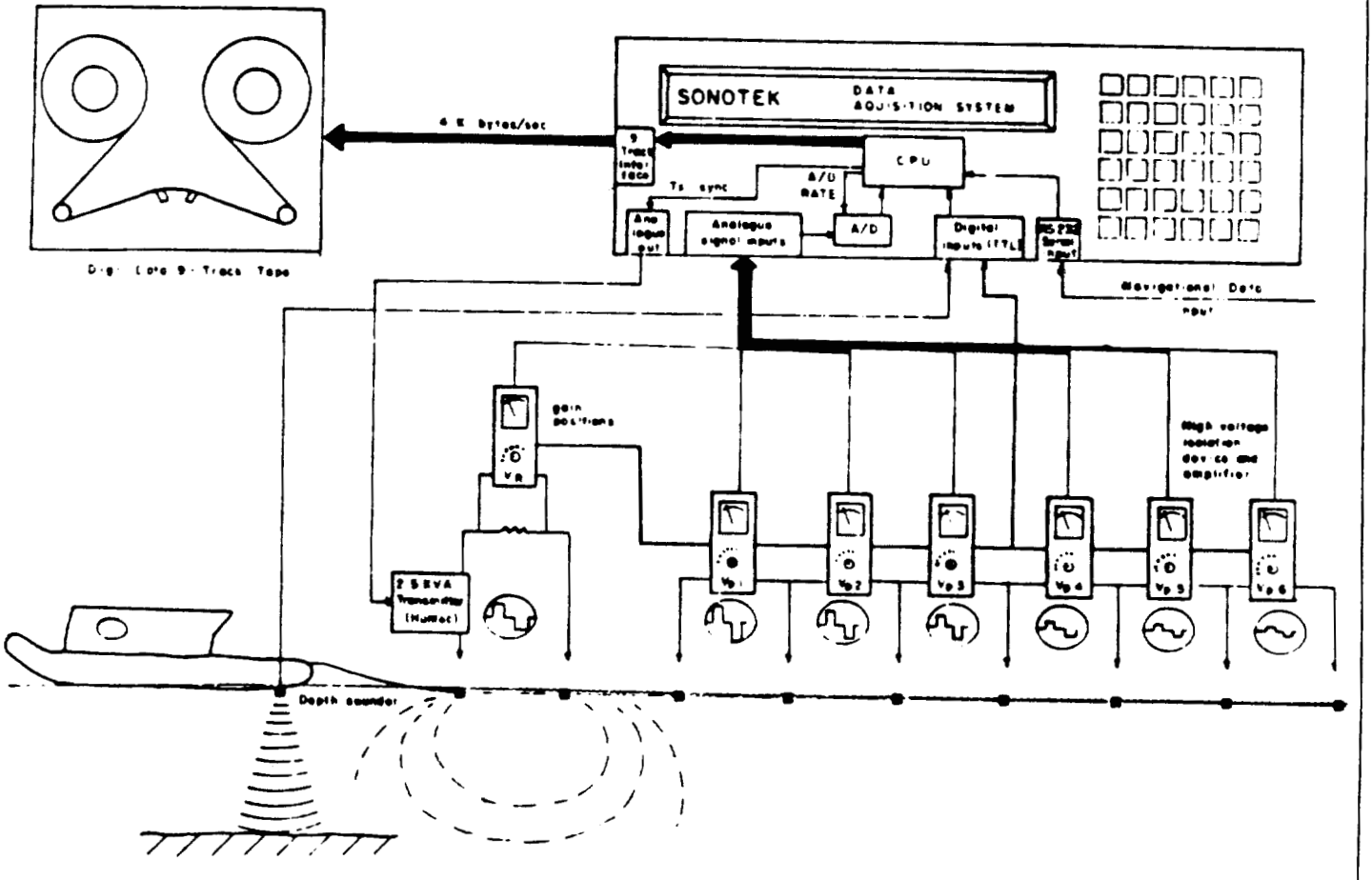

Fig. 1—Schematic illustration of the marine resistivity/induced polarization system.

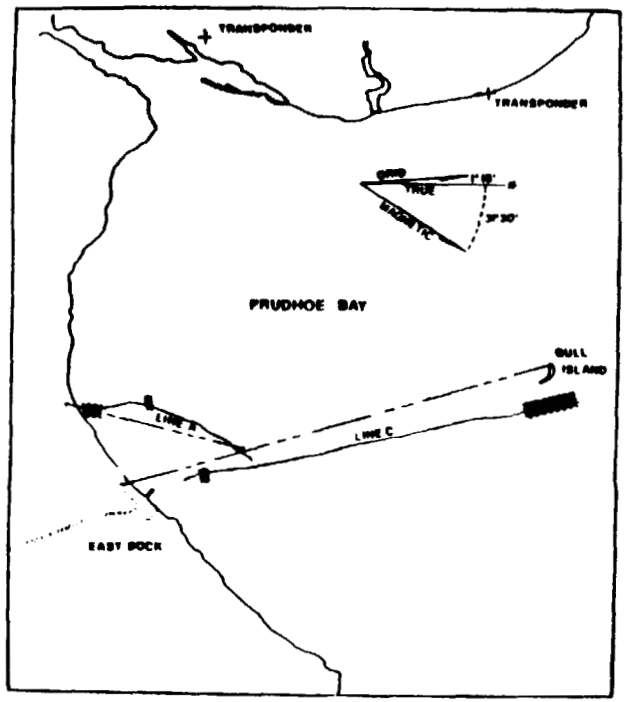

Fig. 2—Survey area in Prudhoe Bay. The cross-hatched areas indicate high-resistivity areas interpreted as gravel.

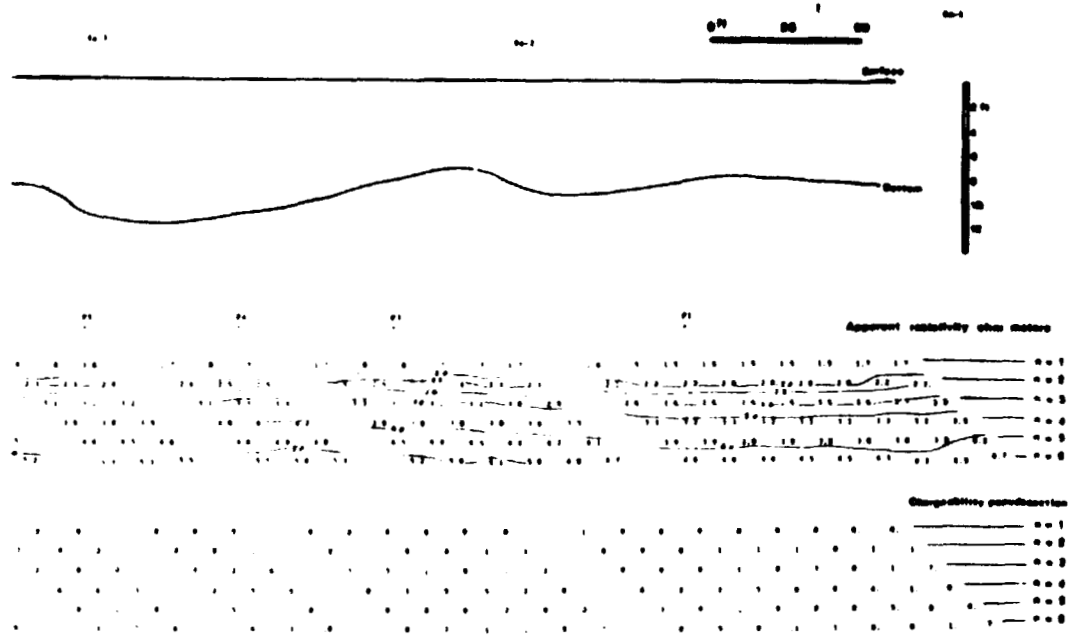

Fig. 3—Water-depth profile and pseudosections from part of the survey with 10-m electrode spacings, corresponding to the cross-hatched area south of Gull Island.

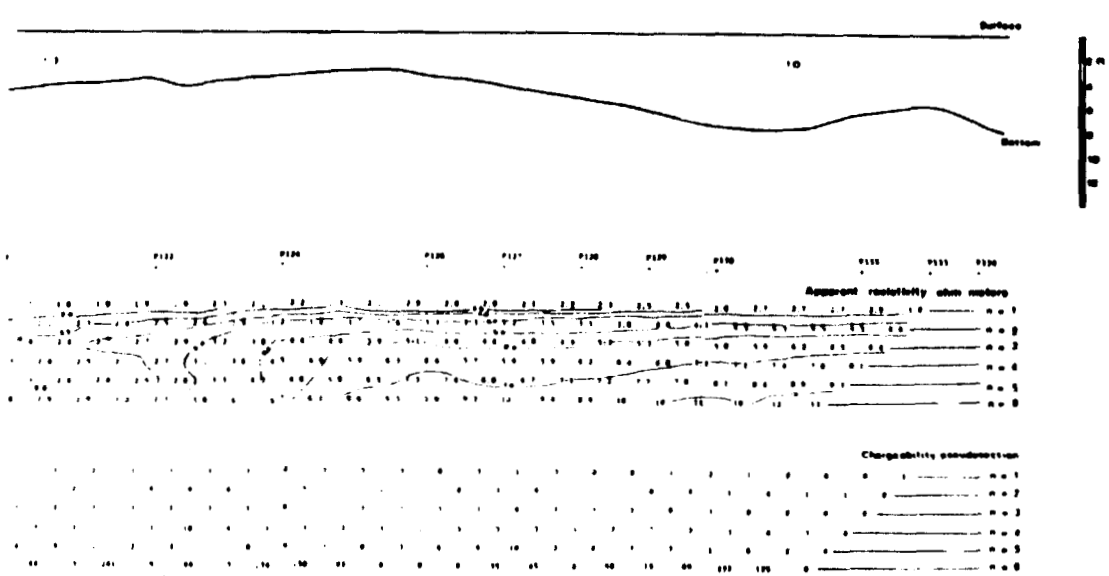

Fig. 4—Water-depth profile and pseudosections from part of the survey with 25-m electrode spacings, in approximately the same position as Fig. 3.

24. WATERBORNE RESISTIVITY/INDUCED POLARIZATION SURVEY OF COLLINS BAY, WOLLASTON LAKE

A.V. Dyck[1], W.J. Scott[2], and J. Lobach[3]

Dyck, A.V., Scott, W.J., and Lobach, J., Waterborne resistivity/induced polarization survey of Collins Bay, Wollaston Lake; in Uranium Exploration in Athabasca Basin, Saskatchewan, Canada, ed. E.M. Cameron; Geological Survey of Canada, Paper 82-11, p. 281-289, 1983.

Abstract

A waterborne resistivity/induced polarization survey was performed on selected areas of Collins Bay in the vicinity of U deposits which underlie the lake. The purpose was to demonstrate the feasibility of mapping, in water-covered areas, the pelite unit which is near the Mudjatik-Wollaston domain junction. The method features a conventional multispaced dipole-dipole array towed continuously along the surface of the water, electronic navigation, and a digital multichannel data acquisition system. Results show elongated zones of anomalously low apparent resistivity and high induced polarization which coincide with the graphitic pelite unit. The waterborne method can be used to obtain good quality data rapidly over lakes. It would thus appear to have wide applicability for mineral exploration in lake covered regions.

Résumé

Dans certaines régions de la baie Collins, on a effectué un levé de polarisation induite et de résistivité, au-dessus de l'eau, à proximité des gîtes d'uranium sous-jacents au fond du lac. Ce levé doit permettre de démontrer la possibilité de dresser la carte, dans des zones recouvertes par l'eau, de l'unité pélitique proche de la jonction des domaines de Mudjatik et Wollaston. Cette méthode consiste à utiliser un appareil classique dipôle-dipôle à intervalles multiples, remorqué de façon continue à la surface de l'eau, ainsi que la navigation électronique et un réseau d'acquisition numérique des données à voies multiples. Les résultats de ce levé montrent l'existence de zones allongées, caractérisées par une résistivité apparente anormalement basse et une polarisation induite élevée, zones qui coïncident avec l'unité pélitique graphiteuse. On peut utiliser cette méthode de levés à la surface de l'eau pour obtenir rapidement des données de bonne qualité pour les lacs. Il semble donc que cette méthode se prêterait parfaitement à la prospection des gîtes minéraux dans les régions recouvertes par des lacs.

INTRODUCTION

The resistivity/induced polarization (IP) method is a standard tool in geophysical exploration for mineral deposits. This paper describes an adaptation of the method to accomodate survey areas that are covered by lakes. Initial development of a system to measure subbottom resistivities was undertaken by the Geological Survey of Canada during the period 1974-79, commencing with permafrost mapping experiments (Scott, 1975). Subsequent encouraging trials with a GSC-built prototype system (W.J. Scott and J. Lobach, unpublished GSC report, 1979) led Hardy Associates (1978) Limited to commence development, in 1980, of a commercial system which was also to incorporate measurement of the SP effect.

The results presented here are from a demonstration survey performed in September, 1981 by Hardy Associates under contract to the GSC. The test areas (Fig. 24.1) were selected in Collins Bay, Wollaston Lake, to delineate water-covered portions of the pelite unit which Sibbald (1983) interpreted as lying at the base of Aphebian metasediments in contact with Archean granitoid gneisses (Archean-Aphebian contact). The pelite unit is near the junction between the Mudjatik and Wollaston domains. Where graphitic, this pelite unit is a prime target for U exploration, and is suitable for detection by resistivity and SP measurements. The pelite unit is known to contain numerous conductors as identified by airborne electromagnetic surveys (Sibbald, 1983).

Acknowledgments

The authors thank the property owners, Eldorado Resources Limited (formerly Gulf Minerals Canada Limited), E and B Exploration, and Noranda Exploration, for permission to carry out the survey and publish the data. Eldorado Resources (formerly Gulf Minerals) also provided kind assistance with logistics. The survey areas were suggested by H. Stolz of the Saskatchewan Geological Survey. We also thank Susan Elsmore for drafting the figures and the reviewers for their helpful suggestions.

DESCRIPTION OF THE METHOD

The principles of the resistivity/IP method have been documented (see, e.g., Sumner, 1976; Hallof, 1980) and need be reviewed only briefly here. Current is injected into the earth through a pair of electrodes (the transmitter 'dipole') using a well-defined current waveform provided by the transmitter. The resulting voltage is measured at a second pair of electrodes (the receiver 'dipole') with a sensitive receiver. The expanding dipole-dipole array is commonly used in mineral exploration and, in land-based surveys, is operated in a station-by-station mode along pre-cut lines. Since electrical contact must be made for each measurement, production is laborious and station spacing is commonly equal to the size of the dipoles used (typically 50 m or greater).

The waterborne adaptation of the technique involves streaming the array of electrodes behind a small boat and collecting measurements from multiple receiving

[1] Geological Survey of Canada, 601 Booth Street, Ottawa, Ontario K1A 0E8
[2] Hardy Associates (1978) Limited, 221-18th Street South East, Calgary, Alberta T2E 6J5
Formerly Hardy Associates, now A-CUBED Inc., 5129 Tomken Road, Mississaga, Ontario L4W 1P1

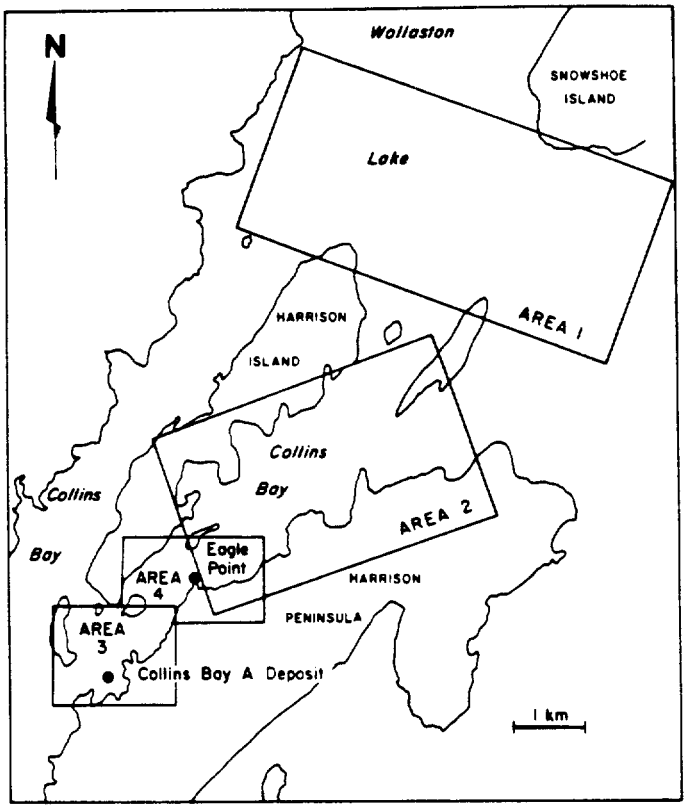

dipoles simultaneously. This not only allows surveys of lake-covered areas which could otherwise be performed only in winter on lake ice, but also improves rate of production and density of coverage along the survey line. An operating crew of two is required.

Instrumentation

Figure 24.2 shows the general configuration of the system. A multiple-dipole array is towed behind the boat on a multiconductor cable. The array consists of one transmitter dipole and six receiver dipoles. The receiver dipoles use copper-copper sulphate electrodes in streamlined nylon holders. Contact with the water is effected through a small porous ceramic plug in the end of each holder. This arrangement allows simultaneous measurements with six transmitter-receiver separations which are multiples of the dipole size (n = 1, 2, 3, 4, 5 and 6). A different cable is required for each dipole size (a = 10, 25 or 50 m). The array is floated at the surface of the water.

Current is supplied by a 2.5 kVa transmitter operating with a time-domain waveform, using a cycle of total length 4 s (one-second on, one-second off, plus reverse polarity), to maximize the number of cycles available for averaging. Acceptable signal strength can be achieved in fresh water for even the largest separation with a transmitter current of 1 A.

Figure 24.1

Waterborne resistivity/IP test survey areas in Collins Bay.

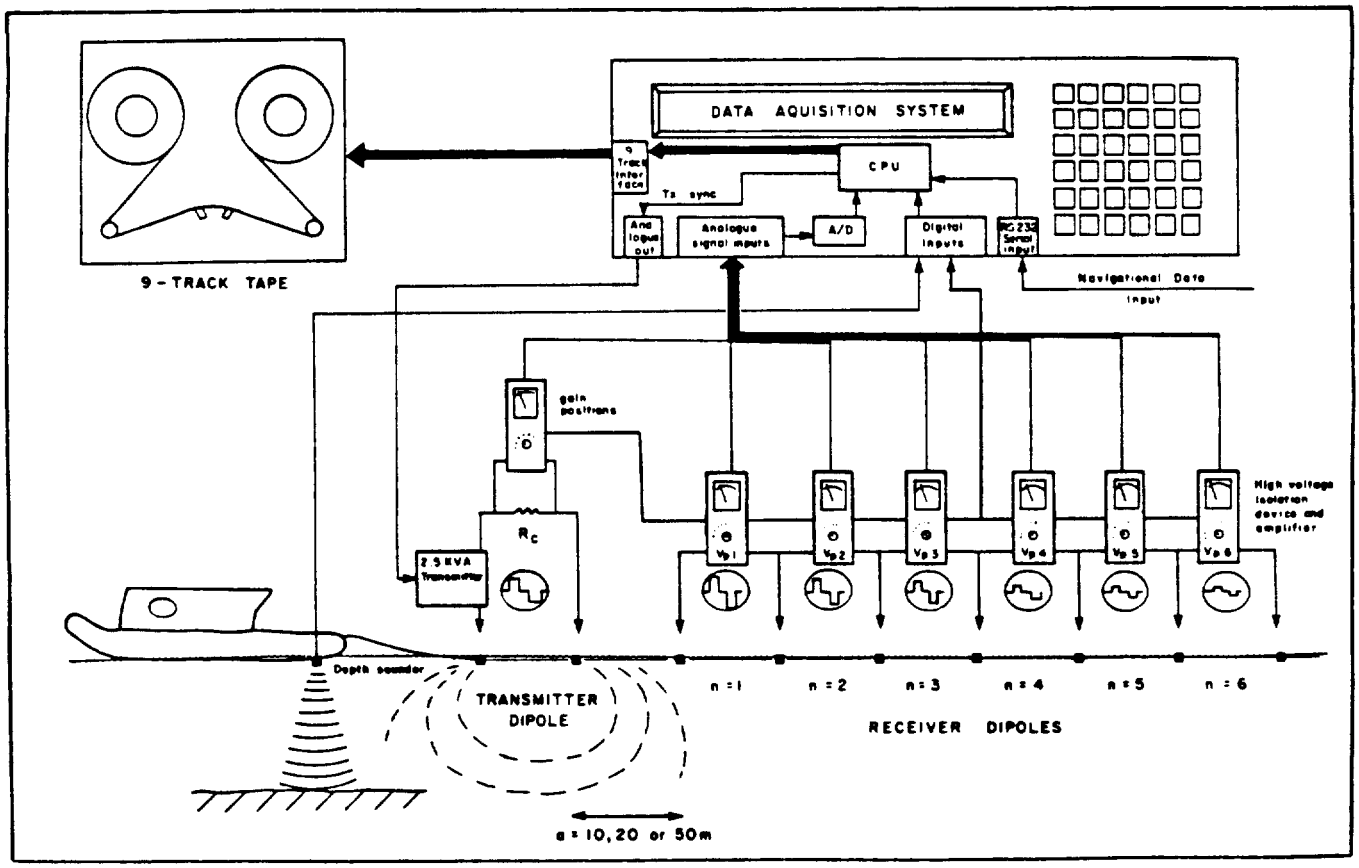

Figure 24.2. *System block diagram.*

The front end of the multichannel measurement system (one channel per dipole) consists of isolation amplifiers to give separation between channels and isolation from the transmitter. Transmitter control and data recording are carried out by the digital acquisition system and nine-track magnetic tape unit. For each transmitter cycle, waveforms of transmitted current and channel voltages are digitized at 1024 equally spaced points, and stored on tape. Performance of the system while the survey is in progress is monitored by the operator through observation of panel meters (one per channel) and apparent resistivities and chargeabilities (measure of the IP effect) calculated for presentation to the operator, but not recorded. Post processing recalculates these parameters, but allows the introduction of various filtering and stacking routines to improve the output quality.

Navigation

Navigation is accomplished by microcomputer-assisted triangulation using a del Norte trisponder system in which the distances between the boat (master transponder) and two known points on land (slave transponders) are measured (Fig. 24.3). Accuracy of the navigation is about ±2 m relative to the location of the slave transponders. Range information is stored on magnetic tape with the electrical data and is also used for real-time instruction to the helmsman via CRT display. Actual path of the boat can be compared to the pre-digitized intended course at any desired scale, so that a regular grid of closely spaced lines can be maintained. Water depth obtained from an echo-sounder is displayed for the helmsman and stored on magnetic tape as well.

Data processing

Resistivity (ρ_a) and chargeability (M) values are determined from the stored voltage data (V_p) for each channel as shown in Figure 24.4. Processing parameters can be chosen just prior to the calculation of these values. For this survey the resistivity window (R_W) was 347.7 ms (89 points) wide and was placed 633 ms after turn-on so as to avoid the transient part of the waveform which immediately followed the turn-on. The transient portion of the waveform following the turn-off (with a delay of 39 ms or 10 points) was used to calculate chargeability over four windows each of length 117 ms (30 points). The chargeability values presented here are normalized numerical integrations of the entire (954 ms) decay portion of the waveform excluding the 39 ms delay (total chargeability). All calculations were averaged over both positive and negative portions of the cycle so as to remove the effect of voltage offset such as is caused by spontaneous polarization.

Presentation can be in the standard form of pseudosections of apparent resistivity and total apparent chargeability. Results can also be presented in the form of contour maps for a particular n-value, as has been done here to demonstrate the mapping of an extended target. Values were averaged over the number of transmitter cycles in a distance of approximately one dipole spacing (approximately 10 cycles for the 50 m dipole) and plotted at the centre of the array, thus reducing the effects of random noise.

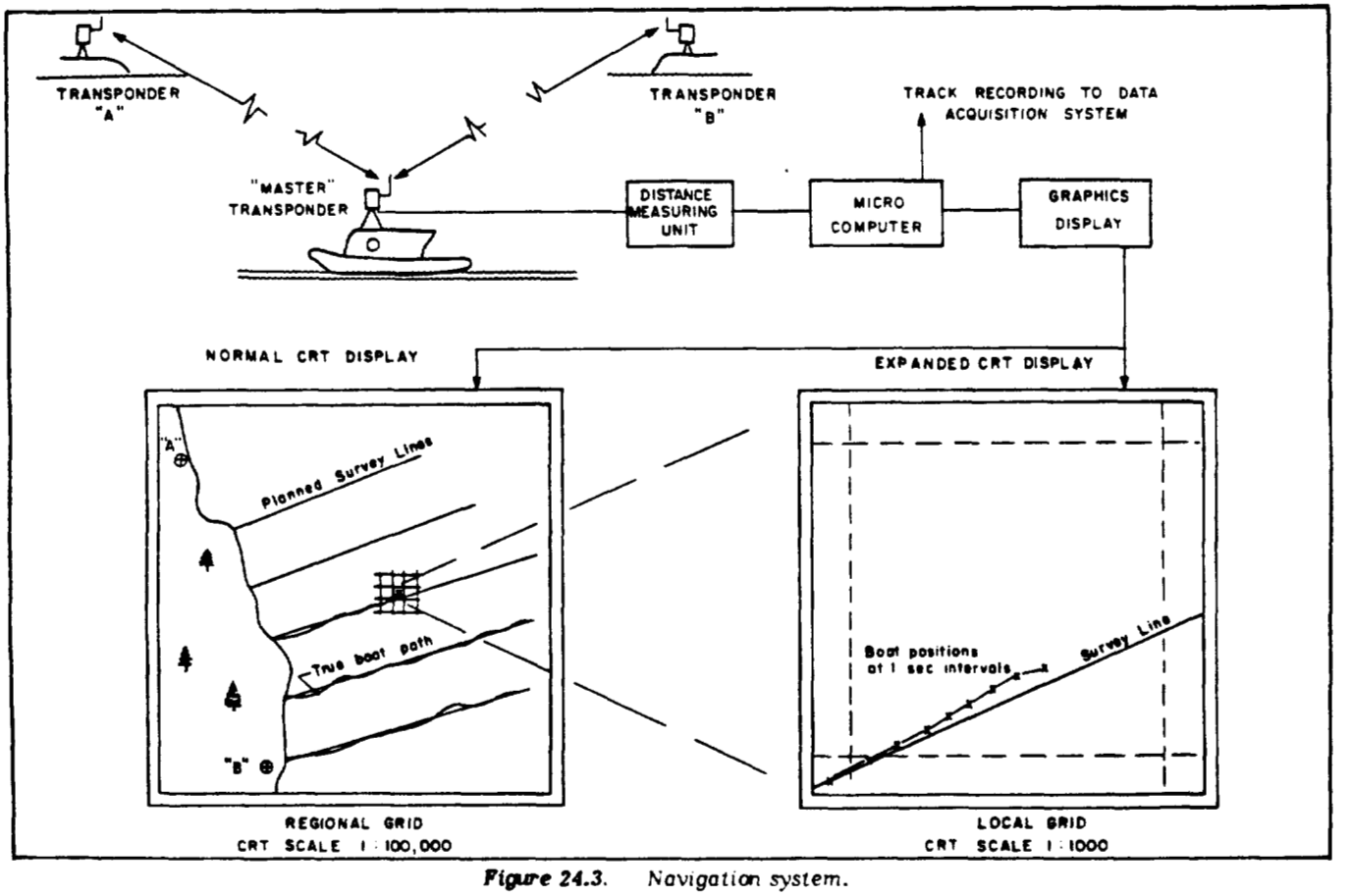

Figure 24.3. Navigation system.

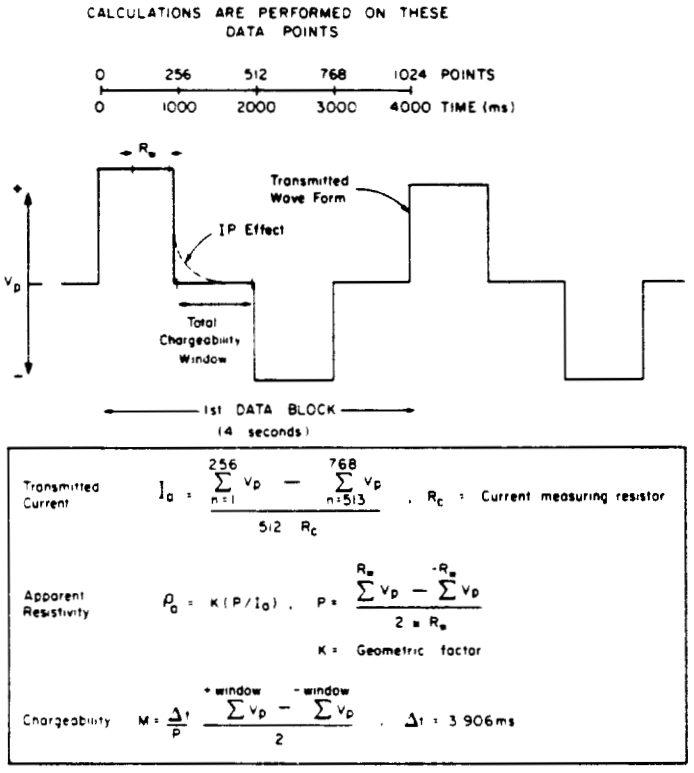

Figure 24.4. Computation of apparent resistivity and chargeability values from the measured waveform.

SURVEY RESULTS

A total of approximately 45 line-km of survey was completed in the four areas shown in Figure 24.1 at an average boat speed of 4-5 km/hour. This represents what is expected to be an average day's output. This productivity was, however, not achieved here because of a variety of malfunctions that occurred during this, the system's first production survey. A number of 'bugs' in the system were identified and eventually corrected, but not without some loss of data. For example, problems with channel four made it impossible to recover reliable chargeabilities for n ≥4. Cable damage resulted in the loss of n = 5 and 6 data for the 50 m dipole array in area 1. Also n = 3 chargeability values from sections of lines 2 and 3 in area 1 appeared excessively noisy and were omitted from the contour map of total chargeability for area 1.

The extent of navigable waters imposes an important operational limitation. Shallow water near the shoreline was particularly critical in areas 3 and 4. This problem could have been overcome by extending the lines with a land-based survey. Water depths of less than 1 m caused the more obvious deviations from straight survey lines. The relatively open waters of areas 1 and 2 were surveyed with the 50 m array (total length 450 m), but the shorter 25 m array (total length 225 m) was used in areas 3 and 4 because of the short survey lines. The results show, however, that the 25 m dipole array was effective in obtaining a response.

A simplified geological-geoelectric model is shown schematically in Figure 24.5. A resistivity contrast across the Archean-Aphebian contact of the order of 10:1, has been indicated by work elsewhere in the Athabasca Basin (H. Stolz, personal communication, 1980). A greater resistivity contrast occurs where the pelite unit is graphitic, or where there is alteration. Water depth is no greater than 25 m and total depth from surface to crystalline basement does not exceed 100 m in the survey area which straddle the margin of the Athabasca Group. A dipole-dipole array using 25 or 50 m dipoles spaced at n = 1 to 6 is thus appropriate to map the pelite unit as shown by the model pseudosection in Figure 24.5b. The operational and temporary problems encountered during the survey impose a constraint on the data available for presentation. A selected set of data has been chosen for display as contours of apparent resistivity and chargeability.

Area 1

Contour maps of apparent resistivity (a = 50 m, n = 4) and total apparent chargeability (a = 50 m, n = 3) are shown in Figure 24.6a and 24.6b, respectively. This area is dominated by a zone of low apparent resistivity which extends northeast from Harrison Island almost to Snowshoe Island. At about 0.5 km southeast of Snowshoe Island the trend changes direction abruptly towards the south. The apparent resistivity falls below 100 ohm-m compared to the background resistivity which is in excess of 1000 ohm-m. Within these low resistivity zones, apparent chargeability values are noticeably higher than elsewhere (approximately 5 to 10 times background). The anomalous zone clearly follows the Archean-Aphebian boundary shown by Sibbald (1983, Figure 1.5) but tends to lie on the Aphebian side of the contact as would be expected since it is the Aphebian pelite unit which is more conductive. This section of the contact was previously mapped by horizontal loop EM profiles (J.H. Reedman, personal communication, 1981) which were obtained during winter surveys on the lake ice.

A second elongated feature, nearly parallel to the first, can be seen about 1 km to the west of Harrison Island. This conductor, also previously known, is conceivably due to a graphitic zone lying in the Aphebian metasediments some distance from the contact.

Area 2

Contour maps of apparent resistivity and total apparent chargeability are shown in Figure 24.7a, b, respectively, for the same electrode spacings as Area 1. Profiles were run in north-south and east-west directions, which are approximately 45° with respect to the expected strike, in order to maximize profile length. This compromise, coupled with some loss of data due to post-processing recovery problems, resulted in rather sparse data for contouring purposes. Nevertheless a northeast-trending anomalous zone can be identified running parallel to the contact shown by Sibbald (1983, Fig. 1.5). The weakness of the response (relative to the Area 1 anomalies) is probably due to a change in the electrical properties of the target unit, and/or an increase in depth to its top.

Area 3 and Area 4

Figure 24.8a and 24.8b are contour maps of apparent resistivity and total apparent chargeability, respectively, for 25 m dipoles with spacing n = 5. The survey lines were fitted in wherever possible as dictated by the relatively crampled manoevring space for even the 25 m array. Again there is a zone of low resistivity trending southwest, a continuation of the zone discussed previously, with associated high chargeability. Unfortunately the anomalous trend occurs very near the shore at the ends of profiles. Three zones of particularly intense response can, however, be identified.

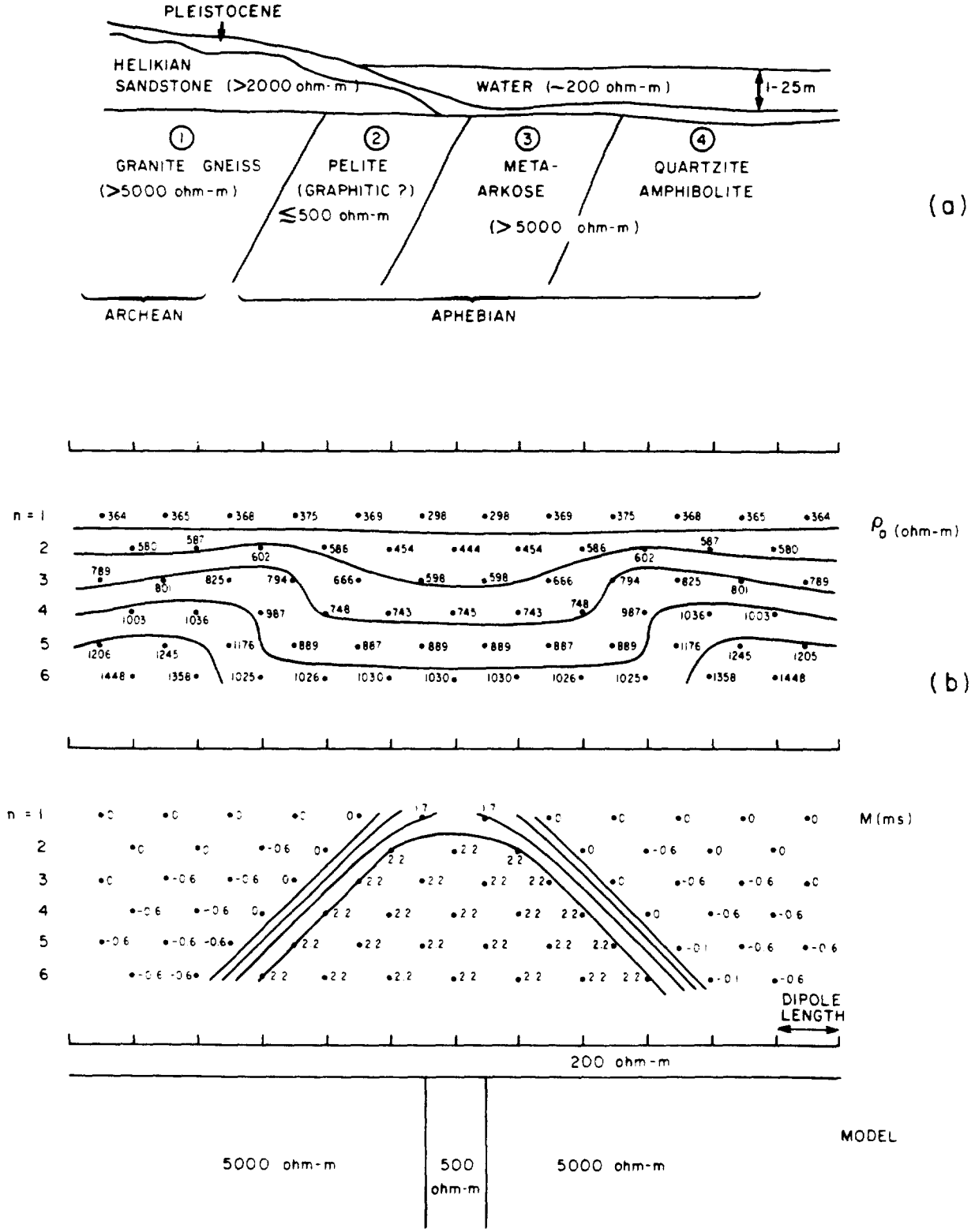

Figure 24.5. *(a) Simplified geoelectric section of the Archean-Aphebian transition zone. (b) Computed 2-D model response to demonstrate detectability of the pelite unit. IP effect was computed in the frequency domain and converted to an approximate chargeability (1.8 PFE = 10 ms) following the method of Van Voorhis (1973).*

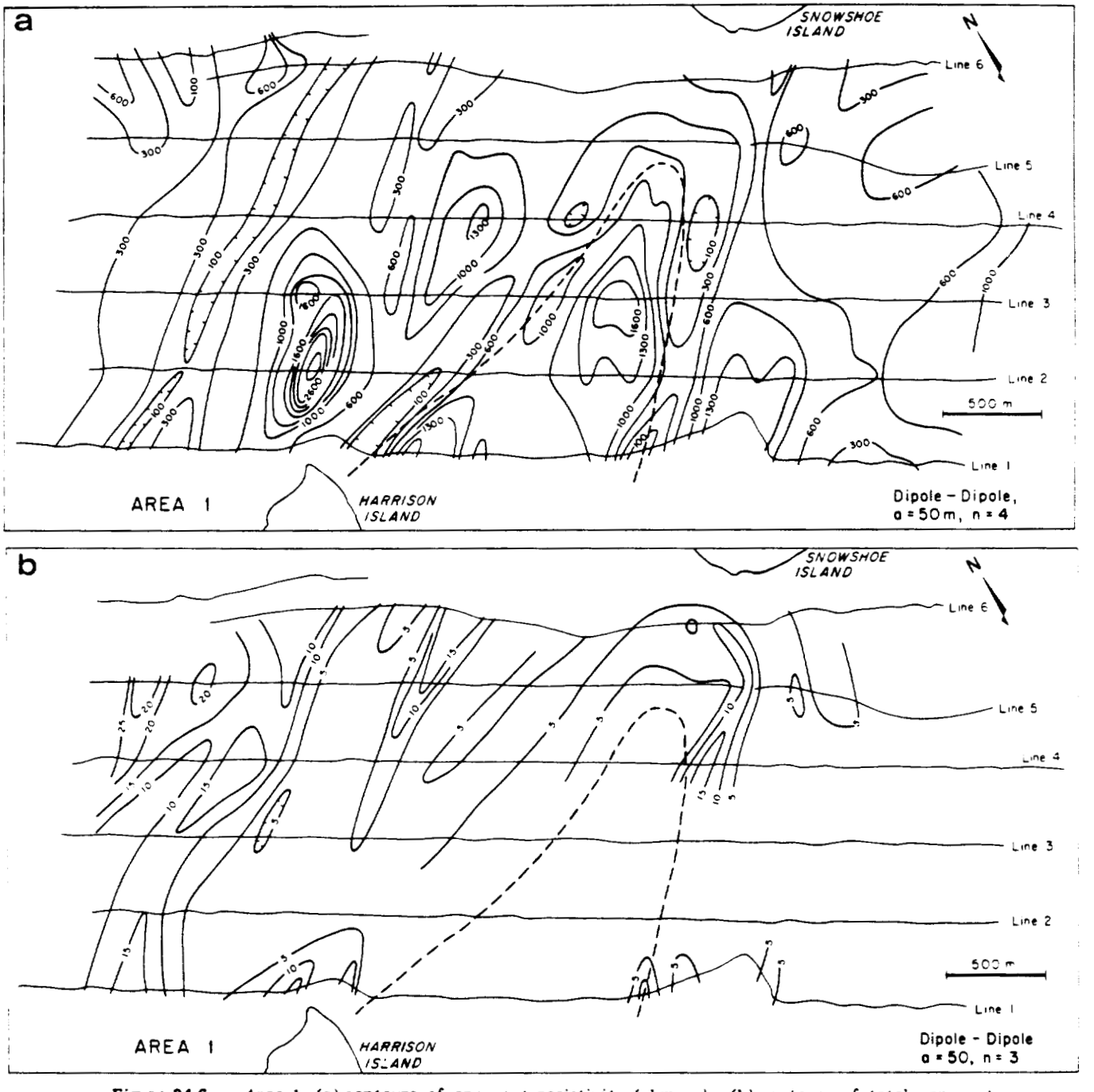

Figure 24.6. *Area 1, (a) contours of apparent resistivity (ohm-m); (b) contours of total apparent chargeability (ms). The dashed line indicates the previously known contact.*

The strongest of these coincides with the location of the Collins Bay A deposit. The apparent resistivity drops to approximately 50 ohm-m and the chargeability peaks at 130 ms. The intense clay alteration and the presence of disseminated base metal mineralization, predominantly pyrite and galena, associated with the deposit (Heine, 1981) are probably responsible.

A second feature occurs about 0.7 km northeast along strike, where the apparent resistivity drops to 85 ohm-m and the apparent chargeability peaks at 100 ms at the east end of Line 3. It is not clear if the source of this anomaly is localized or merely appears so as a consequence of the rather sparse coverage in the vicinity of the shore.

The third feature of interest occurs in Area 4 in the vicinity of the Eagle Point deposit. Immediately north of Eagle Point there is an apparent resistivity low of less than 100 ohm-m and an apparent chargeability peak of 30 ms. About 0.5 km east along Lines 1 and 2 a secondary zone is indicated. The IP response, in particular, suggests the

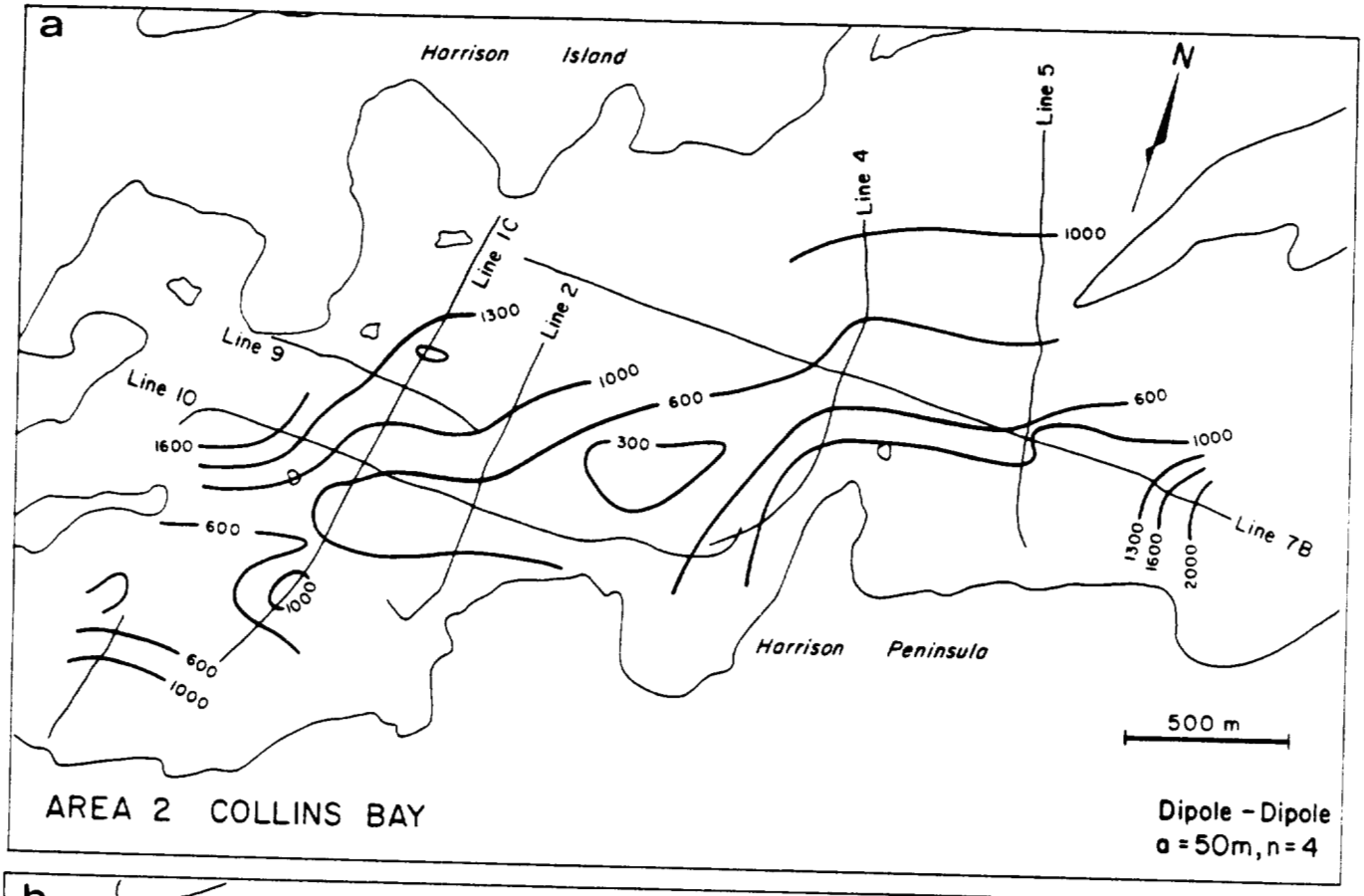

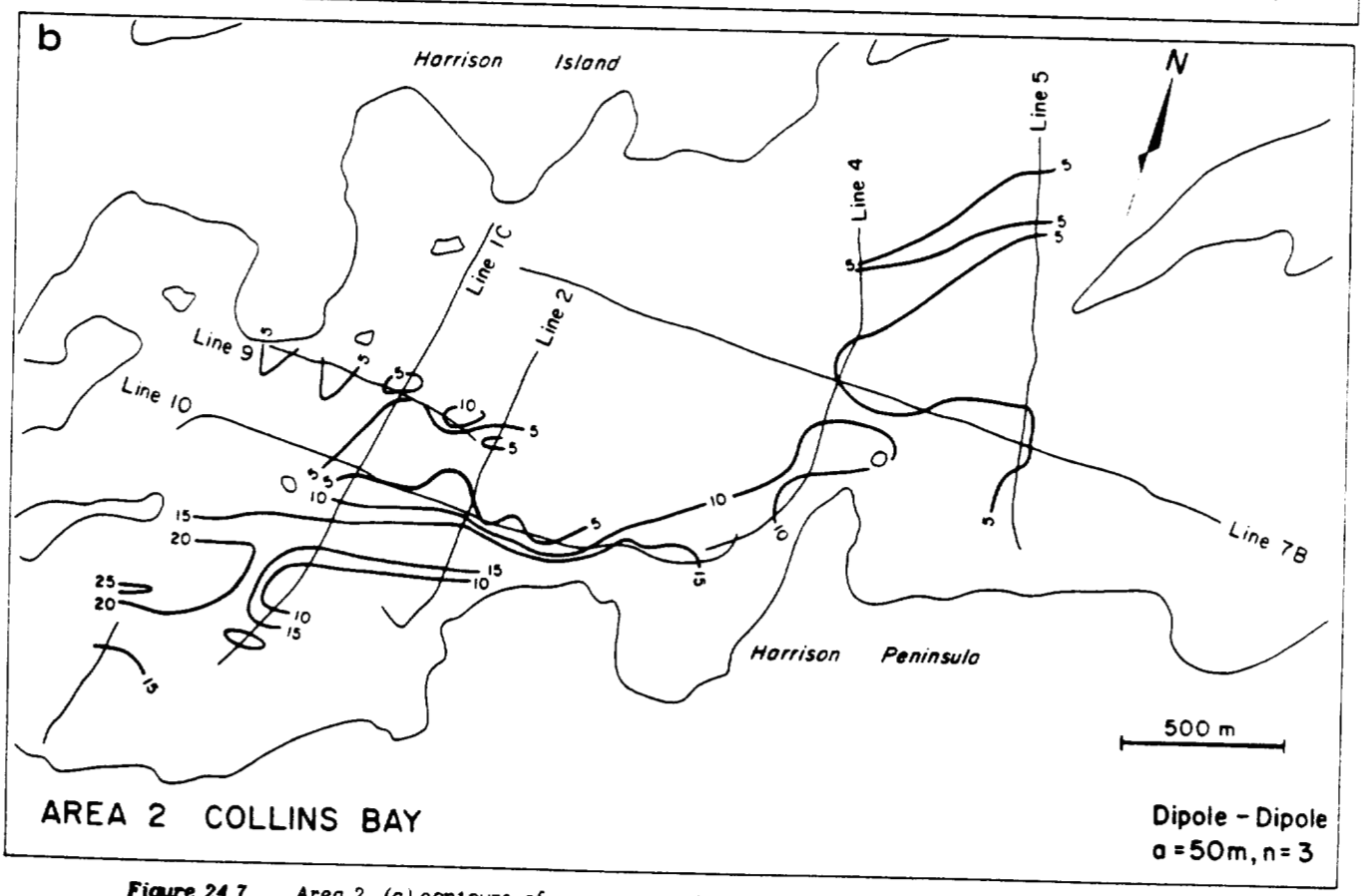

Figure 24.7. *Area 2, (a) contours of apparent resistivity (ohm-m); (b) contours of total apparent chargeability (ms).*

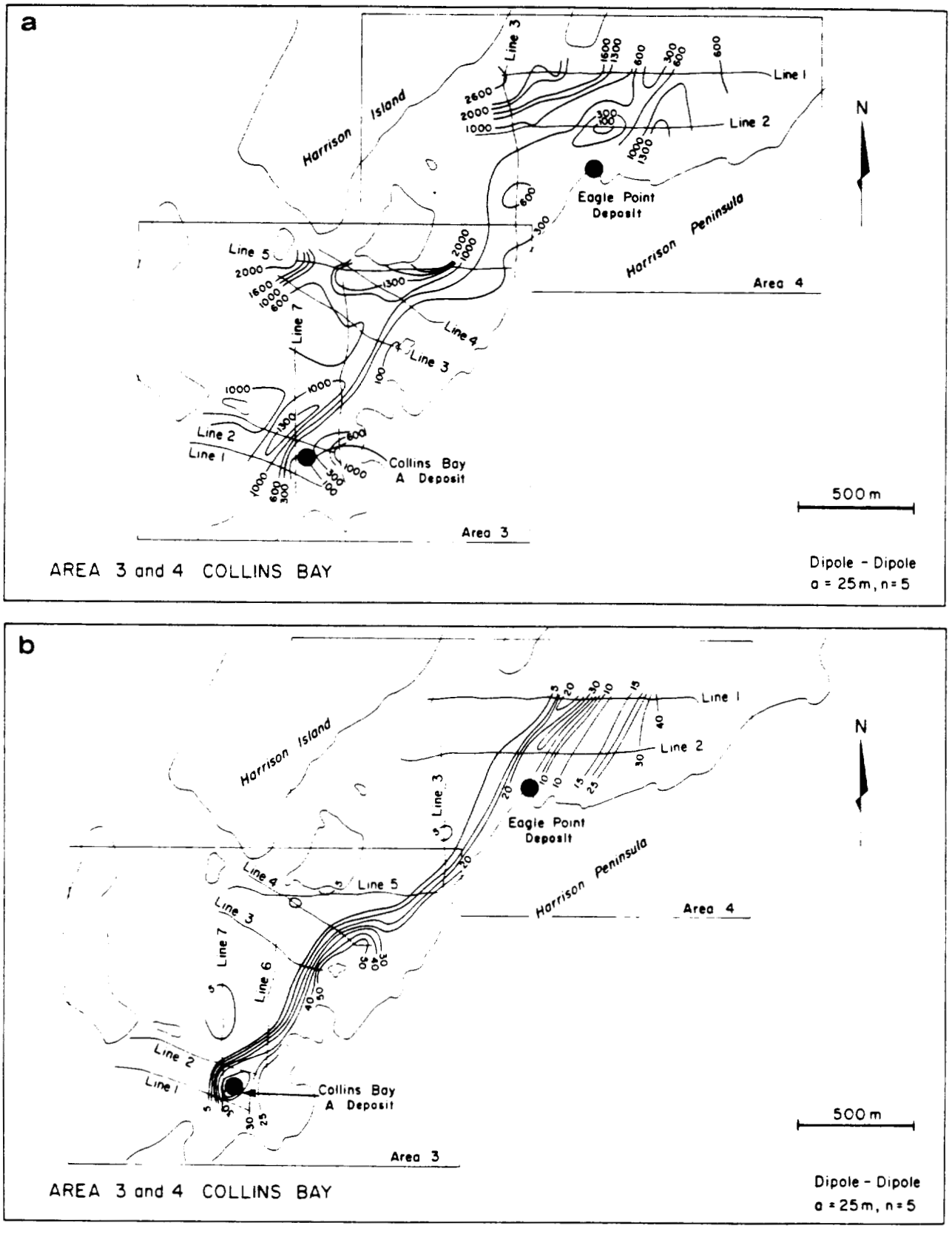

Figure 24.8. *Area 3 and Area 4, (a) contours of apparent resistivity (ohm-m); (b) contours of apparent chargeability (ms).*

presence of two distinct structures. Again, extension of these profiles towards and onto shore would be required for further clarification.

CONCLUSIONS

The results presented here in the form of contour maps of apparent resistivity and total apparent chargeability (induced-polarization response) delineate an anomalous zone which accurately follows the Archean-Aphebian contact underneath Collins Bay. They clearly demonstrate the viability of the waterborne version of the technique, a conclusion reached in spite of a number of technical problems encountered during the survey, and in spite of the very minimal level of interpretation which has been applied to the data.

The ease of exploration of large areas not normally accessible to land-based geophysical coverage is one advantage of the approach. The next generation system will hopefully eliminate the malfunctions and incorporate a number of instrumental improvements which will render the data amenable to quantitative interpretation. Interpretation schemes, such as simple layered earth or two-dimensional inversion, can then be applied using the water as a well-defined top layer of uniform resistivity and measured thickness. In fact, such a uniform, non-polarizable layer could be expected to act as a filter against near-electrode effects from surficial materials, a common source of noise in land-based resistivity/IP surveys. Lake Athabasca, which covers approximately 300 km of the Athabasca boundary, offers a possibility for future application of the system in mapping graphitic horizons and alteration zones.

REFERENCES

Hallof, P.G.
1980: Grounded electrical methods in geophysical exploration; in Practical Geophysics for the Exploration Geologist; Northwest Mining Association, Spokane, Washington, U.S.A., 303 p.

Heine, T.
1981: The Rabbit Lake Deposit and the Collins Bay deposits; in Canadian Institute of Mining and Metallurgy, Geology Division, Uranium Field Excursion Guidebook; The Canadian Institute of Mining and Metallurgy.

Scott, W.J.
1975: Preliminary experiments in marine resistivity near Tuktoyaktuk, District of Mackenzie: in Report of Activities, Part A, Geological Survey of Canada Paper 75-1A, p. 141-145.

Sibbald, T.I.I.
1983: Geology of the crystalline basement, NEA/IAEA Athabasca Test Area; in Uranium Exploration in Athabasca Basin, Saskatchewan, Canada, ed. E.M. Cameron; Geological Survey of Canada, Paper 82-11, report 1.

Sumner, J.S.
1976: Principles of induced polarization for geophysical exploration; Elsevier Scientific Publishing Company, Amsterdam, The Netherlands, 277 p.

Van Voorhis, G.D., Nelson, P.H., and Drake, T.L.
1973: Complex resistivity spectra of porphyry copper mineralization; Geophysics, v. 38, no. 1, p. 49-60.

OFFSHORE TECHNOLOGY CONFERENCE
6200 North Central Expressway
Dallas, Texas 75206

With my compliments,
Edgardo L. Nebrija

PAPER NUMBER OTC 2454

Electrical Prospecting for Copper Veins in Shallow Water

By
Edgardo L. Nebrija, Charles T. Young, Robert P. Meyer and J. Robert Moore, U. Of Wisconsin

THIS PAPER IS SUBJECT TO CORRECTION

ABSTRACT

Electrical measurements using separately a surface-towed Schlumberger resistivity array and a surface-towed, controlled-source audiomagnetotelluric (AMT) system were made in Lake Superior along the north shore of Keweenaw Peninsula. The areas studied were Copper Harbor, where there are known underwater copper veins, and Great Sand Bay, where offshore extensions of onshore copper-bearing fissures may exist.

The Schlumberger array had a 455-foot current electrode separation, sufficient to measure the resistivity of the lake floor in shallow water. The AMT tests were conducted using a circular loop of wire 150-m in diameter laid on the lake bottom and excited by a 400-Hz AC generator as source. With the ship's position regulated by electronic navigation, concentric arcs were traversed about the loop to measure the radial magnetic field, H_r, and the tangential electric field, E_t.

The AMT method yielded distinct and reproducible anomalies in E/H ratios over known copper veins in Copper Harbor and both methods showed correlatable anomalies over expected lithologic contacts in both areas. A previously discovered zone of heavy-mineral concentration inside Great Sand Bay was verified with both methods. A probable underwater vein was also discovered in this area with the surface-towed resistivity array. Other onshore fissures apparently do not extend offshore.

Both methods are strongly affected by bottom topography. For resistivity profiling, a first-order correction for topography has been developed and applied.

References and illustrations at end of paper.

PREFACE

This is the third OTC report on the University of Wisconsin Sea Grant program to investigate the existence of copper deposits under Lake Superior. The emphasis of this report is on the advances in methodology applied to specific targets outlined by Meyer et al. (1975).

INTRODUCTION

Increasing interest in the exploitation of underwater mineral deposits requires a parallel effort in the development of geophysical techniques applicable to their exploration. Electrical prospecting methods are well established in mineral exploration on land; we have applied these methods to underwater exploration. This paper describes the results of exploration for copper vein deposits using surface-towed resistivity profiling and active-source audiomagnetotellurics (AMT) in two areas offshore of Keweenaw Peninsula in freshwater Lake Superior.

Electrical methods employed in the 1974 season (Meyer et al., 1975) demonstrated that known copper veins (and sands with high heavy-mineral content) could be detected with the resistivity method. The 1974 measurements employed a near-bottom-towed 30-foot probe, and while this gave good resolution, keeping the probe close to the bottom made survey work slow and the technique unsuitable for rough bottoms.

In 1975, field trials were undertaken with the two surface-towed electrical techniques to determine the extent to which these could identify lithologic units and differentiate known copper veins from other anomalies with an eye to broad application in areas of probable occurrence of sublake copper veins.

Copper Harbor, where there are known copper veins, was used as a testing ground for the AMT method. Both methods were used at Great Sand Bay, where there are known heavy-mineral sands and probable offshore extensions of copper veins. All work reported here employed an active-radar electronic navigation system.

GEOLOGIC SETTING OF THE KEWEENAW COPPER DEPOSITS

Keweenaw Peninsula was a major copper producer in the United States in the mid-1800's. Here, copper deposits are localized in middle to late Keweenawan lavas and interbedded clastic sediments. Throughout the length of the peninsula, these formations strike parallel to shore and dip homoclinally north. The formation age decreases from the Portage Lake Lava Series in the south-central peninsula to the Copper Harbor Conglomerate and Nonesuch Shale-Freda Sandstone formations to the north. Separating the southernmost and younger Jacobsville Sandstone from the copper district is the Keweenaw Fault, a steep, northward dipping thrust (Figure 1). (Dorr and Eschman, 1971, give an excellent review of the geology and mineral deposits of Keweenaw Peninsula.)

Three types of copper deposits are found: amygdaloidal deposits, conglomeratic deposits, and fissure (or vein) deposits. The amygdaloidal deposits occur within the porous, vesicular, and brecciated tops of lava flows comprising the Portage Lake Lava Series, while the conglomeratic deposits are localized within the conglomerate members of this series. The copper in both is generally in the native state. The most productive mines in the district exploit these two types of deposits.

The vein copper deposits, though not the focus of production now, were the earliest mined. Within calcite veins, ore minerals occur as "leaves" of native copper, or as grains of chalcocite and other copper sulfides. The veins strike normal to and cut across the lavas and conglomerates and are known to outcrop on the nearshore lake bottom at Great Sand Bay, Silver Island, and Copper Harbor.

Although they are generally confined to the Portage Lake Lava Series, veins are also found within the Copper Harbor Conglomerate, the rock formation that underlies both areas surveyed on the north shore of Keweenaw Peninsula.

One of these areas, Copper Harbor, is underlain by two steeply-dipping basalt flows, separated by a medial layer of conglomerate about 150 feet thick (Figure 7). The onshore and peninsular sides of the harbor are composed of conglomerate. In addition, a magnetic high, determined from airborne magnetic measurements, approximately 1 km offshore, marks another probable basalt flow. Two copper-bearing calcite veins strike across the harbor from the Fort Wilkins State Park to the tip of the eastern peninsula (Figure 7). The underwater extensions of these veins can be seen in the shallow nearshore zone of the eastern peninsula.

The other survey area, Great Sand Bay, is underlain by conglomerate but its mouth is marked by an underwater ridge consisting of a basalt flow (Figure 10). Immediately inland, within the Portage Lake Lava Series, are several copper-bearing fissures striking perpendicular to shore and into the lake.

THEORY AND INTERPRETATION TECHNIQUE

Resistivity. In the search for mineralized veins, resistivity prospecting is one of the techniques often applied because mineralized veins have generally lower resistivities than their host rock.

In general land application, a set of electrodes driven into the surface is used to send current, I, into the ground and another set is used to measure the potential difference, ΔV, usually within and along the same line as the current electrodes. The apparent resistivity, ρ_a, is determined from the relation:

$$\rho_a = k \frac{\Delta V}{I} \qquad \text{(Eq. 1)}$$

where k is the geometric factor dependent on the interelectrode spacings used.

$$k = \frac{2\pi}{\frac{1}{R_1} - \frac{1}{R_2} - \frac{1}{R_3} + \frac{1}{R_4}} \qquad \text{(Eq. 2)}$$

where the R's, interelectrode distances, are defined as in Figure 2. In our work, we used the Schlumberger array with a current electrode separation, AB, greater than six times the potential electrode spacing, MN.

In a horizontally-layered earth, the apparent resistivity measured is a weighted average depending on current apportionment between the layers at various depths. The current apportionment depends on the relative resistivities as well as electrode spacing. If half the current electrode separation, a = AB/2, is small compared to the thickness, d, of the first layer (resistivity ρ_1), the apparent resistivity, ρ_a, is approximately equal to the first-layer resistivity, ρ_1. At the other extreme in a two-layered half space, where a is sufficiently greater than d, then ρ_a is approximately equal to the deeper second-layer resistivity, ρ_2. For intermediate values of a, the measured ρ_a lies between ρ_1 and ρ_2. The relation of ρ_a/ρ_1 to a/d for different resistivity contrasts ρ_2/ρ_1 is shown in Figure 3.

For an electrode array towed at the water surface, the first layer is the water and the lower layer is the lake or sea floor. At sea, the low resistivity of salt water (0.25 ohm-meters) (Bannister, 1968) limits current penetration into the sea floor and necessitates very long spacings of current electrodes. However, in fresh water, this "overburden" is about 2-3 orders of magnitude more resistive than sea water so that more practical surface-towed arrays are applicable.

To determine lateral variations in the resistivity of the lake bottom, the array is towed with a fixed electrode spacing. The current electrode separation must be considerably greater than the water depth so that we are in the region where ρ_a is close to the value of ρ_2 (see Figure 3).

Obviously, with constant array spacing, the apparent resistivity correlates with the first layer thickness, i.e., the water depth, and hence with the topography under the array. This requires that the topographically-caused changes in ρ_a be removed so that the desired subbottom properties can be distinguished.

Whiteley (1974) has proposed a method for distinguishing bathymetric effects from true resistivity variations of the subbottom. For this technique, theoretical apparent resistivity profiles are calculated for each of several constant values of the second-layer resistivity. Essentially, the value of ρ_a/ρ_1 is determined from each ρ_a/ρ_1 curve in Figure 3 for each sampling point along the traverse defined by a particular a/d ratio. This assumes that under each calculation point, the bottom is flat and infinite in extent at a depth corresponding to that point. Obviously then, any apparent resistivity variation in the theoretical profiles is just due to changing water depths. On the other hand, any lateral resistivity variation is indicated by non-parallelism between the observed and theoretical profiles.

Another method which is, perhaps, more desirable, is to directly plot the ρ_2/ρ_1 ratios along a profile. Using the observed ρ_a/ρ_1 and a/d ratios for each sample point, we can find, by interpolation, the appropriate ρ_a/ρ_1 curve in Figure 3 to which this pair of values belongs. The ρ_2/ρ_1 value defining the interpolated two-layer curve gives the resistivity contrast under the sample point. Both the determination of ρ_2/ρ_1 values and the formula for calculating ρ_a assume a flat and infinite interface between the water and the bottom beneath the sample point. If the water resistivity, ρ_1, remains fairly constant along a traverse, then the ρ_2/ρ_1 profile gives, in correct proportion, the lateral resistivity changes in the subbottom. If ρ_1 is known, values of ρ_2 can be estimated directly.

Audiomagnetotelluric method. As an alternative to resistivity prospecting, we also made audio-frequency magnetotelluric (AMT) measurements with a controlled source. The magnetotelluric technique uses the ratio of the horizontal AC electric and magnetic fields to determine the surface impedance of the earth. The spatial variation in impedance can be used to locate mineral deposits.

Natural-source AMT has the appropriate depth of penetration for our work, but is dependent on distant unpredictable thunderstorm activity for sources of the AC field, requires several seconds of signal-integration time for each measurement, and gives only roughly reproducible results (Strangway et al., 1973). Our expectation in using 400 Hz controlled-source AMT was to overcome these difficulties, to obtain good penetration into the subbottom, continuous data while towing the apparatus, and high lateral resolution using short electrode separation.

The transmitter was a horizontal circular loop of wire (vertical magnetic dipole). This loop produced a tangential, horizontal electric field (E_t), a vertical magnetic field (H_z), and a radial, horizontal magnetic field (H_r). Along arcs concentric with the loop, the fields are constant in a flat-layered, homogeneous earth. Deviation from constancy indicates inhomogeneity in the ground and by measuring E_t, H_z and H_r along concentric arcs, we should be able to locate conductive bodies such as copper veins beneath the ground.

The horizontal electric to magnetic field ratio, E/H, will drop over conductive bodies. In addition, H_z gives further indication of inhomogeneities. The ratio H_z/H_r should be zero in the plane wave region for a flat-layered earth and should rise in the presence of inhomogeneities.

Skin depth, δ, is defined as the depth at which a plane wave field penetrating into the earth has fallen to 1/e of its value at the surface, given by Vozoff (1972) as:

$$\delta = \sqrt{\frac{2\rho}{\omega\mu}} \quad \text{(meters)} \qquad \text{(Eq. 3)}$$

or in a more practical form to an accuracy of .6% as:

$$\delta = 500\sqrt{\rho/f} \quad \text{(meters)} \qquad \text{(Eq. 4)}$$

where ω = angular frequency; f = frequency in Hz; $2\pi f = \omega$; μ = magnetic permeability of the earth, taken as μ_o, the permeability of free-space, $4\pi \times 10^{-7}$ henry/meter, except for highly magnetic rocks; ρ = resistivity of the earth in ohm-meters. Skin depth gives an approximate depth of penetration for AMT prospecting. For our signals at 400 Hz, the skin depths are 433 meters in Lake Superior water of $\rho \triangleq 300$ ohm-meters and 790 meters in typical metamorphic and igneous rocks of $\rho \triangleq 1{,}000$ ohm-meters.

At great distances from the transmitter, the signals may be treated as plane waves. Operating in the plane-wave region allows the use of interpretation theory that has been developed for the natural-source magneto-telluric method (Strangway and Vozoff, 1967; Ward et al., 1974; Swift, 1971, for examples).

The minimum transmitter-to-receiver distance required for the plane-wave approximation to be valid is about 7δ (Bannister, 1969), or about 3500 meters in Lake Superior water. In Lake Superior, we worked at a maximum distance of 1250 meters. At greater distances, the signal quality was seriously degraded by interference from natural electromagnetic noise (sferics).

For our data in this near-field region, we will not attempt interpretation in terms of lake bottom resistivities; we will interpret the data empirically, identifying anomalous responses due to probable changes in lithology and presence of copper veins by E/H changes.

FIELD PROCEDURE

Resistivity. A schematic diagram of the field set-up of our resistivity array is shown in Figure 2 and a block diagram of the resistivity apparatus is shown and described in Figure 4.

The current electrode separation of 455 feet that we employed was long enough to enable us to measure the subbottom resistivity from the surface. In water depths of 20 to 40 feet, the a/d ratio varies from 10 to 24 which, for resistivity contrasts ρ_2/ρ_1 between 0.30 to 2.5, makes the measured ρ_a approximately equal to ρ_2. For the same current electrode separation, two potential electrode spacings were used and their results were later compared as to their resolution.

In the preliminary resistivity survey of 1974, the bathymetry and the measured potentials were recorded on separate charts and correlating the two was cumbersome. So, in 1975, we recorded potential differences on the same chart as the bathymetry. In this way, it was easier to pick points along the profile where resistivity changes do not correlate with the water depth. However, since the center of the resistivity array was 230 feet behind the boat under which the water depth was measured, a correction for this lateral offset had to be applied in the final plots. A similar correction was applied to the AMT data.

AMT. The field layout for the AMT measurements is shown in Figure 5; a block diagram of the AMT apparatus is shown in Figure 6.

To set up the transmitter antenna, a pontoon boat, which carried the generator and a radar transponder, was anchored where the center of the loop was to be. The loop was then laid out by a second boat which circled the anchored boat, keeping a constant radius by means of a stretched rope. The transmitter loop current was limited to 8 amperes by means of series resistors.

The receiving ship towing the field sensors traversed concentric arcs about the center of the transmitting loop by maintaining a constant range from the radar transponder set up at the loop's center. Along each traverse, radial magnetic field (H_r) and tangential electric field (E_t) were automatically recorded along with bathymetry on the fathometer chart.

DATA ANALYSIS

Resistivity. The apparent resistivity, ρ_a, was calculated using Equation 1 at one-minute intervals along the profiles with shorter sampling intervals used where the potential fluctuated rapidly.

At small a/d ratios (deep water), the ρ_a is approximately equal to the water resistivity, ρ_1. In deep water, the value of ρ_1 was 450 ohm-meters. Compared to reported freshwater resistivities, 20-60 ohm-meters (Boulos, 1972; Unz, 1959), this value is very high. This may be due to the "fresher" nature of Lake Superior water. Beeton (1965) reports the total dissolved solids in Lake Superior as 60 ppm compared to 185 ppm for eutrophic lakes. The water resistivity was assumed to be uniform from nearshore to offshore. Resistivity changes by only a few percent for small temperature fluctuations (Parkhomenko, 1967).

For all traverses, we computed the ρ_a/ρ_1 ratio at each sampling point and plotted this with the a/d and the derived ρ_2/ρ_1 ratios at each point. The difference between the ρ_2/ρ_1 profile and the observed ρ_a/ρ_1 profile is due to the topographic effect. Assuming that the water resistivity, ρ_1, varies only a few percent along the profile, the calculated ρ_2/ρ_1 profile directly indicates lateral resistivity changes. Sections of the profile have been visually divided and an average ρ_2/ρ_1 obtained for each section. The different resistivity regimes so classified are then correlated with the offshore projections of on-land geology.

In deep water ($a/d \leq 1.0$), the ρ_2/ρ_1 value obtained from the two-layer curves of Figure 3 becomes uncertain because the ρ_a/ρ_1 curves for different resistivity contrasts merge.

For one large resistivity anomaly at Great Sand Bay, we also applied the alternative method of distinguishing between topographic and true conductivity anomalies. Theoretical ρ_a/ρ_1 profiles were plotted on the same scale as the observed ρ_a/ρ_1 profile for each of several assumed subbottom resistivities. Along traverses with relatively flat and shallow bottoms, it is not necessary to plot theoretical profiles since the ρ_a/ρ_1 profile gives, in correct proportions, the lateral changes in subbottom resistivity.

AMT. The electric, magnetic and time data from the fathometer chart were digitized with a variable sampling interval; the operator digitized more closely where there were rapid fluctuations in the data.

The electric and magnetic channel outputs recorded on the fathometer chart were converted to impedance values in mV/km/gamma by multiplying by a factor involving sensor sensitivities, amplifier gains and attenuator settings. The value of the factor is derived as follows. The output of the electric channel amplifier, E_O, is related to the electric field in the water, E, by:

$$E_O = ES_eA_{Oe}\ 10^{-\alpha/20} \qquad \text{(Eq. 5)}$$

where:

S_e = sensitivity of the electric detector dipole, in mv output per mv/km input. Numerically equal to dipole length in kilometers.

A_{Oe} = overall gain of electric channel amplifier.

α = electric channel attenuator setting in db.

Similarly, the output of the magnetic channel amplifier, H_O, is related to the incident magnetic field, H, by:

$$H_O = hS_hA_{Oh}\ 10^{-\beta/20} \qquad \text{(Eq. 6)}$$

where:

S_h = sensitivity of induction coil in mv/gamma, at 400 Hz.

A_{Oh} = overall gain of magnetic channel amplifier.

β = magnetic channel attenuator setting in db.

These equations are combined to give a correction factor to convert the ratio of amplifier outputs E_O/H_O to field quantities of mv/km/gamma.

$$\frac{E}{H} = \frac{E_O}{H_O}\left(\frac{S_hA_h\ 10^{-\frac{\beta}{20}}}{S_eA_e\ 10^{-\frac{\alpha}{20}}}\right) \qquad \text{(Eq. 7)}$$

We plotted the E/H values and water depth, and inspected the plots for changes in E/H unrelated to bathymetry. The anomalies thus found are labeled according to strength and plotted on the trackline maps. Interpretation of unknown anomalies is made by comparison with responses we observed over known structures.

In many traverses, the E/H ratios shows a direct correlation with water depth, similar to the response of the resistivity technique. Superimposed on this topographic effect are anomalies due to bedrock changes and copper veins. In the case of the resistivity method, the change in rock type has the predominant effect on the resistivity, much greater than the effect of topography.

RESULTS AND INTERPRETATION

Copper Harbor. Three traverses, AA', BB' and CC' (Figure 7) pass over the known copper-bearing calcite veins. Up to four narrow anomalies of about 2-5% drop in the electric field appear along each traverse including over the extended vein positions. Figure 8 shows the electric field and magnetic field strengths and bottom topography, for traverses AA' and BB' aligned according to a north-south topographic low on the left. As expected with profiles not equidistant from the source, the magnetic field becomes stronger as the sensor goes closer to the loop and as the sensor becomes better aligned with the field. The electric field behaves similarly but with small anomalies superimposed on the regional behavior. The lows, when plotted on the

trackline map (Figure 7), show the two westernmost rows of E/H anomalies fall close to or on the underwater projections of two copper-bearing veins observed on the peninsula. Veins corresponding to the two easternmost lows are not known on shore. Presumably they are short veins.

Along profile CC', the E/H low expected from the Fort Wilkins vein at station 1540 occurs at approximately the same point as a topographic low (Figure 9). The narrow low that we expect for a copper vein, based on traverses AA' and BB' is probably masked by the topography. A strong low between stations 1543 and 1544 is probably due to the boat making a turn there. The turn causes the electric and magnetic field and sensors to become misaligned, producing unpredictable results in the E/H ratio. Another strong low occurs approximately at the basalt-conglomerate boundary. In the other traverse of Great Sand Bay, we found similar strong anomalies at basalt-conglomerate boundaries.

Profiles DD' and EE' outside Copper Harbor show broad lows in an east-west band approximately 500 meters offshore. These lows have no topographic expressions. We interpret them as a low-resistivity layer in the conglomerate and label it CuH2 in Figure 9. In addition, there are three small lows of similar character in profiles DD' and EE'. They occur near the approximate position of the aeromagnetic high indicated in Figure 7. This magnetic high corresponds bathymetrically to a ridge and could be a basalt flow similar to those found along the shore of Copper Harbor and Great Sand Bay. Most probably these small lows are associated with edge effects of the basalt-conglomerate interface.

In the traverses outside of Copper Harbor, we did not find anomalies which can be associated with offshore projections of copper veins exposed on land and known to exist inside the harbor. Either the water is too deep for our system to detect these offshore veins or they extend only a short distance from shore.

Great Sand Bay. Three resistivity regimes are mapped in Great Sand Bay: a low- to medium-resistivity zone (ρ_2 = 0.70 to 1.40 ρ_1) probably related to sands and gravels overlying the Copper Harbor Conglomerate within the bay; a highly resistive region (ρ_2 = 2.2 ρ_1) associated with outcropping basalt flows; and the nearshore, low-resistivity zone (ρ_2 = 0.30 ρ_1) associated with heavy-mineral rich sands. Within each regime, the resistivity varies relatively slowly.

The anomalies associated with underwater copper veins appear sharp and narrow both in the resistivity and EM profiles. They are superimposed on the "regional" resistivity or EM field defining a particular lithologic unit and do not represent as great a resistivity change as is associated with the contact between the basalt flows and the sediment-covered conglomerate unit.

Of the resistivity traverses, only traverse T1 shows such anomalies (marked A, B and C in Figure 11). Anomaly A is interpreted to be a probable underwater vein. Divers have confirmed the presence of a copper vein outcropping on the lake bottom within this area, although an attempt to precisely determine its location in 1974 failed due to poor underwater visibility. This anomaly lies between the straight-line projections of the known copper-bearing Copper Falls and Arnold Fissures onshore. Apparently, this vein does not extend beyond the basalt flow since the EM measurements do not detect it.

Straight-line projections of other onshore fissures do not yield anomalies. The effect of these veins, if they are small, barren, or deeply buried, may be masked by overlying sediments or by the resistivity low associated with the basalt-conglomerate contact. For instance, between stations 1046 and 1050 of traverse T1 in Figure 11, there is a broad resistivity low where the onshore Owl Creek Fissure has been projected. However, this area is also the offshore boundary of the basalt flow exposed on shore. Except in areas where the resistivity measurements are taken within the same lithologic unit, it may be difficult to detect the presence of copper veins.

Anomalies B and C of traverse T1 are more difficult to interpret because they are not as sharp and large as anomaly A. But the fact that they show within the low-resistivity region associated with the basalt-conglomerate boundary indicates that they may be significant. Anomaly C is offset about 70 meters from the fault projection and may indicate the actual location of the fault under the bay. The resistivity low marked as anomaly B anti-correlates with a topographic peak and is probably a short underwater vein since it is not detected in traverse T2.

Over the same area and with the same current electrode separation, the apparent resistivities obtained with different potential electrode spacings must be the same. However, at the tie point between traverses T1 and T2, stations 1127 and 1146 (Figure 10), the computed apparent resistivities are different. This is probably due to the different depths at which the electrodes were towed. Between stations 1140 and 1150 of traverse T2, the boat was maneuvering and moving at a speed about half that of traverse T1. Along adjacent portions of the two traverses where the boat

speed is the same, as between stations 1118 to 1120 and 1156 to 1158, the apparent resistivities are approximately the same.

Theoretically, a shorter potential electrode has a better resolution than a long potential electrode. However, the latter provides a larger signal and smooths smaller variations in resistivity. Two electrode spacings were used in Great Sand Bay and although the sharp anomalies which we interpreted as probable veins were all obtained only with the 12-foot electrode (traverse T1), the 70-foot potential electrode shows ample resolving power, i.e., a sharp change in apparent resistivity, across the basalt-conglomerate boundary in traverse T3. Where the offshore projection of the Arnold Fissure crosses the traverses made with differing potential electrode spacing, neither profile shows an anomaly. Along adjacent portions of traverses T1 and T2 inside Great Sand Bay, variations in the observed resistivity have approximately the same wavelengths (Figures 11 and 13). However, we can not directly compare the responses of the two potential electrode spacings over copper veins because traverses with each electrode spacing were not made over the same profile line.

The main feature of the EM data in Great Sand Bay is the strong response near the basalt-flow boundary (Figures 15 and 16). The southeast side of the flow is marked by strong lows and the north side by weaker lows. The anomaly at station 1654 is over the zone of heavy-mineral concentration found by resistivity. At the eastern end of profile EE' is an anomaly that occurs near the extension of an onshore copper-bearing fissure. This low lies at the edge of our survey area; we do not know whether it would correlate across adjacent EM track lines. The resistivity traverse near this anomaly shows a broad low which resembles more closely that associated with the basalt-conglomerate boundary than the relatively sharp anomalies characterizing copper veins.

All projections of onshore veins are drawn as straight lines. The discrepancy in location between these projections and the anomalies may well be due to offsets along their lengths. Perhaps more plausibly, the veins may not extend far from where they are exposed on land. The longest fissures shown in the geologic maps of Keweenaw Peninsula persist for up to 1.5 km. In Great Sand Bay, unlike in Copper Harbor where a known copper deposit on land is near the shore, the probability of finding veins along the offshore projections of more distant onshore fissures is low. Even in Copper Harbor, the EM traverses made across the offshore projections of the known nearshore veins do not show associated anomalies.

DISCUSSION

Both the resistivity and active-source AMT methods employed proved useful in locating underwater copper veins and delineating boundaries between different lithologic units. The anomalies due to the veins are generally small compared to the large and broad anomalies associated with geologic contacts. Nevertheless, they are sharp and distinguishable. The basalt-conglomerate contact yields a greater than 15% drop in E/H and a broad low in resistivity. Both methods also respond to the presence of heavy-mineral sands and therefore may be applicable in placer exploration.

There are other undulations of 1-5% in the E/H data, and about 5 millivolts in the resistivity data which we did not pick as anomalies. This level represents operational noise level, or limit of detectability, of our systems. Judging from the small, abrupt anomalies over known copper veins in shallow water inside Copper Harbor, the response of similar veins in deep water may be undetectable under the system's noise levels.

Short-electrode, bottom-towed resistivity arrays may have a stronger response in deeper water and better resolution across narrower veins than surface-towed arrays. Meyer et al. (1975) reported a potential drop of about 145 millivolts for the 10-foot electrode spacing bottom-towed Wenner array (current 100 milliamperes) across the Fort Wilkins vein in Copper Harbor. Crossing the probable vein at Great Sand Bay with the Schlumberger array, we obtained a maximum drop of 30 millivolts using the same current and the 12-foot potential electrode. Both veins are at approximately the same depth of about 30 feet. However, we are not aware of a satisfactory way of computing apparent resistivities from the data of bottom-towed arrays, even though theoretical sounding curves for electrodes at the water bottom have been published (Van'Yan, 1956; Patella and Schiavone, 1974). On the other hand, with electrodes near the water surface, the conventional techniques of resistivity interpretation are applicable.

The sensitivity of both methods to narrow anomalies could be improved by the use of a gradient array, consisting of two in-line electrode pairs connected so as to give the algebraic difference of their signals. This array should discriminate against broad lows caused by topography or by the basalt-conglomerate contact and would enhance the response over narrow features such as copper veins.

Further refinements are possible for both resistivity and AMT. For the resistivity

apparatus, multiple sensors in either Schlumberger or dipole-dipole configuration could be devised to allow for several electrode spacings to be used simultaneously. This array would allow different depths of penetration.

For the AMT experiment, we need interpretation curves for the near field. Higher frequency operation would allow plane wave operation near the loop. If our transmitter frequency were stabilized we could achieve narrower bandwidth, resulting in greater resistance to interference from powerline harmonics and natural EM noise, and therefore greater range. Transmitter stability could be improved by regulating the frequency electronically instead of mechanically as is now done.

APPLICABILITY OF THESE TECHNIQUES

Electrical prospecting methods have been adapted for use in fresh water and are capable of locating copper veins, contacts between rock types, and probable heavy-mineral placer deposits. The techniques we developed are likewise applicable to any geologic or engineering problem in shallow freshwater bodies where one needs to know the distribution of rock types or sediments of differing resistivities.

Shallow-water electrical prospecting has decided operational advantages over its land counterpart. Profiling can be done continuously and rapidly. Maintaining continuous electrical contact with the first layer is very simple in water and difficult on land. The water layer has relatively uniform resistivity. With electronic navigation, profile lines can be reliably and rapidly located. Except for the extremely shallow and hazardous parts of a nearshore survey site, most of the area is accessible for measurements. The thickness of the "overburden" is known along the entire profile so that its effect may be isolated from subbottom responses.

In the ocean, the "overburden" is very conductive and masks resistivity changes in the bottom. Resistivity profiling is better conducted with deep-towed arrays to facilitate bottom penetration. In the case of AMT measurements with a 400-Hz source, the skin depth will be reduced by the more conductive water to approximately 12 meters, appropriate for mineral exploration and engineering studies in shallow estuaries, bays and harbors.

ACKNOWLEDGMENTS

We are grateful to the Wisconsin Department of Natural Resources and the U.S. Bureau of Sport Fisheries for the loan of the R/V Salmo, a converted 36-foot surfboat which was used for the field work during the entire month of August, 1975. We gratefully acknowledge the participation during the survey of W. Unger, J. Luetgert, E. Meyer, W. Mooney, R. Meyer, Jr., J. Laurence, D. Laurence, L. Powell, R. Melenberg and K. Huang. We wish to thank L. Powell who designed the timing, recording and resistivity apparatus, D. Novotny and M. Erdman for their great help in rigging the vessel, J. Gallagher for the drafting, D. Kruger for editing and typing the final copy, the Motorola Corporation Marine Electronics Group for the demonstration of an omnidirectional radar transponder, and the Michigan Department of Natural Resources for providing a land base and dockage at Eagle Harbor, Michigan.

This work was supported by the Wisconsin Sea Grant College Program.

REFERENCES

1. Bannister, P. R.: "Determination of the electrical conductivity of the sea bed in shallow waters," Geophysics (1968) 33(6): 995-1003.
2. Bannister, P. R.: "Source distance dependence of the surface impedance conductivity measurement technique," Geophysics (1969) 34(5): 785-788.
3. Beeton, A. M.: "Eutrophication of St. Lawrence Great Lakes," Limnol. and Oceanog. (1965) 10(2): 240-254.
4. Boulos, F. K.: "Electrical sounding on the water-surface at Khor Kundi-El-Bahari in Egypt," Geophys. Prosp. (1972) 20: 304-316.
5. Dorr, J. A., Jr., and Eschman, D. F.: "Geology of Michigan," University of Michigan Press, Ann Arbor (1970) 31-80.
6. Meyer, R. P., Moore, J. R., and Nebrija, E. L.: "Underwater copper exploration in Lake Superior II: Specific targets charted in 1974," OTC Paper 2291 presented at the 7th Ann. Conf. Offshore Tech. Conf., Houston, May 5-8 (1975).
7. Parkhomenko, E. I.: "Electrical Properties of Rocks," G. V. Keller (Ed. and Trans.), Plenum Press, New York (1967) p. 278.
8. Patella, D., and Schiavone, D.: "A theoretical study of the kernel function for resistivity prospecting with a Schlumberger apparatus in water," Annali di Geofisica (1974) 28(1-2): 295-313.
9. Strangway, D. W., and Vozoff, K.: "Mining exploration with natural electromagnetic fields," in Mining and Groundwater Geophys. (I. W. Morley, Ed), Dept. of Energy, Mines and Resources, Ottawa, Canada (1967) 109-122.
10. Strangway, D. W., Swift, C. M., and Holmer, R. C.: "The application of audio-frequency magnetotellurics (AMT) to mineral exploration," Geophysics (1973) 38(6): 1159-1175.
11. Swift, C. M.: "Theoretical magnetotelluric and Turam response from two-dimensional inhomogeneities," Geophysics (1971) 36(1):

38-52.
12. Unz, M.: "Interpretation methods for geophysical exploration of reservoirs," Geophysics (1959) 24(1): 109-141.
13. Van'Yan, L. L.: "Theoretical curves for electrical sea probing with a sea-bottom apparatus," Applied Geophysics, Gostoptekhizdat (1956) 50.
14. Vozoff, K.: "The magnetotelluric method in exploration of sedimentary basins," Geophysics (1972) 37(1): 98-141.
15. Ward, S. H., Ryu, J., Glenn, W. E., Hohman, G. W., Dey, A., and Smith, B. D.: "Electromagnetic methods in conductive terrains," Geoexploration (1974) 12: 121-183.
16. White, W. S.: "The base of the Upper Keweenawan in Michigan and Wisconsin," U.S. Geol. Surv. Bull. 1354-F (1972) 23 p.
17. Whiteley, R. G.: "Design and preliminary testing of a continuous offshore resistivity method," Bull. Aust. Soc. Explor. Geophys. (1974) 5(1): 9-13.
18. Young, C. T.: "Magnetotelluric measurements in the 1- to 50-Hz band in northern Wisconsin," Ph.D. thesis, University of Wisconsin, Madison (1976) in preparation.

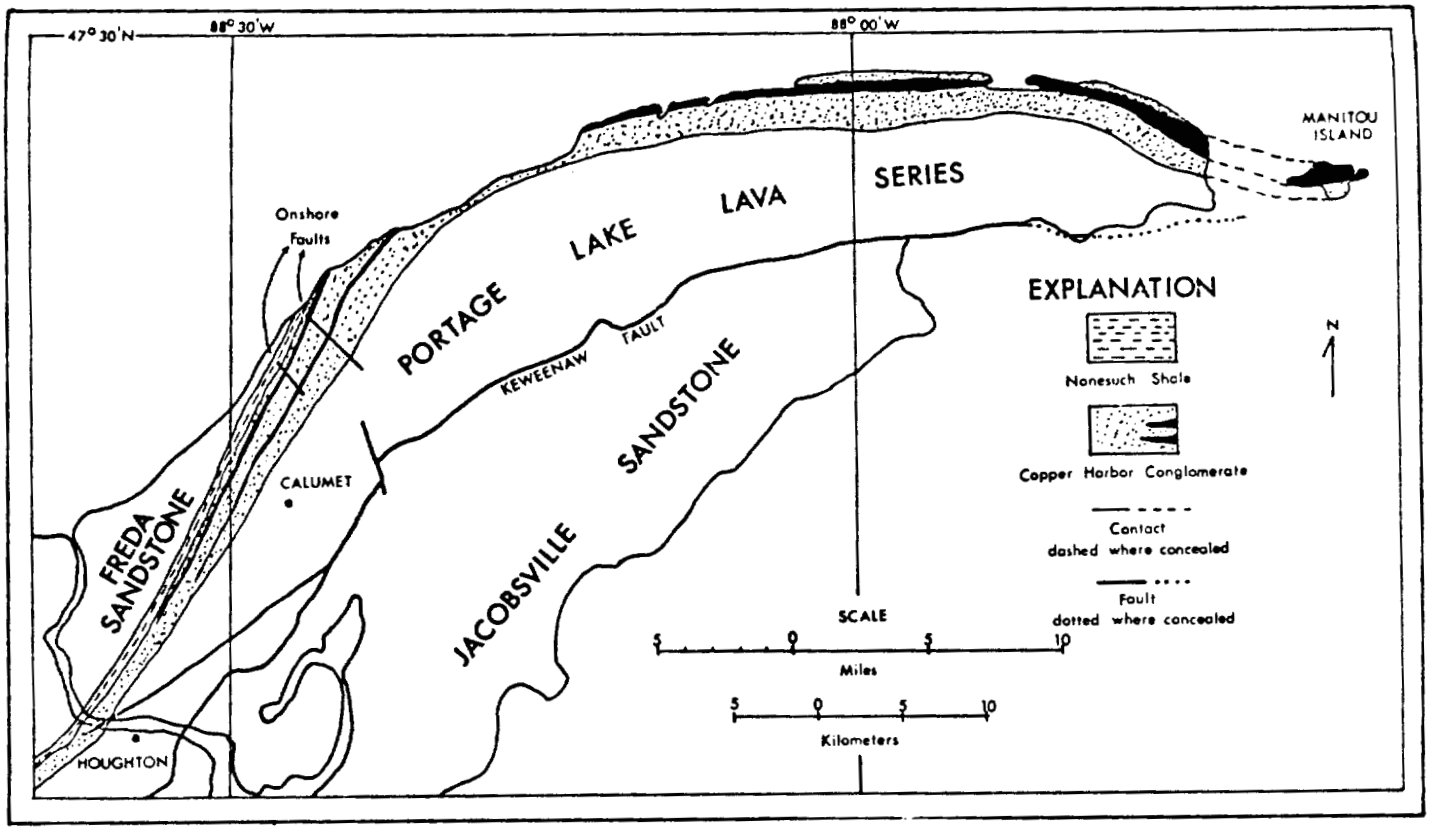

Fig. 1 - Generalized geologic map of Keweenaw Peninsula. Modified from White (1972).

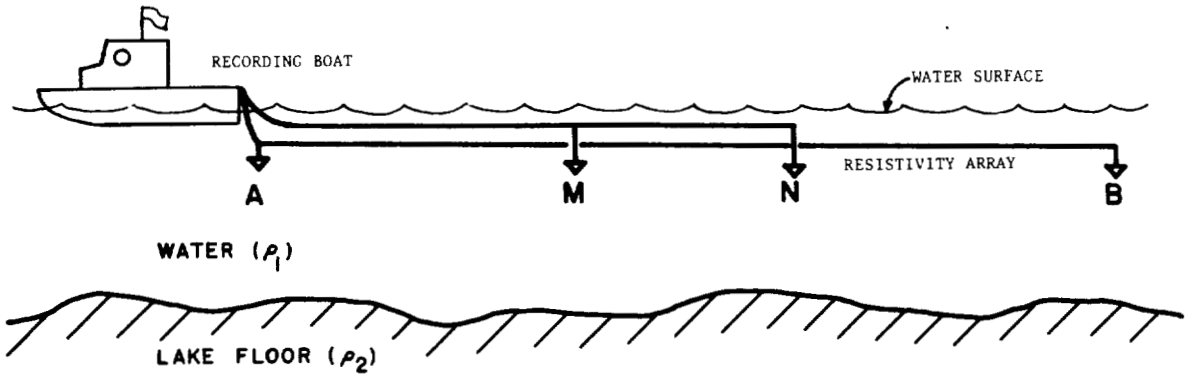

A, B = CURRENT ELECTRODES

M, N = POTENTIAL ELECTRODES

R_1 = AM

R_2 = BM

R_3 = AN

R_4 = BN

FOR 12-FOOT POTENTIAL ELECTRODE

AB = 455 FEET

MN = 12 FEET

FOR 70-FOOT POTENTIAL ELECTRODE

AB = 455 FEET

MN = 70 FEET

Fig. 2 - Field configuration of surface-towed Schlumberger resistivity array. The array used had a 455-foot current electrode separation and potential electrode spacings of either 12 feet or 70 feet. All electrodes were the bared ends of a parallel pair of 18-gauge copper wires. With low-frequency alternating current used as source, electrode polarization was not a problem. The center of the array was 230 feet aft of the 36-foot recording boat.

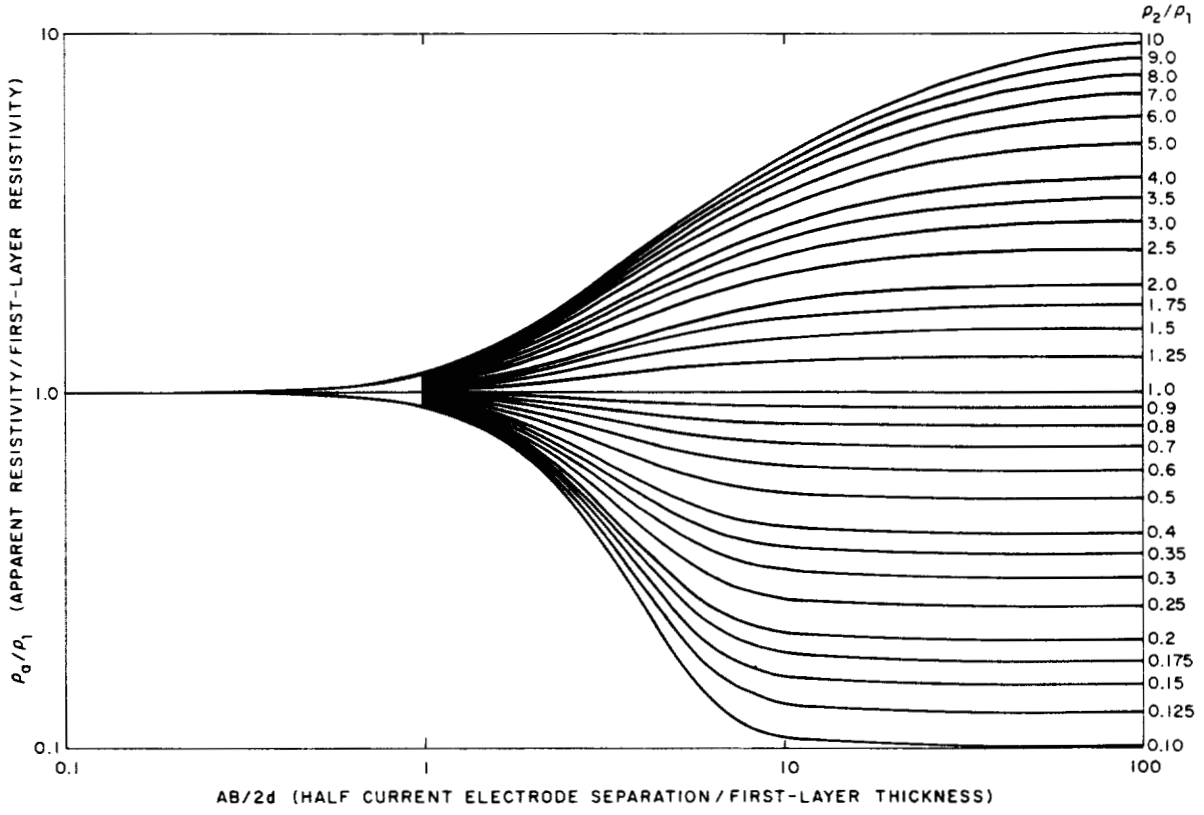

Fig. 3 - Two layer Schlumberger sounding curves. The current electrode half-spacing, AB/2, is generally denoted by a and the abscissa is then simply a/d. For small a/d ratios ($\simeq$ 1.0), $\rho_a/\rho_1 \simeq 1.0$, and for larger a/d ratios, $\rho_a \simeq \rho_2$.

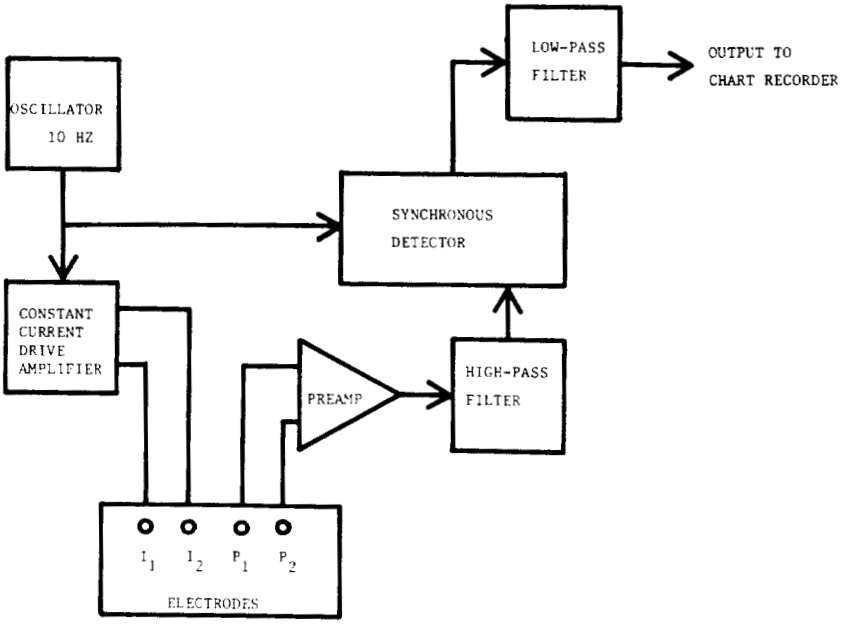

Fig. 4 - Block diagram of resistivity apparatus. An oscillator generates square waves at a frequency of about 10 Hz, controlling a synchronous detector and driving the current electrodes 100 mA through a constant current drive amplifier. The signal present on the potential electrodes is amplified and passed through a high-pass filter with a corner frequency of 1/10 Hz. The resulting zero mean ac is passed through the synchronous detector and then low-pass filtered at 1/10 Hz to remove the operating frequency components. The final slowly-changing dc voltage is then displayed on the same fathometer chart as the bathymetry.

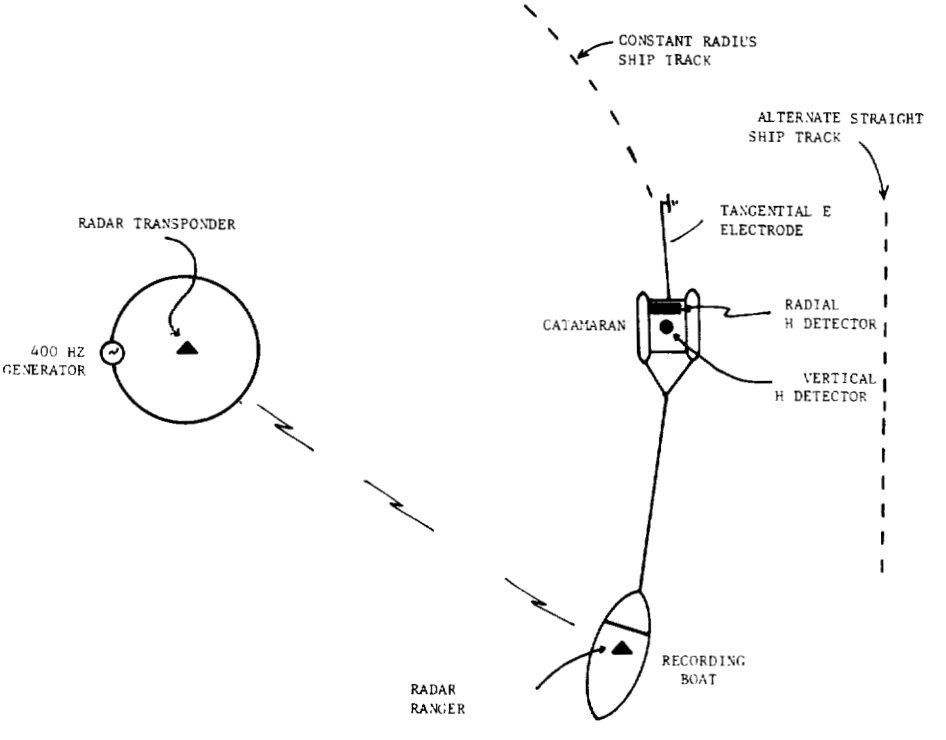

Fig. 5 - Field layout of AMT apparatus. Signal source was a 1.5 kw gasoline generator, delivering approximately 8 amps to the loop, regulated by series resistors. The loop, having a diameter of 150 meters, was laid on lake bottom. Traverses were made at radii ranging from 500 to 1250 meters. Details of receiving apparatus are given in Figure 6.

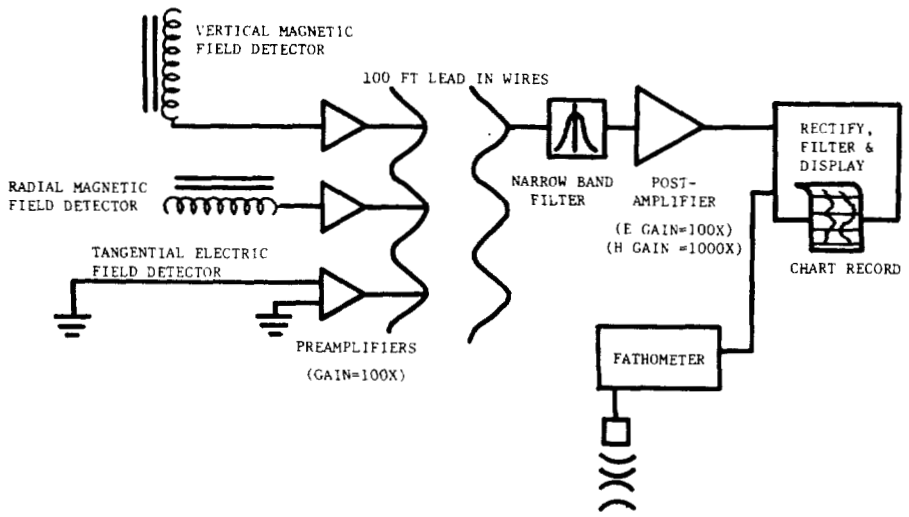

Fig. 6 - Block diagram of AMT apparatus. Sensors and preamplifiers were mounted on an 8-foot long catamaran. The catamaran was towed 100 feet behind the research vessel, a 36-foot converted Coast Guard surf boat. The electric field was detected by measuring the potential difference between twc electrodes, pieces of copper braid in contact with the water. The near electrode was tied to the bottom of the catamaran and the far electrode was towed near the surface at the end of a 70-foot insulated wire. The magnetic sensors consisted of 10,000 turns of 28-gauge wire, wound about a square ferrite core and mounted in waterproof plastic tubes (Young, 1976). Parallel capacitors resonated the coil to 400 Hz. The sensitivity of the coils was approximately 32 millivolts per gamma (one gamma = 10^{-5} gauss), determined using Helmholtz coils. The vertical magnetic field channel was not used in this experiment.

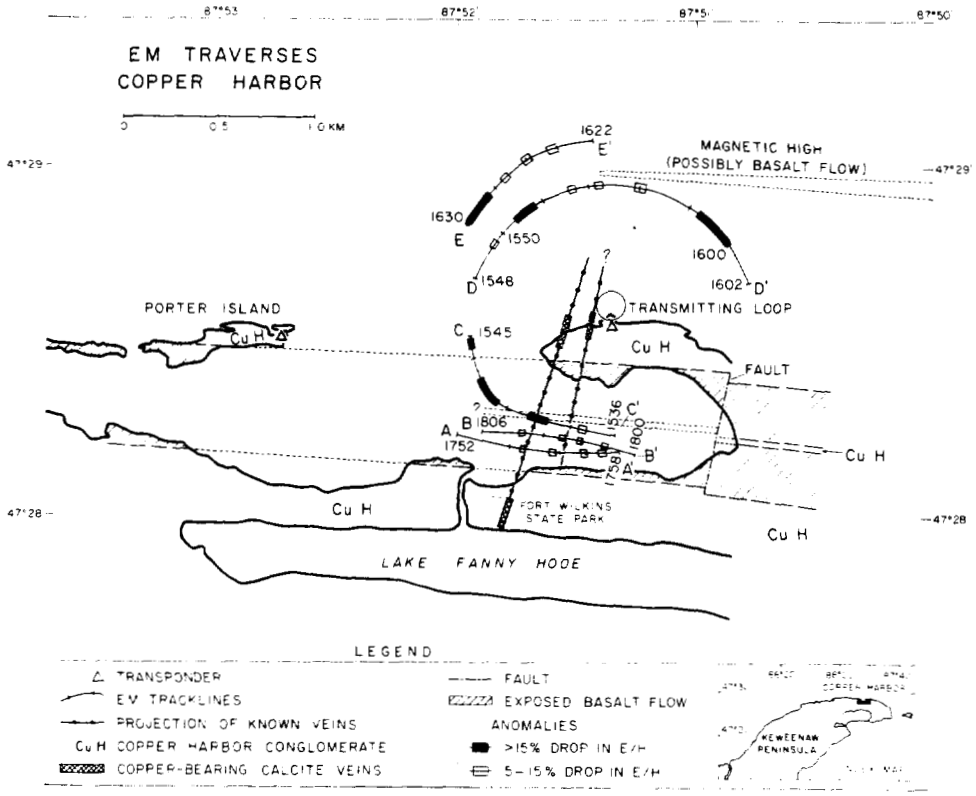

Fig. 7 - Tracklines and location of anomalies from the AMT work at Copper Harbor. Station numbers are clock times, marked at two-minute intervals. Anomalies mark copper veins inside the harbor, transitions from basalt to conglomerate and two parallel bands outside the harbor which we interpret as a low resistivity layer in the conglomerate and as a probable basalt flow. Geology is drawn from USGS Geologic Quadrangle maps GQ 52 & 74.

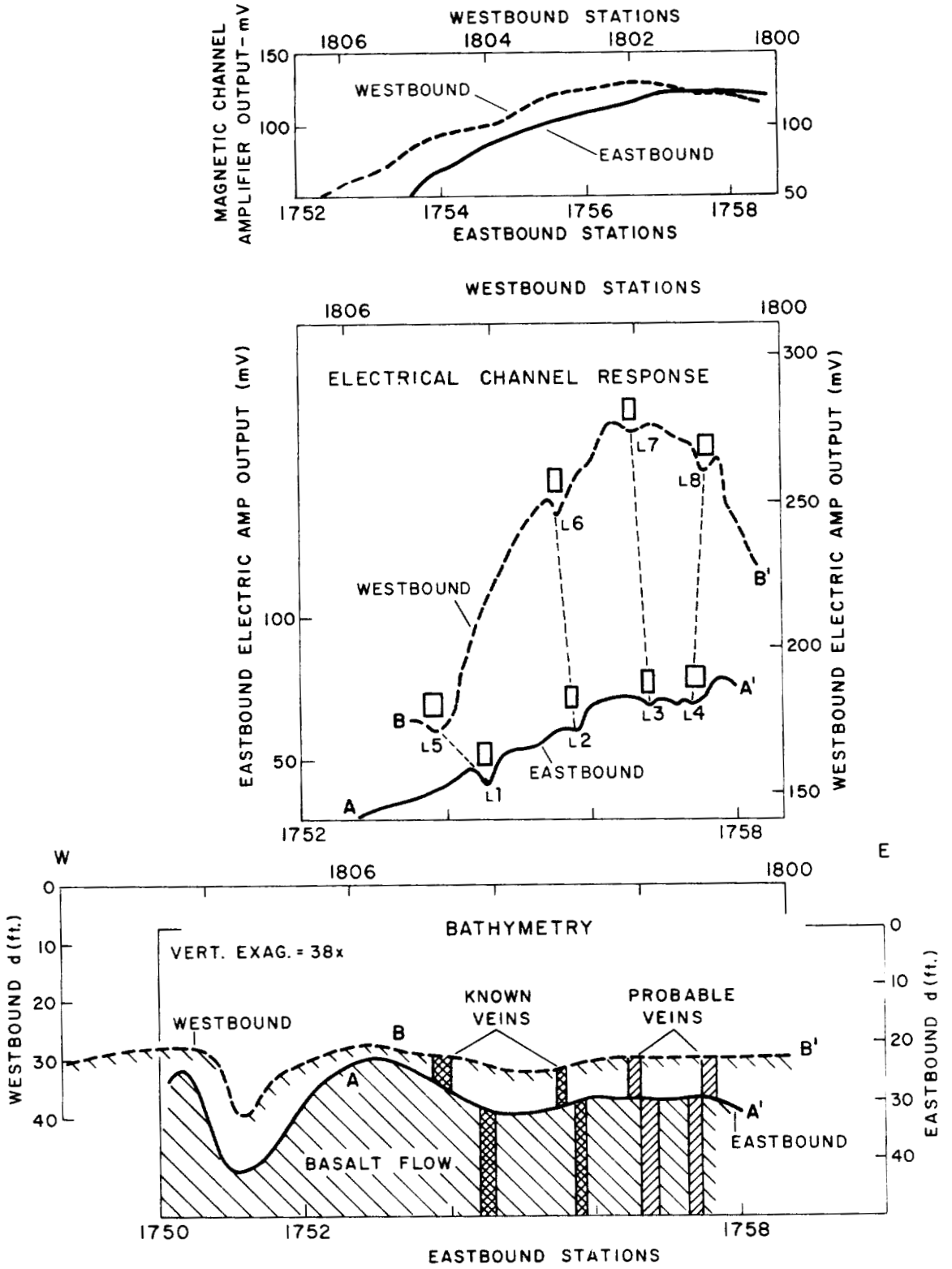

Fig. 8 - Data from traverses AA' and BB'. Copper Harbor. Plots are horizontal magnetic field (transverse to trackline), horizontal electric field (longitudinal to trackline), and bathymetry. Copper veins show as narrow anomalies of three to five percent drop in electric field. The width of the anomalies is approximately the same as the length of the electrode pair, indicating that sharper anomalies might be found with a shorter probe. The anomalies do not appear on the magnetic channel.

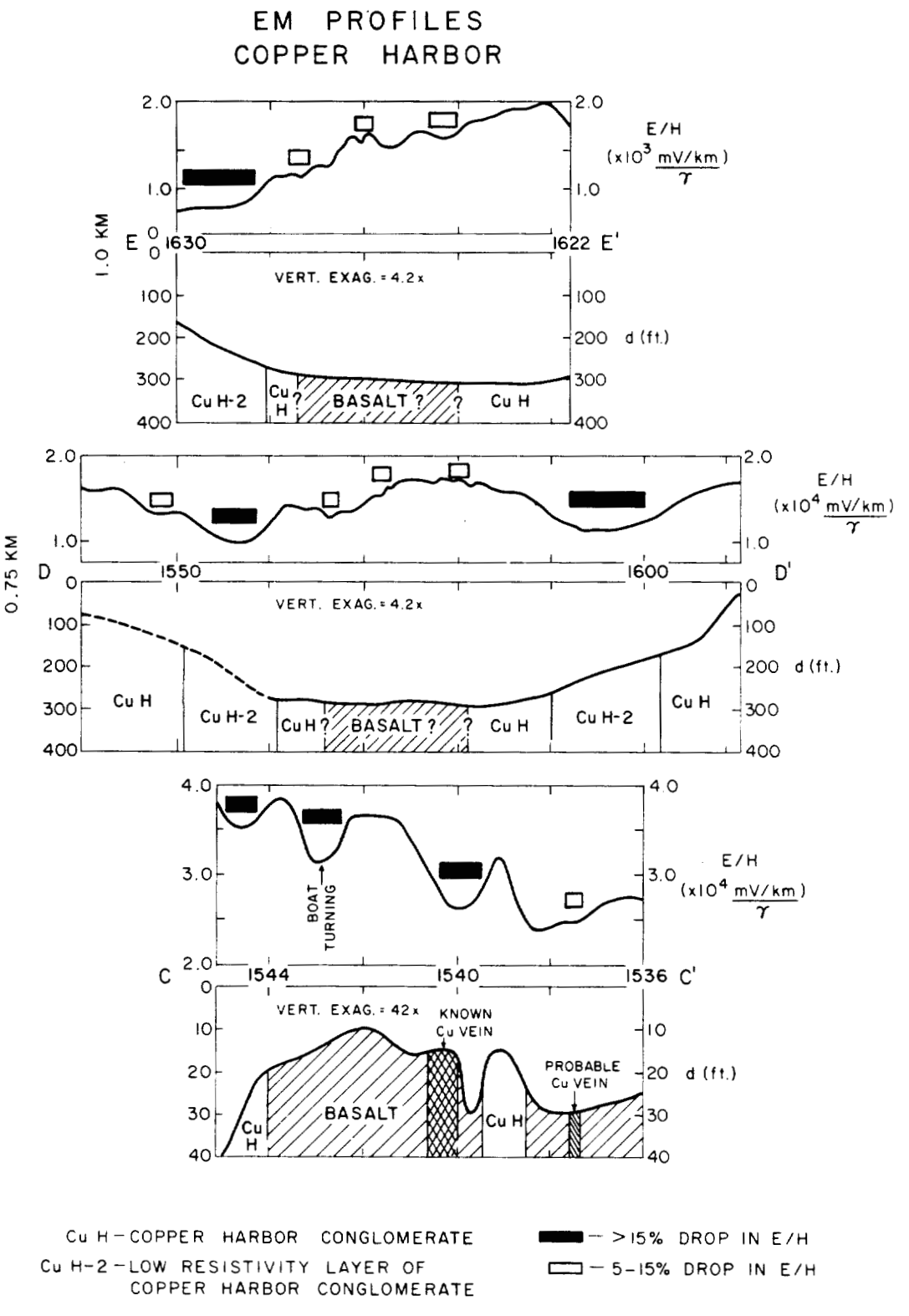

Fig. 9 - AMT profiles CC', DD' and EE' in Copper Harbor. Profile CC' passes over the extension of the Fort Wilkins copper vein (Station 1539), but expected anomaly is possibly masked by the effect of the topographic low.

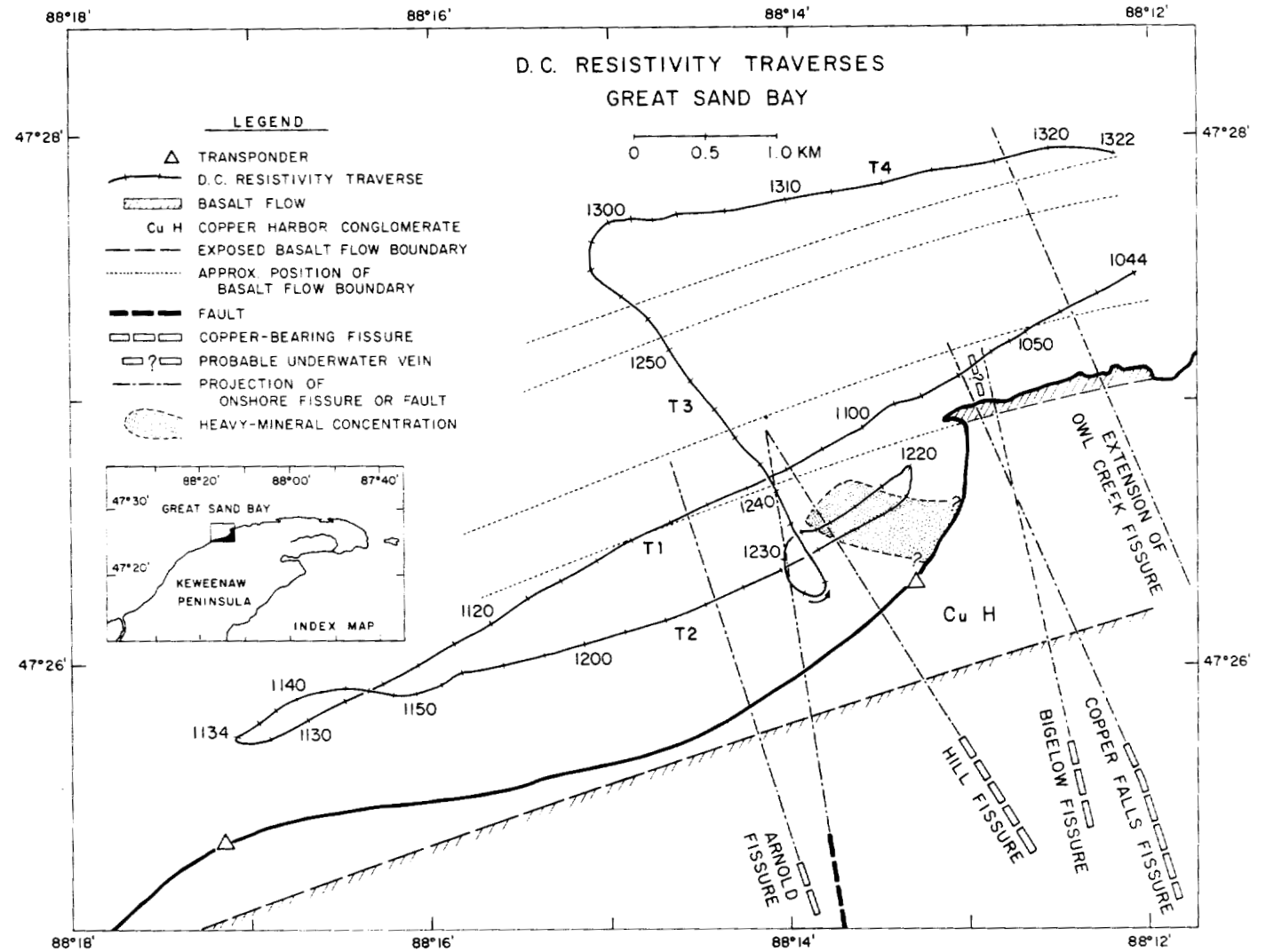

Fig. 10 - Resistivity traverses in Great Sand Bay. Three of these traverses (T1, T2, and T4) are oriented perpendicular to the offshore projections of onshore copper-bearing fissures. Traverse T3 is oriented normal to the geologic strike of the major rock units. Following figures show the resistivity profiles for each traverse, except for T4 which is in deep water and where ρ_a/ρ_1 remains practically constant at 1.0 along the entire profile. Water depths vary from 15 to 40 feet inside the bay and increase to 450 feet outside a scarp making the northern boundary of the nearshore basalt flow. An offshore basalt flow is marked by bathymetry and aeromagnetic measurements. The zone of heavy-mineral concentration discovered in 1974 with a bottom-towed array is confirmed in the present survey with the surface-towed array. The geology is drawn from USGS Beologic Quadrangle map GQ 36.

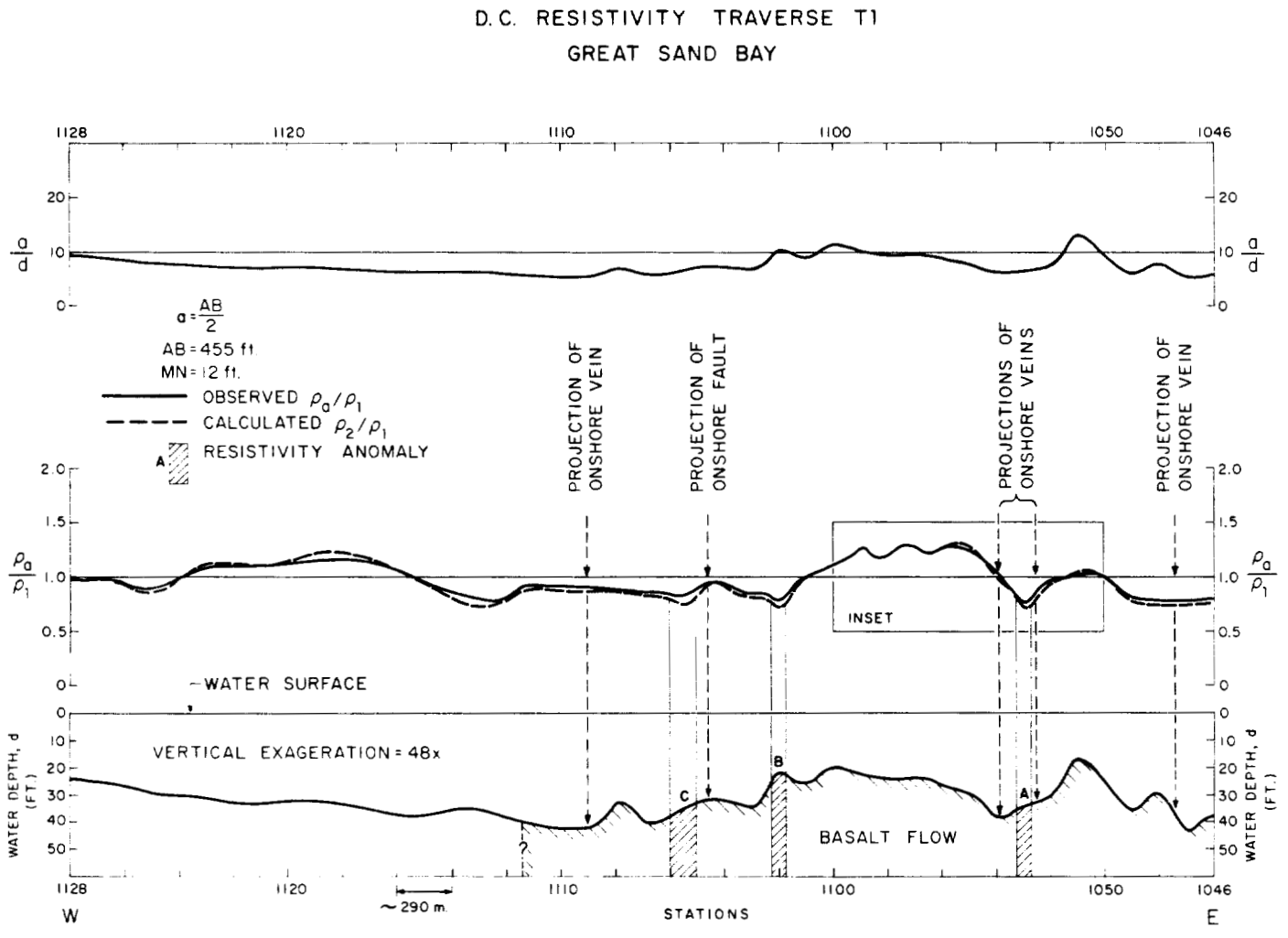

Fig. 11 - Resistivity profile for Traverse T1. Half of the traverse runs longitudinally over a basalt flow characterized by rough topography. Calculated ρ_2/ρ_1 profiles remove, to a first-order approximation, the topographic effect. Many shorter-wave length/resistivity variations may be due to rapid changes in topography. The resistivity anomalies marked A, B and C are discussed in the text. The basalt-flow resistivity obtained here is lower than for Traverse T3 (Figure 14), probably due to the effect of lower-resistivity sediments on one side of the traverse. Inset is shown in Figure 12.

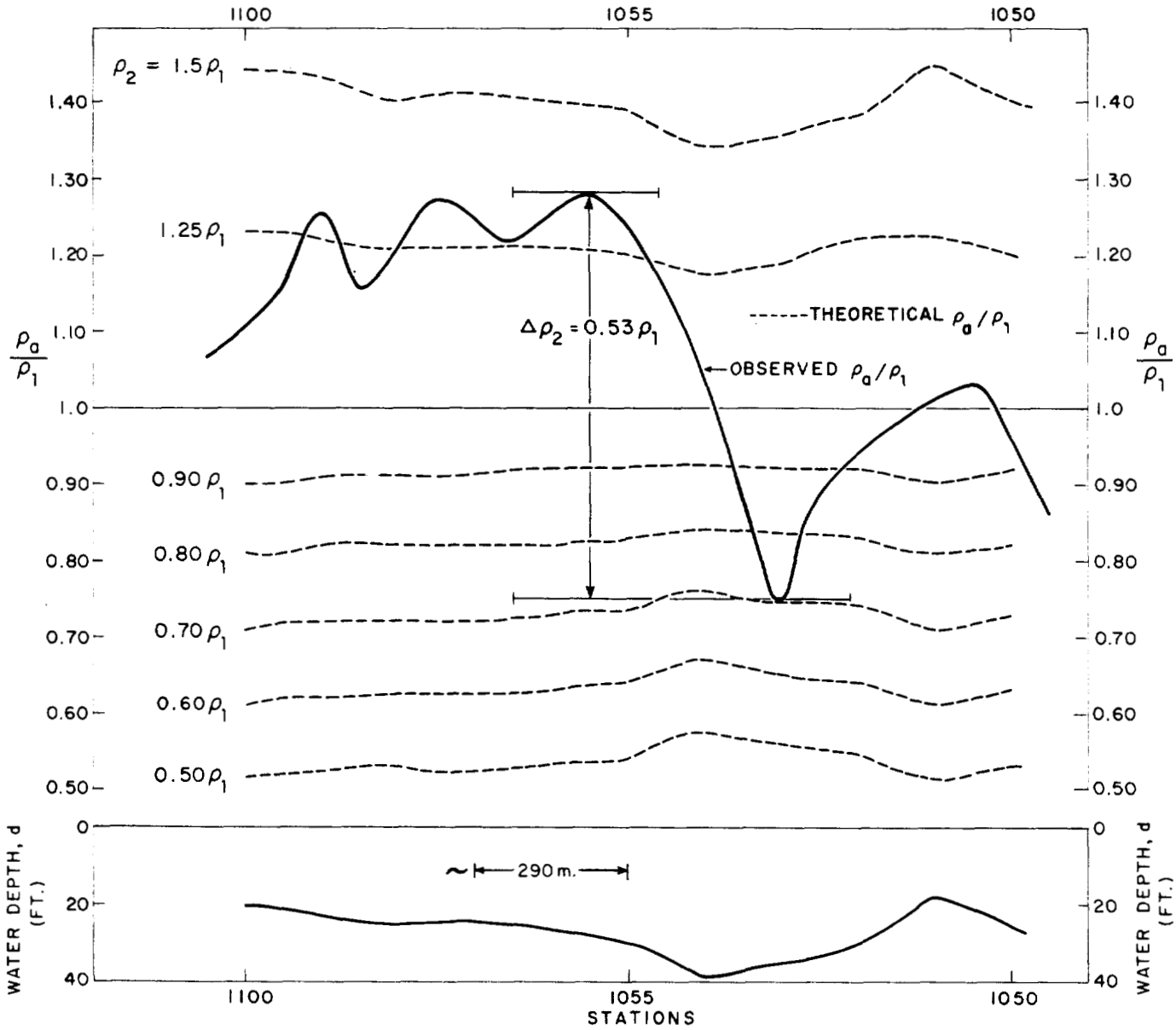

Fig. 12 - Inset of Figure 11. Comparison of observed ρ_a/ρ_1 profile with theoretical ρ_a/ρ_1 profiles across Anomaly A of Traverse T1 after the method of Whiteley (1974). Each theoretical profile is drawn for a constant subbottom resistivity, ρ_2. Theoretical profiles with $\rho_2/\rho_1 < 1.0$ anticorrelate with bottom topography and those for $\rho_2/\rho_1 > 1.0$ correlate with topography. The topographic effect is more pronounced for greater resistivity contrasts between the water and the lake floor. Between stations 1056 to 1100, the observed ρ_a/ρ_1 profile is approximately centered about the theoretical profile for $\rho_a/\rho_1 = 1.30$. Between 1051 and 1055, however, the observed profile intersects the theoretical profiles, indicating an anomaly since the resistivity change in the observed profile cannot be accounted for by topographic changes alone.

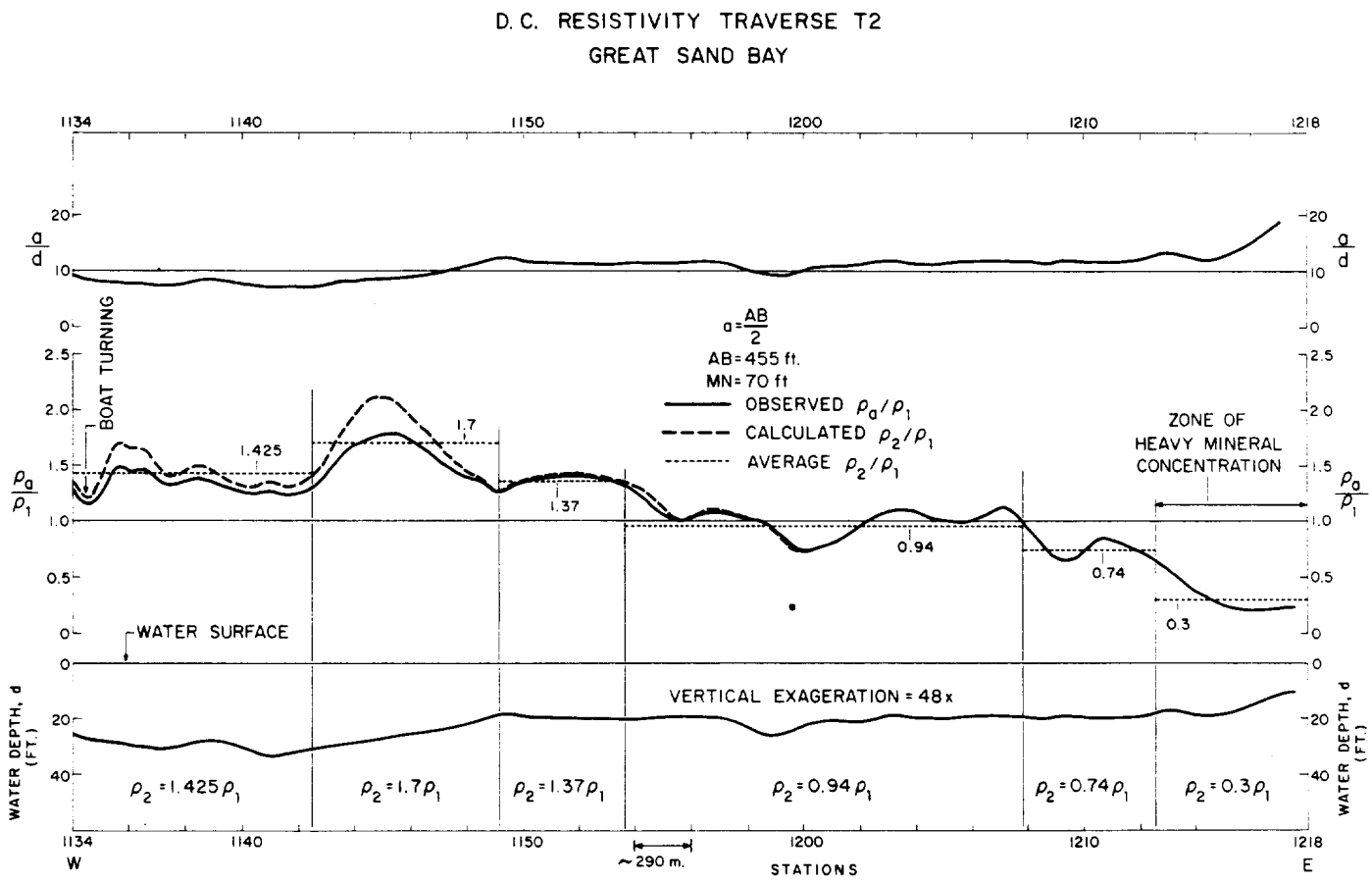

Fig. 13 - Resistivity profile for Traverse T2. The a/d ratio averages about 10 along the profile. The difference between calculated ρ_2/ρ_1 and observed ρ_a/ρ_1 profiles is greater for larger resistivity contrasts and lower a/d ratios. To a first-order approximation, this difference is equal to the "topographic effect." Sections of the profile are grouped visually and the average ρ_2/ρ_1 for each section is calculated. The lake bottom here consists mostly of water-saturated sands and gravels and the variation in ρ_2/ρ_1 along the profile may be due to the varying proportions of the sediment constituents. The zone of heavy-mineral rich sands is characterized by a very low resistivity of 0.30 ρ_1.

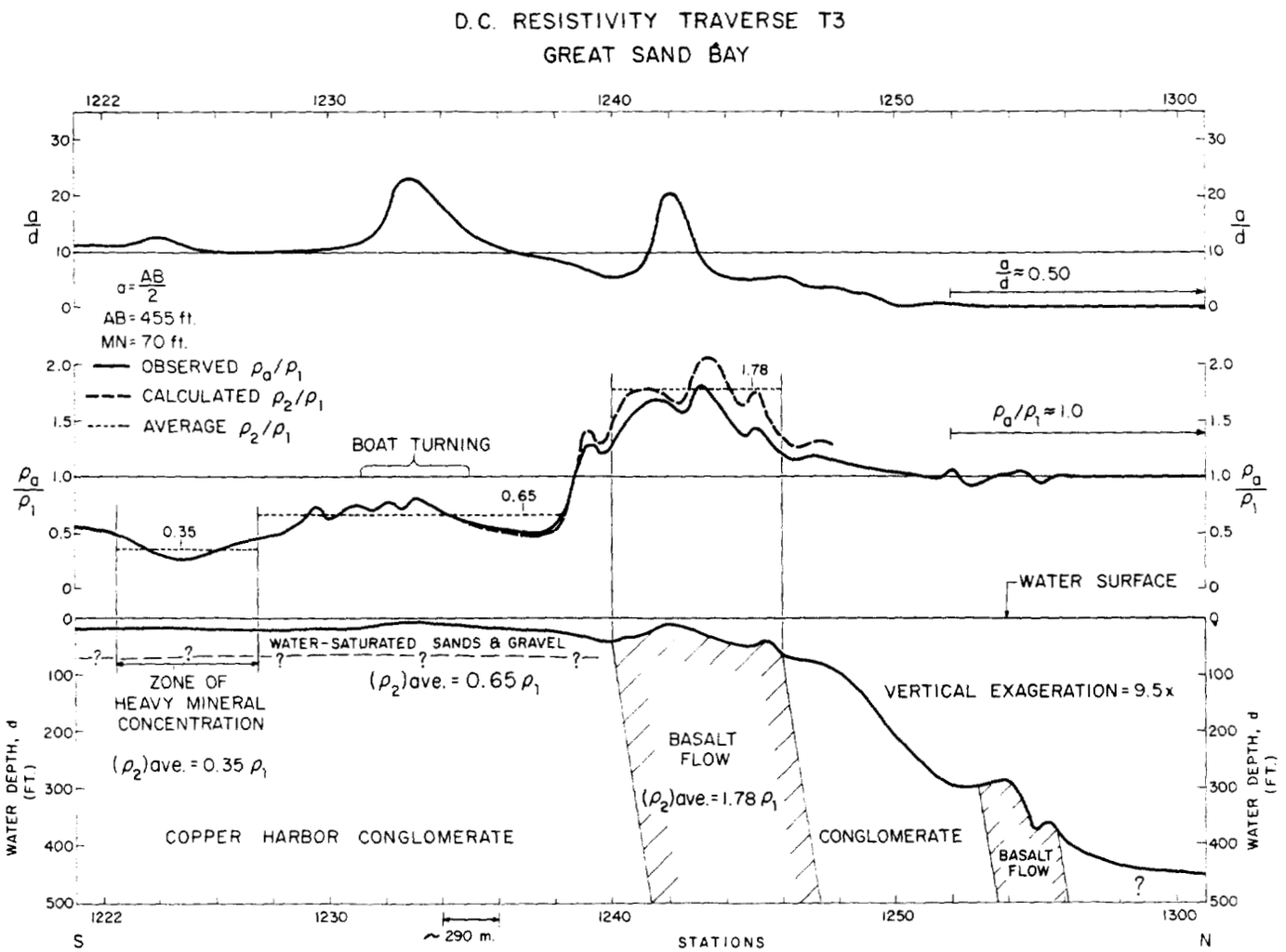

Fig. 14 - Resistivity profile for Traverse T3. This traverse from nearshore to offshore runs normal to the geologic strike. A sharp resistivity change is associated with the basalt-conglomerate boundary. The three resistivity regimes described in the text are indicated. Resistivity fluctuations over the basalt flow may be due to short-wavelength topographic changes not removable with the first-order topographic correction. North of station 1250, the water depth increases rapidly and the value of ρ_2/ρ_1 cannot be accurately determined from the two-layer curves of Figure 3. The small ripples in the resistivity profile at station 1254 indicate that the basalt flow at 300 feet depth still affects the measured apparent resistivity. Beyond 400 feet depth, the measured resistivity is that of the water layer.

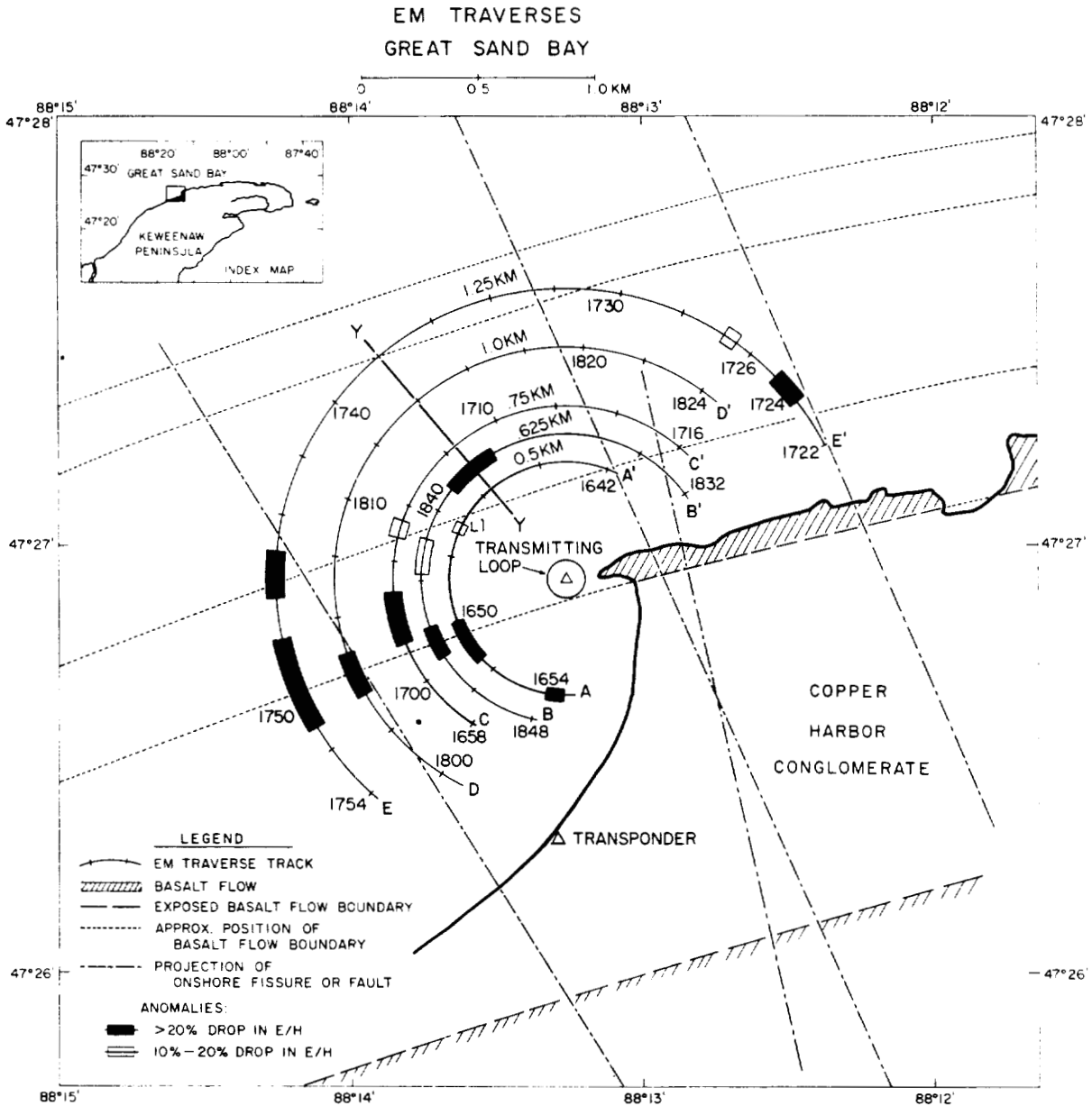

Fig. 15 - AMT traverses at Great Sand Bay. Traverses are along arcs concentric to transmitting loop controlled by keeping the active radar range constant.

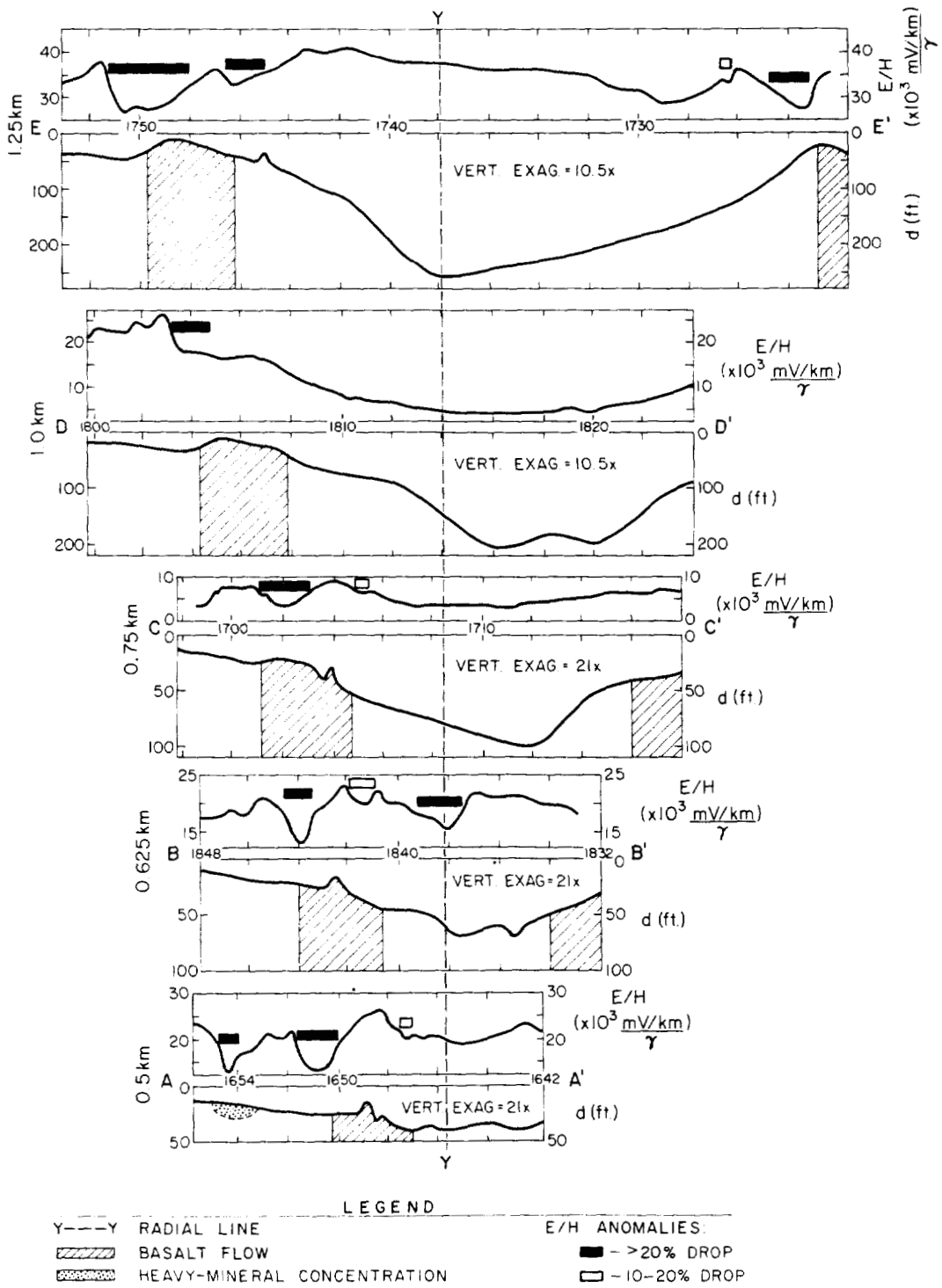

Fig. 16 - AMT profiles at Great Sand Bay. Strong anomalies (solid rectangles) mark the southern edge of the basalt flow, the heavy-mineral concentration sands at station 1654 on traverse AA', the northern edge of the basalt flow at 1724 on traverse EE'. Weaker anomalies (open boxes) mark the northern edge of the basalt flow on profiles AA', BB' and CC'. There is a strong anomaly for which we have not found an associated geological feature bracketing station 1838 on profile BB'.

NATIONAL RESEARCH COUNCIL OF CANADA
ASSOCIATE COMMITTEE ON GEOTECHNICAL RESEARCH

PROCEEDINGS

of a

SYMPOSIUM

on

PERMAFROST GEOPHYSICS (NO. 5)

13 and 14 NOVEMBER 1978

Prepared by

W.J. SCOTT and R.J.E. BROWN

TECHNICAL MEMORANDUM NO. 128

JULY 1980

A SYSTEM FOR RESISTIVITY SURVEYING IN WATER

J. Lobach and W.J. Scott

INTRODUCTION

In 1973 an airborne resistivity survey was flown in the Tuktoyaktuk area to determine the feasibility of measuring permafrost extent from the air (Sellman et al, 1974). The interpreted results of the VLF indicated a good correlation to the then known permafrost distribution and thickness (Scott and Hunter, 1977). Of particular interest were the relatively high resistivities measured over the centres of some of the lakes, specifically Grass Lake (Figure 1). Drilling through the ice in the spring of 1973 indicated that Grass Lake was in fact frozen to the bottom; in places even 30 cm of sediment were also frozen. Therefore, it was suspected that the permafrost did extend from shore out beneath the lake.

However, a D.C. resistivity sounding done in the spring of 1974 in holes drilled through the ice, indicated that there was no permafrost present beneath the lake bottom at least to a depth of 200 m (Scott, 1975). Resistivity studies carried out in the winter through holes drilled in the ice are so cumbersome and slow that obtaining sufficient data to assess the resistivity distribution under Grass Lake appeared difficult. In the summer of 1974 some waterborne resistivity measurements were attempted (Scott, 1975). These attempts included Schlumberger soundings and Wenner profiles. A sounding in Grass Lake confirmed the results of the winter work. The interpreted resistivities and depths relating to the shallow portion of these soundings are consistent with the drilling results on land adjacent to Grass Lake. Two Wenner profiles (a = 5 m and 15 m) were run along the line of the summer soundings. Near the shore high apparent resistivities (ρ_a) indicate the presence of permafrost. In the middle of the lake ρ_a values range from 40 to 50 ohm-m. These values agree well with those from the interpreted soundings. From the data it appears that there is no permafrost along the profile lines at least to a depth of a few metres except near the shore.

Subsequently it was felt that development of a marine resistivity profiling system would be feasible and could yield promising results. In 1975 a six-channel prototype was constructed to measure apparent resistivities with a towed multi-dipole array. Considerable experience and a small amount of data were obtained with the prototype. The system described in this paper was developed in the light of that experience.

In order to allow flexibility in programming, the present system is controlled by a Motorola M6800 microprocessor. A block diagram of the system is shown in Figure 2. The system operates with a towed array consisting of one transmitter dipole and six consecutive receiver dipoles (Figure 3). The transmitter dipole, nearest the boat, is energized by a Huntec Lopo Transmitter, modified to produce a square wave with a period of six seconds. A current reference signal and the voltages from the six receiver dipoles are applied to seven isolation amplifiers with gains manually selected. Under control of the microprocessor, the outputs of the isolation amplifiers for each half cycle are applied in turn through a multiplexer to an autoranging amplifier and an analog-to-digital converter. The digital values are used as inputs to a microprocessor program which calculates apparent resistivities. The current level and the six values of apparent resistivity are recorded on cassette tape, together with time, water depth and positional information.

The depth sounder is a Heath Kit instrument Model No. M1-101 with the time constant shortened 10 microseconds to allow it to resolve water depths as small as three feet. The navigation system is a delNorte Trisponder, which provides radar ranges to slaves in fixed positions on the shore.

The instrumentation was almost completely ready by June 1978. Development work during the summer field season was concentrated on improvement of cable design to minimize movement noise and spontaneous polarization problems. For the 5 m array copper wire wrapped around the axis of the cable produced the best streamlining and, therefore, low electrode noise; self potential was also at a minimum. This cable was only 40 meters long and therefore was successfully streamed through the water at a depth of 30 to 40 cm without flotation material. Submerging it in this way avoided undesirable breaks in the electrode contact caused by temporary surfacing of the cable between waves.

The 30 m array was more than 300 m long and therefore had to be floated on the surface to avoid fouling. In this case copper pipe was suspended about 30 cm below the cable. At low speeds these electrodes did not surface; however, electrode noise was high because of poor streamlining. Low signal levels of 5-10 millivolts (mv) peak to peak were superimposed on approximately 80 mv of self-potential (SP) that varied with position. This SP caused biasing and saturation problems on the input amplifiers. Most of the effort during the 1978 field season was devoted to solving this problem. In 1979 it is planned to use an electrode

design similar to that described by Corwin and Carti (1973) which is expected to minimize noise problems.

SURVEY PROCEDURE

Normal survey procedure consisted of streaming the appropriate cable out behind the boat and making a series of parallel traverses over the area to be surveyed. Figure 4 shows such a series of boat tracks surveyed on Grass Lake. The tick marks on the tracks represent data points separated by about 10 m. A hand calculator was used to calculate the instantaneous positions of the boat from the trisponder readings, which were then plotted on a map as a guide to the helmsman. The time lag between obtaining the trisponder data and plotting the course made it difficult to run an absolutely straight course. By the end of 1979 it is planned that the course recovery will be handled automatically with a much reduced time lag.

During survey runs there was frequent variation in the D.C. offsets observed across the receiver dipoles. The offset was due mostly to changing electrochemical effects as the cable and electrodes moved through the water. It was necessary to monitor and correct for the D.C. offsets constantly during the survey to avoid saturation of the isolation amplifiers. When resistivities changed greatly (such as on crossing from unbonded to ice bonded sediments) it was necessary to alter the transmitter current to prevent saturation of the isolation amplifiers.

DISCUSSION

Three maps of Grass Lake show contoured resistivity data for dipole spacings of nx = 5, 10 and 30 metres (Figures 5, 6 and 7). Previous electrical measurements in the area (Scott, 1975) showed resistivities of the water to be about 40 ohm-m or less and of the sub bottom unfrozen sediments to be from 40 to 70 ohm-m. The water depths were two m on the average. The resistivity contours of Figure 5 (n = 1) are strongly influenced by variations in the water depth. Where the water is more than 2 m deep the apparent resistivity values tend towards 40 ohm-m; where the water depth is less than 2 m,apparent resistivity values increase from 40 to 70 ohm-m. A method of correcting the measured resistivities for varying water depths is under development.

For the multi-dipole spacing of n = 2 the contour map shows the apparent resistivity to be within the range of 40 to 70 ohm-m over most of the lake. The distribution of the resistivity range appears to be uniform over the lake

area. High resistivities are observed only near the shores of the lake. Permafrost is believed to extend out under the lake until water depths exceed 1.5 m. The configuration of this permafrost interface is being studied by electromagnetic techniques at the present time. The map of contoured resistivities measured with n = 6 confirms that a highly resistive permafrost layer extends out a short distance beneath the lake.

These contour maps are preliminary. There are still some data which show the influence of D.C. offsets of different magnitudes on some of the recorder channels which will be numerically corrected.

CONCLUSIONS

A system for measuring apparent electrical resistivities in water has been developed and used successfully in the field, although problems in a design of electrodes and cables still remain to be solved. The resistivities obtained with the system in Grass Lake, near Tuktoyaktuk, N.W.T., are geologically reasonable and agree with measurements made by other means.

ACKNOWLEDGEMENTS

The design and construction of the marine resistivity unit was carried out by C. Gauvreau with assistance of J. Frechette and R. Sloka. Cable construction was undertaken by A. Neiva (Projeto Geofisico Brasil-Canada), B. Todd and E. Farquhar, who also assisted in field trials near Ottawa and near Tuktoyaktuk, N.W.T.

REFERENCES

1. Corwin, R.F. and Carti, U., 1973. A rugged silver-silver chloride electrode for field use. Rev. Sci. Instrum., Vol. 44, No. 6, pp. 708-811.

2. Scott. W.J., 1975. Preliminary experiments in marine resistivity near Tuktoyaktuk, District of Mackenzie. Geol. Surv. Can. Paper 75-1A, pp. 141-145.

3. Scott, W.J. and Hunter, J.A., 1977. Applications of geophysical techniques in permafrost regions. Can. J. Earth Sci., Vol. 14, No. 1, pp. 117-127.

4. Sellmann, P.V., McNeill, J.D. and Scott, W.J., 1974. Airborne E-Phase resistivity surveys of permafrost, Central Alaska and Mackenzie River areas. In Proc. NRC Symp. on Permafrost Geophysics, L.S. Collett and R.J.E. Brown, ed. NRC Tech. Mem. No. 113, pp. 67-71.

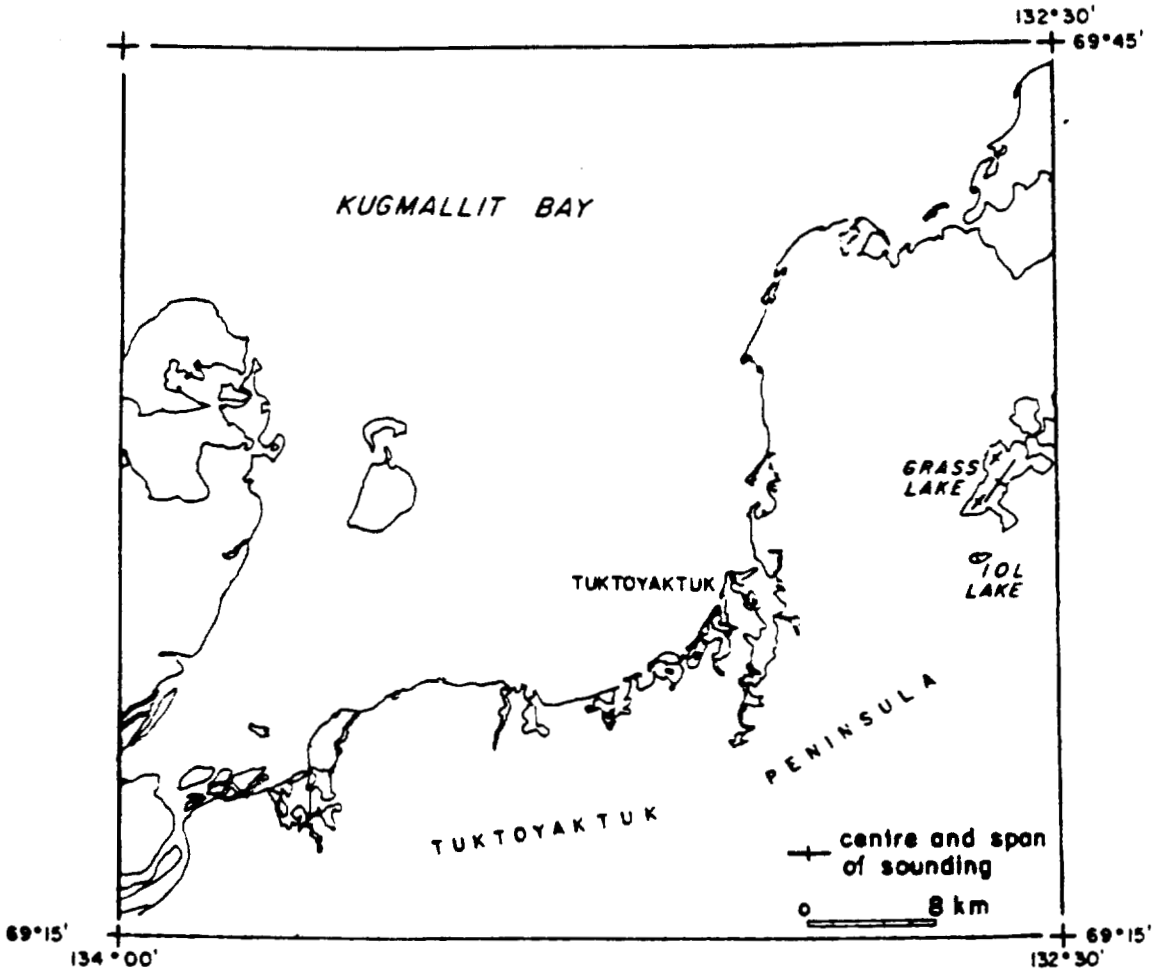

Figure 1 Location map showing position of Grass Lake relative to Tuktoyaktuk, and soundings carried out in 1974

DATA ACQUISITION SYSTEM

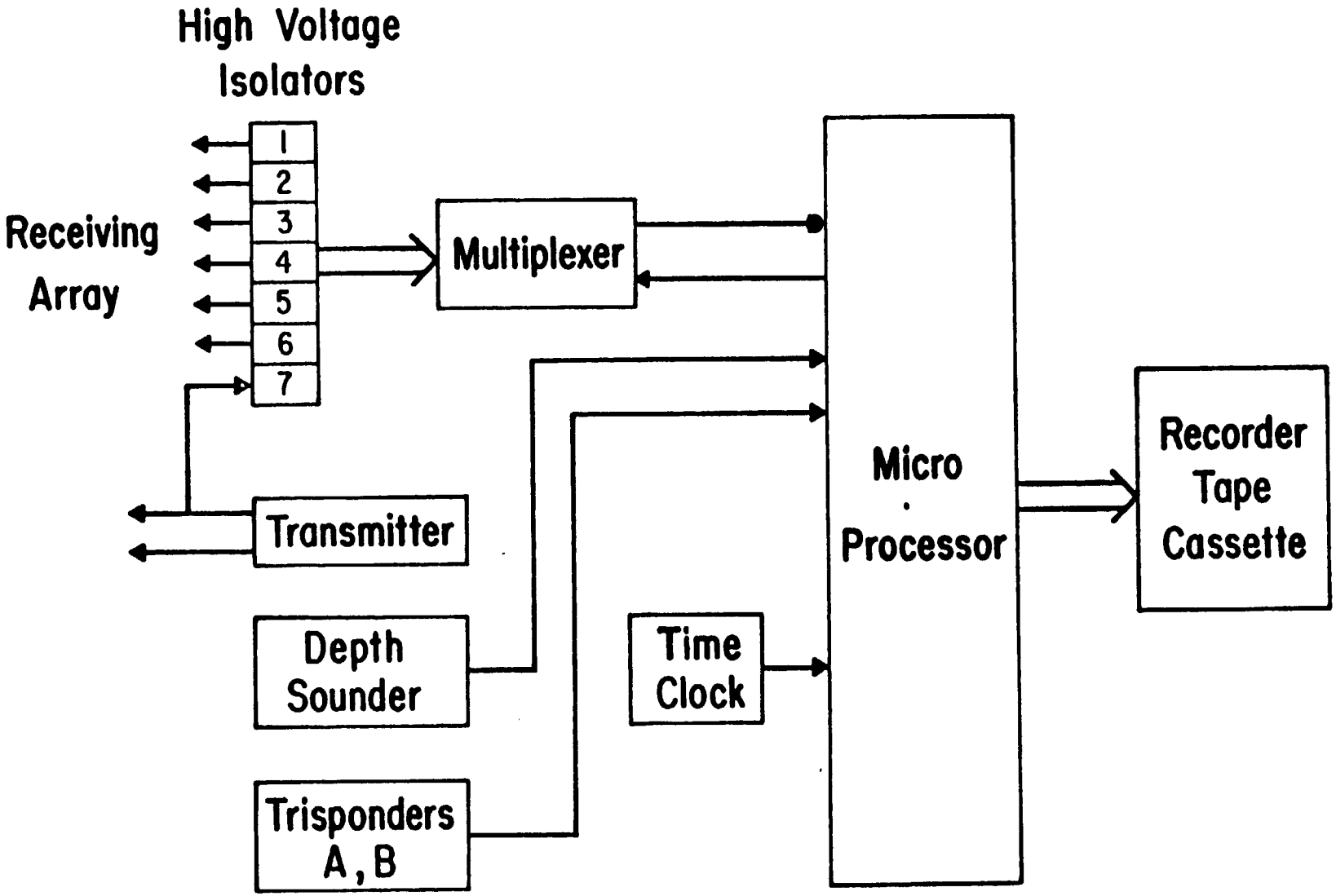

Figure 2 Block diagram of microprocessor-controlled marine resistivity system

ARRAY CONFIGURATION

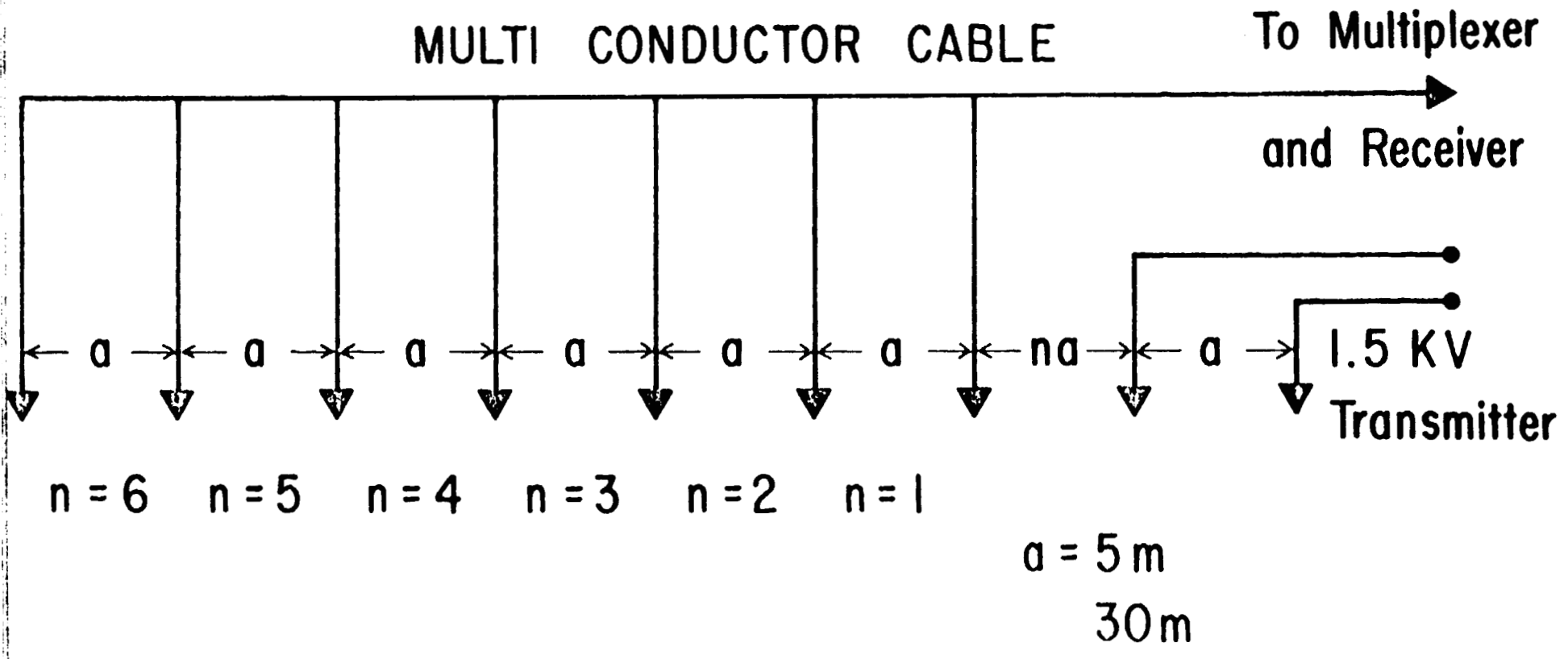

Figure 3 Configuration of the towed multi-dipole electrode array

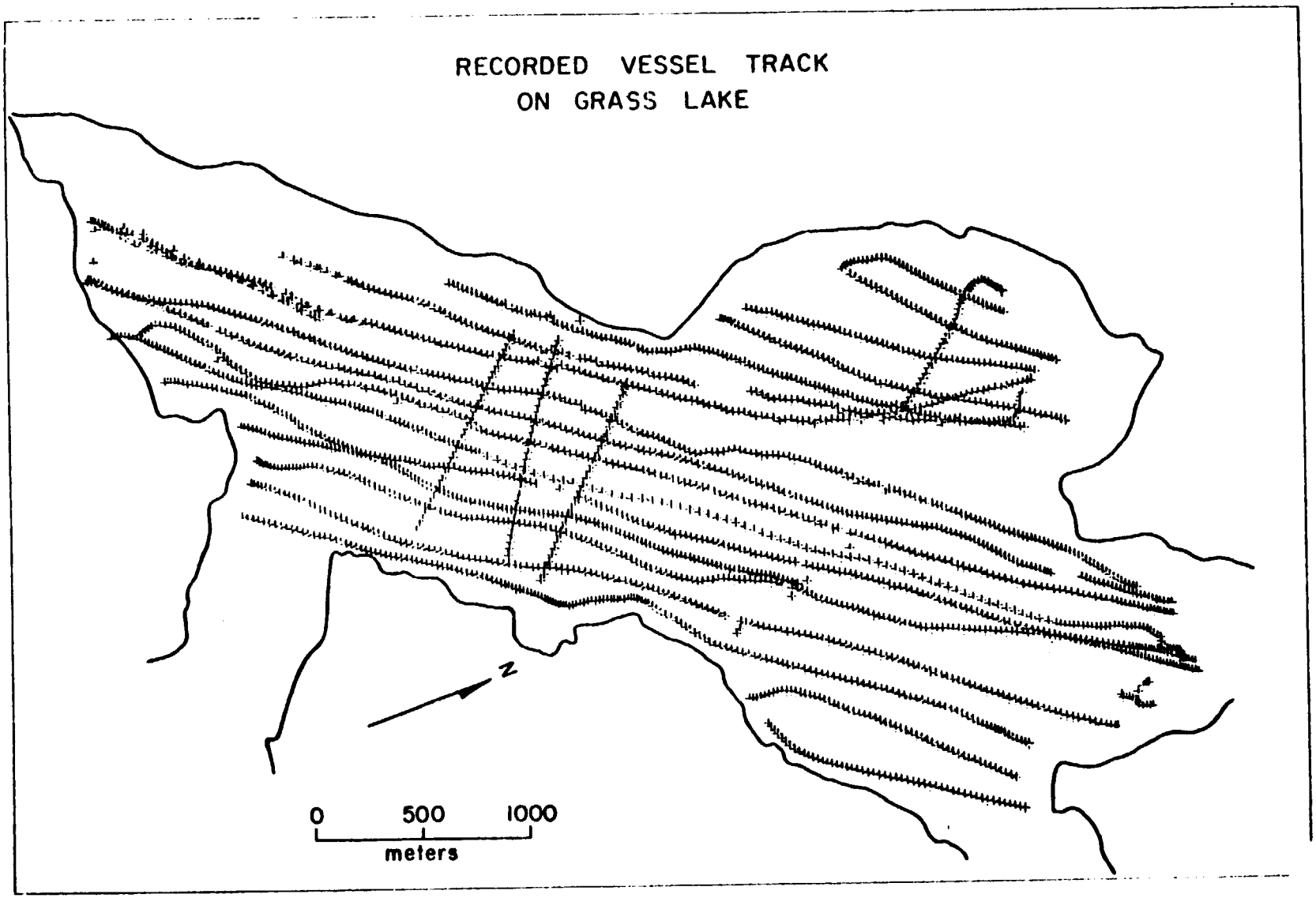

Figure 4 Recorded vessel positions for survey of Grass Lake

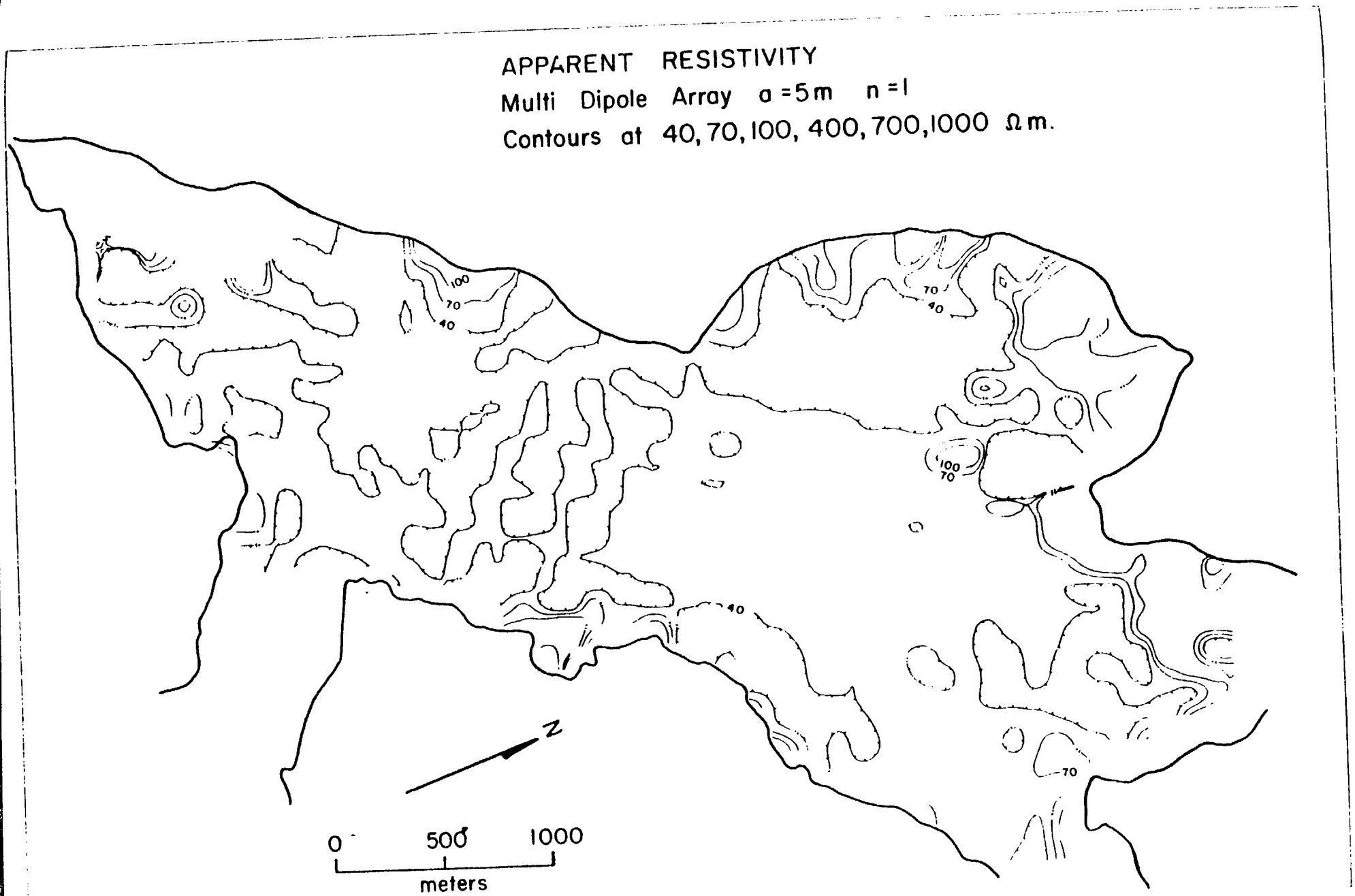

Figure 5 Contour map of apparent resistivity for a = 5 metres, n = 1

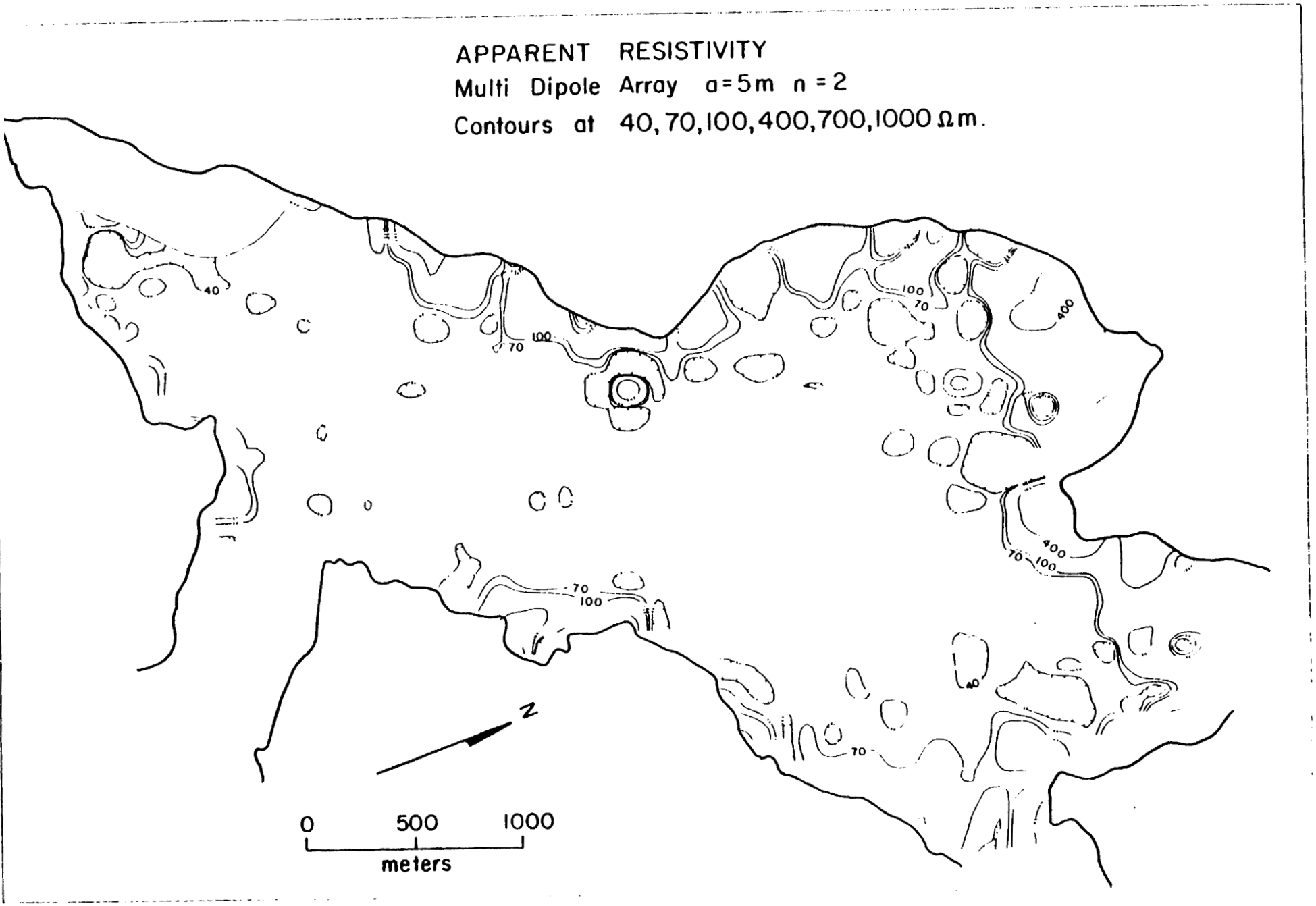

Figure 6 Contour map of apparent resistivity for a = 5 metres, n = 2

Figure 6 Contour map of apparent resistivity for a = 5 metres, n = 2

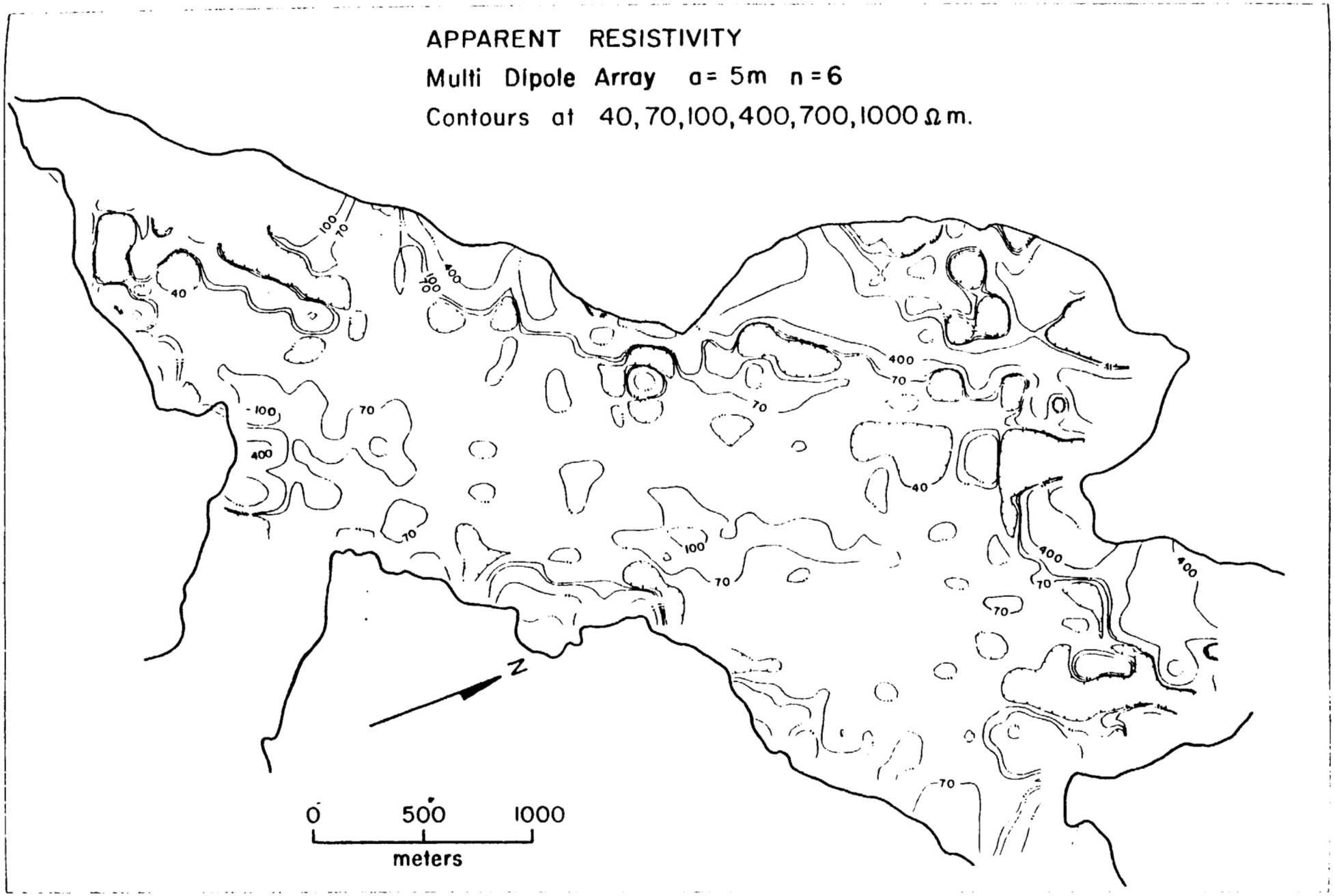

Figure 7 Contour map of apparent resistivity for a = 5 metres, n = 6

APPENDIX "D"

Typical Configurations of Near-Bottom Granular Deposits, Beaufort Sea

4 LAYER MODEL

LAYER	THICKNESS	RESISTIVITY
1	8.0	2
2	20.0	2
3	20.0	1
4		100

N	RHO(10)	RHO(25)	RHO(50)
1	2.0	2.0	1.8
2	2.1	1.8	2.2
3	2.0	1.8	2.9
4	2.0	2.0	3.7
5	1.9	2.3	4.4
6	1.8	2.6	5.2

4 LAYER MODEL

LAYER	THICKNESS	RESISTIVITY
1	8.0	2
2	10.0	2
3	10.0	1
4		500

N	RHO(10)	RHO(25)	RHO(50)
1	2.0	1.9	2.4
2	1.9	2.1	3.8
3	1.8	2.6	5.2
4	1.8	3.3	6.6
5	1.9	4.0	8.0
6	2.0	4.7	9.3

4 LAYER MODEL

LAYER	THICKNESS	RESISTIVITY
1	8.0	2
2	20.0	2
3	20.0	1
4		10

N	RHO(10)	RHO(25)	RHO(50)
1	2.0	2.0	1.8
2	2.1	1.9	2.1
3	2.1	1.8	2.7
4	2.0	1.9	3.2
5	1.9	2.2	3.7
6	1.9	2.4	4.1

4 LAYER MODEL

LAYER	THICKNESS	RESISTIVITY
1	8.0	2
2	20.0	2
3	20.0	1
4		100

N	RHO(10)	RHO(25)	RHO(50)
1	1.9	1.6	1.5
2	1.8	1.5	2.0
3	1.7	1.5	2.7
4	1.6	1.7	3.3
5	1.5	2.0	4.0
6	1.4	2.4	4.7

4 LAYER MODEL

LAYER	THICKNESS	RESISTIVITY
1	8.0	2
2	10.0	2
3	10.0	1
4		500

N	RHO(10)	RHO(25)	RHO(50)
1	1.9	1.6	2.2
2	1.7	1.8	3.5
3	1.6	2.4	4.8
4	1.5	3.0	6.0
5	1.6	3.6	7.3
6	1.8	4.3	8.5

4 LAYER MODEL

LAYER	THICKNESS	RESISTIVITY
1	8.0	2
2	20.0	2
3	20.0	1
4		10

N	RHO(10)	RHO(25)	RHO(50)
1	1.9	1.7	1.5
2	1.8	1.5	1.9
3	1.7	1.5	2.4
4	1.6	1.7	2.9
5	1.5	2.0	3.4
6	1.5	2.2	3.8

5 LAYER MODEL

LAYER	THICKNESS	RESISTIVITY
1	8.0	2
2	2.0	20
3	20.0	2
4	20.0	1
5		100

N	RHO(10)	RHO(25)	RHO(50)
1	2.4	3.1	2.5
2	3.0	2.7	2.4
3	3.2	2.3	3.0
4	3.2	2.3	3.7
5	3.0	2.4	4.4
6	2.8	2.7	5.2

5 LAYER MODEL

LAYER	THICKNESS	RESISTIVITY
1	8.0	2
2	2.0	20
3	10.0	2
4	10.0	1
5		500

N	RHO(10)	RHO(25)	RHO(50)
1	2.3	3.0	2.9
2	2.9	2.8	3.8
3	3.1	2.9	5.2
4	3.0	3.4	6.6
5	2.9	4.0	7.9
6	2.8	4.6	9.3

5 LAYER MODEL

LAYER	THICKNESS	RESISTIVITY
1	8.0	2
2	2.0	20
3	20.0	2
4	20.0	1
5		10

N	RHO(10)	RHO(25)	RHO(50)
1	2.4	3.2	2.6
2	3.0	2.8	2.3
3	3.2	2.4	2.7
4	3.2	2.2	3.2
5	3.0	2.3	3.7
6	2.8	2.5	4.1

5 LAYER MODEL

LAYER	THICKNESS	RESISTIVITY
1	8.0	2
2	2.0	15
3	20.0	2
4	20.0	1
5		100

N	RHO(10)	RHO(25)	RHO(50)
1	2.3	2.7	2.0
2	2.7	2.1	2.0
3	2.8	1.8	2.7
4	2.6	1.9	3.3
5	2.3	2.1	4.0
6	2.1	2.4	4.7

5 LAYER MODEL

LAYER	THICKNESS	RESISTIVITY
1	8.0	2
2	2.0	15
3	10.0	2
4	10.0	1
5		500

N	RHO(10)	RHO(25)	RHO(50)
1	2.3	2.6	2.5
2	2.7	2.3	3.5
3	2.7	2.5	4.7
4	2.5	3.0	6.0
5	2.4	3.6	7.2
6	2.3	4.2	8.5

5 LAYER MODEL

LAYER	THICKNESS	RESISTIVITY
1	8.0	2
2	2.0	15
3	20.0	2
4	20.0	1
5		10

N	RHO(10)	RHO(25)	RHO(50)
1	2.3	2.7	2.0
2	2.7	2.2	2.0
3	2.8	1.9	2.4
4	2.6	1.9	2.9
5	2.4	2.0	3.4
6	2.2	2.2	3.8

5 LAYER MODEL

LAYER	THICKNESS	RESISTIVITY
1	8.0	2
2	5.0	2
3	20.0	2
4	20.0	1
5		100

N	RHO(10)	RHO(25)	RHO(50)
1	1.9	1.9	1.8
2	1.9	1.8	2.1
3	1.9	1.8	2.7
4	1.9	1.9	3.4
5	1.8	2.1	4.1
6	1.8	2.4	4.7

5 LAYER MODEL

LAYER	THICKNESS	RESISTIVITY
1	8.0	2
2	20.0	2
3	10.0	2
4	20.0	1
5		100

N	RHO(10)	RHO(25)	RHO(50)
1	1.9	1.7	1.6
2	1.8	1.6	1.9
3	1.7	1.6	2.4
4	1.7	1.7	3.0
5	1.6	1.9	3.6
6	1.6	2.2	4.2